Aus dem

Institut für Schlaganfall- und Demenzforschung (ISD)

Klinikum der Ludwig-Maximilians-Universität München

Inflammatory pathways as drug targets for autoimmune disease - insights from human genomics

Dissertation

zum Erwerb des Doktorgrades der Medizin

an der Medizinischen Fakultät

der Ludwig-Maximilians-Universität München

vorgelegt von

Dr. Marek Janusz Konieczny

aus

aus Wałbrzych (PL)

Jahr

2025

Mit Genehmigung der Medizinischen Fakultät der
Ludwig-Maximilians-Universität München

Erstes Gutachten:	Dr. Dr. Marios Georgakis
Zweites Gutachten:	Prof. Dr. Sebastian E. Baumeister
Drittes Gutachten:	Prof. Dr. Martin Kerschensteiner
weitere Gutachten:	Honorarprofessor Dr. Hartmut Wekerle

Dekan: Prof. Dr. med. Thomas Gudermann

Tag der mündlichen Prüfung: 07.05.2025

Table of content

Abstract (German)

Inflammation und Entzündungsreaktionen liegen der Pathophysiologie zahlreicher Krankheiten zugrunde, darunter allergische und autoimmune Erkrankungen, kardiometabolische Krankheiten und Krebs. Zirkulierende Zytokine spielen eine zentrale Rolle bei der Regulation von Entzündungen und Immunantworten und haben eine immer größer werdende Bedeutung als Zielstrukturen für pharmakologische Therapien. Tatsächlich sind zytokinbasierte Immuntherapien bereits zugelassen und ein Teil des therapeutischen Arsenals bei der Behandlung von Autoimmunerkrankungen und Krebs. Dennoch spielt die Neupositionierung von zytokinbasierten Wirkstoffen auf andere Indikationsgebiete wie zum Beispiel Herz-Kreislauf-Erkrankungen aufgrund von Wirksamkeits- und Sicherheitsproblemen nur eine untergeordernete Rolle. Aufgrund der niedrigen Kosten und hohen Verfügbarkeit genomischer Daten hat die Entwicklung und Validierung von Wirkstoffen mit Hilfe der Humangenomik in den letzten Jahren viel an Aufmerksamkeit gewonnen und ein enormes Potenzial gezeigt. So haben Studien, die Vorteile der Genomik für die Wirkstoffentwicklung quantifiziert haben, gezeigt das Wirkstoffe die durch In-silico-Daten gestützt werden eine mehr als doppelt so hohe Wahrscheinlichkeit haben eine Marktzulassung zu erhalten im Gegensatz zu Wirkstoffen ohne genetische Unterstützung. Im Rahmen meiner Doktorarbeit führte ich die bislang umfangreichste genomweite Assoziationsstudie (GWAS) an einem Panel von 40 zirkulierenden Zytokinen durch, wobei ich Daten von insgesamt 74.783 Individuen analysiert habe, gefolgt von umfangreichen post-GWAS-Analysen, einschließlich transkriptomweiter Assoziationsstudien mit Mendelscher Randomisierung (TWAS-MR), Mendelscher Randomisierung zur Identifizierung von Wirkstoffzielen (Drug-target MR) und Kolokalisierungsanalysen anwendete, um die genetische Architektur zirkulierender Zytokine zu untersuchen und neue Zielstrukturen für Krankheiten zu identifizieren. In meiner Analyse identifizierte ich insgesamt 359 signifikante Assoziationen zwischen Zytokinspiegeln im Blut und 169 unabhängigen genetischen Varianten. Die Integration der GWAS-Ergebnisse mit Transkriptomdaten zeigte einige wichtigte regulatorische Mechanismen, die der Zytokinexpression zugrunde liegen, auf. Beispielsweise konnte eine signifikante Rolle von ACKR1 bei der Pufferung mehrerer Chemokine, indem es als Abfluss („sink“) fungiert und damit deren Spiegel effektiv reguliert, gezeigt werden. Darüber hinaus habe ich TRAFD1 als einen wichtigen Modulator des durch TNF-Signalgebung induzierten Zytokinsturms identifizieren. Die Cross-Zytokin-MR-Analyse zeigte ein komplexes Netzwerk von Kausalzusammenhängen zwischen Zytokinen auf, wobei TNF-b, VEGF und IL-1ra als zentrale, übergeordnete Akteure mit pleiotropen Downstreameffekten auf mehrere andere Zytokine hervorgingen. Durch die Anwendung von Drug-target MR in Verbindung mit Kolokalisierungsanalysen habe ich vielversprechende Zytokin-basierte Zielstrukturen entdeckt welche einen Kausalzusammenhang mit Autoimmunerkrankungen aufzeigten. Dabei identifizierte ich

G-CSF und CXCL9/MIG als zugrundeliegende Zytokine bei Asthma bzw. Morbus Crohn. Darüber hinaus konnte ich einen protektiven Effekt von TNF-b bei Multipler Sklerose aufzeigen. Meine Ergebnisse bieten umfassende Einsichten in die Genetik von zirkulierenden Zytokinen, und dienen als Grundlage für die Entwicklung gezielter und spezifischer Immuntherapien.

Abstract (English)

Inflammation contributes to the pathophysiology underlying multiple human diseases, including allergic and autoimmune disease, cardiometabolic disease and cancer. Circulating cytokines are central in orchestrating inflammation and immune responses and are increasingly recognized as promising targets for therapeutic interventions. Indeed, cytokine-based immunotherapies are already approved and part of the therapeutic armamentarium for autoimmune diseases and cancer. Nevertheless, repurposing of cytokine-based compounds to other conditions, for example to cardiovascular disease, remains limited due to efficacy and safety issues. Development and validation of drug targets with the help of human genomics received much attention in recent years with increased data availability and low costs showing enormous potential. Researchers quantifying the added value of genomics for drug development have shown that compounds backed-up by in-silico data are more than twice as likely to receive marketing approval compared to targets without genetic support. During my MD project, I conducted the largest genome-wide association study (GWAS) to date on a panel of 40 circulating cytokines, encompassing 74.783 individuals, followed by extensive post-GWAS analyses including transcriptome-wide association studies followed by Mendelian randomization (TWAS-MR), drug-target MR and colocalization to study the genetic architecture of circulating cytokines and uncover novel drug targets for human diseases. In my analysis, I identified a total of 359 significant associations between circulating cytokine levels and genetic variants, spanning 169 distinct genomic loci. By integrating the GWAS findings with transcriptomic data, I uncovered crucial regulatory mechanisms underlying cytokine expression. For instance, the analysis revealed a significant role of ACKR1 in buffering multiple chemokines, acting as a scavenger to regulate their levels effectively. Additionally, I identified TRAFD1 as a key modulator of the cytokine storm induced by TNF signaling. Cross-cytokine MR analysis unveiled a complex network of interconnections among cytokines, with TNF-b, VEGF, and IL-1ra emerging as central players with pleiotropic downstream effects on multiple other cytokines. Employing drug-target MR in conjunction with colocalization analysis, I uncovered potential causal mediators underlying specific diseases. Notably, my analysis identified G-CSF and CXCL9/MIG as potential drivers of asthma and Crohn’s disease, respectively. Additionally, I observed a potentially protective role of TNF-b in multiple sclerosis. My findings offer a comprehensive insight into the genetic landscape governing circulating cytokines, paving the way for targeted immunotherapy development.

List of figures

List of tables

List of abbreviations

ABC1	ATP Binding Cassette Subfamily A Member 1
ACKR1	Atypical chemokine receptor 1
AMD	Age-related macular degeneration
ATF6B	Activating Transcription Factor 6 Beta
B-cells / B-lymphocytes	Bone-marrow cells
BET1L	Bet1 Golgi Vesicular Membrane Trafficking Protein Like
bNGF	Beta nerve growth factor
C4A	Complement C4A
CAD	Carotid artery disease
CANTOS	Cardiovascular Risk Reduction Study
CC	Chemokine in which the first two conserved cysteines residues are adjacent
CCL11/eotaxin-1	Eotaxin
CCL2/MCP-1	Monocyte chemotactic protein-1
CCL27/CTACK	Cutaneous T-cell attracting
CCL3/MIP-1a	Macrophage inflammatory protein-1a
CCL4/MIP-1b	Macrophage inflammatory protein-1b
CCL7/MCP-3	Monocyte specific chemokine 3
CD	Crohn's disease
CFH	Complement factor H
CIRT	Cardiovascular Inflammation Reduction Trial
CRC	Colorectal cancer
CSF	Cerebrospinal fluid
CVD	Cardiovascular disease
CXC	Chemokine that have one amino acid residue separating the first two conserved cysteine residues
CXCL1/GROa	Growth regulated oncogene-a
CXCL10/IP-10	Interferon gamma-induced protein 10
CXCL12/SDF-1a	Stromal cell-derived factor-1 alpha
CXCL8/IL-8	Interleukin-8
CXCL9/MIG	Monokine induced by interferon-gamma
DAMPs	Damage-associated molecular patterns
DMARDs	Disease-modifying anti-rheumatic drugs
DMF	Dimethyl fumarate
DNA	Deoxyribonucleic acid
EDTA	Ethylenediaminetetraacetic acid
eQTL	Expression quantitive trait loci
FCER1A	Fc Epsilon Receptor Ia
FDR-corrected	Benjamin-Hochberg corrected
FGF-b	Basic fibroblast growth factor
FUMA	Functional Mapping and Annotation
G-CSF/CSF-3	Granulocyte colony-stimulating factor
GRCh37 (hg19)	Human genome assembly 19 from Genome Reference Consortium
GWAS	Genome-wide association study
H4C14	H4 Clustered Histone 14
HBV	Hepatitis B virus
HGF	Hepatocyte growth factor
HLA	Human leukocyte antigen

HLA-DRB5	Major Histocompatibility Complex, Class II, DR Beta 5
IBD	Inflammatory bowel disease
IFN-g	Interferon-gamma
IGFBP2	Insulin Like Growth Factor Binding Protein 2
IL-10	Interleukin-10
IL-12p40	Interleukin-12 Subunit p40
IL-12p70	Interleukin-12 Subunit p70
IL-13	Interleukin-13
IL-16	Interleukin-16
IL-17	Interleukin-17
IL-18	Interleukin-18
IL-1b	Interleukin-1-beta
IL-1ra	Interleukin-1 receptor antagonist
IL-2	Interleukin-2
IL-2ra	Interleukin-2 receptor, alpha subunit
IL-4	Interleukin-4
IL-5	Interleukin-5
IL-6	Interleukin-6
IL-7	Interleukin-7
IL-9	Interleukin-9
CXCL-11/IP-9	Interferon Gamma-Inducible Protein 9
IV	Instrumental variable
Kb	Kilobyte
LCMT2	Leucine Carboxyl Methyltransferase 2
LD	Linkage disequilibrium
LDL	Low-density lipoproteins
LDSC	Linkage disequilibrium score regression
LoF	Loss-of-function
MAGMA	Multi-marker Analysis of GenoMic Annotation
Mb	Megabyte
M-CSF/CSF-1	Macrophage colony-stimulating factor
MIF	Macrophage migration inhibitory factor
MR	Mendelian randomization
MR-egger	MR egger regression
MR-IVW	MR inverse variance-weighted
MR-median	MR weighted median estimator
mRNA	Messenger ribonucleic acid
MS	Multiple sclerosis
NELFE	Negative Elongation Factor Complex Member E
NF-kB	Nuclear factor 'kappa-light-chain-enhancer' of activated B-cells
NHGRI	National Human Genome Research Institute
NIH	National Institutes of Health
NLR	Nucleotide Binding Oligomerization Domain
NPX	Normalized expression values
PDGFbb	Platelet derived growth factor BB
PP1	Protein phosphatase 1
PPA	Posterior probability of association

PPI	Protein-protein interactions
PPP1R12A	Protein Phosphatase 1 Regulatory Subunit 12A
PPP1R37	Protein Phosphatase 1 Regulatory Subunit 37
PPP1R3D	Protein Phosphatase 1 Regulatory Subunit 3D
pQTL	Protein-quantitative trait loci
PVR	PVR Cell Adhesion Molecule
RA	Rheumatoid arthritis
RANTES	Regulated on Activation, Normal T Cell Expressed and Secreted
ROC	Receiver operating characteristic
rsID	Rapid stain Identification Series
RTN2	Reticulon 2
SCALLOP	Systematic and Combined AnaLysis of Olink Proteins
SCF	Stem cell factor
SCGF-b	Stem cell growth factor beta
SD	Standard deviation
SKIV2L	SKI2 Subunit Of Superkiller Complex
SMPP1-M	Myosin protein phosphatase 1
SNP	Single-nucleotide polymorphism
STK19B	Serine/Threonine Kinase 19B
SuSIE	SUm of SIngle Effects
T-cells / T-lymphocytes	Thymic cells
TB	Tuberculosis
Th1-cells / Th1-lymphocytes	T-helper cells 1
TLR	Toll-like receptor
TNF	Tumor necrosis factor
TNF-a	Tumor necrosis factor-alpha
TNF-b	Tumor necrosis factor-beta
TNF-R	TNF-receptor
TRAFD1	TRAF-Type Zinc Finger Domain Containing 1
TRAFD2	TRAF-Type Zinc Finger Domain Containing 2
TRAF-proteins	TNF receptor associated factor
TRAIL	TNF-related apoptosis inducing ligand
TWAS	Transcriptome-wide association study
UC	Ulcerative colitis
UKB	UK Biobank
UTR	Untranslated region
VEGF	Vascular endothelial growth factor
YFS	Cardiovascular Risk in Young Finns Study

Contributions to the publication

Contribution to the paper: Konieczny, Marek J., et al. "The Genomic Architecture of Circulating Cytokine Levels Points to Drug Targets for Immune-Related Diseases." medRxiv (2024): 2024-04.

I participated in the study conception and design. I was also responsible for data collection and quality control. For analysis, I established the data processing pipeline for all parts of the manuscript except the cross-assay comparison. This part was contributed by Murad Omarov including statistical analysis and drafting of the figure for the cross-assay comparison. I conducted the statistical analysis of the project, except the cross-assay comparison. Finally, I discussed results with co-authors, drafted the figures (except for the cross-assay comparison) and the manuscript, and revised the manuscript after co-author feedback. All co-authors contributed to the formulations of the discussion. Formulations in the discussion of the dissertation are my own work.

1. Introduction

Chronic inflammation is implicated in a range of diseases spanning allergic and autoimmune conditions, cardiometabolic disorders, and cancer (Konieczny et al., 2024). Key players in this inflammatory cascade are proteins such as cytokines, chemokines, and growth factors, which intricately regulate the immune response (Deckers et al., 2023). Although various immunotherapies targeting circulating cytokines have shown promise in clinical settings, their efficacy in other conditions remains limited, often accompanied by side effects like increased susceptibility to infections (Lutgens et al., 2019; Soehnlein and Libby, 2021). Recent advances in human genetics have enabled an in-silico prioritization of drug targets (Holmes et al., 2021; Minikel et al., 2020), with approval rates more than two times higher than targets without genetic support (King et al., 2019).

Mendelian randomization (MR) leverages data from genome-wide association studies (GWAS) to explore associations between genetic variants in drug target genes and disease traits, offering a robust statistical framework (Gill et al., 2021). Previous MR analyses have demonstrated the potential of integrating GWAS data for circulating proteins, including cytokines, with disease outcomes to unearth novel drug targets (Bouras et al., 2022; Chong et al., 2019; Georgakis et al., 2020, 2019; Kappelmann et al., 2021; Mokry et al., 2019). However, these efforts have often been hindered by the limited sample sizes of GWAS studies focusing on circulating cytokines. To bridge this gap and glean fresh insights into the causal mediators of human diseases, I conducted GWAS across three independent cohorts for 40 circulating cytokines, aggregating data from a total of 74.783 individuals. Making use of post-GWAS methods and transcriptomic data, I characterized the genomic architecture of circulating cytokines including in-depth analysis of inflammatory network relations and key regulatory pathways. Analyzing 15 common human diseases in a two-sample MR setting accompanied by colocalization analysis I found solid evidence for the involvement of specific inflammatory cytokines and chemokines in allergic and autoimmune conditions.

1.1 Inflammation in human disease

Inflammation, once conceived simply as a defensive response to injury or infection that typically resolves quickly under physiological conditions, has emerged as a central player in the pathogenesis of a myriad of human diseases (Pisetsky, 2023). Its intricate involvement spans from the initiation to the resolution phase of various pathological processes, orchestrating a complex interplay of cellular and molecular events (Jin et al., 2024). Understanding the mechanisms of inflammation in human disease is paramount, as it not only elucidates the fundamental processes underlying disease initiation and progression but also unveils novel therapeutic targets (Deckers et al., 2023; Pulendran and Davis, 2020). While recent findings have underscored the significance of immune-mediated

dysregulation in chronic diseases, the precise mechanisms responsible for erroneous inflammatory reactions is still not known (Xiang et al., 2023). Next to the involvement of the immune system in autoimmunity and allergies, there is a considerable contribution of inflammatory dysregulation in cancer and as recently shown also in cardiovascular diseases (Galon et al., 2013; Pisetsky, 2023; Soehnlein and Libby, 2021).

1.1.1 Inflammation in autoimmune disease

In autoimmune diseases, inflammation plays a dual role, serving as both a cause and consequence of the body's immune system mistakenly attacking its own tissues. Under normal circumstances, the immune system is finely regulated to distinguish between self and non-self-antigens, preventing the attack on healthy tissues (Suek et al., 2024). If the process of immune-tolerance is compromised, autoreactive T and B lymphocytes proliferate and attack autoantigens facilitating the development of autoimmune diseases (L. Wang et al., 2015). Firstly, the immune system becomes dysregulated due to various stimuli, leading to the breakdown of immune tolerance (Kubagawa et al., 2024). During this phase, the activated innate immune response triggers the onset of adaptive immunity, causing T and B cells to erroneously identify antigens, thus instigating abnormal immune activity (Damoiseaux et al., 2015). Secondly, the aberrant proliferation of innate immune cells results in the secretion of inflammatory mediators such as cytokines, chemokines and growth factors, driving the abnormal infiltration of T and B cells. Furthermore, chronic inflammation perpetuates autoimmune diseases by sustaining the activation of autoreactive immune cells and release of inflammatory mediators leading to tissue destruction (Davidson and Diamond, 2001). Conversely, the tissue damage resulting from autoimmune attacks can further amplify inflammation through the release of damage-associated molecular patterns (DAMPs) and the activation of innate immune cells, additionally augmenting the vicious cycle of inflammation and tissue destruction (Rodien et al., 1996). Finally, the immune system tries to limit autoimmune responses through intrinsic and extrinsic cellular mechanisms. This stage is characterized by clinical stability and relapses of the disease, underscoring the ongoing potential for disease management (Lou et al., 2022).

1.1.2 Inflammation in cancer

The immune system and inflammation play intricate roles in the complex landscape of cancer development and progression (Yu et al., 2024). Initially perceived solely as a defense mechanism against pathogens, the immune system is now recognized for its pivotal role in recognizing and eliminating aberrant cells, including those undergoing malignant transformation (Sherr, 1996). However, cancer cells have evolved various strategies to evade immune surveillance and harness inflammation to their advantage (Vermeulen et

al., 2003). For example, inflammation can promote tumor initiation by creating a microenvironment conducive to carcinogenesis (Minati et al., 2020; S. Wang et al., 2019). Chronic inflammation, often triggered by persistent infections, environmental toxins, or autoimmune diseases, can lead to DNA damage, genomic instability, and the activation of oncogenic pathways, fostering the development of cancerous lesions (Vermeulen et al., 2003). Moreover, inflammation fuels tumor progression and metastasis through the secretion of pro-inflammatory cytokines, chemokines, and growth factors by both cancer cells and stromal cells within the tumor microenvironment (Lee and Margolin, 2011). These inflammatory mediators stimulate angiogenesis, enhance tumor cell proliferation and survival, facilitate invasion into surrounding tissues, and promote the formation of pre-metastatic niches, thereby facilitating cancer spread (Minati et al., 2020). Conversely, the immune system serves as a critical defense mechanism against cancer by recognizing and eliminating malignant cells through immune surveillance mechanisms (Sherr, 1996). Immune cells, such as cytotoxic T lymphocytes and natural killer cells, can recognize tumor-specific antigens and mount an immune response to eradicate cancer cells (Kambayashi and Laufer, 2014).

1.1.3 Inflammation in cardiovascular disease

Inflammation plays a crucial role in the development and progression of cardiovascular disease (CVD) (Aday and Ridker, 2019). Initially, inflammation was considered merely a response to vascular injury, but it's now understood as a key driver of atherosclerosis, the underlying pathology of most CVD‘s (Gisterå and Hansson, 2017). Atherosclerosis, characterized by the accumulation of lipid-rich plaques in arterial walls, is initiated by endothelial dysfunction, which triggers an inflammatory response. Endothelial cells become activated, expressing adhesion molecules and secreting chemokines, attracting circulating monocytes into the vessel wall (Gerhardt and Ley, 2015). Monocytes differentiate into macrophages, which engulf oxidized low-density lipoproteins (LDL) and transform into foam cells, initiating plaque formation. The inflammatory milieu within plaques promotes further leukocyte recruitment, smooth muscle cell proliferation, and extracellular matrix remodeling, leading to plaque growth and instability (Libby, 2013). Inflammation also contributes to plaque rupture, the primary event triggering acute cardiovascular events such as myocardial infarction and stroke (Croce and Libby, 2007). Vulnerable plaques, characterized by a thin fibrous cap and a lipid-rich core, are prone to rupture due to local inflammation, macrophage activity, and matrix metalloproteinase production, leading to thrombus formation and arterial occlusion (Croce and Libby, 2007). Beyond atherosclerosis, inflammation influences other aspects of CVD. In myocardial infarction, ischemia-reperfusion injury triggers an inflammatory cascade, exacerbating tissue damage (Chen et al., 2022). In heart failure, systemic inflammation contributes to cardiac

remodeling and dysfunction (Prabhu and Frangogiannis, 2016). Additionally, inflammation plays a role in arrhythmias, endothelial dysfunction, and vascular remodeling, further impacting CVD progression (Kamel and Iadecola, 2012).

1.2 Cytokines, chemokines and growth factors as inflammatory mediators

The immune system plays a major role in protecting the host organisms against invading pathogens, aiding in tissue repair and maintenance of tissue homeostasis (Pulendran and Davis, 2020; Unanue et al., 1976). Communication within the immune system is executed through direct cell-to-cell contact or via synthesis and release of cytokines, chemokines and growth factors. These inflammatory proteins are produced and released in response to infections, inflammation, or internal stimuli (Gharaee-Kermani and Phan, 2001). Different classes of cytokines present with distinct functions within the immune system (Altan-Bonnet and Mukherjee, 2019). Cytokines are small proteins secreted by various cells of the immune system, including leukocytes, macrophages, lymphocytes, and endothelial cells (Stanley and Lacy, 2010; Unanue et al., 1976). Cytokines serve as messengers between different immune cells, facilitating communication and coordination of immune responses (Gharaee-Kermani and Phan, 2001). They can activate or inhibit the function of other cells, promoting or suppressing inflammation as needed (Stanley and Lacy, 2010). So-called pro-inflammatory cytokines, including tumor necrosis factor (TNF) have antimicrobial functions and activate the immune responses (Arango Duque and Descoteaux, 2014). Conversely, immunomodulatory or anti-inflammatory cytokines like IL-1 receptor antagonist (IL-1ra) dampen immunostimulatory pathways, reducing inflammation and supporting tissue repair (Opal and DePalo, 2000). Certain cytokines act as chemotactic factors, attracting immune cells such as neutrophils, monocytes, and lymphocytes to sites of infection or tissue injury. These so-called chemokines include CXC and CC chemokine-ligands, guide immune cell migration, facilitating immune surveillance and response (Hughes and Nibbs, 2018). In addition to their role in inflammation, cytokines also contribute to tissue repair and remodeling processes following injury or infection (Zepter et al., 1997). They regulate the production of extracellular matrix components, angiogenesis, and the recruitment of cells involved in tissue regeneration (Gharaee-Kermani and Phan, 2001). Cytokines execute their different functions through a complex network of signaling pathways and interactions with specific receptors on target cells (Unanue et al., 1976). Each cytokine typically interacts with one or more receptor subtypes, and the binding of cytokines to their receptors initiates downstream signaling cascades. Following binding, intracellular pathways trigger biological responses that vary widely depending on the cytokine and cell type involved (Stanley and Lacy, 2010). A key characteristic of cytokines is their ability to induce different phenotypic traits, a concept known as pleiotropy. This occurs because specific cytokine receptors can be expressed

on multiple cell types, resulting in a variety of biological outcomes. Furthermore, certain cytokines can bind to multiple receptors, leading to diverse downstream effects, such as promoting cell differentiation or suppressing effector functions (Lin et al., 1995). Moreover, there is partial functional redundancy among cytokines, where more than one cytokine can perform the same biological function (Stanley and Lacy, 2010). While this redundancy enhances the robustness of the immune system, it complicates therapeutic immunoregulation and the development of cytokine-based immunotherapies (Deckers et al., 2023).

1.3 Targeted cytokine immunotherapies

1.3.1 Development of immunotherapies

Cytokines play crucial roles as key regulators of the human immune system, and their dysregulation is an important feature of various diseases, including allergies and autoimmunity, cardiometabolic disease and cancer (Konieczny et al., 2024; Soehnlein and Libby, 2021; Unanue et al., 1976; Uricoli et al., 2021). Due to their various functions within the immune system, cytokines have attracted considerable attention as potential targets for therapy (Deckers et al., 2023). In conditions characterized by heightened cytokine production, such as autoimmune and inflammatory disorders, inhibiting cytokine activity through monoclonal antibodies or receptor blockers has demonstrated success (Opal and DePalo, 2000). For instance, blocking TNF or Interleukin-6 (IL-6) has proven effective in treating conditions like Crohn's disease (CD) or rheumatoid arthritis, respectively (Monaco et al., 2015; Nishimoto and Kishimoto, 2004). Conversely, cytokines can also be therapeutically administered to modulate immune responses as shown by the effectivity of IL-1ra in CVD (Morton et al., 2015). Advances in recombinant protein technology have led to the development of approved drugs targeting inflammatory proteins, including vascular-endothelial growth factors for age-related macular degeneration (AMD) (Rosenfeld et al., 2005). However, the development of cytokine-based therapeutics presents challenges such as pleiotropic effects, and unfortunate biological distribution, which contribute to their limited efficacy and safety (Deckers et al., 2023). Severe side effects observed in early clinical trials, such as disease exacerbations induced by TNF-inhibitors in trials of multiple sclerosis (MS), underscore the importance of addressing these challenges (Li et al., 2023).

Autoimmune diseases

Immunosuppressive cytokines have been utilized for different therapeutic purposes (Monaco et al., 2015; Morton et al., 2015). These cytokines play a crucial role in attenuating excessive immune reactions, fostering tissue regeneration, and alleviating autoimmune or inflammatory disorders like rheumatoid arthritis (RA) and ulcerative colitis (UC)

(Deckers et al., 2023). In conditions characterized by aberrant immune activation, immunosuppressive cytokines help restore the immune balance by tempering the inflammatory cascade (Opal and DePalo, 2000). Targeting IL-1ra has emerged as a promising therapeutic approach in RA, supported by substantial evidence from preclinical studies, clinical trials, and real-world clinical experience (Fleischmann et al., 2003). Preclinical studies have demonstrated the pivotal role of interleukin-1 (IL-1) in the pathogenesis of RA. IL-1, a pro-inflammatory cytokine, contributes to joint inflammation, cartilage degradation, and bone erosion in RA (Choy and Panayi, 2001). IL-1ra acts as a natural antagonist to IL-1 by competitively inhibiting its binding to the IL-1 receptor, thereby attenuating IL-1-mediated inflammatory responses (Ben-Sasson et al., 2009). Clinical trials investigating the efficacy and safety of IL-1ra blockade in RA have shown encouraging results. One notable study, the IL-1ra in RA (IL-1RA) trial, demonstrated that treatment with IL-1ra by anakinra, a synthetic IL-1ra analogue, significantly reduced disease activity, improved symptoms, and inhibited radiographic progression in patients with RA who had an inadequate response to traditional disease-modifying anti-rheumatic drugs (DMARDs) (Bresnihan et al., 1998). Subsequent studies have corroborated these findings, highlighting the therapeutic potential of IL-1ra in RA management (Cohen et al., 2004; Cunnane et al., 2001; Jiang et al., 2000). Furthermore, the safety profile of IL-1 inhibitors, such as anakinra, has been generally favorable, with adverse events typically being mild to moderate in severity. Common side effects include injection-site reactions and mild infections (Bresnihan, 2001). Importantly, IL-1ra therapy does not appear to increase the risk of serious infections or malignancies (Furst, 2004). On the other hand, anti-TNF antibodies like infliximab and adalimumab, although revolutionizing the treatment of many autoimmune diseases by targeting TNF, a key regulatory cytokine in inflammation and autoimmunity, raise concerns about adverse effects, including an increased risk of cancer and serious infections, including bacterial, viral, fungal, and opportunistic infections which is primarily due to the immunosuppressive effects of TNF inhibition (Andersen et al., 2015; Siegel et al., 2009). Patients need to be monitored closely and appropriate precautions, like vaccinations should be taken to reduce the risk of exposure. Additionally, anti-TNF therapy can lead to the reactivation of latent infections, such as tuberculosis (TB) and hepatitis B virus (HBV) (Lee et al., 2022; Yuk et al., 2024). Lastly, there are concerns that anti-TNF therapy may increase the risk of certain malignancies, especially lymphoma and skin cancers (Siegel et al., 2009). This highlights the potential of immunosuppressive therapies targeting cytokines in managing autoimmune conditions which already proved highly effective for certain diseases and revolutionized patient management it also exemplifies that dampening of important upstream proteins entails serious safety concerns.

Cancer

In contrast to the application of cytokine-based immunotherapy in the field of autoimmune disease, cancer immunology initially had to overcome early skepticism to achieve

significant progress only recently (Galon et al., 2013). Discoveries and experiments which demonstrated the immune rejection of tumors and proposed theories of immune surveillance, reignited interest in cancer immunology (Burnet, 1970; Prehn and Main, 1957; Shankaran et al., 2018). Initial immunological approaches were made using cytokine-based compounds (Galon et al., 2013). A notable example is interferon-alpha (IFN-a), which received its first approval in 1986 for combatting leukemia (Berraondo et al., 2019). Its effectiveness lies in its capacity to induce apoptosis and restrict the proliferation of malignant cells. Following closely, interleukin-2 (IL-2) obtained approval in 1992 specifically for treating metastatic renal cancer (McDermott and Atkins, 2006). Both IFN-a and IL-2 emerged as highly promising treatments, showcasing instances where small groups of patients experienced complete responses (Galon et al., 2013). Nevertheless, when administered systemically, these cytokines often resulted in severe adverse events among many patients, leading to treatment-related fatalities in some cases (Atkins et al., 1999). To harness the benefits of cytokine administration while minimizing off-target effects, engineered cytokine designs have been developed to target specific trafficking into tumor microenvironments (Deckers et al., 2023; Uricoli et al., 2021).

Cardiovascular disease

Cytokine-based therapies in CVD are an area of active research and investigation, but their clinical application remains limited compared to other therapeutic modalities (Soehnlein and Libby, 2021). However, there has been significant interest in targeting specific cytokines implicated in the pathogenesis of atherosclerosis and heart failure (Bonfiglio et al., 2023). Recent clinical trials showed the benefits of repurposed compounds targeting specific cytokine pathways in CVD (Lutgens et al., 2019). IL-1b is a pro-inflammatory cytokine implicated in the initiation and progression of atherosclerosis and other cardiovascular conditions (Bresnihan et al., 1998; Soehnlein and Libby, 2021). Clinical trials have investigated the use of IL-1b inhibitors, such as canakinumab, in patients with a history of myocardial infarction and elevated inflammatory markers (Ridker et al., 2017). While these trials have shown promising results in terms of reducing cardiovascular events, the use of IL-1b inhibitors in clinical practice remains limited due to concerns about safety, cost, and patient selection criteria (Lutgens et al., 2019). TNF is another pro-inflammatory cytokine implicated in the pathogenesis of atherosclerosis and heart failure (Carswell et al., 1975; Sozzani et al., 2014). While TNF inhibitors have been used extensively in the treatment of autoimmune diseases, their role in CVD remains controversial (Bonfiglio et al., 2023). Preclinical studies have suggested potential benefits of TNF inhibitors in reducing inflammation and improving cardiovascular outcomes, but failed to show efficacy in clinical trials. (Atzeni et al., 2021; Chung et al., 2003; Mann et al., 2004). Also, blocking TNF pathways entails the risk for serious side-effects, notably infections and malignancy (Andersen et al., 2015; Lee et al., 2022; Siegel et al., 2009).

IL-6 is another pleiotropic cytokine with diverse effects on inflammation, immune regulation, and cardiovascular function (Nishimoto and Kishimoto, 2004). Elevated levels of IL-6 have been associated with increased risk of cardiovascular events and adverse outcomes in patients with CVD (Interleukin-6 Receptor Mendelian Randomisation Analysis (IL6R MR) Consortium et al., 2012). Therapeutic agents targeting the IL-6 pathway, such as tocilizumab, have been investigated in small-scale studies, but their clinical utility in CVD awaits confirmation in clinical trials (Kleveland et al., 2016). In addition to IL-1b, TNF, and IL-6, other cytokines and inflammatory mediators have been implicated in the pathogenesis of CVD (Bonfiglio et al., 2023). Targeting these pathways with specific cytokine inhibitors or modulators represents a potential therapeutic strategy for CVD (Soehnlein and Libby, 2021). However, further research is needed to elucidate the precise role of these cytokines in CVD pathophysiology and to develop effective and safe cytokine-based therapies.

1.3.2 Need for novel, specific drug targets

Although there has been significant progress in the development of novel, specific compounds coupled with innovative drug designs cytokine-based therapeutics faces challenges due to pleiotropic effects, safety concerns and unfortunate biological distribution, all of which limit their efficacy and applicability in the clinic (Deckers et al., 2023). In the realm of autoimmune disease, interleukin-10 (IL-10) application in CD exhibited minimal side effects and was well tolerated but failed to induce significant remission compared to placebo, possibly due to low local concentrations (Schreiber et al., 2000). To enhance clinical efficacy, many engineered immunosuppressive cytokine designs aim to target specific tissues, receptors, or cell subsets (Deckers et al., 2023). On the other hand, anti-TNF antibodies like infliximab and adalimumab have transformed the treatment of autoimmune diseases, improving symptoms and quality of life (Monaco et al., 2015). However, concerns persist regarding adverse effects, including an elevated risk of cancer, disease exacerbations and serious infections (Andersen et al., 2015; Siegel et al., 2009; Yuk et al., 2024). Similar concerns were observed in CVD. In the first clinical large-scale trial focusing on inflammation it was shown that canakinumab treatment, blocking IL-1b downstream effects, successfully reduced cardiovascular endpoints, including myocardial infarction, stroke or cardiovascular death. Furthermore, an exploratory analysis noted a reduction in cancer and cancer mortality. However, inhibition of the IL-1b pathway showed a slight increase in infections, including fatal ones, in the active treatment arm (Ridker et al., 2017). Nevertheless, targeting inflammatory pathways in CVD represents a promising direction of research (Soehnlein and Libby, 2021). Another anti-inflammatory trial explored the use of low-dose weekly methotrexate in individuals at high risk for coronary events (Ridker et al., 2019). However, the Cardiovascular Inflammation Reduc-

tion Trial (CIRT) was halted prematurely due to futility, showing no reduction in cardiovascular events. Additionally and in contrast to the CANTOS trial, patients in the active treatment group in the CIRT trial showed a significant increase in cutaneous cancer, highlighting a potential limitation of anti-inflammatory therapy in interfering with immune surveillance for malignancy (Ridker et al., 2019). Focusing on targets downstream in the IL-1 pathway, an on-going large scale trial investigating blockage of the IL-6 pathway using ziltivekimab in CVD (ClinicalTrials.gov ID: NCT03926117), a drug target that is efficiently inhibited in the treatment of many autoimmune conditions (Ridker et al., 2021; Soehnlein and Libby, 2021). These challenges, including severe live-threatening side-effects, the low tissue specificity, increased risk for infections or malignancies when blocking immunological pathways represent a major roadblock for the approval of cytokine-based therapies and highlights the necessity for the development of novel, specific drug targets.

1.3.3 In-silico drug target prioritization

Due to the immense costs and high failure rates of clinical drug development programs there is a large unmet need for improved target validation methods (DiMasi et al., 2016; Harrison, 2016). Traditional pre-clinical experiments often fail to accurately predict target perturbation effects in human diseases (Sun et al., 2022). The critical step where most compounds fail is within the late-stage clinical development. At this stage, 90% of compounds have to be discarded due to compound related toxicity or because the target protein fails to show efficacy for the disease indicating that the targeted protein is not causally responsible for the disease (Schmidt et al., 2022). Improving drug development efficiency through better identification of promising targets could help to significantly reduce costs and speed-up the developmental process (DiMasi et al., 2016; Ference, 2018). Advancements in high-throughput genetic technologies have led to a significant reduction in sequencing costs, making it more accessible than ever before. This accessibility, coupled with the exponential growth of sequenced genome data, has revolutionized the landscape of drug discovery (Hukerikar et al., 2024). We now have an unprecedented wealth of genetic information at our fingertips, enabling us to pinpoint and validate potential drug targets with greater precision and efficiency (Lau and So, 2020). This integration of genetic data into drug development processes holds immense promise for accelerating the discovery of novel therapeutic interventions (Schmidt et al., 2022). Despite the wealth of potential drug targets identified through genetic data, the sheer volume can overwhelm traditional wet lab experimentation. This abundance underscores the necessity for systematic methodologies to prioritize targets for further investigation (Hukerikar et al., 2024). Such approaches are crucial for optimizing resources and focusing research efforts on the most promising candidates. By employing systematic target prioritization strategies, researchers can streamline the drug discovery process, increasing the likelihood of

identifying successful therapeutic interventions while minimizing time and resource wastage.

Genome-wide association studies

GWAS are based on data from high-throughput techniques (GWAS arrays) to genotype numerous common genetic markers throughout the genome of a population and assess their association with a particular phenotype (Forgetta et al., 2022; Mountjoy et al., 2021). Due to the cost-effectiveness of genotyping arrays, they can be employed to analyze many different phenotypes in large sample sizes making them highly relevant to drug development (Duncan et al., 2019). Although GWAS can be highly informative there are major limitations to this approach which requires further downstream analyses and validation for reliable drug target identification (Hindorff et al., 2009). In contrast to loss-of-function (LoF) variants which have clear functional implications, GWAS often highlight common genetic variations, predominantly found in non-coding regions proximal to protein-coding genes (Mountjoy et al., 2021; Studer et al., 2013). These variants commonly aggregate into correlated clusters within populations, a phenomenon termed linkage disequilibrium (LD). Deciphering the exact causal variant and gene linked to the association signal poses a formidable challenge due to this genetic clustering (Bulik-Sullivan et al., 2015). Nevertheless, recent advancements in causal gene prediction models shed light on the significance of physical proximity in determining the causal gene. These models indicate that, in many instances, the nearest gene to the associated variant is the primary driver of the observed association (Hukerikar et al., 2024). This underscores the importance of spatial relationships in elucidating the functional implications of GWAS findings. Additionally, the majority of variants identified through GWAS are thought to exert their effects through regulatory mechanisms, impacting the levels of transcripts or proteins rather than directly altering protein functionality (Rose, 2019). Consequently, while GWAS frequently associate these variants with protein-coding genes, it's not inherently assumed that the identified gene is directly involved in protein functions (Mortezaei and Tavallaei, 2021). This highlights the nuanced nature of GWAS findings and the need for further functional validation to elucidate the precise molecular mechanisms underlying the observed associations. Moreover, the direction of effect in a GWAS can be influenced by the selection of the effect allele, adding complexity to the translation of GWAS findings into actionable drug targets (Mortezaei and Tavallaei, 2021). This underscores the necessity for additional information to elucidate the underlying mechanisms. Improving the applicability of GWAS results to drug development frequently entails supplementary analyses such as MR, which inherently addresses these challenges by leveraging genetic variants as instrumental variables (IV) to infer causal relationships between traits and outcomes (Grover et al., 2017). Integrating approaches like MR enhances the robustness and reliability of GWAS findings, facilitating more informed decision-making in drug development endeavors.

Mendelian randomization

MR comprises a collection of methodologies designed to untangle causal associations between genetically determined traits, drawing on insights from human genetics research (Burgess et al., 2013). This framework stands as a pivotal instrument in the drug development pipeline, offering a means to forecast disease trajectories and anticipate potential adverse effects stemming from the modulation of a drug target (Grover et al., 2017). By leveraging genetic variants as IV's, MR provides a rigorous approach to infer causality, thereby aiding in the prioritization of candidate drug targets and guiding decisions throughout the drug development process (Zheng et al., 2017a). Within the MR framework, genetic variants associated with a specific exposure are leveraged to probe for the existence of a dose-response relationship. This relationship elucidates whether the genetic variant's impact on the exposure correlates with its effect on the outcome of interest (Holmes et al., 2017). Initially rooted in IV methodology, MR has evolved into a 'two-sample' paradigm, enabling the amalgamation of non-identifiable genetic data from separate exposure and outcome datasets (Burgess et al., 2016). This innovative approach enhances the statistical power of MR analyses by maximizing sample sizes, a notable advantage over traditional cohort studies (Bandres-Ciga et al., 2020; Fewell et al., 2007). By leveraging genetic information from distinct sources, the two-sample framework broadens the scope of MR investigations, facilitating more robust and comprehensive evaluations of causal relationships between exposures and outcomes in diverse populations and settings (Hartwig et al., 2016). The validity and efficacy of MR rests upon three core principles (Schmidt et al., 2022):

1) Genetic variants must exhibit a robust association with the potential drug target, often achieved by selecting variants identified through GWAS as the focal points of analysis.

2) Genetic variants should not share common causes with the exposure and/or outcome under investigation, a condition typically met owing to the fixed nature of genetic variation within populations.

3) Horizontal pleiotropy pathways, wherein genetic variants influence disease risk independently of the exposure being studied, should be absent. While verifying the validity of this assumption can be challenging, analytical techniques are available to mitigate the potential impact of horizontal pleiotropy.

While the first two principles rely on the characteristics of genetic variants and population genetics, addressing the third principle requires careful consideration and rigorous statistical methods to ensure the reliability of MR findings (Bowden et al., 2015; Kou et al., 2020). These principles collectively underpin the robustness and validity of MR analyses, enabling researchers to draw meaningful and actionable conclusions regarding causal relationships between exposures, outcomes, and potential drug targets. Next to the two-sample MR methodology, the increasing accessibility of protein-quantitative trait loci

(pQTLs) enabled validation of potential proteinergic drug targets (Hukerikar et al., 2024; Wang et al., 2018). This approach called drug-target MR involves sourcing genetic instruments primarily from within or near a small cis-region (i.e. nearby region) of the protein-encoding gene of interest (Ference, 2018; Mokry et al., 2015). MR studies focusing on drug targets have exhibited notable success across various disease categories, underscoring its utility in the validation of potential therapeutic interventions across diverse clinical contexts (King et al., 2019).

Colocalization

Colocalization serves as a crucial analytical tool utilized to determine whether multiple signals detected independently in GWAS originate from a shared underlying causal variant (Franceschini et al., 2018). By integrating data from multiple sources and assessing the overlap of association signals, colocalization aids in distinguishing true genetic associations from spurious correlations, thereby enhancing the accuracy and interpretability of GWAS results (Giambartolomei et al., 2014). Colocalization entails the examination of the convergence between signals detected in GWAS for diseases with signals originating from expression-quantitative trait loci (eQTL) and pQTL (Wallace, 2020). By integrating multiple layers of genomic data, colocalization provides valuable insights into the mechanistic underpinnings of complex traits and diseases, facilitating a deeper understanding of genetic architectures and potential therapeutic targets (Zuber et al., 2022). In the realm of drug target validation, colocalization frequently follows MR as an additional step for prioritization (van der Graaf et al., 2020). Its purpose is to validate whether the identified signal truly originates from the intended exposure (Duncan et al., 2019). Otherwise, it implies the presence of separate genetic associations distinct from those observed in the pQTL underscoring the complexity of genetic influences on diseases and highlighting the need for comprehensive analyses to unravel intricate molecular mechanisms underlying observed associations (Giambartolomei et al., 2014; Zuber et al., 2022).

2. Aims of the thesis

Several lines of research identified inflammation, in particular inflammatory cytokines as important determinants in the pathology of human diseases. As regulators of the immune response these proteins can be used as drug agents for targeted treatment approaches. Indeed, observational studies have demonstrated the potential of targeting specific cytokines in reducing disease endpoints. However, confounding and reverse causation do not allow observational studies to draw causal conclusions that would be relevant for informing drug discovery and development. With the advent of human genetics and the cost-effectiveness of high throughput analysis techniques, genetic research including GWAS, MR and colocalization methods enabled an in-silico identification of inflammatory proteins as drug targets. However, existing efforts have been largely restricted by the small sample sizes of GWAS studies for circulating cytokines. In order to obtain novel insights into the causal mediators of human diseases I will perform GWAS across 3 independent cohorts for 40 circulating cytokines, aggregating data from 74.783 individuals, and MR followed by colocalization analyses for 15 disease phenotypes. The current thesis aims to study the effect of inflammatory cytokines on human diseases by

1. exploring the genomic architecture underlying variations in the levels of circulating cytokines,

2. investigating the effects of genetically predicted cytokine levels on human diseases,

3. dissecting upstream proteomic and transcriptomic changes mediating the effects of circulating cytokines on disease risk.

To gain a deeper understanding of the inflammatory pathomechanisms involved in human disease, I first aimed to explore the genomic profile of circulating cytokine levels. To maximize statistical power, GWAS data for 40 circulating cytokines from 3 publicly available datasets (YFS & FINRISK, SCALLOP Consortium and deCODE Consortium) will be aggregated. In the derived pooled dataset, I then performed fine-mapping, functional annotation, gene-set and pathway analyses to identify causal genes and to obtain insights into the mechanisms regulating the levels of circulating cytokine levels. Using the pooled GWAS dataset, I extracted variants for genetically predicted cytokine levels with the aim to study the effects they exert on allergic and autoimmune disease, cardiometabolic disease and cancer using the MR approach. As a next step, selection of genetic variants was restricted to those around the location of the cytokine-encoding genes (i.e. selection of cis-variants). These genetic variants and their effects on the outcome measures were used to test, in a drug-target MR setting, whether genetic modification of circulating cytokine levels affects the risk for the respective disease. To validate the findings, I performed colocalization analysis and filtered the MR results for associations arising from the same genetic locus. For exploration of additional drug targets, I followed-up on the cytokines that came out significant in drug-target MR and colocalization analyses.

Herein, I aimed to analyze if proteins or transcripts that lie upstream of the cytokine-initiated immune pathway, mediate the effects on disease.

3. Material and Methods

To address my objectives, I calculated GWAS analyses on aggregated data from 3 publicly available, independent cohorts and applied downstream analyses including two-sample, drug-target MR across 15 disease phenotypes (Konieczny et al., 2024). The study cohorts are described in section 3.1., the genomic analysis methodology in section 3.2. The study cohorts and a flowchart of the study design are depicted in **Figure 3.1**.

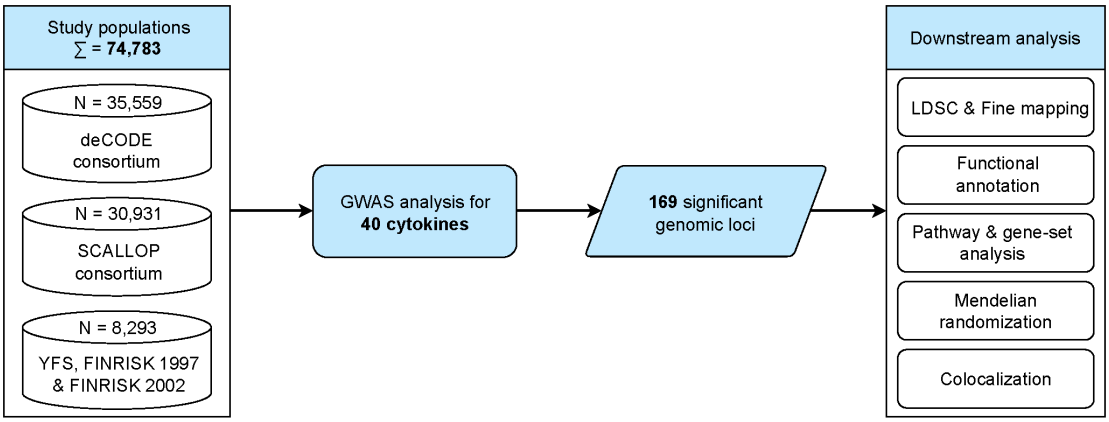

Figure 3.1 Flowchart of the study design. Illustration of the analytical pipeline steps applied in this study to decipher the genetic architecture of circulating cytokines and their relation to allergic and auto-immune, cardiometabolic and cancer outcomes. LDSC, Linkage Disequilibrium Score Regression; SCALLOP, Systematic and Combined AnaLysis of Olink Proteins; SNP, Single-nucleotide polymorphism; TWAS-MR, Transcriptome-wide Mendelian ran-domization analysis; YFS & FINRISK, Cardiovascular Risk in Young Finns Study. Adapted from Konieczny et al., 2024. medRxiv. 2024-04. CC-BY-NC-ND 4.0.

3.1 Material

3.1.1 Study populations

I downloaded publicly available GWAS summary statistics for the circulating levels of up to 40 cytokines from 3 independent cohorts (refer to **Table 3.1**) (Konieczny et al., 2024). Details of the study protocols have been published elsewhere and are outlined below (Ahola-Olli et al., 2017; Ferkingstad et al., 2021; Folkersen et al., 2020). For the GWAS meta-analyses and downstream analyses I included all cytokines that were available in at least 2 cohorts. To ensure that the available cytokines were identical between cohorts I used information provided on the NIH (https://www.ncbi.nlm.nih.gov/gap/) and GeneCards (https://www.genecards.org/) websites and verified synonyms and aliases in the abbreviated and full names of the cytokines. In this regard, I identified a mismatch for the cytokine IL-12 between the YFS & FINRSIK cohort and the deCode cohort. The cytokine IL-12 available in the YFS & FINRSIK cohort was identified as the IL-12 p70 subunit whereas in the deCode cohort the IL-12 p40 subunit was reported. Due to this mismatch, I excluded this cytokine from my analysis. Before further computations, the 3 databases were harmonized regarding

		Total N	YFS and FINRISK 1997 and 2002	Scallop CVD 1	deCode
Mean Age (SD), years	-	-	49 (8)	n/a	55 (18)
Sex, % female	-	-	51	n/a	57
sample size	-	74783	8293	30931	35559
Full length name	**Abbreviation**	-	-	-	-
Beta nerve growth factor	bNGF	70021	3531	30931	35559
Cutaneous T-cell attracting	CCL27/CTACK	39190	3631	n/a	35559
Eotaxin	CCL11/eotaxin-1	43712	8153	n/a	35559
Basic fibroblast growth factor	FGF-b	43124	7565	n/a	35559
Granulocyte colony-stimulating factor	G-CSF/CSF-3	43463	7904	n/a	35559
Growth regulated oncogene-alpha	CXCL1/GROa	69995	3505	30931	35559
Hepatocyte growth factor	HGF	74782	8292	30931	35559
Interferon-gamma	IFN-g	43260	7701	n/a	35559
Interleukin-10	IL-10	43240	7681	n/a	35559
Interleukin-13	IL-13	39116	3557	n/a	35559
Interleukin-16	IL-16	69973	3483	30931	35559
Interleukin-17	IL-17	43319	7760	n/a	35559
Interleukin-18	IL-18	70126	3636	30931	35559
Interleukin-1-beta	IL-1b	38868	3309	n/a	35559
Interleukin-1 receptor antagonist	IL-1ra	70128	3638	30931	35559
Interleukin-2	IL-2	39034	3475	n/a	35559
Interleukin-2 receptor, alpha subunit	IL-2ra	39236	3677	n/a	35559
Interleukin-4	IL-4	43683	8124	n/a	35559
Interleukin-5	IL-5	38923	3364	n/a	35559
Interleukin-6	IL-6	74679	8189	30931	35559
Interleukin-7	IL-7	38968	3409	n/a	35559
Interleukin-8	CXCL8/IL-8	70016	3526	30931	35559
Interleukin-9	IL-9	39193	3634	n/a	35559
Interferon gamma-induced protein 10	CXCL10/IP-10	39244	3685	n/a	35559
Monocyte chemotactic protein-1	CCL2/MCP-1	74783	8293	30931	35559
Monocyte specific chemokine 3	CCL7/MCP-3	36402	843	n/a	35559
Macrophage colony-stimulating factor	M-CSF/CSF-1	67330	840	30931	35559
Macrophage migration inhibitory factor	MIF	39053	3494	n/a	35559
Monokine induced by interferon-gamma	CXCL9/MIG	39244	3685	n/a	35559
Macrophage inflammatory protein-1 alpha	CCL3/MIP-1a	70012	3522	30931	35559
Macrophage inflammatory protein-1 beta	CCL4/MIP-1b	39174	8243	30931	n/a
Platelet derived growth factor BB	PDGFbb	74783	8293	30931	35559
Regulated on Activation, Normal T Cell Expressed and Secreted	RANTES	38980	3421	n/a	35559
Stem cell factor	SCF	74780	8290	30931	35559
Stem cell growth factor beta	SCGF-b	39241	3682	n/a	35559
Stromal cell-derived factor-1 alpha	CXCL12/SDF-1a	41557	5998	n/a	35559
Tumor necrosis factor-alpha	TNF-a	39013	3454	n/a	35559
Tumor necrosis factor-beta	TNF-b	37118	1559	n/a	35559
TNF-related apoptosis inducing ligand	TRAIL	74676	8186	30931	35559
Vascular endothelial growth factor	VEGF	73608	7118	30931	35559

Table 3.1. Characteristics of the included GWAS databases. The table gives an overview of the GWAS databases, including demographic characteristics, where available. Cytokine names and abbreviations were taken from NIH and GeneCards websites. SCALLOP, Systematic and Combined AnaLysis of Olink Proteins; YFS & FINRISK, Cardiovascular Risk in Young Finns Study; N, sample size; SD, standard de-viation; n/a, not available.

the data structure by defining a set of common variables to be included in all datasets, standardizing the cytokine names and aliases and computation of missing data entries (e.g. conversion of odds ratio to standardized beta), where necessary. To define the genomic positions of the data used in this project and provide a standardized framework for understanding the structure, function, and regulation of variants I used human genome assembly GRCh37 (hg19) from Genome Reference Consortium (1000 Genomes Project Consortium et al., 2010).

YFS and FINRISK

Genomic data for 40 cytokines were drawn from up to 8,293 individuals of Finnish background that were included in the YFS & FINRISK cohorts 1997 and 2002, respectively (Ahola-Olli et al., 2017). The Cardiovascular Risk in Young Finns Study (YFS) is a longitudinal investigation initiated in 1980 with follow-up assessments until 2011, involving randomly selected individuals from various Finnish cities and rural areas (Raitakari et al., 2008). This current cross-sectional study focuses on 2,019 unrelated individuals from the 2007 follow-up, examining cytokine levels and genotype data. Additionally, the FINRISK surveys, conducted every five years, monitor chronic disease risk factors in Finland among randomly chosen individuals aged 25 to 74 from five geographical regions (Ritchie et al., 2015). This study analyzed cytokine data from participants in the 1997 and 2002 surveys. Clinical examinations and blood sampling were conducted during the study visit. All participants provided written consent, and the study received approval from local ethics committees. The mean age across both studies was 49 years (standard deviation 8 years). The cytokine measurements were carried out in EDTA plasma for the FINRISK 1997 cohort, in heparin plasma for the FINRISK 2002 cohort and in serum for the YFS cohort using cytokine Luminex®-based multiplex immunoassays from Bio-Rad®. Genotyping was completed using the Illumina HT12 platform for the YFS study and the Illumina 670k HumanHap array for both FINRISK studies. Imputation was performed using the 1000 Genomes reference panel across all cohorts (1000 Genomes Project Consortium et al., 2010). The GWAS meta-analyzing all 3 studies normalized the cytokine distribution using inverse transformation and adjusted the genetic analyses for age, sex and ancestral principal components 1-10. The reported effect sizes were scaled per standard deviation increment in inverse-transformed cytokine levels.

SCALLOP Consortium

Genomic data for 16 cytokines were drawn from up to 30,931 individuals with European background from the SCALLOP consortium, a collaborative framework analyzing gene-

protein associations across 13 studies (Folkersen et al., 2020). The original SCALLOP consortium, consisting of 35 principal investigators from 28 research institutions includes data from over 70,000 patients and controls across 45 cohort studies. Proteins and samples for the current study (i.e. SCALLOP CVD-1) were selected by reviewing literature on protein biomarkers linked to cardiovascular risk in human and animal studies and by consulting leading cardiovascular disease researcher. The cytokine measurements were carried out in plasma samples using the proximity extension assay-based Olink® platform. Genotyping methods across the studies included Cardiometabochip, Immunochip, PsychChip, Illumina HumanCoreExome, Illumina OmniExpress, Metabochip, Illumina OmniExpress 2.5, Affymetrix Axiom UK Biobank array, HumanCytoSNP-12 BeadChip, HapMap300v2, Human Exome, Illumina HumanOmniExpressExome-8 v1, Illumina HumanHap300v1, Omni1, OmniX, Illumina HumanHap300v1 and Infinium PsychArray-24 v1.2. Imputation was performed using the following panels: 1000G phase v5, 1000G phase v3, UK10K reference panel, HRC, HRC r1.1. The GWAS meta-analyzing all 13 studies adjusted the cytokines for age, gender, site, OLINK batch, Olink plate, MDS components, storage time, bleed to processing time (days), smoking status, oral contraceptive usage, blood cell counts, season of venipuncture and ancestral principal components 1-10. The log2-based normalized expression values (NPX) for each protein were rank-based inverse normal transformed and standardized to units of standard deviation.

deCODE

Genomic and proteomic data for 39 cytokines were taken from 35,559 Icelandic individuals included in deCODE (Ferkingstad et al., 2021). deCODE genetics is an industrial research collaboration focused on discovering genetic risk factors for common diseases. The whole cohort, initiated in 1996 gathered genetic and medical data from approximately 500,000 individuals worldwide. In Iceland, they have gathered genotypic and medical data from over 160,000 participants, representing a significant portion of the adult population. On average, participants were 55 years old (standard deviation = 17 years), with 57% being women. All sample donors provided informed consent, and the study was approved by the National Bioethics Committee of Iceland, conducted in accordance with the Data Protection Authority's guidelines. The cytokine measurements were carried out in plasma samples using the aptamer-based SOMAScan® assay. Genotyping was completed using Illumina SNP Chip. Imputation was based on an in-house developed whole genome sequencing reference panel. The genetic analyses were adjusted for age and sex. Cytokine measurements were normalized using rank-inverse normal transformation and standardized to standard deviation increment. To allow alignment with other datasets, I excluded all SNPs that were not covered by the 1000 Genomes reference panel.

3.1.2 Disease outcomes

For the disease endpoints, I downloaded summary level data from the largest publicly available GWAS and performed MR analyses for 3 independent disease groups (Konieczny et al., 2024). Selection of disease phenotypes was based on the unrestricted availability of GWAS summary statistics for common human diseases with case counts (n_{cases}) > 2000 of patients from European ancestry. Following diseases were analyzed for allergic and autoimmune phenotypes: asthma (121,940 cases, 1,254,131 controls) (Tsuo et al., 2022), Crohn's disease (5,956 cases, 14,927 controls) (Liu et al., 2015), ulcerative colitis (6,968 cases, 20,464 controls) (Liu et al., 2015), multiple sclerosis (47,429 cases, 68,374 controls) (International Multiple Sclerosis Genetics Consortium, 2019), psoriasis (4,815 cases, 415,646 controls) (Bycroft et al., 2018), and rheumatoid arthritis (14,361 cases, 43,923 controls) (Okada et al., 2014). For cardiometabolic phenotypes I analyzed peripheral vascular disease (31,307 cases, 211,753 controls) (Klarin et al., 2019), coronary artery disease (60,801 cases, 123,504 controls) (Nikpay et al., 2015), large artery stroke (9,219 cases, 1,503,898 controls) (Mishra et al., 2022) and diabetes mellitus type II (242,283 cases, 1,569,730 controls) (Suzuki et al., 2024). For cancer phenotypes I analyzed breast cancer (133,384 cases, 113,789 controls) (Zhang et al., 2020), colorectal cancer (5,657 cases, 372,016 controls) (Burrows and Haycock, 2021), lung cancer (29,266 cases, 56,450 controls) (McKay et al., 2017), non-Hodgins lymphoma (2,400 cases, 410,350 controls) (Rashkin et al., 2020), and skin cancer (23,694 cases, 372,016 controls) (Burrows and Haycock, 2021). The data sources are detailed in **Table 3.2**.

3.1.3 Online databases

To assess previously reported associations a database search was conducted using the NHGRI-GWAS (National Human Genome Research Institute - Genome-Wide Association Study) catalogue on February 15th, 2023 (Konieczny et al., 2024). The NHGRI-GWAS catalog is a publicly available database that consolidates information from published GWAS and serves as a resource for researchers providing information on genetic variants associated with a wide range of traits (Welter et al., 2014). I analyzed my GWAS hits for associations with any of the 40 cytokines reported here, restricting the results for European-ancestry associations.

Disease group	Disease	Total N	n (cases)	n (controls)	Population
Cardiometabolic	Peripheral vascular disease	243060	31307	211753	European
	Coronary artery disease	184305	60801	123504	European
	Largery artery stroke	1513117	9219	1503898	European
	Diabetes mellitus type II	1812013	242283	1569730	European
Cancer	Breast cancer	247173	133384	113789	European
	Colorectal cancer	377673	5657	372016	European
	Lung cancer	85716	29266	56450	European
	Non-Hodgkins lymphoma	412750	2400	410350	European
	Skin cancer	395710	23694	372016	European
Allergic and Autoimmune	Asthma	1376071	121940	1254131	European
	Crohn's disease	20883	5956	14927	European
	Multiple sclerosis	115803	47429	68374	European
	Psoriasis	420461	4815	415646	European
	Rheumatoid arthritis	58284	14361	43923	European
	Ulcerative colitis	27432	6968	20464	European

Table 3.2. Details of the included disease phenotypes. This table shows sample sizes and geographic ancestry of the 15 disease phenotypes. N, total sample size; n, sample size.

3.1.4 eQTL data

For the transcriptome-wide association study followed by Mendelian randomization (TWAS-MR) analysis I acquired summary statistics for eQTLs in whole blood from the eQTLGen consortium (Konieczny et al., 2024), encompassing transcriptomic profiles for 31,684 individuals, predominantly of European ancestry (Võsa et al., 2021). The eQTL consortium is based on data sampled from the UK Biobank (UKB) (Võsa et al., 2021). The UKB is a population-based cohort of around 500,000 individuals aged 40 to 69, recruited between 2006 and 2010 (Sudlow et al., 2015). It comprises diverse participant data, including genome-wide genotyping, exome sequencing, magnetic resonance imaging, electronic health record linkage, blood and urine biomarker measurements, and physical assessments. Informed consent was obtained from all participants. Quality control procedures ensured data accuracy. Blood samples were collected using EDTA vacutainers and fractionated as per protocol. Protein biomarker measurements utilized the Olink technology, employing proximity extension assay.

3.2 Methods

3.2.1 Cross-assay comparison

To investigate variations in the genomic makeup influencing cytokine levels across 3 studies utilizing diverse measurement assays, I examined the overlap of SNPs within datasets, focusing on variants significant at a p-value threshold of less than 0.05 and direc-

tionally consistent (displaying the same effect estimate direction across all three databases) (Konieczny et al., 2024). Employing raw data, I assessed shared SNPs by treating one dataset as the reference and comparing it with the other two. This comparative analysis highlighted on the degree of agreement and discrepancy in genetic associations with cytokine levels across different measurement platforms and validated my meta-analysis approach.

3.2.2 GWAS analysis

I conducted a fixed-effects inverse variance-weighted meta-analysis for each cytokine across the available cohorts using METAL software (v.2011-03-25) (Konieczny et al., 2024; Willer et al., 2010). The average number of cohorts per cytokine was 2.4, the average sample size per cytokine was n=52.126 (details are provided in **Table 3.1**). Due to variations in the scaling of effect estimates across the 3 datasets, I calculated the meta-analysis using a z-score-based approach with the SCHEME SAMPLESIZE option in METAL. Subsequently, I estimated standardized beta coefficients using p-values, minimum allele frequency, and direction of effects, with weights based on sample sizes (Zhu et al., 2016). To assess the consistency of findings across data sources and ensure validity, reliability, and interpretability of my findings I calculated the heterogeneity of effect sizes applying chi-square test statistics for all included markers. To address genomic inflation, which gives information about potential population stratification of the used sample or usage of an inappropriate model, lambda statistics were computed for each cytokine (de Bakker et al., 2008; Greco M et al., 2015). Variants achieving genome-wide significance ($p<5x10-8$) were considered significant. To identify independent variants after correction for linkage disequilibrium (LD, see below), I performed clumping across significant variants using clump_data from the TwoSampleMR R package version 0.5.6, with an r2 threshold of <0.001 based on the European 1000 Genomes Project reference panel (1000 Genomes Project Consortium et al., 2010). Independent loci were defined as SNPs separated by more than 1 megabyte (Mb) from the next SNPs in the 3' and 5' directions, as previously described (Suzuki et al., 2024).

3.2.3 Linkage Disequilibrium Score Regression (LDSC)

Using the LD score v1.0.1. tool I applied LDSC regression with reference data from the European 1000 Genomes project for calculation of cross-trait LDSC genetic correlations between all 40 cytokines using the GWAS results (1000 Genomes Project Consortium et al., 2010; B. K. Bulik-Sullivan et al., 2015; Konieczny et al., 2024; Zheng et al., 2017b). LDSC is a statistical method to understand the genetic architecture of complex traits and diseases, where LD is defined as the non-random association of alleles at different loci (positions) on a chromosome (B. Bulik-Sullivan et al., 2015). It occurs when certain combinations of alleles at different loci are observed more frequently than expected by

chance. LD patterns are influenced by factors such as genetic recombination and population history. LDSC regression aids to uncover the relationship between genetic variants and complex traits, which are influenced by multiple genetic variants as well as environmental factors, by leveraging the patterns of genetic variation in the human genome.

3.2.4 Fine-mapping

To pinpoint the specific genetic variants responsible for the observed associations, I investigated significant loci associated with cytokines (Konieczny et al., 2024). I employed PLINK v1.9 to compute LD score correlation matrices and further refined the results using SuSiE (susieR R package version 0.12.16) to derive sets of variants, ensuring the inclusion of at least one causal variant with a cumulative probability ≥95% (Purcell et al., 2007; Wellcome Trust Case Control Consortium et al., 2012). This algorithm narrows down the genomic region surrounding an association signal to identify the most likely causal variant. Subsequently, the causal variants were utilized to estimate the total variance explained by the identified loci for individual cytokines (Park et al., 2010).

3.2.5 Functional annotation

For interpretation of the biological significance of genetic variants I annotated the significant variants with functional information using phenoscanner (MendelianRandomization R package version 0.6.0) (Konieczny et al., 2024). Phenoscanner ascribes functional consequences (intron, intergenic, exon, upstream, downsteam, etc.) of single variants using positional mapping (physical distance) (Kamat et al., 2019; Staley et al., 2016). Gene-property analyses was conducted for identification of the tissue specificity of cytokines using the FUMA Gene2Func web database (Watanabe et al., 2017).

3.2.6 Pathway and gene-set analysis

To understand how the significant variants collectively influence biological processes I conducted MAGMA gene-based and gene-set analyses (Konieczny et al., 2024). Gene-based analysis initially calculates p-value association tests for variants mapped to protein coding genes which are then used to calculate gene-set p-values in the gene-set analysis. Using predefined gene-sets, variants with significant associations to genes can then be analyzed to determine their underlying biological pathway or interaction networks, thus enabling mapping of key pathways associated with a particular trait or disease (de Leeuw et al., 2015).

3.2.7 Mendelian randomization

To understand causal relations between exposure and outcome variables I conducted MR analysis leveraging genetic variants associated with circulating cytokine levels as instrumental variables (Konieczny et al., 2024). I employed two-sample MR analysis to enhance statistical power and generalizability considering potential sources of bias and differences between datasets. I used cis-acting variants (i.e. variants that act on genes in their vicinity) as genetic instruments for the MR analyses, as they are associated with a lower risk of pleiotropic effects when compared to trans-acting (i.e. variants that act on distant genes) variants (Schmidt et al., 2020). Pleiotropic effects refer to the phenomenon where a single genetic variant influences multiple, potentially unrelated phenotypes. I derived cis-acting variants by filtering the GWAS results for variants within 300 kilobytes (Kb) around the gene encoding the respective cytokine. I selected variants associated at $p<5x10-5$ and clumped the data at $r2<0.1$. I applied fixed-effects inverse variance-weighted MR analysis (MR-IVW) as the main analytical approach (Burgess et al., 2013). MR-IVW analysis, the most common MR method, combines estimates from individual genetic variants using weighted linear regression, assuming all variants are valid instrumental variables. While MR-IVW provides efficient estimates under the assumption of no horizontal pleiotropy (i.e., genetic variants only affect the outcome through the exposure), it may be sensitive to violations of this assumption. MR egger regression (MR egger) and the weighted median estimator (MR median) were used as sensitivity analyses (Bowden et al., 2016, 2015). MR egger detects and corrects for directional pleiotropy thus providing unbiased estimates in the presence of directional pleiotropy, it may have reduced statistical power compared to the other two MR methods. MR median, a particularly robust MR method when there are concerns about horizontal pleiotropy, takes the median of effect estimates and provides consistent estimates even when 50% of variants violate the instrumental variable assumption. After harmonization of the effect alleles across cytokines I used mr command from the TwoSampleMR R Package (TwoSampleMR version 0.5.6) to extract the respective effect estimates. I used these analyses techniques in 3 different settings to answer specific questions, as outlined below.

3.2.7.1 Cytokines versus cytokines

First, I performed MR analyses exploring the effects of circulating cytokine levels on other cytokines to understand causal interconnections between cytokines (Konieczny et al., 2024). I used cis-acting variants as exposure and the GWAS results as outcome. This approach helped to understand the hierarchical structure within cytokines and to define important networks in inflammation.

3.2.7.2 Cytokines versus disease endpoints

Secondly, I measured the effects of circulating cytokine levels on allergic and autoimmune, cardiometabolic, and cancer disease endpoints for insights into the clinical consequences of genetically proxied levels of the circulating cytokines (Konieczny et al., 2024). Again, I used cis-acting variants as exposure and variants from GWAS's of the disease phenotypes as outcome.

3.2.7.3 eQTLs versus cytokines

Lastly, to further explore whether variant effects on expression of specific genes underlie the genetic underpinnings of circulating cytokine levels, I performed transcriptome-wide inverse variance-weighted two-sample MR analysis (TWAS-MR) (Burgess et al., 2013; Konieczny et al., 2024). Here cis-expression quantitative trait loci (eQTL) gene instruments from the eQTLGen Consortium were used as exposure and the GWAS results of the cytokine panel as outcome.

3.2.8 Colocalization analysis

I followed-up associations with allergic and autoimmune, cardiometabolic, and cancer outcomes showing significant associations in MR analyses by colocalization analyses (Konieczny et al., 2024). Colocalization analysis is a method used to assess whether two different genomic features, such as SNPs' for circulating cytokines and disease outcomes, tend to be located close to each other more often than expected by chance. To analyze shared causal variants between SNPs for circulating cytokines and disease outcomes I used the coloc R package (COLOC version 5.2.2). Coloc is a variant colocalization method that performs tests on shared causal variants in the locus considering the GWAS and disease outcome summary statistics at a locus jointly and probabilistically test if the two signals are likely to be generated by the same causal variant (Giambartolomei et al., 2014). I used the GWAS summary statistics for the significant cytokines restricted to a flanking region ±300 Kb around the genetic location of each cytokine and mapped disease-associated variants by their rapid stain identification series (rsID).

4. Results

I detected 359 significant associations between cytokine levels and variants in 169 independent loci, including 150 trans- and 19 cis-acting loci (Konieczny et al., 2024). Among the trans-acting variants I identified 33 pleiotropic variants, highest number of associated cytokines was found for the locus within the gene encoding CFH (n=12), in line with its function as regulator of the complement system (Parente et al., 2017). Functional analyses revealed that the cytokine-associated genes were predominantly expressed in the liver and the vast majority of them localized within intronic and intergenic regions suggesting that the identified variants primarily determine gene transcription or gene expression (Rose, 2019). Furthermore, gene-set analysis identified 41, mostly immunoregulatory, pathways that showed associations with a total of 13 cytokines. Integration with transcriptomic data identified 245 associations between gene expression and circulating cytokine levels, whereby 22% of gene transcripts exerted pleiotropic effects on up to 9 cytokines. Amongst other, I extended findings for key regulatory mechanisms by discovering additional cytokines affected by the scavenger receptor ACKR1 and TRAFD1-mediated signaling coming from TNF receptor activation (Ahola-Olli et al., 2017; Van Der Graaf et al., 2021; Zhao et al., 2023a). Applying MR, I detected 65 causal associations between circulating cytokines including a network of complex cytokine interconnections with TNF-b, VEGF, and IL-1ra exhibiting pleiotropic downstream effects. Drug target cis-MR focused at 15 diseases including allergic and autoimmune conditions, cardiometabolic phenotypes and cancer identified 11 causal associations, most of them involving autoimmune conditions. Follow-up analysis of the significant ones using colocalization revealed granulocyte colony-stimulating factor (G-CSF/CSF-3) and monokine induced by interferon-gamma (CXCL9/MIG) as potential causal mediators of asthma and CD, respectively, but also a potentially protective role of TNF-b in MS.

4.1 Cross-assay reproducibility

I utilized summary-level GWAS data from 3 distinct datasets, encompassing a total of 74,783 individuals, to investigate genetic associations with 40 circulating cytokines (Konieczny et al., 2024). These datasets included: the Cardiovascular Risk in Young Finns Study (YFS) and FINRISK studies, which utilized Luminex bead-based multiplex immunoassays to measure cytokines in serum (N=8,293); the Systematic and Combined Analysis of Olink Proteins (SCALLOP) study, employing the proximity extension assay-based Olink® platform to measure cytokines in plasma (N=30,931); and a dataset provided by deCODE, which employed the aptamer-based SOMAScan® assay to measure cytokines in plasma (N=35,559). Acknowledging the known differences in assay methodologies, I initiated the analysis by examining the replication rate of significant genetic variants detected within each dataset across the other 2 datasets (Eldjarn et al., 2023) (see

Figure 4.1a). Notably, although the GWAS conducted in the SCALLOP study yielded a lower number of genome-wide significant loci for the analyzed cytokines, these identified variants exhibited the highest reproducibility rate (with a significance threshold of p<5x10-5 and directional consistency) in the other 2 datasets, demonstrating a median reproducibility of 67% in YFS & FINRISK and 63% in deCODE (see **Figure 4.1b**). Conversely, variants detected as significant in the YFS & FINRISK dataset demonstrated a lower reproducibility rate (with a median of 4% in deCODE and 11% in SCALLOP), as did those from the deCODE dataset (with a median of 21% in YFS & FINRISK and 19% in SCALLOP). Of particular interest, monocyte specific cytokine 1 (CCL2/MCP-1) and vascular endothelial growth factor (VEGF) exhibited the highest relative proportion of reproducible single nucleotide polymorphisms (SNPs) across all 3 datasets, irrespective of the specific assay utilized for cytokine measurement.

4.2 GWAS reveals novel trans- and cis-acting variants

Following this, I conducted GWAS's using pooled data from 3 datasets (Konieczny et al., 2024). Through this comprehensive approach, I identified a total of 359 significant associations between genetic variants at 169 independent genomic loci and the circulating levels of one or more of the 40 cytokines (with a stringent significance threshold of $p<5\times10-8$ in fixed-effects analysis, see **Figure 4.2** and **Table A.1** in the appendix for a full list of significant variants). Notably, variants exhibiting significant heterogeneity among the 3 cohorts (indicated by a heterogeneity p-value < 0.1) are detailed in **Table A.2** in the appendix, encompassing 48% of the significant loci (with a range of 0% to 100% across the 40 cytokines). Additionally, to assess the robustness of my findings, I calculated lambda values, ranging between 0.96 for interleukin (IL)-16 and 1.04 for basic fibroblast growth factor (FGFb), indicating the absence of overall inflation in the test statistics (see **Table 4.1**). To contextualize my discoveries within the existing literature, I cross-referenced the identified loci with the GWAS catalogue (https://www.ebi.ac.uk/gwas/), revealing that 156 of these loci had not been previously associated with circulating levels of the 40 cytokines in previous GWAS (refer to **Table A.3** in the appendix). Furthermore, I evaluated the proportion of variance explained by the significant variants, which ranged from 0.0008 for interleukin-17 (IL-17) to 0.033 for stem cell growth factor beta (SCGF-b), providing insights into the genetic determinants influencing cytokine levels (see **Table A.1** in the appendix). Consistent with expectations arising from the larger effect sizes typically associated with rare genetic variants, my analysis revealed a robust inverse correlation between the minimum allele frequency and effect size (Spearman's rho=-0.827, p=5x10-30, as depicted in **Figure 4.3a**). Notably, the majority of the significant loci (150 out of 169) were represented by trans-acting variants,

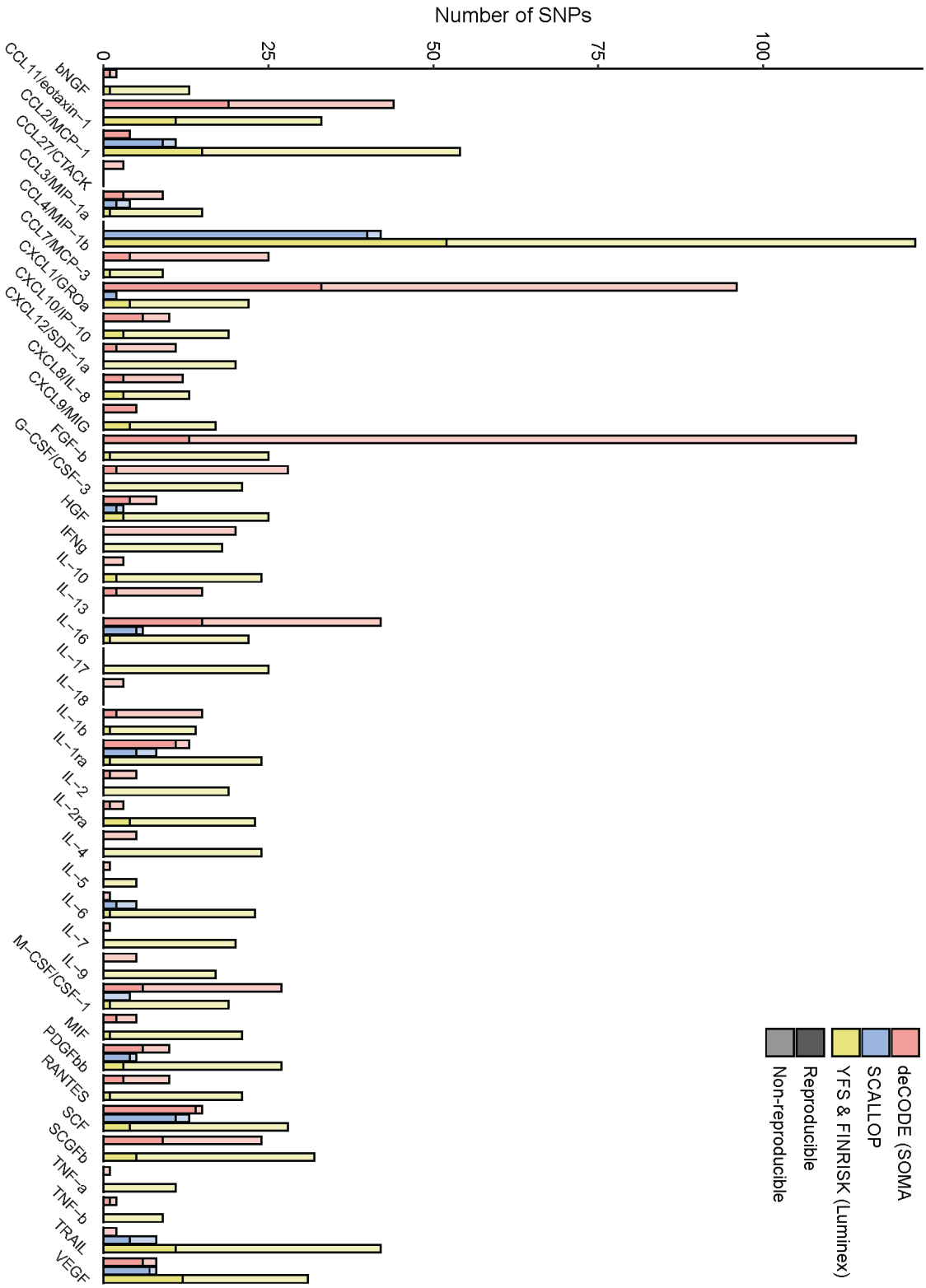

Figure 4.1a. Comparisons of significant genomic loci for 40 circulating cytokines across 3 proteomics assays. Number of reproducible and non-reproducible SNPs per cytokine (depicted as saturated and light-colored bars, respectively) for deCODE, SCALLOP and YFS & FINRISK cohorts. SNP, Single-nucleotide polymorphism; SCALLOP, Systematic and Combined AnaLysis of Olink Proteins; YFS & FINRISK, Cardiovascular Risk in Young Finns Study. Reprinted from Konieczny et al., 2024. medRxiv. 2024-04. CC-BY-NC-ND 4.0.

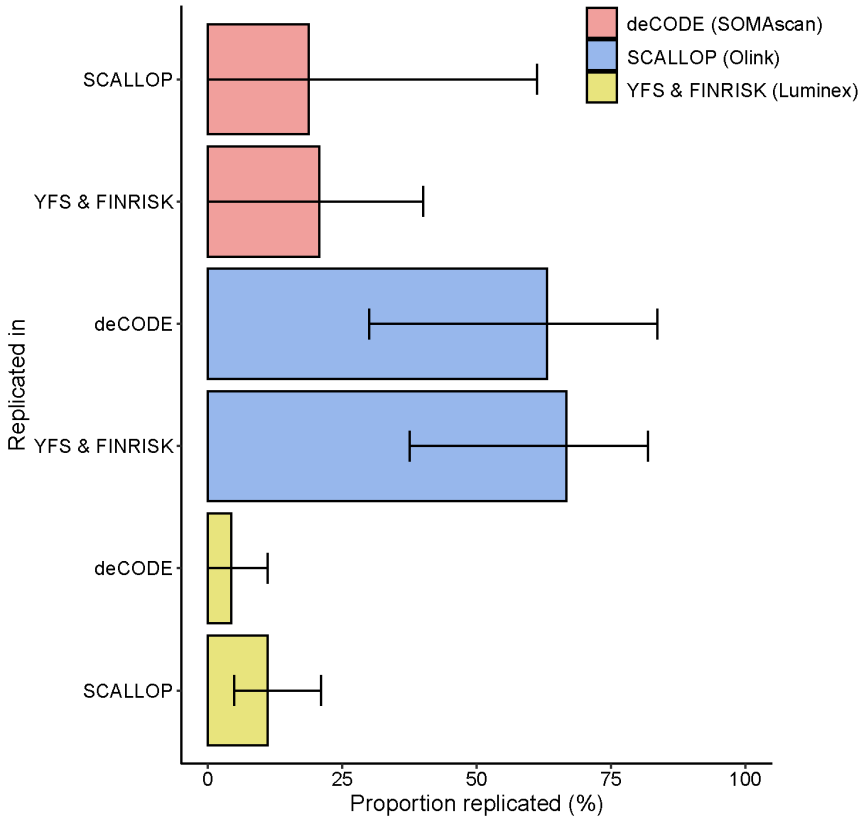

Figure 4.1b. Comparisons of significant genomic loci for 40 circulating cytokines across 3 proteomics assays. Median proportion of replicated SNPs across the 3 platforms (error bars represent the 25th and 75th percentiles). Colored bars represent deCODE consortium in red, SCALLOP consortium in blue and YFS & FINRISK cohorts in yellow. SNP, Single-nucleotide polymorphism; SCALLOP, Systematic and Combined AnaLysis of Olink Proteins; YFS & FINRISK, Cardiovascular Risk in Young Finns Study. Reprinted from Konieczny et al., 2024. medRxiv. 2024-04. CC-BY-NC-ND 4.0.

indicating their influence on cytokine regulation from distant genomic positions. Manhattan plots for each cytokine are provided in the appendix (**Figure A.1**). Upon exclusion of the human leukocyte antigen (HLA) region on chromosome 6, I identified 33 pleiotropic variants exhibiting associations with more than one cytokine among the significant trans-acting variants (refer to **Figure 4.3b**). Notably, a locus hotspot, prominently featuring associations with multiple cytokines, was identified within the gene region encoding complement factor H (CFH). This soluble mediator plays a pivotal role in regulating inflammatory responses mediated by the complement system, providing a plausible mechanism underlying its associations with multiple cytokines (Parente et al., 2017). Residing within CFH the pleiotropic variants rs1329424 and rs12127759 showed associations with 9 and 3 cytokines, respectively (rs1329424 associated with cutaneous T-cell attracting [CTACK/CCL27], interleukin-4 [IL-4], interleukin-5 [IL-5], interleukin-7 [IL-7], interleukin-10 [IL-10], interleukin-17 [IL-17], tumor necrosis factor-alpha [TNF-a], tumor necrosis factor-beta [TNF-b], TRAIL; rs12127759 associated with IFN-g, interleukin-8 [IL-8], interleukin-13 [IL-13]). Furthermore, while at least one significant trans-acting variant was observed for all studied cytokines (with a median number of 5 variants

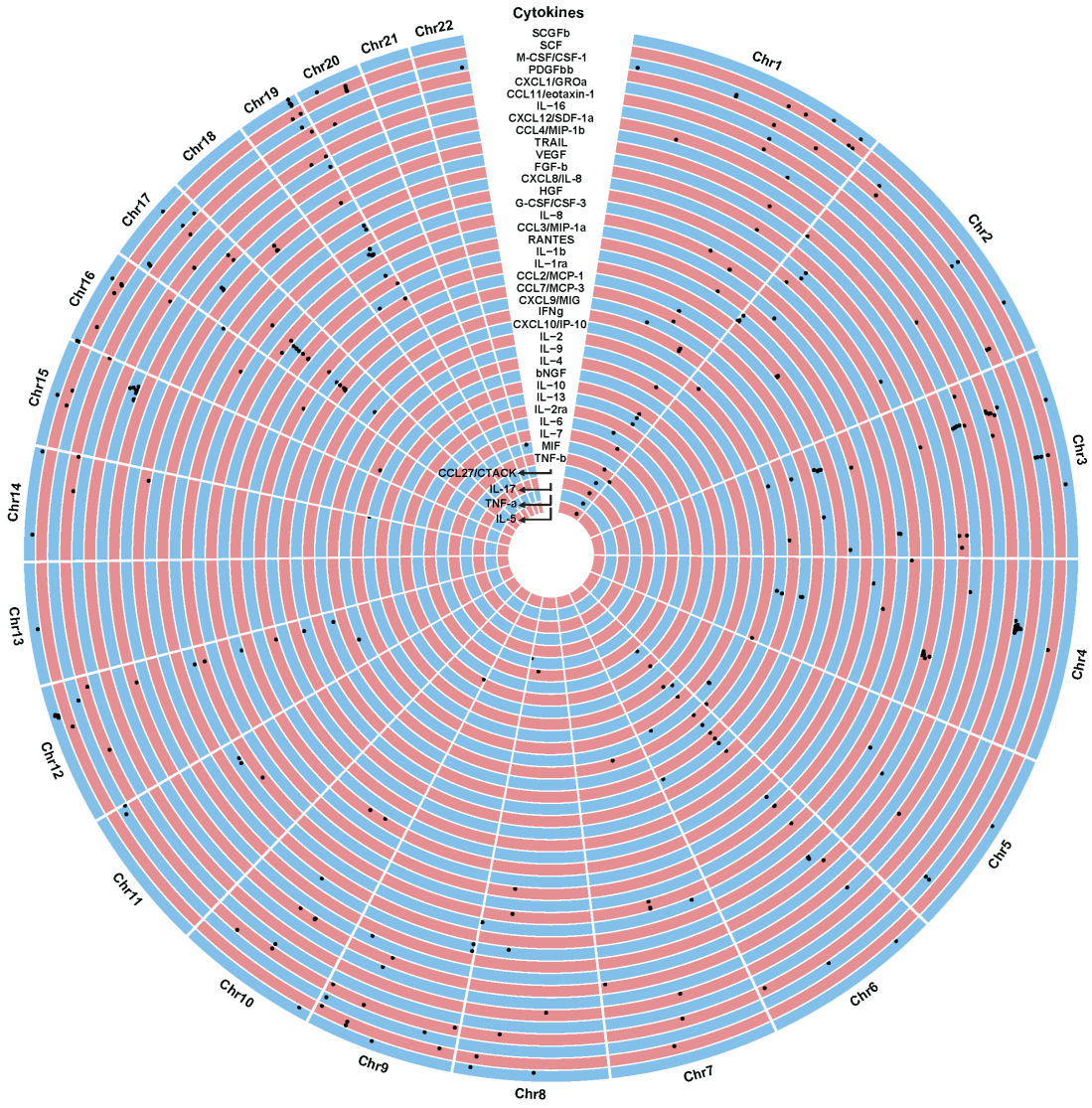

Figure 4.2. Genetic architecture of the circulating levels of the 40 cytokines. Circular Manhattan plot of genomic loci significantly associated with circulating levels of 40 cytokines. The 359 genome-wide significantly associated variants at $p < 5x10{-}8$ are depicted as black dots for the pooled data from YFS & FINRISK, SCALLOP, and deCODE cohorts. The horizontal and vertical location of dots in each single rectangle signify genomic positioning (increasing from left to right) and p-value (decreasing from bottom to top), respectively. SCALLOP, Systematic and Combined AnaLysis of Olink Proteins; YFS & FINRISK, Cardiovascular Risk in Young Finns Study; Chr, chromosome. Reprinted from Konieczny et al., 2024. medRxiv. 2024-04. CC-BY-NC-ND 4.0.

per cytokine, ranging from 1 to 22), I also detected significant cis-acting variants proximal to the encoding gene for 19 cytokines (**see Table 4.1**). Examples of multi-locus-regulated cytokines with a predominance of trans loci were stem cell factor (SCF, n_{trans}=26, n_{cis}=1), macrophage colony-stimulating factor (MCSF, n_{trans}=25, n_{cis}=4), platelet growth factor beta (PDGFb, n_{trans}=21, n_{cis}=1), cytokines with a predominance of cis loci were VEGF (n_{trans}=13, n_{cis}=66), GROa (n_{trans}=17, n_{cis}=57), and MCP3 (n_{trans}=8, n_{cis}=53). Multi-locus-regulated cytokines that showed similar numbers of trans and cis

Cytokine	Lambda	Frequency
bNGF	1,01	2
CCL27/CTACK	1,01	1
CCL11/eotaxin-1	1,03	12
FGF-b	1,04	5
G-CSF/CSF-3	0,99	3
CXCL1/GROa	1,02	7
HGF	1,01	9
IFNg	1,01	9
IL-10	1,00	2
IL-13	1,00	1
IL-16	0,96	11
IL-17	1,02	1
IL-18	1,01	8
IL-1b	0,98	4
IL-1ra	1,03	5
IL-2	1,02	5
IL-2ra	1,01	1
IL-4	1,01	3
IL-5	1,00	1
IL-6	1,02	2
IL-7	1,01	2
CXCL8/IL-8	1,01	7
IL-9	1,03	3
CXCL10/IP-10	1,01	5
M-CSF/CSF-1	1,00	17
CCL2/MCP-1	1,01	5
CCL7/MCP-3	1,02	4
MIF	1,01	1
CXCL9/MIG	1,01	6
CCL3/MIP-1a	1,00	6
CCL4/MIP-1b	1,00	4
PDGFbb	1,02	20
RANTES	1,02	6
SCF	1,00	20
SCGF-b	1,00	22
CXCL12/SDF-1a	1,00	11
TNF-a	1,01	1
TNF-b	1,02	2
TRAIL	1,01	8
VEGF	0,99	6

Table 4.1. Genomic inflation and pleiotropy. This table shows the genomic lambda values (signifying an inflation of the test statistics with increasing deviation from 1), and the number of associated variants for individual cytokines.

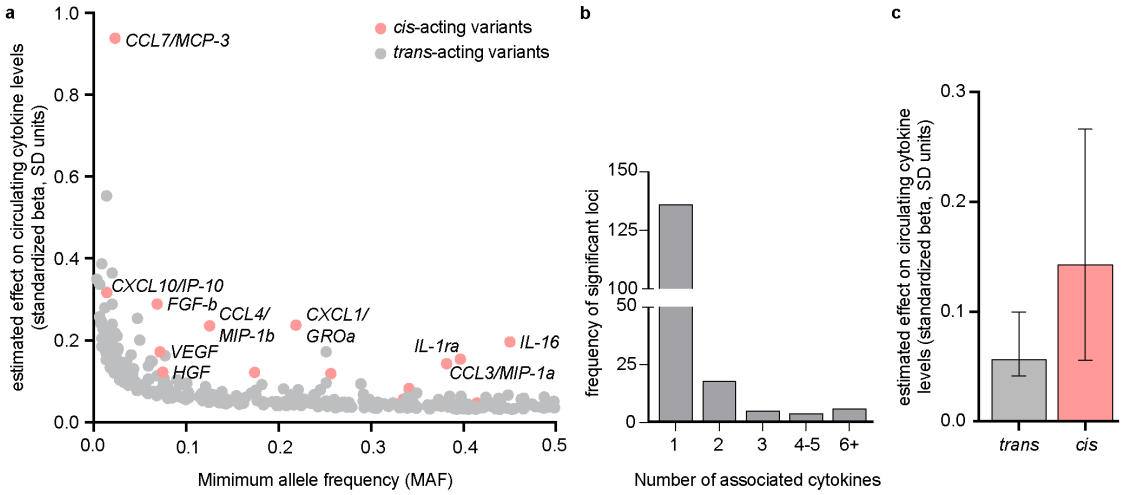

Figure 4.2 Trans- and cis-acting genetic variants underlying circulating cytokines. (a) Inverse correlation between minimum allele frequency and effect size illustrated for trans- and cis-acting loci. (b) Number of pleiotropic loci associated with circulating cytokines (excluding the HLA region on chromosome 6). (c) Cis-acting variants showed stronger associations with cytokine levels when compared with trans-acting variants. Bars and lines represent median and 95% confidence intervals, respectively. HLA, human leukocyte antigen; SD, standard deviation. Reprinted from Konieczny et al., 2024. medRxiv. 2024-04. CC-BY-NC-ND 4.0.

loci were stem cell growth factor beta (SCGFb, n_{trans}=32, n_{cis}=27), SDF1a (n_{trans}=14, n_{cis}=17) and RANTES (n_{trans}=9, n_{cis}=12). Impressively, lead cis-acting variants exhibited stronger associations with cytokine levels (with a mean absolute beta of 0.18, ranging from 0.05 to 0.94) compared to trans-acting variants (with a mean absolute beta of 0.08, ranging from 0.03 to 0.55, p-for-comparison=0.03, see **Figure 4.3c**). Further specifying the distance of the cis-loci to their associated cytokine genomic location I looked at the lead loci (defined as locus with the smallest p-value for each of the cytokines). I found 6 lead loci located 100 Kb around the genes of the cytokines, another 11 lead loci at 50 Kb around the genes and 2 lead loci within the genetic location. To elucidate the causal variants underlying the associations between serum cytokine levels and genes within each of the 169 independent genomic loci, I employed SuSiE fine mapping. This approach utilizes a Bayesian framework to pinpoint credible sets of variants with a posterior probability of association (PPA) of 95%. Across the loci examined, the number of variants within these credible sets ranged from 2 to 50. Remarkably, some loci exhibited a substantial number of variants within their credible sets. Notably, the highest counts were observed at 15q21.3 for stem cell factor (SCF) (n=50), at 19q13.33 for SCGF-b (n=49),

and at 6p21.1 for VEGF (n=44). SuSiE effectively mapped the association test lead variant to the credible sets for 49 genomic loci, indicating that the GWAS lead variants were the most probable causal mutations.

4.3 Functional follow-up analyses highlight immune response regulatory mechanisms

To delve deeper into the biological significance and downstream functional implications of the identified variants, I conducted comprehensive follow-up analyses (Konieczny et al., 2024). Utilizing a MAGMA gene-based analysis, I uncovered 829 significant associations with the levels of circulating cytokines, reaching a significance level defined by Bonferroni correction (detailed in **Table A.4** in the appendix). Remarkably, these associations were linked to 626 uniquely mapped genes, each associated with at least one cytokine. The breadth of gene involvement varied widely across cytokines, ranging from 1 gene for beta nerve growth factor (bNGF), cutaneous T-cell attracting (CCL27/CTACK), IL-10, and tumor necrosis factor-alpha (TNF-a), to as many as 95 genes mapped for SCF, 92 genes for macrophage inflammatory protein-1b (CCL4/MIP-1b), and 51 genes for CCL11/eotaxin-1. Notably, in line with my GWAS results, described above, the abundance of cytokines associated with the CFH gene (n=16) agrees with its function as modulator of the C3 convertase which is a key regulator of downstream inflammatory response of the complement system (Parente et al., 2017). Further analysis revealed genes with exceptionally low p-values, including H4C14 for monocyte specific chemokine 3 (CCL7/MCP-3) ($p=1\times10-50$), DBA4 for interleukin-16 (IL-16) ($p=1.3\times10-45$), and ABC1 for SCF ($p=1.9\times10-29$). Moreover, a gene-property analysis unveiled that cytokine-related genes were predominantly enriched for expression in the liver ($p=4.9\times10-10$), consistent with its established role as a primary source of many cytokines. Additionally, enriched tissues included the spleen ($p=4.9\times10-4$) and lung ($p=5.9\times10-4$, see **Figure 4.4**). In tandem with these findings, a MAGMA gene-set analysis highlighted 41 pathways significantly associated with 13 cytokines, surpassing the Bonferroni-adjusted significance threshold ($p<1.2x10-7$, detailed in **Figure 4.5**). Out of these significant associations 10 cytokines mapped to 33 immunoregulatory pathways, most of them involved in chemokine regulation and antigen-related processes. The remaining pathways revolved around metabolic and developmental processes. My gene-set analysis highlights on the interplay between genetic variants and cytokine regulation and offers insights into the underlying mechanisms driving immune responses. Positional mapping revealed that 79% of significant variants were localized within intronic (54%) and intergenic (25%) regions, indicating their potential roles in modulating gene transcription or gene expression profiles (see **Figure 4.6**) (Rose, 2019). This observation prompted me to integrate the GWAS findings with transcriptomic data, leading to the

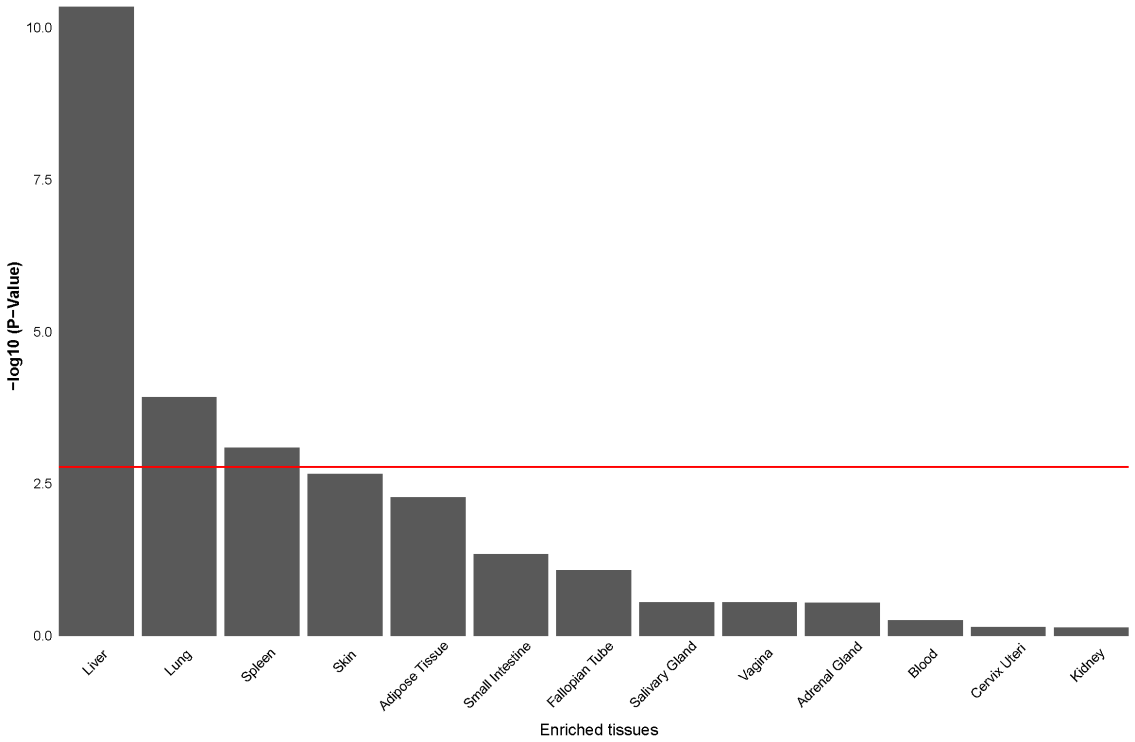

Figure 4.3 Gene property analysis reveals enriched tissues. Tissues that turned-out significant for expression of cytokine-related genes included the liver, spleen and lung. Individual tissues are depicted by separate bars. The red horizontal bar signifies the Bonferroni-corrected significance level.

execution of a TWAS - MR analysis and enabling a deeper exploration of the transcriptional effects underlying my GWAS results. To analyze the gene expression profile associated with my GWAS results, I conducted TWAS-MR analysis utilizing cis-eQTLs as genetic instruments. I identified 245 significant associations between genetically proxied gene expression in whole blood and cytokine levels (refer to **Figure 4.7** and **Table A.5** in the appendix). The number of significant genes associated with each cytokine ranged from 1 to 18. Herein, the cytokine concentration that were influenced by a multitude of different genes were found for SCGF-b (n=18) but also for SCF (n=17), M-CSF (n=16), PDGFbb (n=15), and IL-8 (n=15). Remarkably, while the majority of significant genes (78%) exerted an influence on the levels of a single cytokine, the genetically proxied expression of 54 genes demonstrated effects on circulating levels of up to 9 cytokines. Notably, these genes included SKIV2L (n=9), HLA-DRB5 (n=9), NELFE (n=7), ACKR1 (n=5), FCER1A (n=4), TRAFD1 (n=4), and LCMT2 (n=4). Interestingly, I observed significant cis-effects of the encoding gene expressions on the circulating levels of only 3 out of the 40 respective cytokines. This finding aligns with previous comparisons between eQTLs and pQTLs, indicating that the circulating proteome is not directly dictated by the whole-blood transcriptome (GTEx Consortium, 2020; Zhao et al., 2023b). Upon exclusion of genes within the densely packed HLA region (e.g., SKIV2L, HLA-DRB5, and NELFE), I delved deeper into the biological

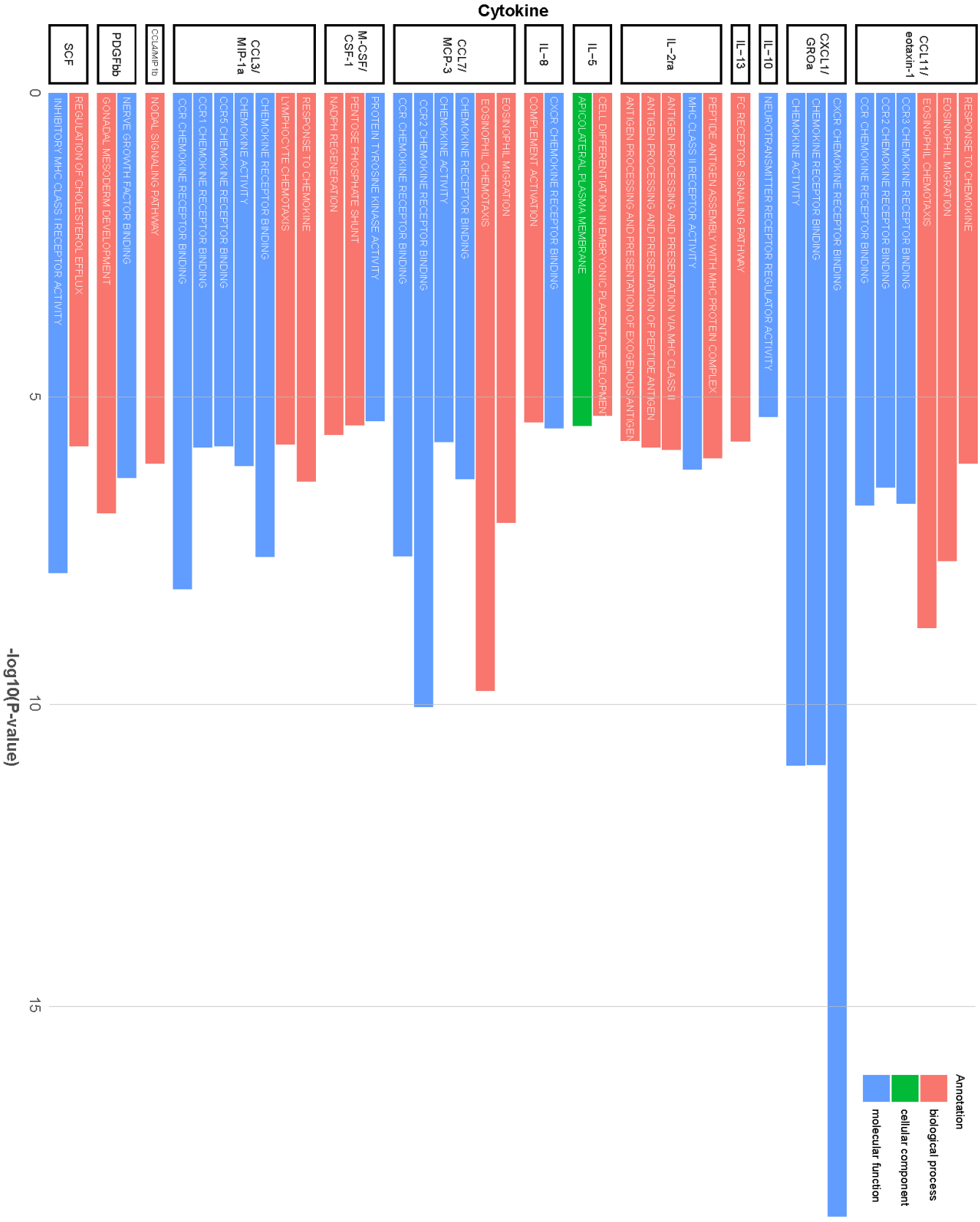

Figure 4.5. Gene-set analysis confirms predominance of immunoregulatory pathways. MAGMA highlighted 41 pathways associated with 13 cytokine related genes, 33 of them involved in immune responses. The rectangles on the left show the cytokines underlying the respective gene pathways aligned on their right side. Pathways are color-coded, with red depicting biological processes, green showing cellular components, and blue signifying molecular mechanisms.

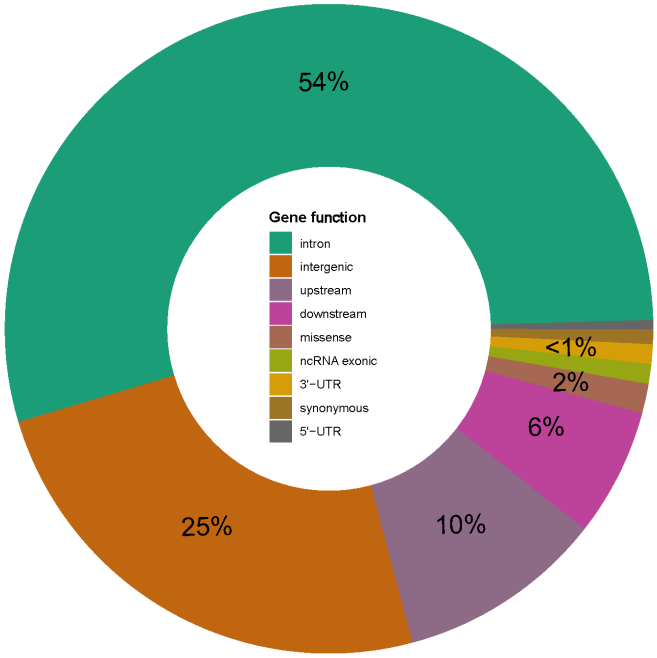

Figure 4.6. Functional significance of cytokine-related variants. The pie-chart visualizes the functional consequences, with 79% of variants determining gene transcription or gene expression (i.e. being located in intronic and intergenic regions), 16% mapped to up- or downstream regions and 2% being located in missense locations. Gene functions are color cod-ed, with green depicting variants in intronic regions, orange depicting variants in intergenic regions, dark violet depicting variants upstream of the respective genes, violet depicting variants downstream of the respective genes, brown depicting missense variants, light green depicting variants in non-coding RNA exonic regions, yellow depicting variants in the 3' untranslated region of the respective genes, dark brown depicting variants in synonymous regions, dark grey depicting variants in the 5' untranslated region of the respective genes.

significance of the pleiotropic genes ACKR1, TRAFD1, and LCMT2. The genetically proxied mRNA levels of ACKR1 exhibited associations with circulating levels of CCL2/MCP-1, CCL7/MCP-3, CCL11/eotaxin-1, growth regulated oncogene-alpha (CXCL1/GROa), and CXCL8/IL-8. ACKR1 encodes a cell-surface receptor known for binding, internalizing, and transporting multiple CC and CXC chemokines, thus facilitating leukocyte transcytosis into the circulation (Korbecki et al., 2022; Schnabel et al., 2010). Acting as a scavenger receptor, ACKR1 modulates cytokine bioavailability, thereby impacting inflammatory responses (Crawford and Volkman, 2023; Szpakowska et al., 2023). The associations identified were predominantly driven by rs12075, a well-characterized missense variant in ACKR1, leading to less efficient chemokine binding due to the loss of a necessary amino acid-sulfation (refer to **Figure 4.8**) (Jiménez-Sousa et al., 2019). This impaired receptor binding results in elevated circulatory chemokine levels, potentially prompting a compensatory increase in ACKR1 expression, thus explaining the positive association between genetically proxied ACKR1 and its ligands (Chen et al., 2020). I replicated previously reported associations between ACKR1

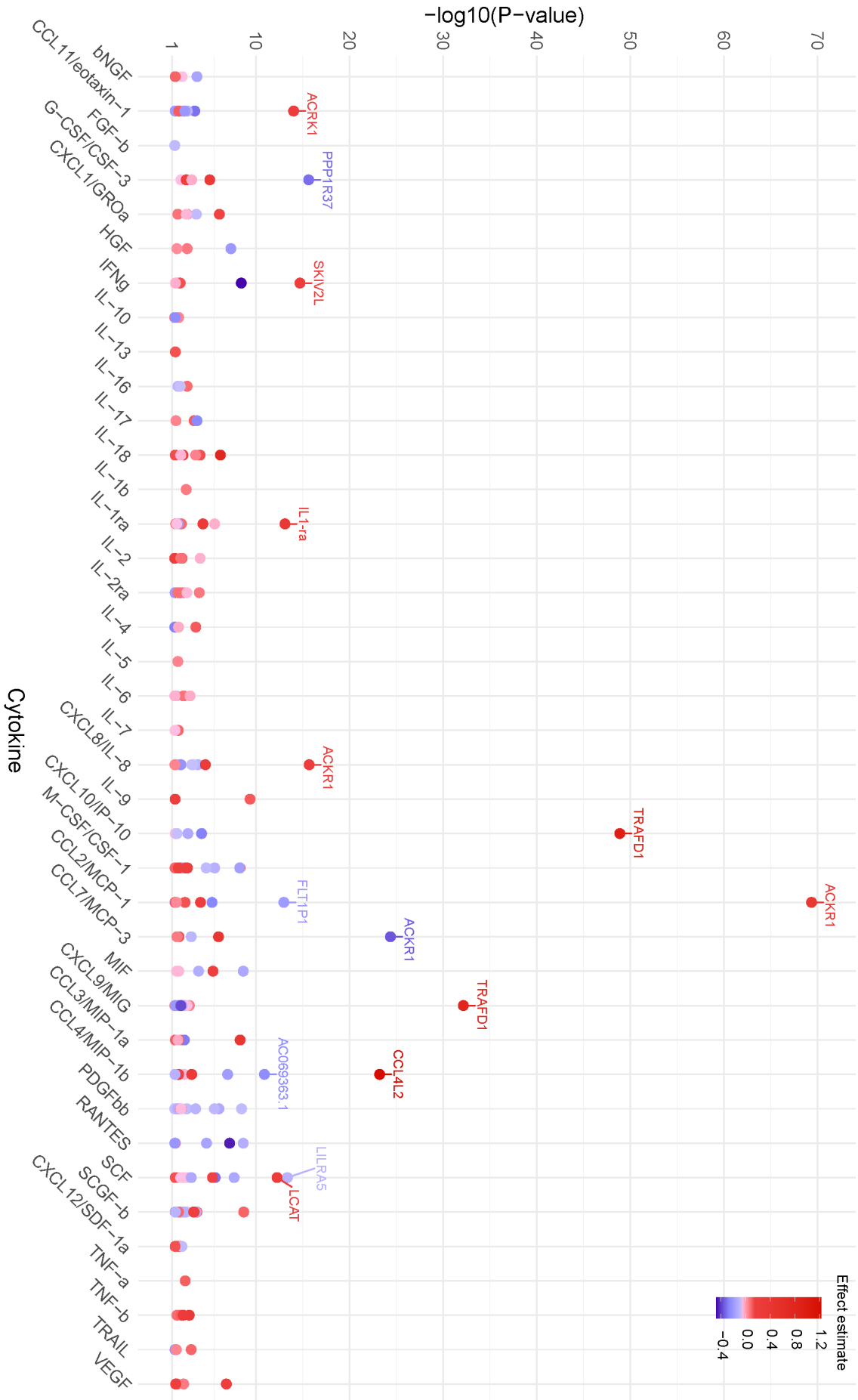

Figure 4.7. Genetically predicted gene expression in peripheral blood partly explains the genetic architecture of 40 circulating cytokine levels. The dots represent genes, the blood expression of which was significantly associated with circulating cytokine levels in a Mendelian randomization-based transcriptome-wide association study. Reprinted from Konieczny et al., 2024. medRxiv. 2024-04. CC-BY-NC-ND 4.0.

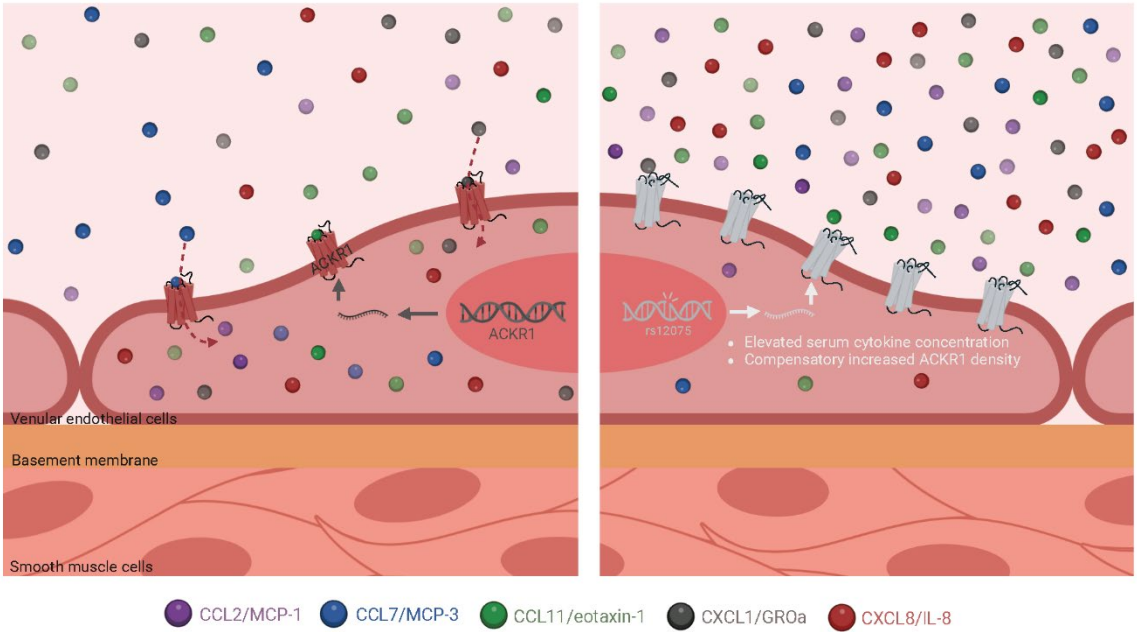

Figure 4.8. Gene expression of ACKR1 exerts pleiotropic effects on multiple cytokine levels. Schematic illustrating the impact of cis-eQTLs for ACKR1 on receptor function. Left hand side shows ACKR1 gene encoding the atypical chemokine receptor 1 functioning as sink for multiple chemokines which are buffered intracellularly in venular endothelial cells. Depicted on the right, is the missense variant rs12075 coding for a dysfunctional receptor with less efficient chemokine binding efficacy. This leads to higher levels of circulating CCL2/MCP-1, CCL7/MCP-3, CCL11/eotaxin-1, CXCL1/GROa, and CXCL8/IL-8 and possibly to a compensatory increase in ACKR1 expression and receptor density. ACKR1, atypical chemokine receptor 1. eQTL, expression quantitative trait loci. Reprinted from Konieczny et al., 2024. medRxiv. 2024-04. CC-BY-NC-ND 4.0.

and levels of CCL2/MCP-1, CCL7/MCP-3, CCL11/eotaxin-1, and CXCL1/GRO-a, while additionally demonstrating an association with CXCL8/IL-8 levels (Ahola-Olli et al., 2017; Zhao et al., 2023b). Similarly, genetically proxied expression of tumor necrosis factor receptor-associated factor 1 (TRAFD1) was linked to multiple circulating cytokine levels, including CCL7/MCP-3, CXCL9/MIG, interferon gamma-induced protein 10 (CXCL10/IP-10), and tumor necrosis factor-beta (TNF-b) (refer to **Figure 4.9**). TRAFD1 serves as an adaptor protein binding to the intracellular domain of TNF receptors on innate and adaptive immune cells. It regulates downstream signaling, particularly involving the nuclear factor 'kappa-light-chain-enhancer' of activated B-cells pathway (NF-kB), thereby modulating the production of several pro-inflammatory cytokines and inflammatory responses (Lalani et al., 2018; Park, 2021; Takechi et al., 2016). Moreover, TRAFD1 is a pivotal regulator of genes involved in interferon-g (IFN-g) signaling and T-cell receptor activation (Van Der Graaf et al., 2021). Additionally, genetically proxied expression of the gene encoding for LCMT2 displayed associations with bNGF, CXCL8/IL-8, CXCL10/IP-10, and platelet-derived growth factor-bb (PDGFbb). LCMT2's involvement in amino acid metabolism suggests a role in regulating hypothalamic gene expression, although limited information exists regarding its biological function (Fantus et al., 2021; Gao et al., 2020).

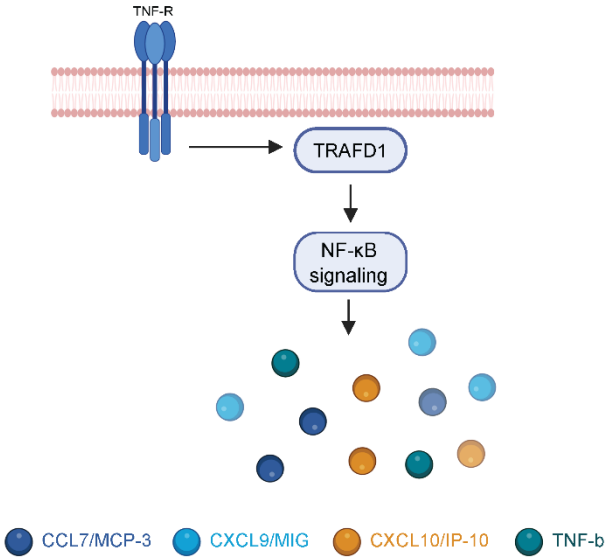

Figure 4.9. Gene expression of TRAFD1 exerts pleiotropic effects on multiple cytokine levels. Schematic illustrating how genetically proxied TRAFD1 expression regulates multiple cytokine levels (CCL7/MCP-3, CXCL9/MIG, CXCL10/IP-10, TNF-b), supporting its regulatory role in TNF-mediated NF-κB signaling. TNF-R, TNF-receptor; NF-κB, nuclear factor 'kappa-light-chain-enhancer' of activated B-cells. Reprinted from Konieczny et al., 2024. medRxiv. 2024-04. CC-BY-NC-ND 4.0.

4.4 Genetic associations point to network interactions between circulating cytokines

Moving forward, I delved into the cross-trait genetic correlations among the circulating levels of the 40 studied cytokines (refer to **Figure 4.10**). Notably, one third of these correlations reached significance at $p<0.05$, with the vast majority (96%) being positive associations. To unravel the causal interconnections between circulating cytokine levels, I conducted MR analysis utilizing cis-variants identified from my GWAS analysis. This analysis revealed significant associations between 65 pairs of cytokines, comprising 53 positive associations and 12 negative associations (see **Figure 4.11** and **Table A.6** in the appendix). Remarkably, genetically proxied levels of certain cytokines — namely, CCL7/MCP-3, stromal cell-derived factor-1alpha (CXCL12/SDF-1a), granulocyte colony-stimulating factor (G-CSF), interleukin-9 (IL-9), tumor necrosis factor-beta (TNF-b), and VEGF — were positively associated with the levels of more than 2 other cytokines. Conversely, genetically proxied levels of CXCL1/GROa and IL-1ra were negatively associated with lower levels of more than 2 other cytokines. Noteworthy significant associations were detected particularly for TNF-b (n=13), VEGF (n=9), IL-1ra (n=7), IL-9 (n=7), and G-CSF (n=7). The pleiotropic effects of VEGF on 9 other cytokines (GROa, HGF, IL-1ra, IL-8, M-CSF, MCP-1, MCP-3, RANTES, TNF-a) might be explained because of the highly pleiotropic cis-acting variants rs3025020 and rs699947 at 6p21.1. A search for the VEGFA gene conducted at the GWAS catalogue confirmed associations with 3 cytokines (IL-1ra, IL-8, TNF-a). A Previous GWAS study already

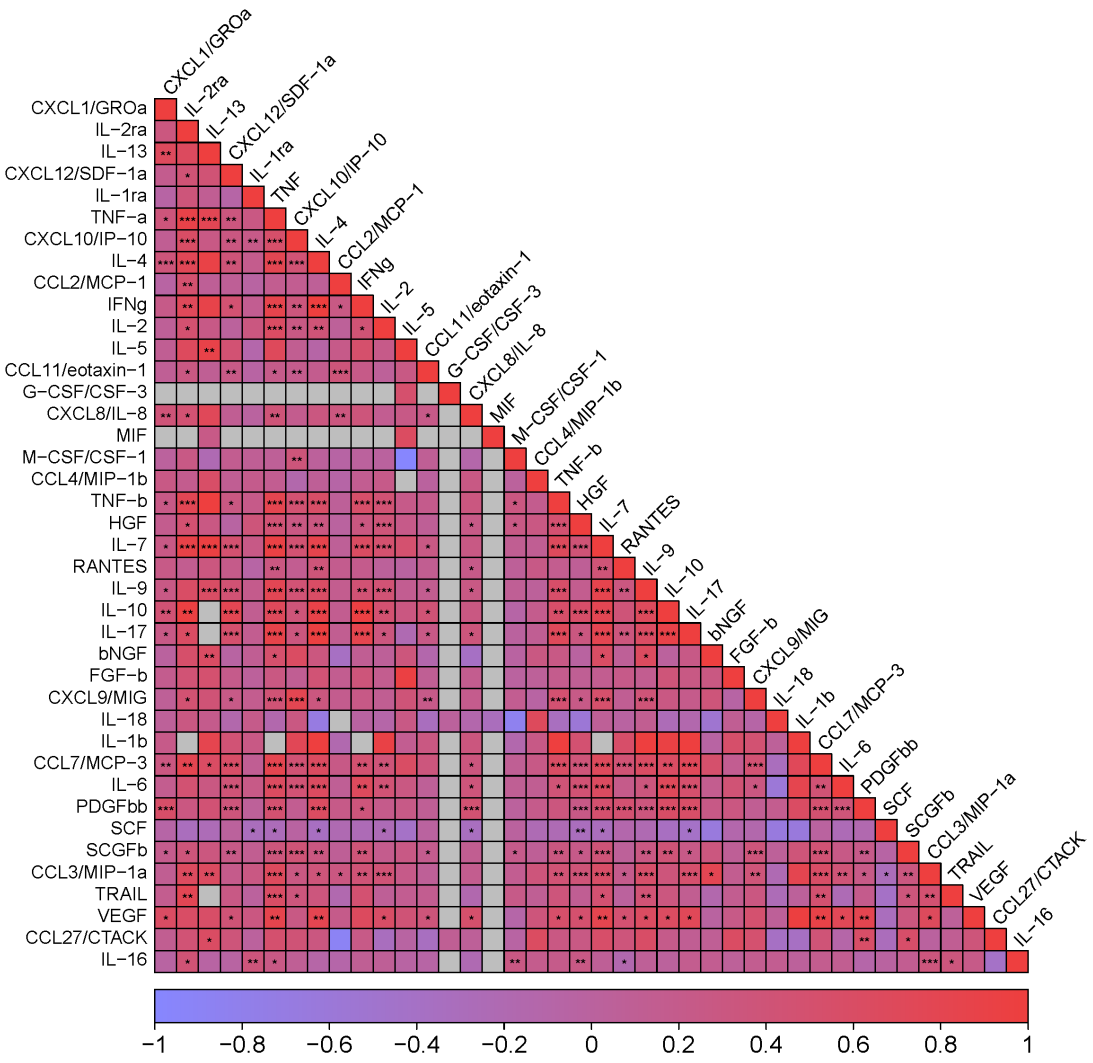

Figure 4.10. LDSC heatmap showing cross-cytokine associations. Genetic correlations with LD-score regression across cytokine serum levels are depicted as correlation heatmap. Stars highlight significance level *, 0.05; **, 0.0001; ***, 0.00001. LD-score correlation coefficients are illustrated according to the legend below spanning from -1 in blue to +1 in red, missing correlation coefficients are depicted in grey. LD, linkage disequilibrium. Reprinted from Konieczny et al., 2024. medRxiv. 2024-04. CC-BY-NC-ND 4.0.

hypothesized about a regulatory mechanism for VEGF on 4 other cytokines (Ahola-Olli et al., 2017). I can confirm these results and add more downstream targets affected by VEGF. The negative associations observed between IL-1ra and several proinflammatory cytokines (CCL7/MCP-3, IL-9, TNF-a, TNF-b), chemokines (macrophage inflammatory protein-1a, CCL3/MIP-1a), and growth factors (hepatocyte growth factor, HGF; VEGF), align well with the immunoregulatory role of the IL-1 pathway and the inhibitory effect of IL-1ra on downstream IL-1 signaling pathways (Basu et al., 2004; Boersma et al., 2021). Of significance, TNF-b emerged as a pivotal player in the network analysis, showcasing characteristics of a master regulator by exhibiting significant associations with higher circulating levels of 13 mostly pro-inflammatory cytokines (bNGF, GROa, IL-1ra, IL-2ra, IL-9, IL-16, MCP-3, MIG, MIP-1a, SCGF-b, TNF-a, TRAIL, VEGF) which might be explained by the variant rs4947328 located at 6p21.33 and coding for the

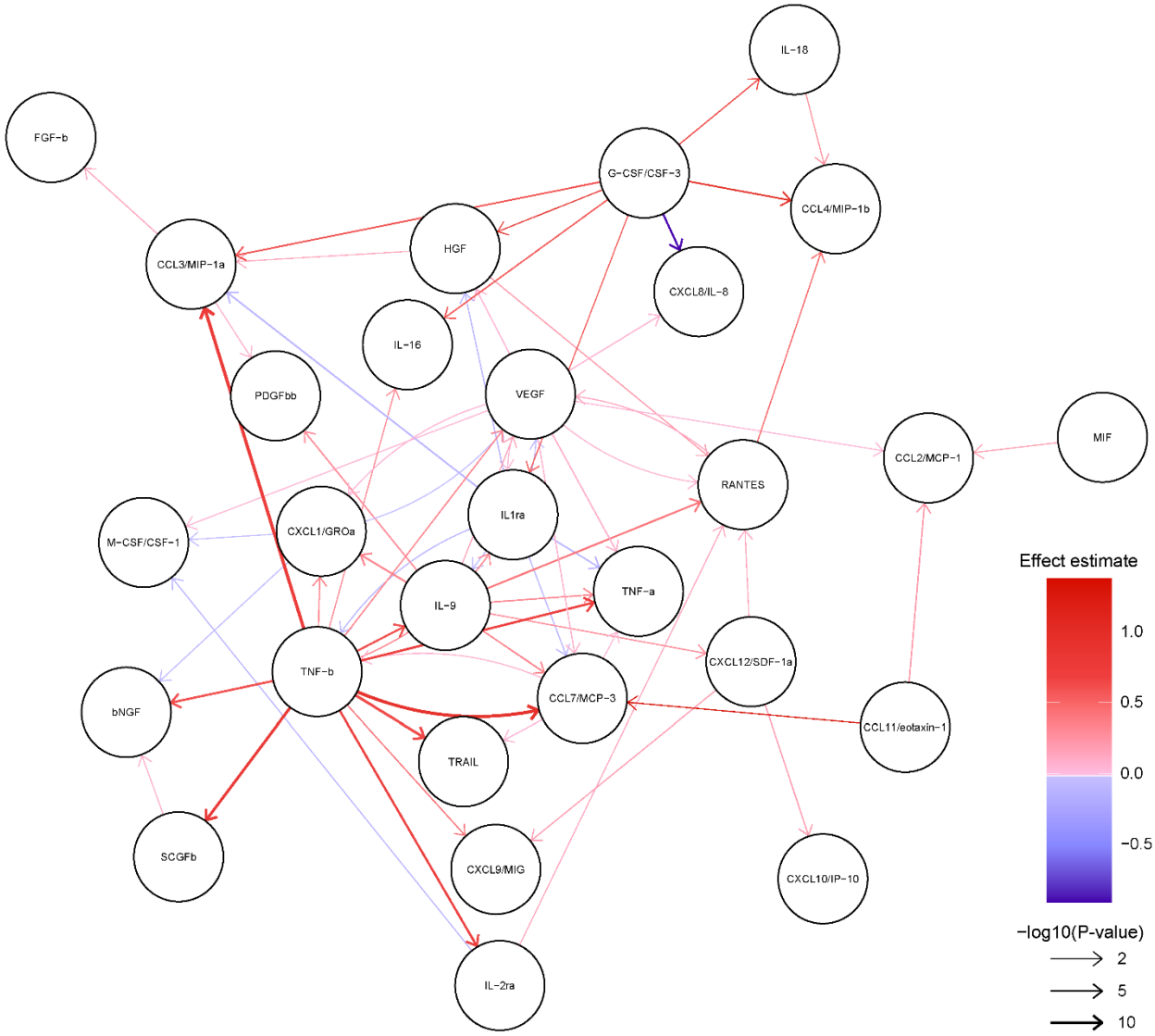

Figure 4.11. Cross-cytokine MR reveals network structure. Cis-Mendelian randomization between genetically proxied circulating cytokine levels identified TNF-b, VEGF and IL-1ra as master regulator. Arrow heads show the direction of causal influence, color gradient indicates the effect estimate and line width the logarithm-adjusted Benjamin-Hochberg corrected significance level. Reprinted from Konieczny et al., 2024. medRxiv. 2024-04. CC-BY-NC-ND 4.0.

natural cytotoxicity triggering receptor 3 (NCR). NCR's are expressed on natural killer (NK) cells, they have multiple ligands (e.g. IL-2 for activation of resting NK cells) and are key regulators of NK cell cytotoxicity (e.g. via TRAIL for induction of apoptosis in tumor cells) and of the cytokine secretion profile of NK cells (e.g. TNF-a, MIP-1a, IL-9) (Barrow et al., 2019). Due to the role TNF-b has for differentiation and recruitment of NK cells it indirectly modulates cytokine concentrations in serum (Calmon-Hamaty et al., 2011). Moreover, TNF-b displayed significant positive LDSC genetic correlations with 7 of the 13 cytokines, indicating a shared genetic architecture within the TNF-b network (**Figure 4.10**). While certain interactions with TNF-b have been well-documented, such as those involving IL-1ra, TNF-a, TNF-related apoptosis-inducing ligand (TRAIL), and VEGF, the majority of interactions have not been previously reported and warrants

further investigation (Daniel and Wilson, 2008; Ding et al., 2016; Okada and Kawada, 1987).

4.5 Cis-Mendelian randomization and colocalization highlight potential drug targets for immune-related diseases

To gain insights into the clinical implications of genetically influenced levels of circulating cytokines, I analyzed associations with allergic and autoimmune, cardiometabolic, and cancer outcomes using drug-target two-sample MR followed by colocalization analyses (see **Figure 4.12** and **Table A.7** in the appendix) (Konieczny et al., 2024). In this analysis, I employed cis-acting genetic variants as instruments, given their lower likelihood of influencing cytokine levels through pleiotropic mechanisms. Additionally, I complemented these analyses with Bayesian colocalization to prioritize associations less susceptible to pleiotropy resulting from LD with neighboring genes (Zuber et al., 2022). Following correction for multiple comparisons, I identified 24 significant MR associations between genetically influenced cytokine levels and disease outcomes, comprising 14 positive and 10 negative associations. Notably, my MR findings provided partial confirmation of established pathogenetic associations with diseases and therapeutic drug targets already in clinical application. For instance, solid evidence links variants increasing IL-2ra to elevated risks for MS and CD (Ahola-Olli et al., 2017). Aldesleukin, a recombinant form of IL-2 approved for cancer indications, is currently under investigation in a phase-2 clinical trial for CD (ClinicalTrials.gov ID: NCT04263831) (Allegretti et al., 2023). Similarly, compounds targeting IL-1 signaling, such as anakinra or canakinumab, represent established treatment strategies for inflammatory joint diseases like RA or juvenile arthritis (Bedaiwi et al., 2021; Shaul et al., 2022). These findings underscore the clinical relevance of genetically influenced cytokine levels and highlight potential therapeutic avenues for various diseases. Out of the 24 signals identified, four also exhibited evidence of significant colocalization, indicating a PPA greater than 80% for shared causal variants between cytokine levels and disease outcomes (refer to **Figure 4.12** and **Table 4.2**). This strengthened the evidence for causality in these 4 cytokine-disease pairs. These noteworthy associations included higher genetically influenced levels of G-CSF being linked to asthma, lower genetically influenced G-CSF levels and higher genetically influenced levels of CXCL9/MIG being associated with CD, and lower genetically influenced TNF-b levels being associated with MS. Additionally, the association between genetically influenced IL-1ra levels and a decreased risk of RA reached a PPA of 68% in colocalization analysis. These findings align with data from preclinical studies (Kwak et al., 2022; Ouyang et al., 2020; H. Wang et al., 2019), observational studies in humans (Åkesson et al., 2023; Hojjati et al., 2023; Huang et al., 2020; Romme Christensen et al., 2012; Walshe et al., 2022), and clinical

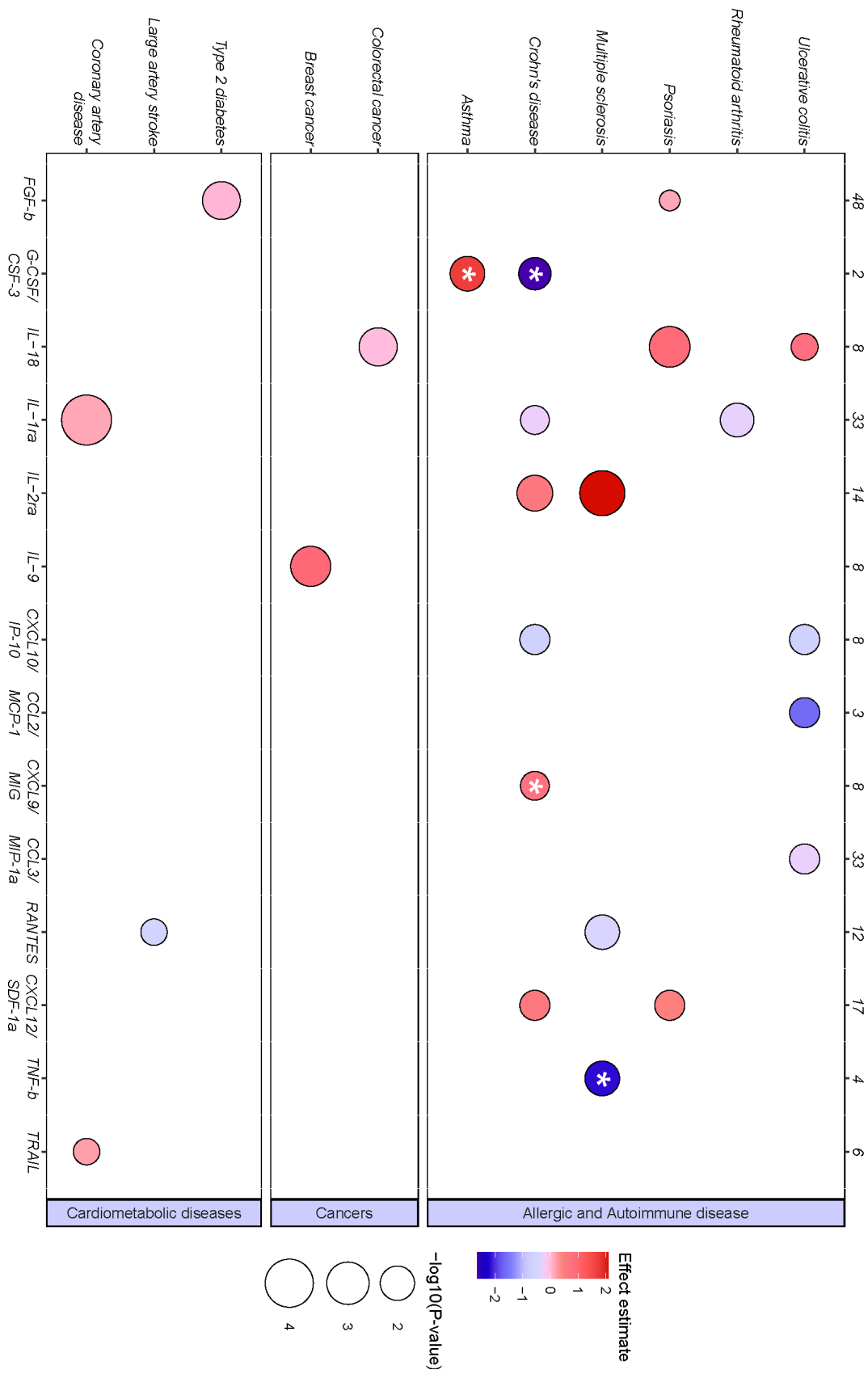

Figure 4.12. *Cis*-Mendelian randomization associations and colocalization analyses between genetically proxied cytokine levels and disease risk. Significant associations between circulating cytokine levels and disease outcomes are shown for allergic and autoimmune, cardiometabolic, and cancer outcomes. Effect sizes and log-transformed, Benjamin-Hochberg corrected p-values are illustrated by color gradient and circle size, respectively. Only cytokines and disease endpoints with at least 1 significant association are depicted. Numbers at the top indicate average number of *cis*-acting genetic variants used as instruments in MR analyses. Stars highlight significant genetic colocalization (posterior probability of association >0.8) for shared causal variants between circulating cytokine levels and disease risk. Reprinted from Konieczny et al., 2024. medRxiv. 2024-04. CC-BY-NC-ND 4.0.

trials (Dejaco et al., 2003; Korzenik and Dieckgraefe, 2005) thereby providing support for potentially promising targeted immunotherapies for these indications. This convergence of evidence underscores the importance of further investigating these cytokine-disease associations and their potential implications for therapeutic interventions.

Cytokine	Disease	PPA for cytokine variants	PPA for disease variants	PPA for unrelated variants	PPA for common variants
G-CSF	**asthma**	0,00	0,00	0,07	**0,92**
IL-9	breast cancer	0,88	0,00	0,00	0,12
G-CSF	**CD**	0,00	0,00	0,02	**0,98**
IL-1RA	CD	0,98	0,00	0,00	0,02
IL-2RA	CD	0,98	0,00	0,00	0,02
IP-10	CD	0,88	0,00	0,00	0,12
MIG	**CD**	0,15	0,00	0,00	**0,85**
SDF-1A	CD	0,98	0,00	0,00	0,01
IL-18	CRC	0,99	0,00	0,00	0,01
IL-1RA	CAD	0,89	0,00	0,00	0,11
TRAIL	CAD	0,90	0,00	0,00	0,09
IL-2RA	MS	0,00	0,00	1,00	0,00
RANTES	MS	0,96	0,00	0,00	0,04
TNF-B	**MS**	0,00	0,01	0,03	**0,96**
FGF-bb	psoriasis	0,95	0,00	0,01	0,04
IL-18	psoriasis	0,86	0,00	0,00	0,13
SDF-1A	psoriasis	0,96	0,00	0,00	0,04
IL-1RA	RA	0,32	0,00	0,00	0,68
RANTES	stroke	0,97	0,00	0,00	0,03
IL-18	UC	0,82	0,00	0,00	0,18
IP-10	UC	0,91	0,00	0,00	0,09
MCP-1	UC	0,80	0,00	0,00	0,17
MIP-1A	UC	0,98	0,00	0,00	0,02

Table 4.2. Colocalization of causal variants associated with circulating cytokine concentrations and disease outcomes. Table compiles results for genomic colocalization between cytokine associated variants and disease associated variants. Values represent (from left to right) the probability (PPA) that the underlying shared association signal is causally linked to cytokine-related variants only, causally linked to disease-related variants only, causally linked to unrelated variants or causally linked to common variants. Colocalization (highlighted in bold) is considered if the PPA exceeds 80% for common causal variants. PPA, posterior probability of association; CD, Crohn's disease; CRC, colorectal cancer; CAD, carotid artery disease; MS, multiple sclerosis; RA, rheumatoid arteritis; UC, ulcerative colitis.

4.6 Integration of cytokine-disease MR and TWAS-MR results implicates additional mediators of disease mechanisms that could represent promising drug targets

In my final step, I aimed to merge the results from the cytokine-disease MR analysis with the TWAS-MR results, with the aim of identifying upstream regulators of potentially

causal cytokines (Konieczny et al., 2024). I conducted MR analyses between the genetically influenced expression of genes significantly associated with G-CSF, CXCL9/MIG, and TNF-b in the TWAS-MR analyses, and the corresponding disease outcomes. My findings revealed that higher genetically influenced expression of PPP1R37 is linked to lower levels of G-CSF, as well as a reduced risk of asthma (see **Figure 4.13a**). Additionally, I observed that higher genetically influenced expression of TRAFD1 is associated with elevated CXCL9/MIG levels and an increased risk of CD (see **Figure 4.13b**). Lastly, I also found that an increase in the genetically influenced expression of TRAFD1 causing higher TNF-b serum levels and an elevated risk for MS (see **Figure 4.13c**). These results provide valuable insights into potential upstream regulators of key cytokines and their implications in disease susceptibility, paving the way for further exploration of therapeutic targets and intervention strategies. Locus zoom plots for each of the cytokine – disease pairings are provided in the appendix (**Figure A.2**).

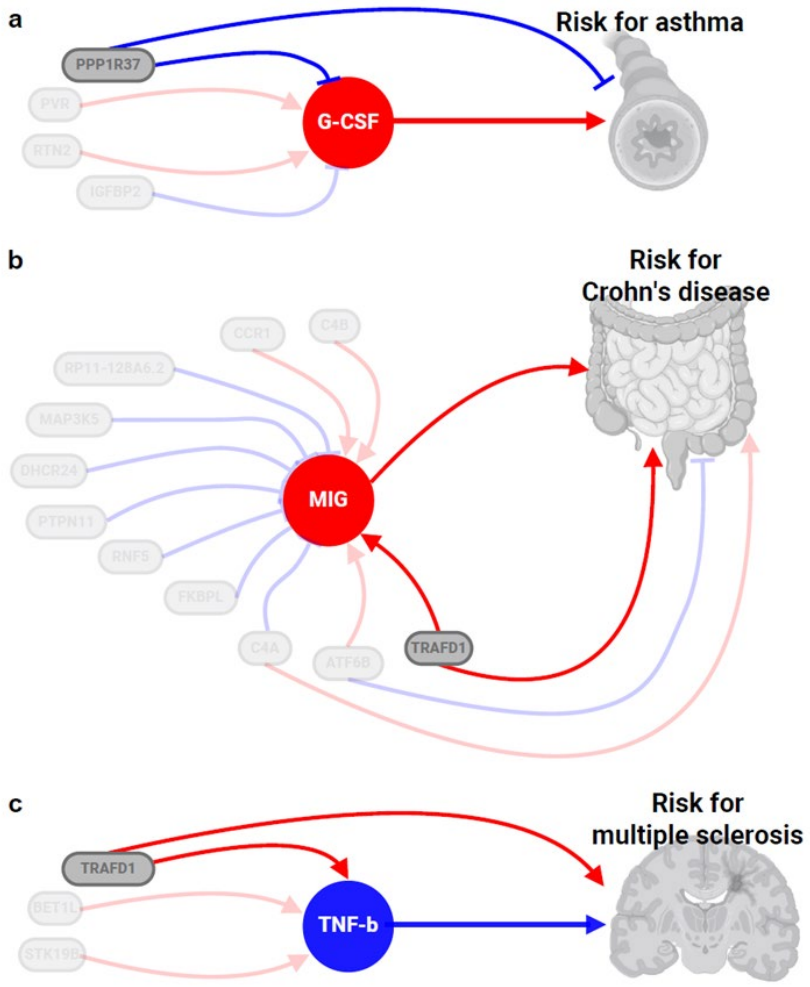

Figure 4.13. Causal associations between genetic regulators for cytokines, circulating cytokine levels and disease risk. (**a**) Genetically proxied mRNA for *PPP1R37*, *PVR*, *RTN2* and *IGFBP2* affect serum G-CSF levels leading to increased risk for asthma. In turn, *PPP1R37* directly lowers disease risk for asthma. (**b**) Genetically proxied mRNA for 11 genes underlying CXCL9/MIG serum levels differentially affect circulating cytokine concentrations which influence the risk for Crohn's disease. Independently, *TRAFD1*, *ATF6B* and *C4A* also modulate disease risk for Crohn's disease. (**c**) Genetically proxied mRNA for *TRAFD1, BET1L, STK19B* genes increase circulating TNF-b levels which lowers the risk for multiple sclerosis. *TRAFD1* is also directly associated with disease risk, leading to higher multiple sclerosis risk. Reprinted from Konieczny et al., 2024. medRxiv. 2024-04. CC-BY-NC-ND 4.0.

5. Discussion

Pooling data from a collective of 74,783 individuals across 3 independent GWAS cohorts, I pinpointed 169 distinct genomic loci exerting influence over the circulating levels of 40 cytokines (Konieczny et al., 2024). Notably, 156 of these loci represent novel findings, not previously associated with circulating cytokine levels in previous GWAS endeavors. Further, I identified 41 immunoregulatory pathways associated with circulating concentrations of 13 cytokines. Integrating my findings with transcriptomic data, I conducted a TWAS-MR analysis, uncovering 245 potentially causal associations between gene expression, particularly of immunoregulatory genes in peripheral blood, and circulating cytokine levels. Delving into the regulatory interactions among cytokines, I identified TNF-b, VEGF, and IL-1ra as pivotal orchestrators, exercising master control over the circulating levels of multiple cytokines. Lastly, I identified genetically proxied serum concentrations of cytokines as risk factors for 11 allergic and autoimmune disease, cardiometabolic disease and cancer. Following-up with colocalization analysis I obtained compelling evidence implicating the circulating levels of 3 cytokines—G-CSF, CXCL9/MIG, and TNF-b—in the pathogenesis of asthma, CD, and MS, respectively. These findings offer invaluable insights for the development of more targeted and specific immunotherapies tailored to these conditions.

In the GWAS analyzing the genomic architecture of 40 inflammatory cytokines I identified 359 significant associations between 169 independent loci and serum concentrations of circulating cytokine concentrations, whereby most of the identified genetic loci have not been associated with serum cytokine levels in previous GWASs. All of the studied cytokines had at least one significant trans-locus and 29 cytokines showed additional associations with one or more significant cis-loci. In expression analysis I found 245 significant associations linking genetically proxied gene expression in whole blood and cytokine levels for all but one of the included cytokines. In a previous approach using the same cytokine panel but only one GWAS cohort, Ahola-Olli et al. identified only 27 GWAS associations with serum cytokine levels and 15 significant eQTL's (Ahola-Olli et al., 2017). My more extensive approach has important implications for deciphering the complex architecture of inflammatory signaling pathways. For example, I could extend the findings of Ahola-Olli on the genetic background for the scavenger receptor ACKR1. This cell-surface receptor binds, internalizes and transports multiple CC and CXC chemokines and promotes leukocyte transcytosis into the circulation with potential relevance for allergic and autoimmune disease, cardiometabolic disease and cancer. (Crawford and Volkman, 2023; Korbecki et al., 2022; Schnabel et al., 2010; Szpakowska et al., 2023). In addition to the previous findings I showed that ACKR1 expression levels affect serum concentrations of 5 inflammatory cytokines in line with the postulated function as buffer and sink for multiple cytokines (Ahola-Olli et al., 2017; Zhao et al., 2023b). Further I

genetically outlined pathways of the TRAFD1 receptor domain which modulates downstream signals coming from TNF receptors, TLR and NLR (Edilova et al., 2018; Lalani et al., 2018; Park, 2021). In my approach linking expression levels of genes underlying cytokine concentrations, serum levels of cytokines and disease risks I identified TRAFD1 as upstream regulator of multiple cytokines levels and disease risk of T-cell mediated autoimmune disorders, in line with previous research showing involvement in Coeliac disease (Van Der Graaf et al., 2021).

In the network analysis, I observed that over 80 % of the significant interactions between cytokines resulted in an increase in downstream cytokine concentrations. This finding suggests the presence of a self-perpetuating feedback mechanism, particularly dominated by pro-inflammatory cytokines, driving robust inflammatory responses. It indicates a widespread trend where cytokines mutually activate each other, amplifying their immune reactions. Specifically, within the IL-1ra and TNF-b network, I expanded the repertoire of downstream affected cytokines. TNF-b emerged as a prominent master regulator, exerting significant downstream effects on 13 other cytokines. This observation underscores the pivotal role of TNF-b in orchestrating immune responses. It is consistent with existing literature on TRAFD1's downstream effects, which influence various cytokine-encoding genes such as CXCL10/IP-10 and IFN-g (Van Der Graaf et al., 2021). This aligns with the notion that cytokine networks are intricately interconnected and regulated, contributing to the complexity of immune responses.

Clinical management of many autoimmune diseases relies on rather unspecific treatment options including corticosteroids, immunosuppressives and often also chemotherapeutic agents (Lemanske and Busse, 2010; Rahman et al., 2024; Reich et al., 2018; L. Wang et al., 2015). These treatment regimens do not only suffer from modest efficacy but also come along with serious or life-threating adverse effects which affects compliance and quality of life of affected patients. Therefore, insight into molecular mechanisms and identification of disease-specific drug targets amenable for pharmaceutical modulation is of paramount importance for development of specific and efficient biological therapies (Pisetsky, 2023). Proteinergic inflammatory signaling molecules have been implicated in a range of human diseases (Xiang et al., 2023). By means of large-scale observational studies, particular cytokines have been identified and linked to specific disease conditions (Damoiseaux et al., 2015; Uricoli et al., 2021). Yet, the mechanistic importance and causal significance of these findings often remained elusive. For insights into the clinical consequences of chronically elevated inflammatory mediators I analyzed causal relations between the genetically proxied circulating cytokine profile and allergic and autoimmune disease, cardiometabolic disease and cancer conditions in a two-sample MR setting (Konieczny et al., 2024). In total, I identified 24 potentially causal associations, unsurprisingly most of them with autoimmune diseases. My MR findings partially confirm already established pathogenetic associations with diseases and therapeutic drug targets

already in clinical application. For example, there is solid evidence linking IL-2ra increasing variants to elevated risk for MS and CD (Ahola-Olli et al., 2017). Aldesleukin, a recombinant IL-2 protein approved for the treatment of cancers by the US European regulatory agencies, is currently under investigation in a phase-2 clinical trial for CD (ClinicalTrials.gov ID: NCT04263831) (Allegretti et al., 2023). Also, monoclonal antibodies targeting IL-1ra, anakinra or canakinumab, represent established treatment algorithms for inflammatory joint diseases like RA or juvenile arthritis (Bedaiwi et al., 2021; Shaul et al., 2022). On the other hand, my results implicating serum IL-1ra levels as risk factor underlying myocardial infarction are in line with previous observational findings from population based studies but contradict the results from the CANTOS trial showing effi-cacy of canakinumab in reducing cardiovascular events (Herder et al., 2017; Ridker et al., 2017). This indicates that despite MR evidence linking circulating cytokine levels and disease risk, the direction of putative effects must be interpreted with caution (Schmidt et al., 2020). Complex biological mechanisms like compensatory feedback loops between receptors and ligands indirectly affect serum levels of cytokines or disease specific local inflammatory reactions that do not directly translate into corresponding changes in the circulating cytokine profile have to be considered when interpreting MR findings (Ahola-Olli et al., 2017; Schmidt et al., 2020; Zhao et al., 2023b). To further corroborate the robustness of my MR findings causally linking cytokine levels to disease risk, I used colocalization analyses to test if the found associations underly shared causal variants (Zuber et al., 2022). Out of the 24 significant MR associations 4 cytokine – disease rela-tions showed colocalization between cytokine and disease associated variants (Konieczny et al., 2024). These findings offer genetic backing for potentially promising targeted im-munotherapies aimed at addressing asthma, CD, and MS. Importantly, my results are strongly aligned with preclinical, epidemiological, and, in some cases, clinical evidence.

For example, G-CSF, a pro-inflammatory cytokine has been implicated in the pathogenesis of asthma (Ouyang et al., 2020; Tsioumpekou et al., 2023). Asthma is a chronic inflammatory disease of the airways, characterized by recurring wheezing, coughing, chest tightness, and shortness of breath due to reversible airflow obstruction, and easily trig-gered bronchospasms (Lemanske and Busse, 2010). Next to environmental factors, there is considerable genetic contribution including genes for cytokines and inflammatory pro-teins underlying asthma (Yawn, 2008). There are different subtypes of asthma (e.g. atopic asthma including eosinophilic and neutrophilic disease variants) that characterize the pre-dominant immune mechanism triggering the disease (Crisford et al., 2021). G-CSF is a pro-inflammatory cytokine involved in neutrophil differentiation and systemic mobiliza-tion and has been implicated in the pathogenesis of neutrophilic airway diseases including asthma (Ouyang et al., 2020; Tsioumpekou et al., 2023). Preclinical studies conducted in asthma models have consistently demonstrated that blocking upstream inducers or the

receptor of G-CSF can lead to reductions in circulating cytokine levels, mitigation of airway inflammatory responses, and improvements in disease outcomes (Kwak et al., 2022; Ouyang et al., 2020; H. Wang et al., 2019; Wang et al., 2021). Furthermore, there is evidence suggesting that G-CSF levels in the sputum of asthma patients may serve as a marker of airway neutrophilic inflammation (Kim et al., 2020). My genetic findings lend robust support to the notion of targeting G-CSF in the context of asthma, with potential emphasis on patients exhibiting neutrophilic asthma (Konieczny et al., 2024). Exploring the upstream genetic regulators for circulating cytokine levels in a TWAS-MR setting I identified protein phosphatase 1 regulatory subunit 37 (PPP1R37) as G-CSF-increasing transcript that was also causally associated with reduced asthma risk. PPP1R37 codes for a regulatory subunit of protein phosphatase 1 (PP1) ("PPP1R37 protein phosphatase 1 regulatory subunit 37 [Homo sapiens (human)]," 2023). There is only limited information available about the function of PPP1R37 suggesting an inhibitory effect on PP1 phosphatase activity. PP1 has an essential role in different physiological processes including glycogen metabolism, cell progression, apoptosis and muscle contraction. PP1 binds and complexes with various regulatory subunits to define its substrate specificity or inhibit its own function (Yadav et al., 2017). Prior investigations into related regulatory subunits have shed light on potential biological mechanisms through which these molecules might influence immune responses and disease characteristics (Haystead, 2005; Yadav et al., 2017). For example, myosin protein phosphatase 1 (SMPP1-M) functions as dephosphorylating enzyme without specific substrate preference. Only when SMPP1-M forms a complex with the PPP1**R12A** regulatory subunit the phosphatase specifically targets and dephosphorylates the myosin light chains of smooth muscle cells (Haystead, 2005). In the bronchial musculature dephosphorylation of the myosin light chain decreases smooth muscle contraction and thereby attenuates airway hyperresponsiveness which is one hallmark of asthma (Goto et al., 2008). Genetic studies have also implicated other protein phosphatase regulatory subunits as contributing factors to airway diseases (Andiappan et al., 2016; Freidin and Polonikov, 2013; Kidwai et al., 2023). For instance, genetically influenced expression of PPP1**R3D** has been linked to asthma-related traits such as mucosal immunity, cellular metabolism, airway remodeling, and predicted responsiveness to omalizumab therapy (Kidwai et al., 2023). Although the precise biological mechanism underlying my discovery remains elusive, it is plausible to speculate that the diverse range of functions associated with PP1, could be implicated in the observed associations (Konieczny et al., 2024). These findings highlight the intricate interplay between genetic factors and immune regulation in the pathogenesis of asthma and underscore the need for further exploration to elucidate the underlying mechanisms. My MR findings for the eQTL for PPP1R37 showing a protective effect for asthma were not described so far and need to be mechanistically validated. Similarly, the found association between the eQTL for PPP1R37 and circulating G-CSF needs further validation and substantiation.

My MR findings provided support for a connection between genetically influenced circulating levels of six cytokines and CD. Notably, the associations of higher CXCL9/MIG levels and lower G-CSF levels with CD were further bolstered by colocalization evidence (Konieczny et al., 2024). CD is an autoimmune-mediated IBD presenting with pain, diarrhea, fever and malabsorption caused by stenosis, inflammation, fistulization or abscesses and affecting any part of the gastrointestinal tract. While the exact cause is currently not known, T-lymphocytes are believed to be central in the underlying pathophysiology (Singh et al., 2007). CXCL9/MIG is a proinflammatory CXC-chemokine and growth-factor that is released locally upon physical stress or microbial invasion (Lasagni et al., 2003). Together with the closely related, neighboring CXCL10/IP-10 and CXCL11/IP-9 chemokines they all bind CXC-receptor 3 (CXRC3) and form the CXCL9/MIG – CXCL10/IP-10 – CXCL11/IP-9 – CXCR3 axis that has particular relevance in IBD (Tokunaga et al., 2018). Chemotactic signaling by these cytokines orchestrate an inflammatory response directed at CXCR3 positive NK cells, innate immune cells and Th1-cells which then start migrating to the lesion side (Singh et al., 2007). At the same time, stimulated CXCR3 positive Th1-cells secrete IFN-g and TNF-a which in turn increase the local release of CXCL9/MIG thus creating a self-amplifying loop which results in a hyperinflammatory state (Tokunaga et al., 2018). Recent studies suggest that the CXCL9/MIG – CXCL10/IP-10 – CXCL11/IP-9 – CXCR3 axis might be implicated in the local immune response at the gastrointestinal mucosa in IBD (Caruso, 2019). For example, identification of serum proteins for prognostication of CD recurrence revealed strongest association with circulating CXCL9/MIG levels, thus confirming CXCL9/MIG as risk factor underlying CD. Interestingly, stratification of the associations according to anti-TNF therapy revealed that the found association was limited to patients currently treated with infliximab indicating that the CXCR3 axis is particular important in patients with treatment refractory inflammation or indicates that treatment of downstream targets, like for example CXCL9/MIG, might be more efficient (Walshe et al., 2022). Causal evidence for the role of the CXCR3 axis in IBD was provided by a phase II study. Here blockage of the CXC3 axis by a monoclonal antibody against CXCL10/IP-10 (MDX-1100) proved to be effective and safe in patients with UC by inducing clinical response, remission, and mucosal healing in a dose dependent manner (Mayer et al., 2014). In addition to its pro-inflammatory effects reported above, exogenous administration of G-CSF has been linked to immunoregulatory effects, such as modulation of T-cell responses (Martins et al., 2010). Also, G-CSF supports immune homeostasis in organs such as the gastrointestinal tract that shows constitutively high G-CSF levels (Dejaco et al., 2003). In preclinical models, G-CSF deficient animals benefit from G-CSF injections and show a return to physiological neutrophil concentrations (Sainathan et al., 2008). Immunoregulatory effects, like downregulation of circulating cytokines, induction of tolerant dendritic cells and switching from a pro-inflammatory cytokine profile into an anti-inflammatory profile in T-cells were observed in humans after G-CSF administration (Martins et al.,

2010). The pathogenesis underlying CD is not well understood but the prevailing etiological explanation assumes an excessive inflammatory reaction based on defective interactions between innate and adaptive immune systems. An alternative hypothesis focuses on a failure of innate humoral mechanisms in the intestinal immune system which exposes cells of the mucosa to luminal pathogens and resulting in chronic inflammation maintained by T-cells (Korzenik and Dieckgraefe, 2000). In accordance with this line of thinking G-CSF treatment was administered to augment the innate immune response and modulate T-cell responses. In 2 open-label studies subcutaneous G-CSF proved efficious by inducing clinical remission, mucosal healing and normalized cell counts and cytokine responses together with an acceptable safety profile (Dejaco et al., 2003; Korzenik and Dieckgraefe, 2005). By integrating my findings that associate CD with circulating levels of CXCL9/MIG, I uncovered the genetically influenced expression of TRAFD1 as a potential upstream causal regulator of CXCL9/MIG levels and, consequently, the risk of CD (Huang et al., 2023; Liu et al., 2023; Walshe et al., 2022). TRAFD1 is an adaptor protein that is bound to the intracellular domain of TNF receptors expressed on innate and adaptive immune cells and modulates downstream signaling influencing pro-inflammatory cytokine production and inflammatory responses (Lalani et al., 2018; Park, 2021). Moreover, there is evidence for an expanded influence of TRAFD1 on the inflammatory response by binding to TLR and NLR receptors and interacting with TRAF**D2** for augmentation of the immune response (Edilova et al., 2018). Involvement of TRAFD1 in IBD was studied in colon biopsies of coeliac disease patients and showed TRAFD1-dependent upregulation of IFN-g signaling via CXCL10/IP-10 (Van Der Graaf et al., 2021). Subsequently, cytotoxic T-cells become activated and destroy the integrity of the mucosal barrier, one hallmark of coeliac disease. Altogether, the authors concluded using a combination of genomic, in-silico and in-vitro approaches that TRAFD1 is a master regulator of genes involved in IFN-g signaling and T-cell activation (Van Der Graaf et al., 2021). Due to the importance of TNF-a in the disease pathology and as drug target in treatment approaches the involvement of TRAFD1 and TRAF**D2** was explored in patients with CD and UC (Andersen et al., 2015; Qiao et al., 2013). Both TRAF domains were significantly upregulated in the mucosa from IBD patients compared to control and also higher in currently inflamed lesions of the colon compared to healthy colon biopsies. Furthermore, in ROC analyses serum levels of TRAF's discriminated both IBD groups from controls, where TRAFD1 showed superiority over TRAF**D2** in both patient groups for sensitivity and specificity parameters (Qiao et al., 2013). Back then, the authors concluded that the observed increase of TRAF levels and expression profile in mucosal lesions might constitute an early event in the pathogenesis of IBD. More recent insights showing that TRAFD1 stimulates survival of T-cells increases the relevance of their findings and indicates that TRAFD1 is not only important in initiation of lesions but also a key factor in maintenance of the disease (Edilova et al., 2018). In the TWAS-MR analyses, mRNA of

the TRAFD1 gene was causally related to increased risk for CD and an increase in circulating CXCL9/MIG levels (Konieczny et al., 2024). Also, I have shown earlier that the transcriptional variant for TRAFD1 increases circulating serum levels for CXCL10/IP-10, CCL7/MCP-3, CXCL9/MIG and TNF-b. Together my results confirmed contemporary findings for the importance of TRAFD1 in the pathology of IBD and as modulator of inflammatory reactions through effects on cytokine levels, providing causal evidence for TRAFD1 as potential drug target. Research on pharmacological targeting of TRAF's identified specific binding pockets that enable protein-protein interactions (PPI) between TRAF domains and receptors which provide sufficient specificity and experimentally inhibited the downstream cellular signal (Park, 2021). TRAF**D6** was tested in a preclinical model of RA. Using a small interfering RNA to inhibit binding between TRAF**D6** and CD40 successfully reduced the severity of arthritis and inflammation (H. Wang et al., 2015). In pre-clinical studies, Atrosab has been used to inhibit binding of TNF-a and TNF-b to the pro-inflammatory TNF-R1 showing lowered immune cell infiltration and amelioration of disease severity (Williams et al., 2018). Interestingly, the mechanism of action induces conformational changes to the binding pockets of TNF-R1 which makes binding of TRAF domains impossible and precludes downstream signaling (Richter et al., 2013). These collective findings underscore the significance of TRAFD1 in the pathology of CD and reinforce the potential therapeutic relevance of targeting TRAFD1 in CD.

Lastly, my analysis also unveiled an intriguing inverse association between genetically influenced circulating levels of TNF-b and the risk of MS (Konieczny et al., 2024). MS is an autoimmune-mediated central nervous system (CNS) disease defined by partially or fully reversible episodes of neurological disability including opticus neuritis and myelitis and corresponding focal white matter lesions visible on MRI (Reich et al., 2018). The pathogenesis of CNS lesions involves a complex interaction between cells of the innate and adaptive immune system, glial cells and neurons. TNF-b is a soluble cytokine from the TNF superfamily and shares 50% homology to the more prominent TNF-a which exists in soluble and membrane bound configurations (Smookler et al., 2006). TNF-b is released by CD4 and CD8 T cells, B cells, and other cells from the lymphoid lineage, and is a ligand for the pro-inflammatory TNF-R1 and the anti-inflammatory TNF-R2 (Ruddle, 2014). TNF-b has been evaluated as biomarker in multiple studies and showed promising results associating with clinical remission following dimethyl fumarate (DMF) and natalizumab treatment (Hojjati et al., 2023). These and other studies collected samples from peripheral blood and CSF and uniformly reported an inverse relation between serum levels and CSF levels of TNF-b in line with my results (Åkesson et al., 2023; Hojjati et al., 2023; Huang et al., 2020; Romme Christensen et al., 2012). In a randomized phase 2 trial, the TNF inhibitor lenercept was investigated for its safety and efficacy in MS. However,

the trial had to be terminated prematurely due to a dose-dependent increase in the frequency and severity of MS exacerbations observed during the interim analysis (The Lenercept Multiple Sclerosis Study Group and The University of British Columbia MS/MRI Analysis Group, 2011). Unlike other TNF blockers such as infliximab, adalimumab, and golimumab, lenercept offers equal inhibitory efficacy for both TNF-a and TNF-b (Mitoma et al., 2018; Ruddle, 2014). While TNF inhibition has shown efficacy in treating autoimmune diseases like RA or psoriasis, patients receiving anti-TNF therapy for these conditions are at risk of developing demyelinating CNS lesions, suggesting a disease-specific effect (Ding et al., 2016; Li et al., 2023). Supporting these clinical observations, GWAS in MS have identified alleles associated with lower levels of both TNF-a and TNF-b, correlating with a higher risk for MS (Gregory et al., 2012; Zhao et al., 2023b). My findings provide additional genetic evidence in line with observational, clinical, and GWAS data, suggesting a potentially protective role of TNF-b in MS pathogenesis (Konieczny et al., 2024). These results underscore the complexity of cytokine-mediated immune responses in MS and highlight the need for further research to elucidate the underlying mechanisms. Next, I showed in the TWAS-MR setting that TRAFD1 is a transcriptional determinant underlying increased serum TNF-b levels as well as elevated risk for MS. As described above TRAFD1 is an important immune mediator (Edilova et al., 2018; Lalani et al., 2018; Park, 2021). Currently, there is no evidence linking the TRAFD1 protein to multiple sclerosis, only 2 genetic studies showing associations of unknown functional relevance (Hecker et al., 2022; Smits et al., 2023).

My study has several limitations that warrants careful consideration. Firstly, in aggregating my GWAS dataset I pooled data across 3 cohorts, each employing distinct affinity-based assay methods to quantify circulating cytokines. The use of different assay technologies can introduce significant variability in protein measurements (Eldjarn et al., 2023). Notably, my analysis revealed a higher replication rate for signals detected using the Olink assay. This finding aligns with previous cross-assay comparisons between Olink and SomaScan assays, which have shown significant differences in the proportion of detected pQTLs. Specifically, Olink-based assays tend to demonstrate higher detection rates for pQTLs compared to SomaScan (Eldjarn et al., 2023). These differences suggest that the Olink platform may have superior sensitivity or specificity in certain contexts, which could influence its utility and effectiveness in proteomic studies. To better understand these assay discrepancies, further exploration across larger cohorts is necessary. Expanding the investigation to include more diverse and extensive datasets will allow for a more comprehensive assessment of the feasibility and accuracy of integrating genetic explorations across studies that utilize different proteomic platforms. This broader analysis will help identify the strengths and limitations of each assay method, facilitating more informed decisions on their application in various research contexts. Ultimately, such ef-

forts will enhance the robustness and reproducibility of proteomic data in genetic research, ensuring that findings are consistent and reliable across different studies and assay technologies. This will also contribute to the development of standardized protocols and best practices for proteomic analyses, fostering greater collaboration and data sharing within the scientific community. Secondly, discrepancies in reporting effect sizes for genetic variants across the GWAS source data constrained my ability to perform more detailed analyses. Specifically, these inconsistencies made it impossible for me to calculate p-value-based analyses rather than more comprehensive effect size-based analyses. This constraint necessitated the indirect estimation of pooled effect sizes based on derived p-values and variant allele frequencies. Such estimations are inherently less precise than direct effect size reporting, potentially introducing inaccuracies that could significantly impact downstream analyses reliant on these effect sizes. Future studies should prioritize direct effect size measurements to improve the quality and reliability of genetic research outcomes. Thirdly, my analyses were limited to a selection of 40 cytokines due to the constraints of data availability. This limited scope restricts the breadth of my findings and may overlook important cytokines involved in inflammatory processes. Future studies utilizing high-throughput proteomic technologies could expand the range of investigated proteins to include a more extensive array of inflammatory markers. Such an approach would allow for a more comprehensive analysis, potentially uncovering additional insights into the complex network of cytokines and their roles in inflammation and disease. Fourthly, my study population comprised individuals of European, Finnish, and Icelandic ancestry, which may limit the generalizability of my findings to populations with different ancestral backgrounds. Genetic and proteomic variations can differ significantly across diverse populations, and the associations I identified may not be applicable to other groups. To improve the applicability and relevance of my results, future research should include more diverse cohorts representing a broader range of ancestries. This would help to ensure that findings are more universally applicable and can provide insights into genetic and proteomic influences across different populations, thereby enhancing the overall robustness and inclusivity of genetic research. Fifthly, due to the large number of cytokines analyzed, I adjusted the significance level to account for multiple testing. This stringent correction likely reduced the likelihood of type I errors but may have also led to the omission of potentially important findings that did not meet the adjusted significance threshold. Future studies employing a hypothesis-driven approach could revisit my results to identify additional targets that may have been missed in my analysis. By focusing on specific cytokines or pathways of interest, these studies can explore associations that may not have reached significance in my broader analysis, potentially uncovering novel insights and enhancing our understanding of cytokine-related genetic influences. Sixthly, my GWAS analysis was conducted on population-based cohorts without a predominant presence of inflammatory diseases. While this approach offers valuable insights into genetic influences on cytokine levels in general populations, it may not fully capture the

nuanced effects of genetic variants in specific inflammatory contexts. For example, genetic variants may exert greater influence on cytokine levels during responses to infections or other pro-inflammatory stimuli, which were not explicitly addressed in my analysis. Future studies focusing on cohorts with defined inflammatory conditions or incorporating experimental models of inflammation could provide a more comprehensive understanding of the genetic determinants of cytokine regulation in disease-relevant contexts. By exploring these specific scenarios, researchers can elucidate the role of genetic variants in modulating cytokine responses under different physiological conditions, thus contributing to a more nuanced understanding of cytokine biology and its implications for health and disease. Overall, my study offers valuable insights into the genetic architecture of circulating cytokines. However, it is important to interpret my findings cautiously in light of the identified limitations. These limitations, including variations in assay methodologies, constraints on data availability, and the specific characteristics of my study population, underscore the need for careful consideration when extrapolating conclusions. Moreover, they highlight promising avenues for future research to overcome these challenges and build upon my findings. By addressing these limitations head-on and leveraging advancements in technology and methodology, future studies can further elucidate the complex interplay between genetics and cytokine regulation, ultimately advancing our understanding of inflammatory processes and their implications for health and disease.

Conclusion

In summary, by analyzing data from a large-scale cohort of 74,783 individuals, I identified 169 genomic loci that influence circulating cytokine levels. Notably, many of these loci had not been previously associated with cytokine regulation, highlighting novel genetic factors that may play critical roles in immune function and inflammation. Through subsequent analyses, I conducted an in-depth examination of the identified signals, revealing intricate pathways that underlie immune responses. This detailed exploration provided new insights into the molecular mechanisms and regulatory networks that govern cytokine activity and immune function. By combining my findings with genetic data on human disease susceptibility, I provided genetic support for potential therapeutic targets for immune-related disorders such as asthma, Crohn’s disease, and multiple sclerosis. Specifically, I highlighted G-CSF, CXCL9/MIG, and TNF-b as promising candidates. These targets warrant prioritization for further investigation in clinical trials to assess their efficacy and potential in treating these conditions. The comprehensive summary statistics generated from my study serve as a valuable resource for future genomics studies. This dataset supports the advancement of precision medicine by enabling deeper insights into the genetic underpinnings of disease and the development of targeted therapeutic interventions.

6. References

1000 Genomes Project Consortium, Abecasis, G.R., Altshuler, D., Auton, A., Brooks, L.D., Durbin, R.M., Gibbs, R.A., Hurles, M.E., McVean, G.A., 2010. A map of human genome variation from population-scale sequencing. Nature 467, 1061–1073. https://doi.org/10.1038/nature09534

Aday, A.W., Ridker, P.M., 2019. Targeting Residual Inflammatory Risk: A Shifting Paradigm for Atherosclerotic Disease. Front. Cardiovasc. Med. 6, 16. https://doi.org/10.3389/fcvm.2019.00016

Ahola-Olli, A.V., Würtz, P., Havulinna, A.S., Aalto, K., Pitkänen, N., Lehtimäki, T., Kähönen, M., Lyytikäinen, L.-P., Raitoharju, E., Seppälä, I., Sarin, A.-P., Ripatti, S., Palotie, A., Perola, M., Viikari, J.S., Jalkanen, S., Maksimow, M., Salomaa, V., Salmi, M., Kettunen, J., Raitakari, O.T., 2017. Genome-wide Association Study Identifies 27 Loci Influencing Concentrations of Circulating Cytokines and Growth Factors. Am. J. Hum. Genet. 100, 40–50. https://doi.org/10.1016/j.ajhg.2016.11.007

Åkesson, J., Hojjati, S., Hellberg, S., Raffetseder, J., Khademi, M., Rynkowski, R., Kockum, I., Altafini, C., Lubovac-Pilav, Z., Mellergård, J., Jenmalm, M.C., Piehl, F., Olsson, T., Ernerudh, J., Gustafsson, M., 2023. Proteomics reveal biomarkers for diagnosis, disease activity and long-term disability outcomes in multiple sclerosis. Nat. Commun. 14, 6903. https://doi.org/10.1038/s41467-023-42682-9

Allegretti, J.R., Mitsialis, V., Canavan, J.B., Low-Dose IL2 UC Study Group, Snapper, S.B., 2023. Low-Dose Interleukin 2 for the Treatment of Moderate to Severe Ulcerative Colitis. Gastroenterology 165, 492-495.e2. https://doi.org/10.1053/j.gastro.2023.03.230

Altan-Bonnet, G., Mukherjee, R., 2019. Cytokine-mediated communication: a quantitative appraisal of immune complexity. Nat. Rev. Immunol. 19, 205–217. https://doi.org/10.1038/s41577-019-0131-x

Andersen, N.N., Pasternak, B., Friis-Møller, N., Andersson, M., Jess, T., 2015. Association between tumour necrosis factor-α inhibitors and risk of serious infections in people with inflammatory bowel disease: nationwide Danish cohort study. BMJ 350, h2809. https://doi.org/10.1136/bmj.h2809

Andiappan, A.K., Sio, Y.Y., Lee, B., Suri, B.K., Matta, S.A., Lum, J., Foo, S., Koh, G., Liu, J., Zolezzi, F., Poidinger, M., Wang, D.Y., Rotzschke, O., Chew, F.T., 2016. Functional variants of 17q12-21 are associated with allergic asthma but not allergic rhinitis. J. Allergy Clin. Immunol. 137, 758-766.e3. https://doi.org/10.1016/j.jaci.2015.08.038

Arango Duque, G., Descoteaux, A., 2014. Macrophage cytokines: involvement in immunity and infectious diseases. Front. Immunol. 5, 491. https://doi.org/10.3389/fimmu.2014.00491

Atkins, M.B., Lotze, M.T., Dutcher, J.P., Fisher, R.I., Weiss, G., Margolin, K., Abrams, J., Sznol, M., Parkinson, D., Hawkins, M., Paradise, C., Kunkel, L., Rosenberg, S.A., 1999. High-dose recombinant interleukin 2 therapy for patients with metastatic melanoma: analysis of 270 patients treated between 1985 and 1993. J. Clin. Oncol. Off. J. Am. Soc. Clin. Oncol. 17, 2105–2116. https://doi.org/10.1200/JCO.1999.17.7.2105

Atzeni, F., Rodríguez-Carrio, J., Popa, C.D., Nurmohamed, M.T., Szűcs, G., Szekanecz, Z., 2021. Cardiovascular effects of approved drugs for rheumatoid arthritis. Nat. Rev. Rheumatol. 17, 270–290. https://doi.org/10.1038/s41584-021-00593-3

Bandres-Ciga, S., Noyce, A.J., Traynor, B.J., 2020. Mendelian Randomization-A Journey From Obscurity to Center Stage With a Few Potholes Along the Way. JAMA Neurol. 77, 7–8. https://doi.org/10.1001/jamaneurol.2019.3419

Barrow, A.D., Martin, C.J., Colonna, M., 2019. The Natural Cytotoxicity Receptors in Health and Disease. Front. Immunol. 10, 909. https://doi.org/10.3389/fimmu.2019.00909

Basu, A., Krady, J.K., Levison, S.W., 2004. Interleukin-1: A master regulator of neuroinflammation. J. Neurosci. Res. 78, 151–156. https://doi.org/10.1002/jnr.20266

Bedaiwi, M.K., Almaghlouth, I., Omair, M.A., 2021. Effectiveness and adverse effects of anakinra in treatment of rheumatoid arthritis: a systematic review. Eur. Rev. Med. Pharmacol. Sci. 25, 7833–7839. https://doi.org/10.26355/eurrev_202112_27630

Ben-Sasson, S.Z., Hu-Li, J., Quiel, J., Cauchetaux, S., Ratner, M., Shapira, I., Dinarello, C.A., Paul, W.E., 2009. IL-1 acts directly on CD4 T cells to enhance their antigen-driven expansion and differentiation. Proc. Natl. Acad. Sci. U. S. A. 106, 7119–7124. https://doi.org/10.1073/pnas.0902745106

Berraondo, P., Sanmamed, M.F., Ochoa, M.C., Etxeberria, I., Aznar, M.A., Pérez-Gracia, J.L., Rodríguez-Ruiz, M.E., Ponz-Sarvise, M., Castañón, E., Melero, I., 2019. Cytokines in clinical cancer immunotherapy. Br. J. Cancer 120, 6–15. https://doi.org/10.1038/s41416-018-0328-y

Boersma, B., Jiskoot, W., Lowe, P., Bourquin, C., 2021. The interleukin-1 cytokine family members: Role in cancer pathogenesis and potential therapeutic applications in cancer immunotherapy. Cytokine Growth Factor Rev. 62, 1–14. https://doi.org/10.1016/j.cytogfr.2021.09.004

Bonfiglio, C.A., Weber, C., Atzler, D., Lutgens, E., 2023. Immunotherapy and cardiovascular diseases: novel avenues for immunotherapeutic approaches. QJM Mon. J. Assoc. Physicians 116, 271–278. https://doi.org/10.1093/qjmed/hcab207

Bouras, E., Karhunen, V., Gill, D., Huang, J., Haycock, P.C., Gunter, M.J., Johansson, M., Brennan, P., Key, T., Lewis, S.J., Martin, R.M., Murphy, N., Platz, E.A., Travis, R., Yarmolinsky, J., Zuber, V., Martin, P., Katsoulis, M., Freisling, H., Nøst, T.H., Schulze, M.B., Dossus, L., Hung, R.J., Amos, C.I., Ahola-Olli, A., Palaniswamy, S., Männikkö, M., Auvinen, J., Herzig, K.-H., Keinänen-Kiukaanniemi, S., Lehtimäki, T., Salomaa, V., Raitakari, O., Salmi, M., Jalkanen, S., PRACTICAL consortium, Jarvelin, M.-R., Dehghan, A., Tsilidis, K.K., 2022. Circulating inflammatory cytokines and risk of five cancers: a Mendelian randomization analysis. BMC Med. 20, 3. https://doi.org/10.1186/s12916-021-02193-0

Bowden, J., Davey Smith, G., Burgess, S., 2015. Mendelian randomization with invalid instruments: effect estimation and bias detection through Egger regression. Int. J. Epidemiol. 44, 512–525. https://doi.org/10.1093/ije/dyv080

Bowden, J., Davey Smith, G., Haycock, P.C., Burgess, S., 2016. Consistent Estimation in Mendelian Randomization with Some Invalid Instruments Using a Weighted

Median Estimator. Genet. Epidemiol. 40, 304–314. https://doi.org/10.1002/gepi.21965

Bresnihan, B., 2001. The safety and efficacy of interleukin-1 receptor antagonist in the treatment of rheumatoid arthritis. Semin. Arthritis Rheum. 30, 17–20. https://doi.org/10.1053/sarh.2001.23701

Bresnihan, B., Alvaro-Gracia, J.M., Cobby, M., Doherty, M., Domljan, Z., Emery, P., Nuki, G., Pavelka, K., Rau, R., Rozman, B., Watt, I., Williams, B., Aitchison, R., McCabe, D., Musikic, P., 1998. Treatment of rheumatoid arthritis with recombinant human interleukin-1 receptor antagonist. Arthritis Rheum. 41, 2196–2204. https://doi.org/10.1002/1529-0131(199812)41:12<2196::AID-ART15>3.0.CO;2-2

Bulik-Sullivan, B., Finucane, H.K., Anttila, V., Gusev, A., Day, F.R., Loh, P.-R., ReproGen Consortium, Psychiatric Genomics Consortium, Genetic Consortium for Anorexia Nervosa of the Wellcome Trust Case Control Consortium 3, Duncan, L., Perry, J.R.B., Patterson, N., Robinson, E.B., Daly, M.J., Price, A.L., Neale, B.M., 2015. An atlas of genetic correlations across human diseases and traits. Nat. Genet. 47, 1236–1241. https://doi.org/10.1038/ng.3406

Bulik-Sullivan, B.K., Loh, P.-R., Finucane, H.K., Ripke, S., Yang, J., Schizophrenia Working Group of the Psychiatric Genomics Consortium, Patterson, N., Daly, M.J., Price, A.L., Neale, B.M., 2015. LD Score regression distinguishes confounding from polygenicity in genome-wide association studies. Nat. Genet. 47, 291–295. https://doi.org/10.1038/ng.3211

Burgess, S., Butterworth, A., Thompson, S.G., 2013. Mendelian randomization analysis with multiple genetic variants using summarized data. Genet. Epidemiol. 37, 658–665. https://doi.org/10.1002/gepi.21758

Burgess, S., Davies, N.M., Thompson, S.G., 2016. Bias due to participant overlap in two-sample Mendelian randomization. Genet. Epidemiol. 40, 597–608. https://doi.org/10.1002/gepi.21998

Burnet, F.M., 1970. The concept of immunological surveillance. Prog. Exp. Tumor Res. 13, 1–27. https://doi.org/10.1159/000386035

Burrows, K., Haycock, P., 2021. Genome-wide Association Study of Cancer Risk in UK Biobank. https://doi.org/10.5523/BRIS.AED0U12W0EDE20OLB0M77P4B9

Bycroft, C., Freeman, C., Petkova, D., Band, G., Elliott, L.T., Sharp, K., Motyer, A., Vukcevic, D., Delaneau, O., O'Connell, J., Cortes, A., Welsh, S., Young, A., Effingham, M., McVean, G., Leslie, S., Allen, N., Donnelly, P., Marchini, J., 2018. The UK Biobank resource with deep phenotyping and genomic data. Nature 562, 203–209. https://doi.org/10.1038/s41586-018-0579-z

Calmon-Hamaty, F., Combe, B., Hahne, M., Morel, J., 2011. Lymphotoxin α revisited: general features and implications in rheumatoid arthritis. Arthritis Res. Ther. 13, 232. https://doi.org/10.1186/ar3376

Carswell, E.A., Old, L.J., Kassel, R.L., Green, S., Fiore, N., Williamson, B., 1975. An endotoxin-induced serum factor that causes necrosis of tumors. Proc. Natl. Acad. Sci. U. S. A. 72, 3666–3670. https://doi.org/10.1073/pnas.72.9.3666

Caruso, C., 2019. MIG in Crohn's disease. Clin. Ter. 170, e206–e210. https://doi.org/10.7417/CT.2019.2134

Chen, C., Yu, L.-T., Cheng, B.-R., Xu, J.-L., Cai, Y., Jin, J.-L., Feng, R.-L., Xie, L., Qu, X.-Y., Li, D., Liu, J., Li, Y., Cui, X.-Y., Lu, J.-J., Zhou, K., Lin, Q., Wan, J., 2022. Promising Therapeutic Candidate for Myocardial Ischemia/Reperfusion Injury: What Are the Possible Mechanisms and Roles of Phytochemicals? Front. Cardiovasc. Med. 8, 792592. https://doi.org/10.3389/fcvm.2021.792592

Chen, M.-H., Raffield, L.M., Mousas, A., Sakaue, S., Huffman, J.E., Moscati, A., Trivedi, B., Jiang, T., Akbari, P., Vuckovic, D., Bao, E.L., Zhong, X., Manansala, R., Laplante, V., Chen, M., Lo, K.S., Qian, H., Lareau, C.A., Beaudoin, M., Hunt, K.A., Akiyama, M., Bartz, T.M., Ben-Shlomo, Y., Beswick, A., Bork-Jensen, J., Bottinger, E.P., Brody, J.A., Van Rooij, F.J.A., Chitrala, K., Cho, K., Choquet, H., Correa, A., Danesh, J., Di Angelantonio, E., Dimou, N., Ding, J., Elliott, P., Esko, T., Evans, M.K., Floyd, J.S., Broer, L., Grarup, N., Guo, M.H., Greinacher, A., Haessler, J., Hansen, T., Howson, J.M.M., Huang, Q.Q., Huang, W., Jorgenson, E., Kacprowski, T., Kähönen, M., Kamatani, Y., Kanai, M., Karthikeyan, S., Koskeridis, F., Lange, L.A., Lehtimäki, T., Lerch, M.M., Linneberg, A., Liu, Y., Lyytikäinen, L.-P., Manichaikul, A., Martin, H.C., Matsuda, K., Mohlke, K.L., Mononen, N., Murakami, Y., Nadkarni, G.N., Nauck, M., Nikus, K., Ouwehand, W.H., Pankratz, N., Pedersen, O., Preuss, M., Psaty, B.M., Raitakari, O.T., Roberts, D.J., Rich, S.S., Rodriguez, B.A.T., Rosen, J.D., Rotter, J.I., Schubert, P., Spracklen, C.N., Surendran, P., Tang, H., Tardif, J.-C., Trembath, R.C., Ghanbari, M., Völker, U., Völzke, H., Watkins, N.A., Zonderman, A.B., Wilson, P.W.F., Li, Y., Butterworth, A.S., Gauchat, J.-F., Chiang, C.W.K., Li, B., Loos, R.J.F., Astle, W.J., Evangelou, E., Van Heel, D.A., Sankaran, V.G., Okada, Y., Soranzo, N., Johnson, A.D., Reiner, A.P., Auer, P.L., Lettre, G., 2020. Trans-ethnic and Ancestry-Specific Blood-Cell Genetics in 746,667 Individuals from 5 Global Populations. Cell 182, 1198-1213.e14. https://doi.org/10.1016/j.cell.2020.06.045

Chong, M., Sjaarda, J., Pigeyre, M., Mohammadi-Shemirani, P., Lali, R., Shoamanesh, A., Gerstein, H.C., Paré, G., 2019. Novel Drug Targets for Ischemic Stroke Identified Through Mendelian Randomization Analysis of the Blood Proteome. Circulation 140, 819–830. https://doi.org/10.1161/CIRCULATIONAHA.119.040180

Choy, E.H., Panayi, G.S., 2001. Cytokine pathways and joint inflammation in rheumatoid arthritis. N. Engl. J. Med. 344, 907–916. https://doi.org/10.1056/NEJM200103223441207

Chung, E.S., Packer, M., Lo, K.H., Fasanmade, A.A., Willerson, J.T., Anti-TNF Therapy Against Congestive Heart Failure Investigators, 2003. Randomized, double-blind, placebo-controlled, pilot trial of infliximab, a chimeric monoclonal antibody to tumor necrosis factor-alpha, in patients with moderate-to-severe heart failure: results of the anti-TNF Therapy Against Congestive Heart Failure (ATTACH) trial. Circulation 107, 3133–3140. https://doi.org/10.1161/01.CIR.0000077913.60364.D2

Cohen, S.B., Moreland, L.W., Cush, J.J., Greenwald, M.W., Block, S., Shergy, W.J., Hanrahan, P.S., Kraishi, M.M., Patel, A., Sun, G., Bear, M.B., 990145 Study Group, 2004. A multicentre, double blind, randomised, placebo controlled trial of anakinra (Kineret), a recombinant interleukin 1 receptor antagonist, in patients with rheumatoid arthritis treated with background methotrexate. Ann. Rheum. Dis. 63, 1062–1068. https://doi.org/10.1136/ard.2003.016014

Crawford, K.S., Volkman, B.F., 2023. Prospects for targeting ACKR1 in cancer and other diseases. Front. Immunol. 14, 1111960. https://doi.org/10.3389/fimmu.2023.1111960

Crisford, H., Sapey, E., Rogers, G.B., Taylor, S., Nagakumar, P., Lokwani, R., Simpson, J.L., 2021. Neutrophils in asthma: the good, the bad and the bacteria. Thorax 76, 835–844. https://doi.org/10.1136/thoraxjnl-2020-215986

Croce, K., Libby, P., 2007. Intertwining of thrombosis and inflammation in atherosclerosis. Curr. Opin. Hematol. 14, 55–61. https://doi.org/10.1097/00062752-200701000-00011

Cunnane, G., Madigan, A., Murphy, E., FitzGerald, O., Bresnihan, B., 2001. The effects of treatment with interleukin-1 receptor antagonist on the inflamed synovial membrane in rheumatoid arthritis. Rheumatol. Oxf. Engl. 40, 62–69. https://doi.org/10.1093/rheumatology/40.1.62

Damoiseaux, J., Andrade, L.E., Fritzler, M.J., Shoenfeld, Y., 2015. Autoantibodies 2015: From diagnostic biomarkers toward prediction, prognosis and prevention. Autoimmun. Rev. 14, 555–563. https://doi.org/10.1016/j.autrev.2015.01.017

Daniel, D., Wilson, N.S., 2008. Tumor necrosis factor: renaissance as a cancer therapeutic? Curr. Cancer Drug Targets 8, 124–131. https://doi.org/10.2174/156800908783769346

Davidson, A., Diamond, B., 2001. Autoimmune diseases. N. Engl. J. Med. 345, 340–350. https://doi.org/10.1056/NEJM200108023450506

de Bakker, P.I.W., Ferreira, M.A.R., Jia, X., Neale, B.M., Raychaudhuri, S., Voight, B.F., 2008. Practical aspects of imputation-driven meta-analysis of genome-wide association studies. Hum. Mol. Genet. 17, R122-128. https://doi.org/10.1093/hmg/ddn288

de Leeuw, C.A., Mooij, J.M., Heskes, T., Posthuma, D., 2015. MAGMA: generalized gene-set analysis of GWAS data. PLoS Comput. Biol. 11, e1004219. https://doi.org/10.1371/journal.pcbi.1004219

Deckers, J., Anbergen, T., Hokke, A.M., De Dreu, A., Schrijver, D.P., De Bruin, K., Toner, Y.C., Beldman, T.J., Spangler, J.B., De Greef, T.F.A., Grisoni, F., Van Der Meel, R., Joosten, L.A.B., Merkx, M., Netea, M.G., Mulder, W.J.M., 2023. Engineering cytokine therapeutics. Nat. Rev. Bioeng. 1, 286–303. https://doi.org/10.1038/s44222-023-00030-y

Dejaco, C., Lichtenberger, C., Miehsler, W., Oberhuber, G., Herbst, F., Vogelsang, H., Gangl, A., Reinisch, W., 2003. An open-label pilot study of granulocyte colony-stimulating factor for the treatment of severe endoscopic postoperative recurrence in Crohn's disease. Digestion 68, 63–70. https://doi.org/10.1159/000074517

DiMasi, J.A., Grabowski, H.G., Hansen, R.W., 2016. Innovation in the pharmaceutical industry: New estimates of R&D costs. J. Health Econ. 47, 20–33. https://doi.org/10.1016/j.jhealeco.2016.01.012

Ding, Si., Xie, J., Wan, Q., 2016. Association Between Cytokines and Their Receptor Antagonist Gene Polymorphisms and Clinical Risk Factors and Acute Rejection Following Renal Transplantation. Med. Sci. Monit. Int. Med. J. Exp. Clin. Res. 22, 4736–4741. https://doi.org/10.12659/msm.898193

Duncan, L.E., Ostacher, M., Ballon, J., 2019. How genome-wide association studies (GWAS) made traditional candidate gene studies obsolete. Neuropsychopharmacology 44, 1518–1523. https://doi.org/10.1038/s41386-019-0389-5

Edilova, M.I., Abdul-Sater, A.A., Watts, T.H., 2018. TRAF1 Signaling in Human Health and Disease. Front. Immunol. 9.

Eldjarn, G.H., Ferkingstad, E., Lund, S.H., Helgason, H., Magnusson, O.T., Gunnarsdottir, K., Olafsdottir, T.A., Halldorsson, B.V., Olason, P.I., Zink, F., Gudjonsson, S.A., Sveinbjornsson, G., Magnusson, M.I., Helgason, A., Oddsson, A., Halldorsson, G.H., Magnusson, M.K., Saevarsdottir, S., Eiriksdottir, T., Masson, G., Stefansson, H., Jonsdottir, I., Holm, H., Rafnar, T., Melsted, P., Saemundsdottir, J., Norddahl, G.L., Thorleifsson, G., Ulfarsson, M.O., Gudbjartsson, D.F., Thorsteinsdottir, U., Sulem, P., Stefansson, K., 2023. Large-scale plasma proteomics comparisons through genetics and disease associations. Nature 622, 348–358. https://doi.org/10.1038/s41586-023-06563-x

Fantus, R.J., Na, R., Wei, J., Shi, Z., Resurreccion, W.K., Halpern, J.A., Franco, O., Hayward, S.W., Isaacs, W.B., Zheng, S.L., Xu, J., Helfand, B.T., 2021. Genetic Susceptibility for Low Testosterone in Men and Its Implications in Biology and Screening: Data from the UK Biobank. Eur. Urol. Open Sci. 29, 36–46. https://doi.org/10.1016/j.euros.2021.04.010

Ference, B.A., 2018. How to use Mendelian randomization to anticipate the results of randomized trials. Eur. Heart J. 39, 360–362. https://doi.org/10.1093/eurheartj/ehx462

Ferkingstad, E., Sulem, P., Atlason, B.A., Sveinbjornsson, G., Magnusson, M.I., Styrmisdottir, E.L., Gunnarsdottir, K., Helgason, A., Oddsson, A., Halldorsson, B.V., Jensson, B.O., Zink, F., Halldorsson, G.H., Masson, G., Arnadottir, G.A., Katrinardottir, H., Juliusson, K., Magnusson, M.K., Magnusson, O.T., Fridriksdottir, R., Saevarsdottir, S., Gudjonsson, S.A., Stacey, S.N., Rognvaldsson, S., Eiriksdottir, T., Olafsdottir, T.A., Steinthorsdottir, V., Tragante, V., Ulfarsson, M.O., Stefansson, H., Jonsdottir, I., Holm, H., Rafnar, T., Melsted, P., Saemundsdottir, J., Norddahl, G.L., Lund, S.H., Gudbjartsson, D.F., Thorsteinsdottir, U., Stefansson, K., 2021. Large-scale integration of the plasma proteome with genetics and disease. Nat. Genet. 53, 1712–1721. https://doi.org/10.1038/s41588-021-00978-w

Fewell, Z., Davey Smith, G., Sterne, J.A.C., 2007. The impact of residual and unmeasured confounding in epidemiologic studies: a simulation study. Am. J. Epidemiol. 166, 646–655. https://doi.org/10.1093/aje/kwm165

Fleischmann, R.M., Schechtman, J., Bennett, R., Handel, M.L., Burmester, G.-R., Tesser, J., Modafferi, D., Poulakos, J., Sun, G., 2003. Anakinra, a recombinant human interleukin-1 receptor antagonist (r-metHuIL-1ra), in patients with rheumatoid arthritis: A large, international, multicenter, placebo-controlled trial. Arthritis Rheum. 48, 927–934. https://doi.org/10.1002/art.10870

Folkersen, L., Gustafsson, S., Wang, Q., Hansen, D.H., Hedman, Å.K., Schork, A., Page, K., Zhernakova, D.V., Wu, Y., Peters, J., Eriksson, N., Bergen, S.E., Boutin, T.S., Bretherick, A.D., Enroth, S., Kalnapenkis, A., Gådin, J.R., Suur, B.E., Chen, Y., Matic, L., Gale, J.D., Lee, J., Zhang, W., Quazi, A., Ala-Korpela, M., Choi, S.H., Claringbould, A., Danesh, J., Davey Smith, G., de Masi, F., Elmståhl, S., Engström, G., Fauman, E., Fernandez, C., Franke, L.,

Franks, P.W., Giedraitis, V., Haley, C., Hamsten, A., Ingason, A., Johansson, Å., Joshi, P.K., Lind, L., Lindgren, C.M., Lubitz, S., Palmer, T., Macdonald-Dunlop, E., Magnusson, M., Melander, O., Michaelsson, K., Morris, A.P., Mägi, R., Nagle, M.W., Nilsson, P.M., Nilsson, J., Orho-Melander, M., Polasek, O., Prins, B., Pålsson, E., Qi, T., Sjögren, M., Sundström, J., Surendran, P., Võsa, U., Werge, T., Wernersson, R., Westra, H.-J., Yang, J., Zhernakova, A., Ärnlöv, J., Fu, J., Smith, J.G., Esko, T., Hayward, C., Gyllensten, U., Landen, M., Siegbahn, A., Wilson, J.F., Wallentin, L., Butterworth, A.S., Holmes, M.V., Ingelsson, E., Mälarstig, A., 2020. Genomic and drug target evaluation of 90 cardiovascular proteins in 30,931 individuals. Nat. Metab. 2, 1135–1148. https://doi.org/10.1038/s42255-020-00287-2

Forgetta, V., Jiang, L., Vulpescu, N.A., Hogan, M.S., Chen, S., Morris, J.A., Grinek, S., Benner, C., Jang, D.-K., Hoang, Q., Burtt, N., Flannick, J.A., McCarthy, M.I., Fauman, E., Greenwood, C.M.T., Maurano, M.T., Richards, J.B., 2022. An effector index to predict target genes at GWAS loci. Hum. Genet. 141, 1431–1447. https://doi.org/10.1007/s00439-022-02434-z

Franceschini, N., Giambartolomei, C., de Vries, P.S., Finan, C., Bis, J.C., Huntley, R.P., Lovering, R.C., Tajuddin, S.M., Winkler, T.W., Graff, M., Kavousi, M., Dale, C., Smith, A.V., Hofer, E., van Leeuwen, E.M., Nolte, I.M., Lu, L., Scholz, M., Sargurupremraj, M., Pitkänen, N., Franzén, O., Joshi, P.K., Noordam, R., Marioni, R.E., Hwang, S.-J., Musani, S.K., Schminke, U., Palmas, W., Isaacs, A., Correa, A., Zonderman, A.B., Hofman, A., Teumer, A., Cox, A.J., Uitterlinden, A.G., Wong, A., Smit, A.J., Newman, A.B., Britton, A., Ruusalepp, A., Sennblad, B., Hedblad, B., Pasaniuc, B., Penninx, B.W., Langefeld, C.D., Wassel, C.L., Tzourio, C., Fava, C., Baldassarre, D., O'Leary, D.H., Teupser, D., Kuh, D., Tremoli, E., Mannarino, E., Grossi, E., Boerwinkle, E., Schadt, E.E., Ingelsson, E., Veglia, F., Rivadeneira, F., Beutner, F., Chauhan, G., Heiss, G., Snieder, H., Campbell, H., Völzke, H., Markus, H.S., Deary, I.J., Jukema, J.W., de Graaf, J., Price, J., Pott, J., Hopewell, J.C., Liang, J., Thiery, J., Engmann, J., Gertow, K., Rice, K., Taylor, K.D., Dhana, K., Kiemeney, L.A.L.M., Lind, L., Raffield, L.M., Launer, L.J., Holdt, L.M., Dörr, M., Dichgans, M., Traylor, M., Sitzer, M., Kumari, M., Kivimaki, M., Nalls, M.A., Melander, O., Raitakari, O., Franco, O.H., Rueda-Ochoa, O.L., Roussos, P., Whincup, P.H., Amouyel, P., Giral, P., Anugu, P., Wong, Q., Malik, R., Rauramaa, R., Burkhardt, R., Hardy, R., Schmidt, R., de Mutsert, R., Morris, R.W., Strawbridge, R.J., Wannamethee, S.G., Hägg, S., Shah, S., McLachlan, S., Trompet, S., Seshadri, S., Kurl, S., Heckbert, S.R., Ring, S., Harris, T.B., Lehtimäki, T., Galesloot, T.E., Shah, T., de Faire, U., Plagnol, V., Rosamond, W.D., Post, W., Zhu, X., Zhang, X., Guo, X., Saba, Y., MEGASTROKE Consortium, Dehghan, A., Seldenrijk, A., Morrison, A.C., Hamsten, A., Psaty, B.M., van Duijn, C.M., Lawlor, D.A., Mook-Kanamori, D.O., Bowden, D.W., Schmidt, H., Wilson, J.F., Wilson, J.G., Rotter, J.I., Wardlaw, J.M., Deanfield, J., Halcox, J., Lyytikäinen, L.-P., Loeffler, M., Evans, M.K., Debette, S., Humphries, S.E., Völker, U., Gudnason, V., Hingorani, A.D., Björkegren, J.L.M., Casas, J.P., O'Donnell, C.J., 2018. GWAS and colocalization analyses implicate carotid intima-media thickness and carotid plaque loci in cardiovascular outcomes. Nat. Commun. 9, 5141. https://doi.org/10.1038/s41467-018-07340-5

Freidin, M.B., Polonikov, A.V., 2013. Validation of PPP1R12B as a candidate gene for childhood asthma in Russians. J. Genet. 92, 93–96. https://doi.org/10.1007/s12041-013-0210-x

Furst, D.E., 2004. Anakinra: review of recombinant human interleukin-I receptor antagonist in the treatment of rheumatoid arthritis. Clin. Ther. 26, 1960–1975. https://doi.org/10.1016/j.clinthera.2004.12.019

Galon, J., Angell, H.K., Bedognetti, D., Marincola, F.M., 2013. The Continuum of Cancer Immunosurveillance: Prognostic, Predictive, and Mechanistic Signatures. Immunity 39, 11–26. https://doi.org/10.1016/j.immuni.2013.07.008

Gao, M.-M., Hu, F., Zeng, X.-D., Tang, H.-L., Zhang, H., Jiang, W., Yan, H.-J., Shi, H., Shu, Y., Long, Y.-S., 2020. Hypothalamic proteome changes in response to nicotine and its withdrawal are potentially associated with alteration in body weight. J. Proteomics 214, 103633. https://doi.org/10.1016/j.jprot.2020.103633

Georgakis, M.K., Gill, D., Rannikmäe, K., Traylor, M., Anderson, C.D., Lee, J.-M., Kamatani, Y., Hopewell, J.C., Worrall, B.B., Bernhagen, J., Sudlow, C.L.M., Malik, R., Dichgans, M., 2019. Genetically Determined Levels of Circulating Cytokines and Risk of Stroke. Circulation 139, 256–268. https://doi.org/10.1161/CIRCULATIONAHA.118.035905

Georgakis, M.K., Malik, R., Gill, D., Franceschini, N., Sudlow, C.L.M., Dichgans, M., INVENT Consortium,CHARGE Inflammation Working Group, 2020. Interleukin-6 Signaling Effects on Ischemic Stroke and Other Cardiovascular Outcomes: A Mendelian Randomization Study. Circ. Genomic Precis. Med. 13, e002872. https://doi.org/10.1161/CIRCGEN.119.002872

Gerhardt, T., Ley, K., 2015. Monocyte trafficking across the vessel wall. Cardiovasc. Res. 107, 321–330. https://doi.org/10.1093/cvr/cvv147

Gharaee-Kermani, M., Phan, S.H., 2001. Role of cytokines and cytokine therapy in wound healing and fibrotic diseases. Curr. Pharm. Des. 7, 1083–1103. https://doi.org/10.2174/1381612013397573

Giambartolomei, C., Vukcevic, D., Schadt, E.E., Franke, L., Hingorani, A.D., Wallace, C., Plagnol, V., 2014. Bayesian Test for Colocalisation between Pairs of Genetic Association Studies Using Summary Statistics. PLoS Genet. 10, e1004383. https://doi.org/10.1371/journal.pgen.1004383

Gill, D., Georgakis, M.K., Walker, V.M., Schmidt, A.F., Gkatzionis, A., Freitag, D.F., Finan, C., Hingorani, A.D., Howson, J.M.M., Burgess, S., Swerdlow, D.I., Davey Smith, G., Holmes, M.V., Dichgans, M., Scott, R.A., Zheng, J., Psaty, B.M., Davies, N.M., 2021. Mendelian randomization for studying the effects of perturbing drug targets. Wellcome Open Res. 6, 16. https://doi.org/10.12688/wellcomeopenres.16544.2

Gisterå, A., Hansson, G.K., 2017. The immunology of atherosclerosis. Nat. Rev. Nephrol. 13, 368–380. https://doi.org/10.1038/nrneph.2017.51

Goto, K., Chiba, Y., Sakai, H., Misawa, M., 2008. Glucocorticoids inhibited airway hyperresponsiveness through downregulation of CPI-17 in bronchial smooth muscle. Eur. J. Pharmacol. 591, 231–236. https://doi.org/10.1016/j.ejphar.2008.06.021

Greco M, F.D., Minelli, C., Sheehan, N.A., Thompson, J.R., 2015. Detecting pleiotropy in Mendelian randomisation studies with summary data and a continuous outcome. Stat. Med. 34, 2926–2940. https://doi.org/10.1002/sim.6522

Gregory, A.P., Dendrou, C.A., Attfield, K.E., Haghikia, A., Xifara, D.K., Butter, F., Poschmann, G., Kaur, G., Lambert, L., Leach, O.A., Prömel, S., Punwani, D., Felce, J.H., Davis, S.J., Gold, R., Nielsen, F.C., Siegel, R.M., Mann, M., Bell, J.I., McVean, G., Fugger, L., 2012. TNF receptor 1 genetic risk mirrors outcome of anti-TNF therapy in multiple sclerosis. Nature 488, 508–511. https://doi.org/10.1038/nature11307

Grover, S., Del Greco M, F., Stein, C.M., Ziegler, A., 2017. Mendelian Randomization. Methods Mol. Biol. Clifton NJ 1666, 581–628. https://doi.org/10.1007/978-1-4939-7274-6_29

GTEx Consortium, 2020. The GTEx Consortium atlas of genetic regulatory effects across human tissues. Science 369, 1318–1330. https://doi.org/10.1126/science.aaz1776

Harrison, R.K., 2016. Phase II and phase III failures: 2013-2015. Nat. Rev. Drug Discov. 15, 817–818. https://doi.org/10.1038/nrd.2016.184

Hartwig, F.P., Davies, N.M., Hemani, G., Davey Smith, G., 2016. Two-sample Mendelian randomization: avoiding the downsides of a powerful, widely applicable but potentially fallible technique. Int. J. Epidemiol. 45, 1717–1726. https://doi.org/10.1093/ije/dyx028

Haystead, T.A.J., 2005. ZIP kinase, a key regulator of myosin protein phosphatase 1. Cell. Signal. 17, 1313–1322. https://doi.org/10.1016/j.cellsig.2005.05.008

Hecker, M., Fitzner, B., Putscher, E., Schwartz, M., Winkelmann, A., Meister, S., Dudesek, A., Koczan, D., Lorenz, P., Boxberger, N., Zettl, U.K., 2022. Implication of genetic variants in primary microRNA processing sites in the risk of multiple sclerosis. EBioMedicine 80, 104052. https://doi.org/10.1016/j.ebiom.2022.104052

Herder, C., de Las Heras Gala, T., Carstensen-Kirberg, M., Huth, C., Zierer, A., Wahl, S., Sudduth-Klinger, J., Kuulasmaa, K., Peretz, D., Ligthart, S., Bongaerts, B.W.C., Dehghan, A., Ikram, M.A., Jula, A., Kee, F., Pietilä, A., Saarela, O., Zeller, T., Blankenberg, S., Meisinger, C., Peters, A., Roden, M., Salomaa, V., Koenig, W., Thorand, B., 2017. Circulating Levels of Interleukin 1-Receptor Antagonist and Risk of Cardiovascular Disease: Meta-Analysis of Six Population-Based Cohorts. Arterioscler. Thromb. Vasc. Biol. 37, 1222–1227. https://doi.org/10.1161/ATVBAHA.117.309307

Hindorff, L.A., Sethupathy, P., Junkins, H.A., Ramos, E.M., Mehta, J.P., Collins, F.S., Manolio, T.A., 2009. Potential etiologic and functional implications of genome-wide association loci for human diseases and traits. Proc. Natl. Acad. Sci. U. S. A. 106, 9362–9367. https://doi.org/10.1073/pnas.0903103106

Hojjati, S., Ernerudh, J., Vrethem, M., Mellergård, J., Raffetseder, J., 2023. Dimethyl fumarate treatment in relapsing remitting MS changes the inflammatory CSF protein profile by a prominent decrease in T-helper 1 immunity. Mult. Scler. Relat. Disord. 80, 105126. https://doi.org/10.1016/j.msard.2023.105126

Holmes, M.V., Ala-Korpela, M., Smith, G.D., 2017. Mendelian randomization in cardiometabolic disease: challenges in evaluating causality. Nat. Rev. Cardiol. 14, 577–590. https://doi.org/10.1038/nrcardio.2017.78

Holmes, M.V., Richardson, T.G., Ference, B.A., Davies, N.M., Davey Smith, G., 2021. Integrating genomics with biomarkers and therapeutic targets to invigorate cardiovascular drug development. Nat. Rev. Cardiol. 18, 435–453. https://doi.org/10.1038/s41569-020-00493-1

Huang, J., Khademi, M., Fugger, L., Lindhe, Ö., Novakova, L., Axelsson, M., Malmeström, C., Constantinescu, C., Lycke, J., Piehl, F., Olsson, T., Kockum, I., 2020. Inflammation-related plasma and CSF biomarkers for multiple sclerosis. Proc. Natl. Acad. Sci. 117, 12952–12960. https://doi.org/10.1073/pnas.1912839117

Huang, J., Su, B., Karhunen, V., Gill, D., Zuber, V., Ahola-Olli, A., Palaniswamy, S., Auvinen, J., Herzig, K.-H., Keinänen-Kiukaanniemi, S., Salmi, M., Jalkanen, S., Lehtimäki, T., Salomaa, V., Raitakari, O.T., Matthews, P.M., Elliott, P., Tsilidis, K.K., Jarvelin, M., Tzoulaki, I., Dehghan, A., 2023. Inflammatory Diseases, Inflammatory Biomarkers, and Alzheimer Disease: An Observational Analysis and Mendelian Randomization. Neurology 100. https://doi.org/10.1212/WNL.0000000000201489

Hughes, C.E., Nibbs, R.J.B., 2018. A guide to chemokines and their receptors. FEBS J. 285, 2944–2971. https://doi.org/10.1111/febs.14466

Hukerikar, N., Hingorani, A.D., Asselbergs, F.W., Finan, C., Schmidt, A.F., 2024. Prioritising genetic findings for drug target identification and validation. Atherosclerosis 390, 117462. https://doi.org/10.1016/j.atherosclerosis.2024.117462

Interleukin-6 Receptor Mendelian Randomisation Analysis (IL6R MR) Consortium, Swerdlow, D.I., Holmes, M.V., Kuchenbaecker, K.B., Engmann, J.E.L., Shah, T., Sofat, R., Guo, Y., Chung, C., Peasey, A., Pfister, R., Mooijaart, S.P., Ireland, H.A., Leusink, M., Langenberg, C., Li, K.W., Palmen, J., Howard, P., Cooper, J.A., Drenos, F., Hardy, J., Nalls, M.A., Li, Y.R., Lowe, G., Stewart, M., Bielinski, S.J., Peto, J., Timpson, N.J., Gallacher, J., Dunlop, M., Houlston, R., Tomlinson, I., Tzoulaki, I., Luan, J., Boer, J.M.A., Forouhi, N.G., Onland-Moret, N.C., van der Schouw, Y.T., Schnabel, R.B., Hubacek, J.A., Kubinova, R., Baceviciene, M., Tamosiunas, A., Pajak, A., Topor-Madry, R., Malyutina, S., Baldassarre, D., Sennblad, B., Tremoli, E., de Faire, U., Ferrucci, L., Bandenelli, S., Tanaka, T., Meschia, J.F., Singleton, A., Navis, G., Mateo Leach, I., Bakker, S.J.L., Gansevoort, R.T., Ford, I., Epstein, S.E., Burnett, M.S., Devaney, J.M., Jukema, J.W., Westendorp, R.G.J., Jan de Borst, G., van der Graaf, Y., de Jong, P.A., Mailand-van der Zee, A.-H., Klungel, O.H., de Boer, A., Doevendans, P.A., Stephens, J.W., Eaton, C.B., Robinson, J.G., Manson, J.E., Fowkes, F.G., Frayling, T.M., Price, J.F., Whincup, P.H., Morris, R.W., Lawlor, D.A., Smith, G.D., Ben-Shlomo, Y., Redline, S., Lange, L.A., Kumari, M., Wareham, N.J., Verschuren, W.M.M., Benjamin, E.J., Whittaker, J.C., Hamsten, A., Dudbridge, F., Delaney, J.A.C., Wong, A., Kuh, D., Hardy, R., Castillo, B.A., Connolly, J.J., van der Harst, P., Brunner, E.J., Marmot, M.G., Wassel, C.L., Humphries, S.E., Talmud, P.J., Kivimaki, M., Asselbergs, F.W., Voevoda, M., Bobak, M., Pikhart, H., Wilson, J.G., Hakonarson, H., Reiner, A.P., Keating, B.J., Sattar, N., Hingorani, A.D., Casas, J.P., 2012. The interleukin-6 receptor as a target for prevention of coronary heart disease: a

mendelian randomisation analysis. Lancet Lond. Engl. 379, 1214–1224. https://doi.org/10.1016/S0140-6736(12)60110-X

International Multiple Sclerosis Genetics Consortium, 2019. Multiple sclerosis genomic map implicates peripheral immune cells and microglia in susceptibility. Science 365, eaav7188. https://doi.org/10.1126/science.aav7188

Jiang, Y., Genant, H.K., Watt, I., Cobby, M., Bresnihan, B., Aitchison, R., McCabe, D., 2000. A multicenter, double-blind, dose-ranging, randomized, placebo-controlled study of recombinant human interleukin-1 receptor antagonist in patients with rheumatoid arthritis: radiologic progression and correlation of Genant and Larsen scores. Arthritis Rheum. 43, 1001–1009. https://doi.org/10.1002/1529-0131(200005)43:5<1001::AID-ANR7>3.0.CO;2-P

Jiménez-Sousa, Gómez-Moreno, Pineda-Tenor, Sánchez-Ruano, Artaza-Varasa, Martin-Vicente, Fernández-Rodríguez, Martínez, Resino, 2019. Impact of DARC rs12075 Variants on Liver Fibrosis Progression in Patients with Chronic Hepatitis C: A Retrospective Study. Biomolecules 9, 143. https://doi.org/10.3390/biom9040143

Jin, H., Li, M., Jeong, E., Castro-Martinez, F., Zuker, C.S., 2024. A body-brain circuit that regulates body inflammatory responses. Nature. https://doi.org/10.1038/s41586-024-07469-y

Kamat, M.A., Blackshaw, J.A., Young, R., Surendran, P., Burgess, S., Danesh, J., Butterworth, A.S., Staley, J.R., 2019. PhenoScanner V2: an expanded tool for searching human genotype-phenotype associations. Bioinforma. Oxf. Engl. 35, 4851–4853. https://doi.org/10.1093/bioinformatics/btz469

Kambayashi, T., Laufer, T.M., 2014. Atypical MHC class II-expressing antigen-presenting cells: can anything replace a dendritic cell? Nat. Rev. Immunol. 14, 719–730. https://doi.org/10.1038/nri3754

Kamel, H., Iadecola, C., 2012. Brain-immune interactions and ischemic stroke: clinical implications. Arch. Neurol. 69, 576–581. https://doi.org/10.1001/archneurol.2011.3590

Kappelmann, N., Arloth, J., Georgakis, M.K., Czamara, D., Rost, N., Ligthart, S., Khandaker, G.M., Binder, E.B., 2021. Dissecting the Association Between Inflammation, Metabolic Dysregulation, and Specific Depressive Symptoms: A Genetic Correlation and 2-Sample Mendelian Randomization Study. JAMA Psychiatry 78, 161–170. https://doi.org/10.1001/jamapsychiatry.2020.3436

Kidwai, S., Barbiero, P., Meijerman, I., Tonda, A., Perez-Pardo, P., Lio´, P., Van Der Maitland-Zee, A.H., Oberski, D.L., Kraneveld, A.D., Lopez-Rincon, A., 2023. A robust mRNA signature obtained via recursive ensemble feature selection predicts the responsiveness of omalizumab in moderate-to-severe asthma. Clin. Transl. Allergy 13, e12306. https://doi.org/10.1002/clt2.12306

Kim, Y.-M., Kim, H., Lee, Seungwon, Kim, S., Lee, J.-U., Choi, Y., Park, H.W., You, G., Kang, H., Lee, Seyoung, Park, J.-S., Park, Y., Park, H.-S., Park, C.-S., Lee, S.-W., 2020. Airway G-CSF identifies neutrophilic inflammation and contributes to asthma progression. Eur. Respir. J. 55, 1900827. https://doi.org/10.1183/13993003.00827-2019

King, E.A., Davis, J.W., Degner, J.F., 2019. Are drug targets with genetic support twice as likely to be approved? Revised estimates of the impact of genetic support for

drug mechanisms on the probability of drug approval. PLOS Genet. 15, e1008489. https://doi.org/10.1371/journal.pgen.1008489

Klarin, D., Lynch, J., Aragam, K., Chaffin, M., Assimes, T.L., Huang, J., Lee, K.M., Shao, Q., Huffman, J.E., Natarajan, P., Arya, S., Small, A., Sun, Y.V., Vujkovic, M., Freiberg, M.S., Wang, L., Chen, J., Saleheen, D., Lee, J.S., Miller, D.R., Reaven, P., Alba, P.R., Patterson, O.V., DuVall, S.L., Boden, W.E., Beckman, J.A., Gaziano, J.M., Concato, J., Rader, D.J., Cho, K., Chang, K.-M., Wilson, P.W.F., O'Donnell, C.J., Kathiresan, S., VA Million Veteran Program, Tsao, P.S., Damrauer, S.M., 2019. Genome-wide association study of peripheral artery disease in the Million Veteran Program. Nat. Med. 25, 1274–1279. https://doi.org/10.1038/s41591-019-0492-5

Kleveland, O., Kunszt, G., Bratlie, M., Ueland, T., Broch, K., Holte, E., Michelsen, A.E., Bendz, B., Amundsen, B.H., Espevik, T., Aakhus, S., Damås, J.K., Aukrust, P., Wiseth, R., Gullestad, L., 2016. Effect of a single dose of the interleukin-6 receptor antagonist tocilizumab on inflammation and troponin T release in patients with non-ST-elevation myocardial infarction: a double-blind, randomized, placebo-controlled phase 2 trial. Eur. Heart J. 37, 2406–2413. https://doi.org/10.1093/eurheartj/ehw171

Konieczny, M.J., Omarov, M., Malik, R., Richardson, T.G., Baumeister, S.-E., Bernhagen, J., Dichgans, M., Georgakis, M.K., 2025. The genomic architecture of circulating cytokine levels points to drug targets for immune-related diseases. Commun Biol. 2025 Jan 10;8(1):34. doi: 10.1038/s42003-025-07453-w. PMID: 39794498; PMCID: PMC11724035.

Korbecki, J., Barczak, K., Gutowska, I., Chlubek, D., Baranowska-Bosiacka, I., 2022. CXCL1: Gene, Promoter, Regulation of Expression, mRNA Stability, Regulation of Activity in the Intercellular Space. Int. J. Mol. Sci. 23, 792. https://doi.org/10.3390/ijms23020792

Korzenik, J.R., Dieckgraefe, B.K., 2005. An open-labelled study of granulocyte colony-stimulating factor in the treatment of active Crohn's disease. Aliment. Pharmacol. Ther. 21, 391–400. https://doi.org/10.1111/j.1365-2036.2005.02287.x

Korzenik, J.R., Dieckgraefe, B.K., 2000. Is Crohn's disease an immunodeficiency? A hypothesis suggesting possible early events in the pathogenesis of Crohn's disease. Dig. Dis. Sci. 45, 1121–1129. https://doi.org/10.1023/a:1005541700805

Kou, N., Zhou, W., He, Y., Ying, X., Chai, S., Fei, T., Fu, W., Huang, J., Liu, H., 2020. A Mendelian Randomization Analysis to Expose the Causal Effect of IL-18 on Osteoporosis Based on Genome-Wide Association Study Data. Front. Bioeng. Biotechnol. 8, 201. https://doi.org/10.3389/fbioe.2020.00201

Kubagawa, H., Mahmoudi Aliabadi, P., Al-Qaisi, K., Jani, P.K., Honjo, K., Izui, S., Radbruch, A., Melchers, F., 2024. Functions of IgM fc receptor (FcμR) related to autoimmunity. Autoimmunity 57, 2323563. https://doi.org/10.1080/08916934.2024.2323563

Kwak, D.-W., Park, D., Kim, J.-H., 2022. Leukotriene B4 Receptor 2 Mediates the Production of G-CSF That Plays a Critical Role in Steroid-Resistant Neutrophilic Airway Inflammation. Biomedicines 10, 2979. https://doi.org/10.3390/biomedicines10112979

Lalani, A.I., Zhu, S., Gokhale, S., Jin, J., Xie, P., 2018. TRAF Molecules in Inflammation and Inflammatory Diseases. Curr. Pharmacol. Rep. 4, 64–90. https://doi.org/10.1007/s40495-017-0117-y

Lasagni, L., Francalanci, M., Annunziato, F., Lazzeri, E., Giannini, S., Cosmi, L., Sagrinati, C., Mazzinghi, B., Orlando, C., Maggi, E., Marra, F., Romagnani, S., Serio, M., Romagnani, P., 2003. An alternatively spliced variant of CXCR3 mediates the inhibition of endothelial cell growth induced by IP-10, Mig, and I-TAC, and acts as functional receptor for platelet factor 4. J. Exp. Med. 197, 1537–1549. https://doi.org/10.1084/jem.20021897

Lau, A., So, H.-C., 2020. Turning genome-wide association study findings into opportunities for drug repositioning. Comput. Struct. Biotechnol. J. 18, 1639–1650. https://doi.org/10.1016/j.csbj.2020.06.015

Lee, J.M., Wei, S.-C., Lee, K.-M., Ye, B.D., Mao, R., Kim, H.-S., Park, S.J., Park, S.H., Oh, E.H., Im, J.P., Jang, B.I., Kim, D.B., Takeuchi, K., 2022. Clinical Course of Hepatitis B Viral Infection in Patients Undergoing Anti-Tumor Necrosis Factor α Therapy for Inflammatory Bowel Disease. Gut Liver 16, 396–403. https://doi.org/10.5009/gnl210081

Lee, S., Margolin, K., 2011. Cytokines in cancer immunotherapy. Cancers 3, 3856–3893. https://doi.org/10.3390/cancers3043856

Lemanske, R.F., Busse, W.W., 2010. Asthma: clinical expression and molecular mechanisms. J. Allergy Clin. Immunol. 125, S95-102. https://doi.org/10.1016/j.jaci.2009.10.047

Li, L., Aviña-Zubieta, J.A., Bernstein, C.N., Kaplan, G.G., Tremlett, H., Xie, H., Peña-Sánchez, J.-N., Marrie, R.A., Etminan, M., 2023. Risk of Multiple Sclerosis Among Users of Antitumor Necrosis Factor α in 4 Canadian Provinces: A Population-Based Study. Neurology 100. https://doi.org/10.1212/WNL.0000000000201472

Libby, P., 2013. Mechanisms of acute coronary syndromes and their implications for therapy. N. Engl. J. Med. 368, 2004–2013. https://doi.org/10.1056/NEJMra1216063

Lin, J.X., Migone, T.S., Tsang, M., Friedmann, M., Weatherbee, J.A., Zhou, L., Yamauchi, A., Bloom, E.T., Mietz, J., John, S., 1995. The role of shared receptor motifs and common Stat proteins in the generation of cytokine pleiotropy and redundancy by IL-2, IL-4, IL-7, IL-13, and IL-15. Immunity 2, 331–339. https://doi.org/10.1016/1074-7613(95)90141-8

Liu, B., Qian, Y., Li, Y., Shen, X., Ye, D., Mao, Y., Sun, X., 2023. Circulating levels of cytokines and risk of inflammatory bowel disease: evidence from genetic data. Front. Immunol. 14, 1310086. https://doi.org/10.3389/fimmu.2023.1310086

Liu, J.Z., van Sommeren, S., Huang, H., Ng, S.C., Alberts, R., Takahashi, A., Ripke, S., Lee, J.C., Jostins, L., Shah, T., Abedian, S., Cheon, J.H., Cho, J., Dayani, N.E., Franke, L., Fuyuno, Y., Hart, A., Juyal, R.C., Juyal, G., Kim, W.H., Morris, A.P., Poustchi, H., Newman, W.G., Midha, V., Orchard, T.R., Vahedi, H., Sood, A., Sung, J.Y., Malekzadeh, R., Westra, H.-J., Yamazaki, K., Yang, S.-K., International Multiple Sclerosis Genetics Consortium, International IBD Genetics Consortium, Barrett, J.C., Alizadeh, B.Z., Parkes, M., Bk, T., Daly, M.J., Kubo, M., Anderson, C.A., Weersma, R.K., 2015. Association analyses identify 38 susceptibility loci for inflammatory bowel disease and highlight

shared genetic risk across populations. Nat. Genet. 47, 979–986. https://doi.org/10.1038/ng.3359

Lou, H., Ling, G.S., Cao, X., 2022. Autoantibodies in systemic lupus erythematosus: From immunopathology to therapeutic target. J. Autoimmun. 132, 102861. https://doi.org/10.1016/j.jaut.2022.102861

Lutgens, E., Atzler, D., Döring, Y., Duchene, J., Steffens, S., Weber, C., 2019. Immunotherapy for cardiovascular disease. Eur. Heart J. 40, 3937–3946. https://doi.org/10.1093/eurheartj/ehz283

Mann, D.L., McMurray, J.J.V., Packer, M., Swedberg, K., Borer, J.S., Colucci, W.S., Djian, J., Drexler, H., Feldman, A., Kober, L., Krum, H., Liu, P., Nieminen, M., Tavazzi, L., van Veldhuisen, D.J., Waldenstrom, A., Warren, M., Westheim, A., Zannad, F., Fleming, T., 2004. Targeted anticytokine therapy in patients with chronic heart failure: results of the Randomized Etanercept Worldwide Evaluation (RENEWAL). Circulation 109, 1594–1602. https://doi.org/10.1161/01.CIR.0000124490.27666.B2

Martins, A., Han, J., Kim, S.O., 2010. The multifaceted effects of granulocyte colony-stimulating factor in immunomodulation and potential roles in intestinal immune homeostasis. IUBMB Life 62, 611–617. https://doi.org/10.1002/iub.361

Mayer, L., Sandborn, W.J., Stepanov, Y., Geboes, K., Hardi, R., Yellin, M., Tao, X., Xu, L.A., Salter-Cid, L., Gujrathi, S., Aranda, R., Luo, A.Y., 2014. Anti-IP-10 antibody (BMS-936557) for ulcerative colitis: a phase II randomised study. Gut 63, 442–450. https://doi.org/10.1136/gutjnl-2012-303424

McDermott, D.F., Atkins, M.B., 2006. Interleukin-2 therapy of metastatic renal cell carcinoma--predictors of response. Semin. Oncol. 33, 583–587. https://doi.org/10.1053/j.seminoncol.2006.06.004

McKay, J.D., Hung, R.J., Han, Y., Zong, X., Carreras-Torres, R., Christiani, D.C., Caporaso, N.E., Johansson, Mattias, Xiao, X., Li, Y., Byun, J., Dunning, A., Pooley, K.A., Qian, D.C., Ji, X., Liu, G., Timofeeva, M.N., Bojesen, S.E., Wu, X., Le Marchand, L., Albanes, D., Bickeböller, H., Aldrich, M.C., Bush, W.S., Tardon, A., Rennert, G., Teare, M.D., Field, J.K., Kiemeney, L.A., Lazarus, P., Haugen, A., Lam, S., Schabath, M.B., Andrew, A.S., Shen, H., Hong, Y.-C., Yuan, J.-M., Bertazzi, P.A., Pesatori, A.C., Ye, Y., Diao, N., Su, L., Zhang, R., Brhane, Y., Leighl, N., Johansen, J.S., Mellemgaard, A., Saliba, W., Haiman, C.A., Wilkens, L.R., Fernandez-Somoano, A., Fernandez-Tardon, G., van der Heijden, H.F.M., Kim, J.H., Dai, J., Hu, Z., Davies, M.P.A., Marcus, M.W., Brunnström, H., Manjer, J., Melander, O., Muller, D.C., Overvad, K., Trichopoulou, A., Tumino, R., Doherty, J.A., Barnett, M.P., Chen, C., Goodman, G.E., Cox, A., Taylor, F., Woll, P., Brüske, I., Wichmann, H.-E., Manz, J., Muley, T.R., Risch, A., Rosenberger, A., Grankvist, K., Johansson, Mikael, Shepherd, F.A., Tsao, M.-S., Arnold, S.M., Haura, E.B., Bolca, C., Holcatova, I., Janout, V., Kontic, M., Lissowska, J., Mukeria, A., Ognjanovic, S., Orlowski, T.M., Scelo, G., Swiatkowska, B., Zaridze, D., Bakke, P., Skaug, V., Zienolddiny, S., Duell, E.J., Butler, L.M., Koh, W.-P., Gao, Y.-T., Houlston, R.S., McLaughlin, J., Stevens, V.L., Joubert, P., Lamontagne, M., Nickle, D.C., Obeidat, M., Timens, W., Zhu, B., Song, L., Kachuri, L., Artigas, M.S., Tobin, M.D., Wain, L.V., SpiroMeta Consortium, Rafnar, T., Thorgeirsson, T.E., Reginsson, G.W., Stefansson, K., Hancock, D.B., Bierut, L.J., Spitz, M.R., Gaddis, N.C., Lutz, S.M., Gu, F., Johnson, E.O., Kamal, A., Pikielny, C., Zhu,

D., Lindströem, S., Jiang, X., Tyndale, R.F., Chenevix-Trench, G., Beesley, J., Bossé, Y., Chanock, S., Brennan, P., Landi, M.T., Amos, C.I., 2017. Large-scale association analysis identifies new lung cancer susceptibility loci and heterogeneity in genetic susceptibility across histological subtypes. Nat. Genet. 49, 1126–1132. https://doi.org/10.1038/ng.3892

Minati, R., Perreault, C., Thibault, P., 2020. A Roadmap Toward the Definition of Actionable Tumor-Specific Antigens. Front. Immunol. 11, 583287. https://doi.org/10.3389/fimmu.2020.583287

Minikel, Eric Vallabh, Karczewski, K.J., Martin, H.C., Cummings, B.B., Whiffin, N., Rhodes, D., Alföldi, J., Trembath, R.C., Van Heel, D.A., Daly, M.J., Genome Aggregation Database Production Team, Alföldi, J., Armean, I.M., Banks, E., Bergelson, L., Cibulskis, K., Collins, R.L., Connolly, K.M., Covarrubias, M., Cummings, B.B., Daly, M.J., Donnelly, S., Farjoun, Y., Ferriera, S., Francioli, L., Gabriel, S., Gauthier, L.D., Gentry, J., Gupta, N., Jeandet, T., Kaplan, D., Karczewski, K.J., Laricchia, K.M., Llanwarne, C., Minikel, Eric V., Munshi, R., Neale, B.M., Novod, S., O'Donnell-Luria, A.H., Petrillo, N., Poterba, T., Roazen, D., Ruano-Rubio, V., Saltzman, A., Samocha, K.E., Schleicher, M., Seed, C., Solomonson, M., Soto, J., Tiao, G., Tibbetts, K., Tolonen, C., Vittal, C., Wade, G., Wang, A., Wang, Q., Ware, J.S., Watts, N.A., Weisburd, B., Whiffin, N., Genome Aggregation Database Consortium, Aguilar Salinas, C.A., Ahmad, T., Albert, C.M., Ardissino, D., Atzmon, G., Barnard, J., Beaugerie, L., Benjamin, E.J., Boehnke, M., Bonnycastle, L.L., Bottinger, E.P., Bowden, D.W., Bown, M.J., Chambers, J.C., Chan, J.C., Chasman, D., Cho, J., Chung, M.K., Cohen, B., Correa, A., Dabelea, D., Daly, M.J., Darbar, D., Duggirala, R., Dupuis, J., Ellinor, P.T., Elosua, R., Erdmann, J., Esko, T., Färkkilä, M., Florez, J., Franke, A., Getz, G., Glaser, B., Glatt, S.J., Goldstein, D., Gonzalez, C., Groop, L., Haiman, C., Hanis, C., Harms, M., Hiltunen, M., Holi, M.M., Hultman, C.M., Kallela, M., Kaprio, J., Kathiresan, S., Kim, B.-J., Kim, Y.J., Kirov, G., Kooner, J., Koskinen, S., Krumholz, H.M., Kugathasan, S., Kwak, S.H., Laakso, M., Lehtimäki, T., Loos, R.J.F., Lubitz, S.A., Ma, R.C.W., MacArthur, D.G., Marrugat, J., Mattila, K.M., McCarroll, S., McCarthy, M.I., McGovern, D., McPherson, R., Meigs, J.B., Melander, O., Metspalu, A., Neale, B.M., Nilsson, P.M., O'Donovan, M.C., Ongur, D., Orozco, L., Owen, M.J., Palmer, C.N.A., Palotie, A., Park, K.S., Pato, C., Pulver, A.E., Rahman, N., Remes, A.M., Rioux, J.D., Ripatti, S., Roden, D.M., Saleheen, D., Salomaa, V., Samani, N.J., Scharf, J., Schunkert, H., Shoemaker, M.B., Sklar, P., Soininen, H., Sokol, H., Spector, T., Sullivan, P.F., Suvisaari, J., Tai, E.S., Teo, Y.Y., Tiinamaija, T., Tsuang, M., Dan Turner, T., Tusie-Luna, T., Vartiainen, E., Vawter, M.P., Ware, James.S., Watkins, H., Weersma, R.K., Wessman, M., Wilson, J.G., Xavier, R.J., Schreiber, S.L., MacArthur, D.G., 2020. Evaluating drug targets through human loss-of-function genetic variation. Nature 581, 459–464. https://doi.org/10.1038/s41586-020-2267-z

Mishra, A., Malik, R., Hachiya, T., Jürgenson, T., Namba, S., Posner, D.C., Kamanu, F.K., Koido, M., Le Grand, Q., Shi, M., He, Y., Georgakis, M.K., Caro, I., Krebs, K., Liaw, Y.-C., Vaura, F.C., Lin, K., Winsvold, B.S., Srinivasasainagendra, V., Parodi, L., Bae, H.-J., Chauhan, G., Chong, M.R., Tomppo, L., Akinyemi, R., Roshchupkin, G.V., Habib, N., Jee, Y.H., Thomassen, J.Q., Abedi, V., Cárcel-Márquez, J., Nygaard, M., Leonard, H.L., Yang, C., Yonova-Doing, E., Knol, M.J., Lewis, A.J., Judy, R.L., Ago, T., Amouyel, P., Armstrong, N.D., Bakker, M.K., Bartz, T.M., Bennett, D.A., Bis,

J.C., Bordes, C., Børte, S., Cain, A., Ridker, P.M., Cho, K., Chen, Z., Cruchaga, C., Cole, J.W., de Jager, P.L., de Cid, R., Endres, M., Ferreira, L.E., Geerlings, M.I., Gasca, N.C., Gudnason, V., Hata, J., He, J., Heath, A.K., Ho, Y.-L., Havulinna, A.S., Hopewell, J.C., Hyacinth, H.I., Inouye, M., Jacob, M.A., Jeon, C.E., Jern, C., Kamouchi, M., Keene, K.L., Kitazono, T., Kittner, S.J., Konuma, T., Kumar, A., Lacaze, P., Launer, L.J., Lee, K.-J., Lepik, K., Li, J., Li, L., Manichaikul, A., Markus, H.S., Marston, N.A., Meitinger, T., Mitchell, B.D., Montellano, F.A., Morisaki, T., Mosley, T.H., Nalls, M.A., Nordestgaard, B.G., O'Donnell, M.J., Okada, Y., Onland-Moret, N.C., Ovbiagele, B., Peters, A., Psaty, B.M., Rich, S.S., Rosand, J., Sabatine, M.S., Sacco, R.L., Saleheen, D., Sandset, E.C., Salomaa, V., Sargurupremraj, M., Sasaki, M., Satizabal, C.L., Schmidt, C.O., Shimizu, A., Smith, N.L., Sloane, K.L., Sutoh, Y., Sun, Y.V., Tanno, K., Tiedt, S., Tatlisumak, T., Torres-Aguila, N.P., Tiwari, H.K., Trégouët, D.-A., Trompet, S., Tuladhar, A.M., Tybjærg-Hansen, A., van Vugt, M., Vibo, R., Verma, S.S., Wiggins, K.L., Wennberg, P., Woo, D., Wilson, P.W.F., Xu, H., Yang, Q., Yoon, K., COMPASS Consortium, INVENT Consortium, Dutch Parelsnoer Initiative (PSI) Cerebrovascular Disease Study Group, Estonian Biobank, PRECISE4Q Consortium, FinnGen Consortium, NINDS Stroke Genetics Network (SiGN), MEGASTROKE Consortium, SIREN Consortium, China Kadoorie Biobank Collaborative Group, VA Million Veteran Program, International Stroke Genetics Consortium (ISGC), Biobank Japan, CHARGE Consortium, GIGASTROKE Consortium, Millwood, I.Y., Gieger, C., Ninomiya, T., Grabe, H.J., Jukema, J.W., Rissanen, I.L., Strbian, D., Kim, Y.J., Chen, P.-H., Mayerhofer, E., Howson, J.M.M., Irvin, M.R., Adams, H., Wassertheil-Smoller, S., Christensen, K., Ikram, M.A., Rundek, T., Worrall, B.B., Lathrop, G.M., Riaz, M., Simonsick, E.M., Kõrv, J., França, P.H.C., Zand, R., Prasad, K., Frikke-Schmidt, R., de Leeuw, F.-E., Liman, T., Haeusler, K.G., Ruigrok, Y.M., Heuschmann, P.U., Longstreth, W.T., Jung, K.J., Bastarache, L., Paré, G., Damrauer, S.M., Chasman, D.I., Rotter, J.I., Anderson, C.D., Zwart, J.-A., Niiranen, T.J., Fornage, M., Liaw, Y.-P., Seshadri, S., Fernández-Cadenas, I., Walters, R.G., Ruff, C.T., Owolabi, M.O., Huffman, J.E., Milani, L., Kamatani, Y., Dichgans, M., Debette, S., 2022. Stroke genetics informs drug discovery and risk prediction across ancestries. Nature 611, 115–123. https://doi.org/10.1038/s41586-022-05165-3

Mitoma, H., Horiuchi, T., Tsukamoto, H., Ueda, N., 2018. Molecular mechanisms of action of anti-TNF-α agents – Comparison among therapeutic TNF-α antagonists. Cytokine 101, 56–63. https://doi.org/10.1016/j.cyto.2016.08.014

Mokry, L.E., Ahmad, O., Forgetta, V., Thanassoulis, G., Richards, J.B., 2015. Mendelian randomisation applied to drug development in cardiovascular disease: a review. J. Med. Genet. 52, 71–79. https://doi.org/10.1136/jmedgenet-2014-102438

Mokry, L.E., Zhou, S., Guo, C., Scott, R.A., Devey, L., Langenberg, C., Wareham, N., Waterworth, D., Cardon, L., Sanseau, P., Davey Smith, G., Richards, J.B., 2019. Interleukin-18 as a drug repositioning opportunity for inflammatory bowel disease: A Mendelian randomization study. Sci. Rep. 9, 9386. https://doi.org/10.1038/s41598-019-45747-2

Monaco, C., Nanchahal, J., Taylor, P., Feldmann, M., 2015. Anti-TNF therapy: past, present and future. Int. Immunol. 27, 55–62. https://doi.org/10.1093/intimm/dxu102

Mortezaei, Z., Tavallaei, M., 2021. Recent innovations and in-depth aspects of post-genome wide association study (Post-GWAS) to understand the genetic basis of complex phenotypes. Heredity 127, 485–497. https://doi.org/10.1038/s41437-021-00479-w

Morton, A.C., Rothman, A.M.K., Greenwood, J.P., Gunn, J., Chase, A., Clarke, B., Hall, A.S., Fox, K., Foley, C., Banya, W., Wang, D., Flather, M.D., Crossman, D.C., 2015. The effect of interleukin-1 receptor antagonist therapy on markers of inflammation in non-ST elevation acute coronary syndromes: the MRC-ILA Heart Study. Eur. Heart J. 36, 377–384. https://doi.org/10.1093/eurheartj/ehu272

Mountjoy, E., Schmidt, E.M., Carmona, M., Schwartzentruber, J., Peat, G., Miranda, A., Fumis, L., Hayhurst, J., Buniello, A., Karim, M.A., Wright, D., Hercules, A., Papa, E., Fauman, E.B., Barrett, J.C., Todd, J.A., Ochoa, D., Dunham, I., Ghoussaini, M., 2021. An open approach to systematically prioritize causal variants and genes at all published human GWAS trait-associated loci. Nat. Genet. 53, 1527–1533. https://doi.org/10.1038/s41588-021-00945-5

Nikpay, M., Goel, A., Won, H.-H., Hall, L.M., Willenborg, C., Kanoni, S., Saleheen, D., Kyriakou, T., Nelson, C.P., Hopewell, J.C., Webb, T.R., Zeng, L., Dehghan, A., Alver, M., Armasu, S.M., Auro, K., Bjonnes, A., Chasman, D.I., Chen, S., Ford, I., Franceschini, N., Gieger, C., Grace, C., Gustafsson, S., Huang, Jie, Hwang, S.-J., Kim, Y.K., Kleber, M.E., Lau, K.W., Lu, X., Lu, Y., Lyytikäinen, L.-P., Mihailov, E., Morrison, A.C., Pervjakova, N., Qu, L., Rose, L.M., Salfati, E., Saxena, R., Scholz, M., Smith, A.V., Tikkanen, E., Uitterlinden, A., Yang, X., Zhang, W., Zhao, W., de Andrade, M., de Vries, P.S., van Zuydam, N.R., Anand, S.S., Bertram, L., Beutner, F., Dedoussis, G., Frossard, P., Gauguier, D., Goodall, A.H., Gottesman, O., Haber, M., Han, B.-G., Huang, Jianfeng, Jalilzadeh, S., Kessler, T., König, I.R., Lannfelt, L., Lieb, W., Lind, L., Lindgren, C.M., Lokki, M.-L., Magnusson, P.K., Mallick, N.H., Mehra, N., Meitinger, T., Memon, F.-U.-R., Morris, A.P., Nieminen, M.S., Pedersen, N.L., Peters, A., Rallidis, L.S., Rasheed, A., Samuel, M., Shah, S.H., Sinisalo, J., Stirrups, K.E., Trompet, S., Wang, L., Zaman, K.S., Ardissino, D., Boerwinkle, E., Borecki, I.B., Bottinger, E.P., Buring, J.E., Chambers, J.C., Collins, R., Cupples, L.A., Danesh, J., Demuth, I., Elosua, R., Epstein, S.E., Esko, T., Feitosa, M.F., Franco, O.H., Franzosi, M.G., Granger, C.B., Gu, D., Gudnason, V., Hall, A.S., Hamsten, A., Harris, T.B., Hazen, S.L., Hengstenberg, C., Hofman, A., Ingelsson, E., Iribarren, C., Jukema, J.W., Karhunen, P.J., Kim, B.-J., Kooner, J.S., Kullo, I.J., Lehtimäki, T., Loos, R.J.F., Melander, O., Metspalu, A., März, W., Palmer, C.N., Perola, M., Quertermous, T., Rader, D.J., Ridker, P.M., Ripatti, S., Roberts, R., Salomaa, V., Sanghera, D.K., Schwartz, S.M., Seedorf, U., Stewart, A.F., Stott, D.J., Thiery, J., Zalloua, P.A., O'Donnell, C.J., Reilly, M.P., Assimes, T.L., Thompson, J.R., Erdmann, J., Clarke, R., Watkins, H., Kathiresan, S., McPherson, R., Deloukas, P., Schunkert, H., Samani, N.J., Farrall, M., 2015. A comprehensive 1,000 Genomes-based genome-wide association meta-analysis of coronary artery disease. Nat. Genet. 47, 1121–1130. https://doi.org/10.1038/ng.3396

Nishimoto, N., Kishimoto, T., 2004. Inhibition of IL-6 for the treatment of inflammatory diseases. Curr. Opin. Pharmacol. 4, 386–391. https://doi.org/10.1016/j.coph.2004.03.005

Okada, T., Kawada, T., 1987. [Function of implanted prosthetic heart valves]. Kokyu To Junkan 35, 1053–1058.

Okada, Y., Wu, D., Trynka, G., Raj, T., Terao, C., Ikari, K., Kochi, Y., Ohmura, K., Suzuki, A., Yoshida, S., Graham, R.R., Manoharan, A., Ortmann, W., Bhangale, T., Denny, J.C., Carroll, R.J., Eyler, A.E., Greenberg, J.D., Kremer, J.M., Pappas, D.A., Jiang, L., Yin, J., Ye, L., Su, D.-F., Yang, J., Xie, G., Keystone, E., Westra, H.-J., Esko, T., Metspalu, A., Zhou, X., Gupta, N., Mirel, D., Stahl, E.A., Diogo, D., Cui, J., Liao, K., Guo, M.H., Myouzen, K., Kawaguchi, T., Coenen, M.J.H., van Riel, P.L.C.M., van de Laar, M.A.F.J., Guchelaar, H.-J., Huizinga, T.W.J., Dieudé, P., Mariette, X., Bridges, S.L., Zhernakova, A., Toes, R.E.M., Tak, P.P., Miceli-Richard, C., Bang, S.-Y., Lee, H.-S., Martin, J., Gonzalez-Gay, M.A., Rodriguez-Rodriguez, L., Rantapää-Dahlqvist, S., Arlestig, L., Choi, H.K., Kamatani, Y., Galan, P., Lathrop, M., RACI consortium, GARNET consortium, Eyre, S., Bowes, J., Barton, A., de Vries, N., Moreland, L.W., Criswell, L.A., Karlson, E.W., Taniguchi, A., Yamada, R., Kubo, M., Liu, J.S., Bae, S.-C., Worthington, J., Padyukov, L., Klareskog, L., Gregersen, P.K., Raychaudhuri, S., Stranger, B.E., De Jager, P.L., Franke, L., Visscher, P.M., Brown, M.A., Yamanaka, H., Mimori, T., Takahashi, A., Xu, H., Behrens, T.W., Siminovitch, K.A., Momohara, S., Matsuda, F., Yamamoto, K., Plenge, R.M., 2014. Genetics of rheumatoid arthritis contributes to biology and drug discovery. Nature 506, 376–381. https://doi.org/10.1038/nature12873

Opal, S.M., DePalo, V.A., 2000. Anti-inflammatory cytokines. Chest 117, 1162–1172. https://doi.org/10.1378/chest.117.4.1162

Ouyang, S., Liu, C., Xiao, J., Chen, X., Lui, A.C., Li, X., 2020. Targeting IL-17A/glucocorticoid synergy to CSF3 expression in neutrophilic airway diseases. JCI Insight 5, e132836, 132836. https://doi.org/10.1172/jci.insight.132836

Parente, R., Clark, S.J., Inforzato, A., Day, A.J., 2017. Complement factor H in host defense and immune evasion. Cell. Mol. Life Sci. CMLS 74, 1605–1624. https://doi.org/10.1007/s00018-016-2418-4

Park, H.H., 2021. Structural feature of TRAFs, their related human diseases and therapeutic intervention. Arch. Pharm. Res. 44, 475–486. https://doi.org/10.1007/s12272-021-01330-w

Park, J.-H., Wacholder, S., Gail, M.H., Peters, U., Jacobs, K.B., Chanock, S.J., Chatterjee, N., 2010. Estimation of effect size distribution from genome-wide association studies and implications for future discoveries. Nat. Genet. 42, 570–575. https://doi.org/10.1038/ng.610

Pisetsky, D.S., 2023. Pathogenesis of autoimmune disease. Nat. Rev. Nephrol. 19, 509–524. https://doi.org/10.1038/s41581-023-00720-1

PPP1R37 protein phosphatase 1 regulatory subunit 37 [Homo sapiens (human)] [WWW Document], 2023. . Gene - NCBI. URL https://www.ncbi.nlm.nih.gov/gene/284352.

Prabhu, S.D., Frangogiannis, N.G., 2016. The Biological Basis for Cardiac Repair After Myocardial Infarction: From Inflammation to Fibrosis. Circ. Res. 119, 91–112. https://doi.org/10.1161/CIRCRESAHA.116.303577

Prehn, R.T., Main, J.M., 1957. Immunity to methylcholanthrene-induced sarcomas. J. Natl. Cancer Inst. 18, 769–778.

Pulendran, B., Davis, M.M., 2020. The science and medicine of human immunology. Science 369, eaay4014. https://doi.org/10.1126/science.aay4014

Purcell, S., Neale, B., Todd-Brown, K., Thomas, L., Ferreira, M.A.R., Bender, D., Maller, J., Sklar, P., de Bakker, P.I.W., Daly, M.J., Sham, P.C., 2007. PLINK: a tool set for whole-genome association and population-based linkage analyses. Am. J. Hum. Genet. 81, 559–575. https://doi.org/10.1086/519795

Qiao, Y.Q., Shen, J., Gu, Y., Tong, J.L., Xu, X.T., Huang, M.L., Ran, Z.H., 2013. Gene expression of tumor necrosis factor receptor associated-factor (TRAF)-1 and TRAF -2 in inflammatory bowel disease. J. Dig. Dis. 14, 244–250. https://doi.org/10.1111/1751-2980.12044

Rahman, S., Patel, R.K., Boden, E., Tsikitis, V.L., 2024. Medical Management of Inflammatory Bowel Disease. Surg. Clin. North Am. 104, 657–671. https://doi.org/10.1016/j.suc.2023.12.005

Raitakari, O.T., Juonala, M., Rönnemaa, T., Keltikangas-Järvinen, L., Räsänen, L., Pietikäinen, M., Hutri-Kähönen, N., Taittonen, L., Jokinen, E., Marniemi, J., Jula, A., Telama, R., Kähönen, M., Lehtimäki, T., Åkerblom, H.K., Viikari, J.S., 2008. Cohort Profile: The Cardiovascular Risk in Young Finns Study. Int. J. Epidemiol. 37, 1220–1226. https://doi.org/10.1093/ije/dym225

Rashkin, S.R., Graff, R.E., Kachuri, L., Thai, K.K., Alexeeff, S.E., Blatchins, M.A., Cavazos, T.B., Corley, D.A., Emami, N.C., Hoffman, J.D., Jorgenson, E., Kushi, L.H., Meyers, T.J., Van Den Eeden, S.K., Ziv, E., Habel, L.A., Hoffmann, T.J., Sakoda, L.C., Witte, J.S., 2020. Pan-cancer study detects genetic risk variants and shared genetic basis in two large cohorts. Nat. Commun. 11, 4423. https://doi.org/10.1038/s41467-020-18246-6

Reich, D.S., Lucchinetti, C.F., Calabresi, P.A., 2018. Multiple Sclerosis. N. Engl. J. Med. 378, 169–180. https://doi.org/10.1056/NEJMra1401483

Richter, F., Liebig, T., Guenzi, E., Herrmann, A., Scheurich, P., Pfizenmaier, K., Kontermann, R.E., 2013. Antagonistic TNF Receptor One-Specific Antibody (ATROSAB): Receptor Binding and In Vitro Bioactivity. PLoS ONE 8, e72156. https://doi.org/10.1371/journal.pone.0072156

Ridker, P.M., Devalaraja, M., Baeres, F.M.M., Engelmann, M.D.M., Hovingh, G.K., Ivkovic, M., Lo, L., Kling, D., Pergola, P., Raj, D., Libby, P., Davidson, M., 2021. IL-6 inhibition with ziltivekimab in patients at high atherosclerotic risk (RESCUE): a double-blind, randomised, placebo-controlled, phase 2 trial. The Lancet 397, 2060–2069. https://doi.org/10.1016/S0140-6736(21)00520-1

Ridker, P.M., Everett, B.M., Pradhan, A., MacFadyen, J.G., Solomon, D.H., Zaharris, E., Mam, V., Hasan, A., Rosenberg, Y., Iturriaga, E., Gupta, M., Tsigoulis, M., Verma, S., Clearfield, M., Libby, P., Goldhaber, S.Z., Seagle, R., Ofori, C., Saklayen, M., Butman, S., Singh, N., Le May, M., Bertrand, O., Johnston, J., Paynter, N.P., Glynn, R.J., CIRT Investigators, 2019. Low-Dose Methotrexate for the Prevention of Atherosclerotic Events. N. Engl. J. Med. 380, 752–762. https://doi.org/10.1056/NEJMoa1809798

Ridker, P.M., Everett, B.M., Thuren, T., MacFadyen, J.G., Chang, W.H., Ballantyne, C., Fonseca, F., Nicolau, J., Koenig, W., Anker, S.D., Kastelein, J.J.P., Cornel, J.H., Pais, P., Pella, D., Genest, J., Cifkova, R., Lorenzatti, A., Forster, T., Kobalava, Z., Vida-Simiti, L., Flather, M., Shimokawa, H., Ogawa, H., Dellborg, M., Rossi, P.R.F., Troquay, R.P.T., Libby, P., Glynn, R.J., 2017. Antiinflammatory Therapy with Canakinumab for Atherosclerotic Disease. N. Engl. J. Med. 377, 1119–1131. https://doi.org/10.1056/NEJMoa1707914

Ritchie, S.C., Würtz, P., Nath, A.P., Abraham, G., Havulinna, A.S., Fearnley, L.G., Sarin, A.-P., Kangas, A.J., Soininen, P., Aalto, K., Seppälä, I., Raitoharju, E., Salmi, M., Maksimow, M., Männistö, S., Kähönen, M., Juonala, M., Ripatti, S., Lehtimäki, T., Jalkanen, S., Perola, M., Raitakari, O., Salomaa, V., Ala-Korpela, M., Kettunen, J., Inouye, M., 2015. The Biomarker GlycA Is Associated with Chronic Inflammation and Predicts Long-Term Risk of Severe Infection. Cell Syst. 1, 293–301. https://doi.org/10.1016/j.cels.2015.09.007

Rodien, P., Madec, A.M., Ruf, J., Rajas, F., Bornet, H., Carayon, P., Orgiazzi, J., 1996. Antibody-dependent cell-mediated cytotoxicity in autoimmune thyroid disease: relationship to antithyroperoxidase antibodies. J. Clin. Endocrinol. Metab. 81, 2595–2600. https://doi.org/10.1210/jcem.81.7.8675583

Romme Christensen, J., Börnsen, L., Hesse, D., Krakauer, M., Sørensen, P.S., Søndergaard, H.B., Sellebjerg, F., 2012. Cellular sources of dysregulated cytokines in relapsing-remitting multiple sclerosis. J. Neuroinflammation 9, 215. https://doi.org/10.1186/1742-2094-9-215

Rose, A.B., 2019. Introns as Gene Regulators: A Brick on the Accelerator. Front. Genet. 9.

Rosenfeld, P.J., Moshfeghi, A.A., Puliafito, C.A., 2005. Optical Coherence Tomography Findings After an Intravitreal Injection of Bevacizumab (Avastin®) for Neovascular Age-Related Macular Degeneration. Ophthalmic Surg. Lasers Imaging Retina 36, 331–335. https://doi.org/10.3928/1542-8877-20050701-14

Ruddle, N.H., 2014. Lymphotoxin and TNF: How it all began—A tribute to the travelers. Cytokine Growth Factor Rev. 25, 83–89. https://doi.org/10.1016/j.cytogfr.2014.02.001

Sainathan, S.K., Hanna, E.M., Gong, Q., Bishnupuri, K.S., Luo, Q., Colonna, M., White, F.V., Croze, E., Houchen, C., Anant, S., Dieckgraefe, B.K., 2008. Granulocyte macrophage colony-stimulating factor ameliorates DSS-induced experimental colitis. Inflamm. Bowel Dis. 14, 88–99. https://doi.org/10.1002/ibd.20279

Schmidt, A.F., Finan, C., Gordillo-Marañón, M., Asselbergs, F.W., Freitag, D.F., Patel, R.S., Tyl, B., Chopade, S., Faraway, R., Zwierzyna, M., Hingorani, A.D., 2020. Genetic drug target validation using Mendelian randomisation. Nat. Commun. 11, 3255. https://doi.org/10.1038/s41467-020-16969-0

Schmidt, A.F., Hingorani, A.D., Finan, C., 2022. Human Genomics and Drug Development. Cold Spring Harb. Perspect. Med. 12, a039230. https://doi.org/10.1101/cshperspect.a039230

Schnabel, R.B., Baumert, J., Barbalic, M., Dupuis, J., Ellinor, P.T., Durda, P., Dehghan, A., Bis, J.C., Illig, T., Morrison, A.C., Jenny, N.S., Keaney, J.F., Gieger, C., Tilley, C., Yamamoto, J.F., Khuseyinova, N., Heiss, G., Doyle, M., Blankenberg, S., Herder, C., Walston, J.D., Zhu, Y., Vasan, R.S., Klopp, N., Boerwinkle, E., Larson, M.G., Psaty, B.M., Peters, A., Ballantyne, C.M., Witteman, J.C.M., Hoogeveen, R.C., Benjamin, E.J., Koenig, W., Tracy, R.P., 2010. Duffy antigen receptor for chemokines (Darc) polymorphism regulates circulating concentrations of monocyte chemoattractant protein-1 and other inflammatory mediators. Blood 115, 5289–5299. https://doi.org/10.1182/blood-2009-05-221382

Schreiber, S., Fedorak, R.N., Nielsen, O.H., Wild, G., Williams, C.N., Nikolaus, S., Jacyna, M., Lashner, B.A., Gangl, A., Rutgeerts, P., Isaacs, K., van Deventer, S.J., Koningsberger, J.C., Cohard, M., LeBeaut, A., Hanauer, S.B., 2000. Safety and efficacy of recombinant human interleukin 10 in chronic active Crohn's disease. Crohn's Disease IL-10 Cooperative Study Group. Gastroenterology 119, 1461–1472. https://doi.org/10.1053/gast.2000.20196

Shankaran, V., Ikeda, H., Bruce, A.T., White, J.M., Swanson, P.E., Old, L.J., Schreiber, R.D., 2018. Pillars Article: IFNγ and Lymphocytes Prevent Primary Tumour Development and Shape Tumour Immunogenicity. Nature. 2001. 410: 1107-1111. J. Immunol. Baltim. Md 1950 201, 827–831.

Shaul, E., Conrad, M.A., Dawany, N., Patel, T., Canavan, M.C., Baccarella, A., Weinbrom, S., Aleynick, D., Sullivan, K.E., Kelsen, J.R., 2022. Canakinumab for the treatment of autoinflammatory very early onset- inflammatory bowel disease. Front. Immunol. 13, 972114. https://doi.org/10.3389/fimmu.2022.972114

Sherr, C.J., 1996. Cancer cell cycles. Science 274, 1672–1677. https://doi.org/10.1126/science.274.5293.1672

Siegel, C.A., Marden, S.M., Persing, S.M., Larson, R.J., Sands, B.E., 2009. Risk of Lymphoma Associated With Combination Anti–Tumor Necrosis Factor and Immunomodulator Therapy for the Treatment of Crohn's Disease: A Meta-Analysis. Clin. Gastroenterol. Hepatol. 7, 874–881. https://doi.org/10.1016/j.cgh.2009.01.004

Singh, U.P., Venkataraman, C., Singh, R., Lillard, J.W., 2007. CXCR3 axis: role in inflammatory bowel disease and its therapeutic implication. Endocr. Metab. Immune Disord. Drug Targets 7, 111–123. https://doi.org/10.2174/187153007780832109

Smits, D.J., Dekker, J., Schot, R., Tabarki, B., Alhashem, A., Demmers, J.A.A., Dekkers, D.H.W., Romito, A., Van Der Spek, P.J., Van Ham, T.J., Bertoli-Avella, A.M., Mancini, G.M.S., 2023. CLEC16A interacts with retromer and TRIM27, and its loss impairs endosomal trafficking and neurodevelopment. Hum. Genet. 142, 379–397. https://doi.org/10.1007/s00439-022-02511-3

Smookler, D.S., Mohammed, F.F., Kassiri, Z., Duncan, G.S., Mak, T.W., Khokha, R., 2006. Cutting Edge: Tissue Inhibitor of Metalloproteinase 3 Regulates TNF-Dependent Systemic Inflammation. J. Immunol. 176, 721–725. https://doi.org/10.4049/jimmunol.176.2.721

Soehnlein, O., Libby, P., 2021. Targeting inflammation in atherosclerosis - from experimental insights to the clinic. Nat. Rev. Drug Discov. 20, 589–610. https://doi.org/10.1038/s41573-021-00198-1

Sozzani, S., Abbracchio, M.P., Annese, V., Danese, S., De Pità, O., De Sarro, G., Maione, S., Olivieri, I., Parodi, A., Sarzi-Puttini, P., 2014. Chronic inflammatory diseases: do immunological patterns drive the choice of biotechnology drugs? A critical review. Autoimmunity 47, 287–306. https://doi.org/10.3109/08916934.2014.897333

Staley, J.R., Blackshaw, J., Kamat, M.A., Ellis, S., Surendran, P., Sun, B.B., Paul, D.S., Freitag, D., Burgess, S., Danesh, J., Young, R., Butterworth, A.S., 2016. PhenoScanner: a database of human genotype-phenotype associations.

Bioinforma. Oxf. Engl. 32, 3207–3209. https://doi.org/10.1093/bioinformatics/btw373

Stanley, A.C., Lacy, P., 2010. Pathways for cytokine secretion. Physiol. Bethesda Md 25, 218–229. https://doi.org/10.1152/physiol.00017.2010

Studer, R.A., Dessailly, B.H., Orengo, C.A., 2013. Residue mutations and their impact on protein structure and function: detecting beneficial and pathogenic changes. Biochem. J. 449, 581–594. https://doi.org/10.1042/BJ20121221

Sudlow, C., Gallacher, J., Allen, N., Beral, V., Burton, P., Danesh, J., Downey, P., Elliott, P., Green, J., Landray, M., Liu, B., Matthews, P., Ong, G., Pell, J., Silman, A., Young, A., Sprosen, T., Peakman, T., Collins, R., 2015. UK biobank: an open access resource for identifying the causes of a wide range of complex diseases of middle and old age. PLoS Med. 12, e1001779. https://doi.org/10.1371/journal.pmed.1001779

Suek, N., Young, T., Fu, J., 2024. Immune cell profiling in intestinal transplantation. Hum. Immunol. 110808. https://doi.org/10.1016/j.humimm.2024.110808

Sun, D., Gao, W., Hu, H., Zhou, S., 2022. Why 90% of clinical drug development fails and how to improve it? Acta Pharm. Sin. B 12, 3049–3062. https://doi.org/10.1016/j.apsb.2022.02.002

Suzuki, K., Hatzikotoulas, K., Southam, L., Taylor, H.J., Yin, X., Lorenz, K.M., Mandla, R., Huerta-Chagoya, A., Melloni, G.E.M., Kanoni, S., Rayner, N.W., Bocher, O., Arruda, A.L., Sonehara, K., Namba, S., Lee, S.S.K., Preuss, M.H., Petty, L.E., Schroeder, P., Vanderwerff, B., Kals, M., Bragg, F., Lin, K., Guo, X., Zhang, W., Yao, J., Kim, Y.J., Graff, M., Takeuchi, F., Nano, J., Lamri, A., Nakatochi, M., Moon, S., Scott, R.A., Cook, J.P., Lee, J.-J., Pan, I., Taliun, D., Parra, E.J., Chai, J.-F., Bielak, L.F., Tabara, Y., Hai, Y., Thorleifsson, G., Grarup, N., Sofer, T., Wuttke, M., Sarnowski, C., Gieger, C., Nousome, D., Trompet, S., Kwak, S.-H., Long, J., Sun, M., Tong, L., Chen, W.-M., Nongmaithem, S.S., Noordam, R., Lim, V.J.Y., Tam, C.H.T., Joo, Y.Y., Chen, C.-H., Raffield, L.M., Prins, B.P., Nicolas, A., Yanek, L.R., Chen, G., Brody, J.A., Kabagambe, E., An, P., Xiang, A.H., Choi, H.S., Cade, B.E., Tan, J., Broadaway, K.A., Williamson, A., Kamali, Z., Cui, J., Thangam, M., Adair, L.S., Adeyemo, A., Aguilar-Salinas, C.A., Ahluwalia, T.S., Anand, S.S., Bertoni, A., Bork-Jensen, J., Brandslund, I., Buchanan, T.A., Burant, C.F., Butterworth, A.S., Canouil, M., Chan, J.C.N., Chang, L.-C., Chee, M.-L., Chen, J., Chen, S.-H., Chen, Y.-T., Chen, Z., Chuang, L.-M., Cushman, M., Danesh, J., Das, S.K., De Silva, H.J., Dedoussis, G., Dimitrov, L., Doumatey, A.P., Du, S., Duan, Q., Eckardt, K.-U., Emery, L.S., Evans, D.S., Evans, M.K., Fischer, K., Floyd, J.S., Ford, I., Franco, O.H., Frayling, T.M., Freedman, B.I., Genter, P., Gerstein, H.C., Giedraitis, V., González-Villalpando, C., González-Villalpando, M.E., Gordon-Larsen, P., Gross, M., Guare, L.A., Hackinger, S., Hakaste, L., Han, S., Hattersley, A.T., Herder, C., Horikoshi, M., Howard, A.-G., Hsueh, W., Huang, M., Huang, W., Hung, Y.-J., Hwang, M.Y., Hwu, C.-M., Ichihara, S., Ikram, M.A., Ingelsson, M., Islam, Md.T., Isono, M., Jang, H.-M., Jasmine, F., Jiang, G., Jonas, J.B., Jørgensen, T., Kamanu, F.K., Kandeel, F.R., Kasturiratne, A., Katsuya, T., Kaur, V., Kawaguchi, T., Keaton, J.M., Kho, A.N., Khor, C.-C., Kibriya, M.G., Kim, D.-H., Kronenberg, F., Kuusisto, J., Läll, K., Lange, L.A., Lee, K.M., Lee, M.-S., Lee, N.R., Leong, A., Li, L., Li, Y., Li-Gao, R., Ligthart, S., Lindgren, C.M., Linneberg, A., Liu, C.-T., Liu, J., Locke, A.E., Louie, T., Luan, J., Luk, A.O., Luo, X., Lv, J., Lynch, J.A., Lyssenko, V., Maeda, S.,

Mamakou, V., Mansuri, S.R., Matsuda, K., Meitinger, T., Melander, O., Metspalu, A., Mo, H., Morris, A.D., Moura, F.A., Nadler, J.L., Nalls, M.A., Nayak, U., Ntalla, I., Okada, Y., Orozco, L., Patel, S.R., Patil, S., Pei, P., Pereira, M.A., Peters, A., Pirie, F.J., Polikowsky, H.G., Porneala, B., Prasad, G., Rasmussen-Torvik, L.J., Reiner, A.P., Roden, M., Rohde, R., Roll, K., Sabanayagam, C., Sandow, K., Sankareswaran, A., Sattar, N., Schönherr, S., Shahriar, M., Shen, B., Shi, J., Shin, D.M., Shojima, N., Smith, J.A., So, W.Y., Stančáková, A., Steinthorsdottir, V., Stilp, A.M., Strauch, K., Taylor, K.D., Thorand, B., Thorsteinsdottir, U., Tomlinson, B., Tran, T.C., Tsai, F.-J., Tuomilehto, J., Tusie-Luna, T., Udler, M.S., Valladares-Salgado, A., Van Dam, R.M., Van Klinken, J.B., Varma, R., Wacher-Rodarte, N., Wheeler, E., Wickremasinghe, A.R., Van Dijk, K.W., Witte, D.R., Yajnik, C.S., Yamamoto, Ken, Yamamoto, Kenichi, Yoon, K., Yu, C., Yuan, J.-M., Yusuf, S., Zawistowski, M., Zhang, L., Zheng, W., VA Million Veteran Program, AMED GRIFIN Diabetes Initiative Japan, Biobank Japan Project, Penn Medicine BioBank, Regeneron Genetics Center, Genes & Health Research Team, Kanona, S., Van Heel, D.A., eMERGE Consortium, International Consortium of Blood Pressure (ICBP), Meta-Analyses of Glucose and Insulin-Related Traits Consortium (MAGIC), Raffel, L.J., Igase, M., Ipp, E., Redline, S., Cho, Y.S., Lind, L., Province, M.A., Fornage, M., Hanis, C.L., Ingelsson, E., Zonderman, A.B., Psaty, B.M., Wang, Y.-X., Rotimi, C.N., Becker, D.M., Matsuda, F., Liu, Y., Yokota, M., Kardia, S.L.R., Peyser, P.A., Pankow, J.S., Engert, J.C., Bonnefond, A., Froguel, P., Wilson, J.G., Sheu, W.H.H., Wu, J.-Y., Hayes, M.G., Ma, R.C.W., Wong, T.-Y., Mook-Kanamori, D.O., Tuomi, T., Chandak, G.R., Collins, F.S., Bharadwaj, D., Paré, G., Sale, M.M., Ahsan, H., Motala, A.A., Shu, X.-O., Park, K.-S., Jukema, J.W., Cruz, M., Chen, Y.-D.I., Rich, S.S., McKean-Cowdin, R., Grallert, H., Cheng, C.-Y., Ghanbari, M., Tai, E.-S., Dupuis, J., Kato, N., Laakso, M., Köttgen, A., Koh, W.-P., Bowden, D.W., Palmer, C.N.A., Kooner, J.S., Kooperberg, C., Liu, S., North, K.E., Saleheen, D., Hansen, T., Pedersen, O., Wareham, N.J., Lee, J., Kim, B.-J., Millwood, I.Y., Walters, R.G., Stefansson, K., Ahlqvist, E., Goodarzi, M.O., Mohlke, K.L., Langenberg, C., Haiman, C.A., Loos, R.J.F., Florez, J.C., Rader, D.J., Ritchie, M.D., Zöllner, S., Mägi, R., Marston, N.A., Ruff, C.T., Van Heel, D.A., Finer, S., Denny, J.C., Yamauchi, T., Kadowaki, T., Chambers, J.C., Ng, M.C.Y., Sim, X., Below, J.E., Tsao, P.S., Chang, K.-M., McCarthy, M.I., Meigs, J.B., Mahajan, A., Spracklen, C.N., Mercader, J.M., Boehnke, M., Rotter, J.I., Vujkovic, M., Voight, B.F., Morris, A.P., Zeggini, E., 2024. Genetic drivers of heterogeneity in type 2 diabetes pathophysiology. Nature. https://doi.org/10.1038/s41586-024-07019-6

Szpakowska, M., D'Uonnolo, G., Luís, R., Alonso Bartolomé, A., Thelen, M., Legler, D.F., Chevigné, A., 2023. New pairings and deorphanization among the atypical chemokine receptor family — physiological and clinical relevance. Front. Immunol. 14, 1133394. https://doi.org/10.3389/fimmu.2023.1133394

Takechi, R., Galay, R.L., Matsuo, T., Maeda, H., Kusakisako, K., Talactac, M.R., Mochizuki, M., Fujisaki, K., Tanaka, T., 2016. Role of the tumor necrosis factor receptor-associated factor-type zinc finger domain containing protein 1 (TRAFD1) from the hard tick Haemaphysalis longicornis in immunity against bacterial infection. Ticks Tick-Borne Dis. 7, 36–45. https://doi.org/10.1016/j.ttbdis.2015.08.002

The Lenercept Multiple Sclerosis Study Group and The University of British Columbia MS/MRI Analysis Group, 2011. TNF neutralization in MS: Results of a randomized, placebo-controlled multicenter study. Neurology 77, 1382–1382. https://doi.org/10.1212/01.wnl.0000406608.85830.82

Tokunaga, R., Zhang, W., Naseem, M., Puccini, A., Berger, M.D., Soni, S., McSkane, M., Baba, H., Lenz, H.-J., 2018. CXCL9, CXCL10, CXCL11/CXCR3 axis for immune activation - A target for novel cancer therapy. Cancer Treat. Rev. 63, 40–47. https://doi.org/10.1016/j.ctrv.2017.11.007

Tsioumpekou, M., Krijgsman, D., Leusen, J.H.W., Olofsen, P.A., 2023. The Role of Cytokines in Neutrophil Development, Tissue Homing, Function and Plasticity in Health and Disease. Cells 12, 1981. https://doi.org/10.3390/cells12151981

Tsuo, K., Zhou, W., Wang, Y., Kanai, M., Namba, S., Gupta, R., Majara, L., Nkambule, L.L., Morisaki, T., Okada, Y., Neale, B.M., Global Biobank Meta-analysis Initiative, Daly, M.J., Martin, A.R., 2022. Multi-ancestry meta-analysis of asthma identifies novel associations and highlights the value of increased power and diversity. Cell Genomics 2, 100212. https://doi.org/10.1016/j.xgen.2022.100212

Unanue, E.R., Beller, D.I., Calderon, J., Kiely, J.M., Stadecker, M.J., 1976. Regulation of immunity and inflammation by mediators from macrophages. Am. J. Pathol. 85, 465–478.

Uricoli, B., Birnbaum, L.A., Do, P., Kelvin, J.M., Jain, J., Costanza, E., Chyong, A., Porter, C.C., Rafiq, S., Dreaden, E.C., 2021. Engineered Cytokines for Cancer and Autoimmune Disease Immunotherapy. Adv. Healthc. Mater. 10, 2002214. https://doi.org/10.1002/adhm.202002214

van der Graaf, A., Claringbould, A., Rimbert, A., BIOS Consortium, Westra, H.-J., Li, Y., Wijmenga, C., Sanna, S., 2020. Mendelian randomization while jointly modeling cis genetics identifies causal relationships between gene expression and lipids. Nat. Commun. 11, 4930. https://doi.org/10.1038/s41467-020-18716-x

Van Der Graaf, A., Zorro, M.M., Claringbould, A., Võsa, U., Aguirre-Gamboa, R., Li, C., Mooiweer, J., Ricaño-Ponce, I., Borek, Z., Koning, F., Kooy-Winkelaar, Y., Sollid, L.M., Qiao, S.-W., Kumar, V., Li, Y., Franke, L., Withoff, S., Wijmenga, C., Sanna, S., Jonkers, I., BIOS Consortium, 2021. Systematic Prioritization of Candidate Genes in Disease Loci Identifies TRAFD1 as a Master Regulator of IFNγ Signaling in Celiac Disease. Front. Genet. 11, 562434. https://doi.org/10.3389/fgene.2020.562434

Vermeulen, K., Van Bockstaele, D.R., Berneman, Z.N., 2003. The cell cycle: a review of regulation, deregulation and therapeutic targets in cancer. Cell Prolif. 36, 131–149. https://doi.org/10.1046/j.1365-2184.2003.00266.x

Võsa, U., Claringbould, A., Westra, H.-J., Bonder, M.J., Deelen, P., Zeng, B., Kirsten, H., Saha, A., Kreuzhuber, R., Yazar, S., Brugge, H., Oelen, R., de Vries, D.H., van der Wijst, M.G.P., Kasela, S., Pervjakova, N., Alves, I., Favé, M.-J., Agbessi, M., Christiansen, M.W., Jansen, R., Seppälä, I., Tong, L., Teumer, A., Schramm, K., Hemani, G., Verlouw, J., Yaghootkar, H., Sönmez Flitman, R., Brown, A., Kukushkina, V., Kalnapenkis, A., Rüeger, S., Porcu, E., Kronberg, J., Kettunen, J., Lee, B., Zhang, F., Qi, T., Hernandez, J.A., Arindrarto, W., Beutner, F., BIOS Consortium, i2QTL Consortium, Dmitrieva, J., Elansary, M., Fairfax, B.P., Georges, M., Heijmans, B.T., Hewitt, A.W., Kähönen, M., Kim,

Y., Knight, J.C., Kovacs, P., Krohn, K., Li, S., Loeffler, M., Marigorta, U.M., Mei, H., Momozawa, Y., Müller-Nurasyid, M., Nauck, M., Nivard, M.G., Penninx, B.W.J.H., Pritchard, J.K., Raitakari, O.T., Rotzschke, O., Slagboom, E.P., Stehouwer, C.D.A., Stumvoll, M., Sullivan, P., 't Hoen, P.A.C., Thiery, J., Tönjes, A., van Dongen, J., van Iterson, M., Veldink, J.H., Völker, U., Warmerdam, R., Wijmenga, C., Swertz, M., Andiappan, A., Montgomery, G.W., Ripatti, S., Perola, M., Kutalik, Z., Dermitzakis, E., Bergmann, S., Frayling, T., van Meurs, J., Prokisch, H., Ahsan, H., Pierce, B.L., Lehtimäki, T., Boomsma, D.I., Psaty, B.M., Gharib, S.A., Awadalla, P., Milani, L., Ouwehand, W.H., Downes, K., Stegle, O., Battle, A., Visscher, P.M., Yang, J., Scholz, M., Powell, J., Gibson, G., Esko, T., Franke, L., 2021. Large-scale cis- and trans-eQTL analyses identify thousands of genetic loci and polygenic scores that regulate blood gene expression. Nat. Genet. 53, 1300–1310. https://doi.org/10.1038/s41588-021-00913-z

Wallace, C., 2020. Eliciting priors and relaxing the single causal variant assumption in colocalisation analyses. PLOS Genet. 16, e1008720. https://doi.org/10.1371/journal.pgen.1008720

Walshe, M., Nayeri, S., Ji, J., Hernandez-Rocha, C., Sabic, K., Hu, L., Giri, M., Nayar, S., Brant, S., McGovern, D.P.B., Rioux, J.D., Duerr, R.H., Cho, J.H., Schumm, P.L., Lazarev, M., Silverberg, M.S., 2022. A Role for CXCR3 Ligands as Biomarkers of Post-Operative Crohn's Disease Recurrence. J. Crohns Colitis 16, 900–910. https://doi.org/10.1093/ecco-jcc/jjab186

Wang, H., Aloe, C., McQualter, J., Papanicolaou, A., Vlahos, R., Wilson, N., Bozinovski, S., 2021. G-CSFR antagonism reduces mucosal injury and airways fibrosis in a virus-dependent model of severe asthma. Br. J. Pharmacol. 178, 1869–1885. https://doi.org/10.1111/bph.15415

Wang, H., Chen, W., Wang, L., Li, F., Zhang, C., Xu, L., 2015. Tumor necrosis factor receptor-associated factor 6 promotes migration of rheumatoid arthritis fibroblast-like synoviocytes. Mol. Med. Rep. 11, 2761–2766. https://doi.org/10.3892/mmr.2014.3104

Wang, H., FitzPatrick, M., Wilson, N.J., Anthony, D., Reading, P.C., Satzke, C., Dunne, E.M., Licciardi, P.V., Seow, H.J., Nichol, K., Adcock, I.M., Chung, K.F., Anderson, G.P., Vlahos, R., Wark, P., Bozinovski, S., 2019. CSF3R/CD114 mediates infection-dependent transition to severe asthma. J. Allergy Clin. Immunol. 143, 785-788.e6. https://doi.org/10.1016/j.jaci.2018.10.001

Wang, L., Wang, F., Gershwin, M.E., 2015. Human autoimmune diseases: a comprehensive update. J. Intern. Med. 278, 369–395. https://doi.org/10.1111/joim.12395

Wang, M., Roux, F., Bartoli, C., Huard-Chauveau, C., Meyer, C., Lee, H., Roby, D., McPeek, M.S., Bergelson, J., 2018. Two-way mixed-effects methods for joint association analysis using both host and pathogen genomes. Proc. Natl. Acad. Sci. U. S. A. 115, E5440–E5449. https://doi.org/10.1073/pnas.1710980115

Wang, S., He, Z., Wang, X., Li, H., Liu, X.-S., 2019. Antigen presentation and tumor immunogenicity in cancer immunotherapy response prediction. eLife 8, e49020. https://doi.org/10.7554/eLife.49020

Watanabe, K., Taskesen, E., Van Bochoven, A., Posthuma, D., 2017. Functional mapping and annotation of genetic associations with FUMA. Nat. Commun. 8, 1826. https://doi.org/10.1038/s41467-017-01261-5

Wellcome Trust Case Control Consortium, Maller, J.B., McVean, G., Byrnes, J., Vukcevic, D., Palin, K., Su, Z., Howson, J.M.M., Auton, A., Myers, S., Morris, A., Pirinen, M., Brown, M.A., Burton, P.R., Caulfield, M.J., Compston, A., Farrall, M., Hall, A.S., Hattersley, A.T., Hill, A.V.S., Mathew, C.G., Pembrey, M., Satsangi, J., Stratton, M.R., Worthington, J., Craddock, N., Hurles, M., Ouwehand, W., Parkes, M., Rahman, N., Duncanson, A., Todd, J.A., Kwiatkowski, D.P., Samani, N.J., Gough, S.C.L., McCarthy, M.I., Deloukas, P., Donnelly, P., 2012. Bayesian refinement of association signals for 14 loci in 3 common diseases. Nat. Genet. 44, 1294–1301. https://doi.org/10.1038/ng.2435

Welter, D., MacArthur, J., Morales, J., Burdett, T., Hall, P., Junkins, H., Klemm, A., Flicek, P., Manolio, T., Hindorff, L., Parkinson, H., 2014. The NHGRI GWAS Catalog, a curated resource of SNP-trait associations. Nucleic Acids Res. 42, D1001–D1006. https://doi.org/10.1093/nar/gkt1229

Willer, C.J., Li, Y., Abecasis, G.R., 2010. METAL: fast and efficient meta-analysis of genomewide association scans. Bioinforma. Oxf. Engl. 26, 2190–2191. https://doi.org/10.1093/bioinformatics/btq340

Williams, S.K., Fairless, R., Maier, O., Liermann, P.C., Pichi, K., Fischer, R., Eisel, U.L.M., Kontermann, R., Herrmann, A., Weksler, B., Romero, N., Couraud, P.-O., Pfizenmaier, K., Diem, R., 2018. Anti-TNFR1 targeting in humanized mice ameliorates disease in a model of multiple sclerosis. Sci. Rep. 8, 13628. https://doi.org/10.1038/s41598-018-31957-7

Xiang, Y., Zhang, M., Jiang, D., Su, Q., Shi, J., 2023. The role of inflammation in autoimmune disease: a therapeutic target. Front. Immunol. 14. https://doi.org/10.3389/fimmu.2023.1267091

Yadav, L., Tamene, F., Göös, H., Van Drogen, A., Katainen, R., Aebersold, R., Gstaiger, M., Varjosalo, M., 2017. Systematic Analysis of Human Protein Phosphatase Interactions and Dynamics. Cell Syst. 4, 430-444.e5. https://doi.org/10.1016/j.cels.2017.02.011

Yawn, B.P., 2008. Factors accounting for asthma variability: achieving optimal symptom control for individual patients. Prim. Care Respir. J. J. Gen. Pract. Airw. Group 17, 138–147. https://doi.org/10.3132/pcrj.2008.00004

Yu, Q., Ding, J., Li, S., Li, Y., 2024. Autophagy in cancer immunotherapy: Perspective on immune evasion and cell death interactions. Cancer Lett. 590, 216856. https://doi.org/10.1016/j.canlet.2024.216856

Yuk, J.-M., Kim, J.K., Kim, I.S., Jo, E.-K., 2024. TNF in Human Tuberculosis: A Double-Edged Sword. Immune Netw. 24, e4. https://doi.org/10.4110/in.2024.24.e4

Zepter, K., Häffner, A., Soohoo, L.F., De Luca, D., Tang, H.P., Fisher, P., Chavinson, J., Elmets, C.A., 1997. Induction of biologically active IL-1 beta-converting enzyme and mature IL-1 beta in human keratinocytes by inflammatory and immunologic stimuli. J. Immunol. Baltim. Md 1950 159, 6203–6208.

Zhang, H., Ahearn, T.U., Lecarpentier, J., Barnes, D., Beesley, J., Qi, G., Jiang, X., O'Mara, T.A., Zhao, N., Bolla, M.K., Dunning, A.M., Dennis, J., Wang, Q., Ful,

Z.A., Aittomäki, K., Andrulis, I.L., Anton-Culver, H., Arndt, V., Aronson, K.J., Arun, B.K., Auer, P.L., Azzollini, J., Barrowdale, D., Becher, H., Beckmann, M.W., Behrens, S., Benitez, J., Bermisheva, M., Bialkowska, K., Blanco, A., Blomqvist, C., Bogdanova, N.V., Bojesen, S.E., Bonanni, B., Bondavalli, D., Borg, A., Brauch, H., Brenner, H., Briceno, I., Broeks, A., Brucker, S.Y., Brüning, T., Burwinkel, B., Buys, S.S., Byers, H., Caldés, T., Caligo, M.A., Calvello, M., Campa, D., Castelao, J.E., Chang-Claude, J., Chanock, S.J., Christiaens, M., Christiansen, H., Chung, W.K., Claes, K.B.M., Clarke, C.L., Cornelissen, S., Couch, F.J., Cox, A., Cross, S.S., Czene, K., Daly, M.B., Devilee, P., Diez, O., Domchek, S.M., Dörk, T., Dwek, M., Eccles, D.M., Ekici, A.B., Evans, D.G., Fasching, P.A., Figueroa, J., Foretova, L., Fostira, F., Friedman, E., Frost, D., Gago-Dominguez, M., Gapstur, S.M., Garber, J., García-Sáenz, J.A., Gaudet, M.M., Gayther, S.A., Giles, G.G., Godwin, A.K., Goldberg, M.S., Goldgar, D.E., González-Neira, A., Greene, M.H., Gronwald, J., Guénel, P., Häberle, L., Hahnen, E., Haiman, C.A., Hake, C.R., Hall, P., Hamann, U., Harkness, E.F., Heemskerk-Gerritsen, B.A.M., Hillemanns, P., Hogervorst, F.B.L., Holleczek, B., Hollestelle, A., Hooning, M.J., Hoover, R.N., Hopper, J.L., Howell, A., Huebner, H., Hulick, P.J., Imyanitov, E.N., kConFab Investigators, ABCTB Investigators, Isaacs, C., Izatt, L., Jager, A., Jakimovska, M., Jakubowska, A., James, P., Janavicius, R., Janni, W., John, E.M., Jones, M.E., Jung, A., Kaaks, R., Kapoor, P.M., Karlan, B.Y., Keeman, R., Khan, S., Khusnutdinova, E., Kitahara, C.M., Ko, Y.-D., Konstantopoulou, I., Koppert, L.B., Koutros, S., Kristensen, V.N., Laenkholm, A.-V., Lambrechts, D., Larsson, S.C., Laurent-Puig, P., Lazaro, C., Lazarova, E., Lejbkowicz, F., Leslie, G., Lesueur, F., Lindblom, A., Lissowska, J., Lo, W.-Y., Loud, J.T., Lubinski, J., Lukomska, A., MacInnis, R.J., Mannermaa, A., Manoochehri, M., Manoukian, S., Margolin, S., Martinez, M.E., Matricardi, L., McGuffog, L., McLean, C., Mebirouk, N., Meindl, A., Menon, U., Miller, A., Mingazheva, E., Montagna, M., Mulligan, A.M., Mulot, C., Muranen, T.A., Nathanson, K.L., Neuhausen, S.L., Nevanlinna, H., Neven, P., Newman, W.G., Nielsen, F.C., Nikitina-Zake, L., Nodora, J., Offit, K., Olah, E., Olopade, O.I., Olsson, H., Orr, N., Papi, L., Papp, J., Park-Simon, T.-W., Parsons, M.T., Peissel, B., Peixoto, A., Peshkin, B., Peterlongo, P., Peto, J., Phillips, K.-A., Piedmonte, M., Plaseska-Karanfilska, D., Prajzendanc, K., Prentice, R., Prokofyeva, D., Rack, B., Radice, P., Ramus, S.J., Rantala, J., Rashid, M.U., Rennert, G., Rennert, H.S., Risch, H.A., Romero, A., Rookus, M.A., Rübner, M., Rüdiger, T., Saloustros, E., Sampson, S., Sandler, D.P., Sawyer, E.J., Scheuner, M.T., Schmutzler, R.K., Schneeweiss, A., Schoemaker, M.J., Schöttker, B., Schürmann, P., Senter, L., Sharma, P., Sherman, M.E., Shu, X.-O., Singer, C.F., Smichkoska, S., Soucy, P., Southey, M.C., Spinelli, J.J., Stone, J., Stoppa-Lyonnet, D., EMBRACE Study, GEMO Study Collaborators, Swerdlow, A.J., Szabo, C.I., Tamimi, R.M., Tapper, W.J., Taylor, J.A., Teixeira, M.R., Terry, M., Thomassen, M., Thull, D.L., Tischkowitz, M., Toland, A.E., Tollenaar, R.A.E.M., Tomlinson, I., Torres, D., Troester, M.A., Truong, T., Tung, N., Untch, M., Vachon, C.M., van den Ouweland, A.M.W., van der Kolk, L.E., van Veen, E.M., vanRensburg, E.J., Vega, A., Wappenschmidt, B., Weinberg, C.R., Weitzel, J.N., Wildiers, H., Winqvist, R., Wolk, A., Yang, X.R., Yannoukakos, D., Zheng, W., Zorn, K.K., Milne, R.L., Kraft, P., Simard, J., Pharoah, P.D.P., Michailidou, K., Antoniou, A.C., Schmidt, M.K., Chenevix-Trench, G., Easton, D.F., Chatterjee, N., García-Closas, M., 2020. Genome-wide association study identifies 32 novel breast cancer susceptibility loci from overall and subtype-

specific analyses. Nat. Genet. 52, 572–581. https://doi.org/10.1038/s41588-020-0609-2

Zhao, J.H., Stacey, D., Eriksson, N., Macdonald-Dunlop, E., Hedman, Å.K., Kalnapenkis, A., Enroth, S., Cozzetto, D., Digby-Bell, J., Marten, J., Folkersen, L., Herder, C., Jonsson, L., Bergen, S.E., Gieger, C., Needham, E.J., Surendran, P., Estonian Biobank Research Team, Metspalu, A., Milani, L., Mägi, R., Nelis, M., Hudjašov, G., Paul, D.S., Polasek, O., Thorand, B., Grallert, H., Roden, M., Võsa, U., Esko, T., Hayward, C., Johansson, Å., Gyllensten, U., Powell, N., Hansson, O., Mattsson-Carlgren, N., Joshi, P.K., Danesh, J., Padyukov, L., Klareskog, L., Landén, M., Wilson, J.F., Siegbahn, A., Wallentin, L., Mälarstig, A., Butterworth, A.S., Peters, J.E., 2023a. Genetics of circulating inflammatory proteins identifies drivers of immune-mediated disease risk and therapeutic targets. Nat. Immunol. 24, 1540–1551. https://doi.org/10.1038/s41590-023-01588-w

Zhao, J.H., Stacey, D., Eriksson, N., Macdonald-Dunlop, E., Hedman, Å.K., Kalnapenkis, A., Enroth, S., Cozzetto, D., Digby-Bell, J., Marten, J., Folkersen, L., Herder, C., Jonsson, L., Bergen, S.E., Gieger, C., Needham, E.J., Surendran, P., Estonian Biobank Research Team, Metspalu, A., Milani, L., Mägi, R., Nelis, M., Hudjašov, G., Paul, D.S., Polasek, O., Thorand, B., Grallert, H., Roden, M., Võsa, U., Esko, T., Hayward, C., Johansson, Å., Gyllensten, U., Powell, N., Hansson, O., Mattsson-Carlgren, N., Joshi, P.K., Danesh, J., Padyukov, L., Klareskog, L., Landén, M., Wilson, J.F., Siegbahn, A., Wallentin, L., Mälarstig, A., Butterworth, A.S., Peters, J.E., 2023b. Genetics of circulating inflammatory proteins identifies drivers of immune-mediated disease risk and therapeutic targets. Nat. Immunol. 24, 1540–1551. https://doi.org/10.1038/s41590-023-01588-w

Zheng, J., Baird, D., Borges, M.-C., Bowden, J., Hemani, G., Haycock, P., Evans, D.M., Smith, G.D., 2017a. Recent Developments in Mendelian Randomization Studies. Curr. Epidemiol. Rep. 4, 330–345. https://doi.org/10.1007/s40471-017-0128-6

Zheng, J., Erzurumluoglu, A.M., Elsworth, B.L., Kemp, J.P., Howe, L., Haycock, P.C., Hemani, G., Tansey, K., Laurin, C., Early Genetics and Lifecourse Epidemiology (EAGLE) Eczema Consortium, Pourcain, B.S., Warrington, N.M., Finucane, H.K., Price, A.L., Bulik-Sullivan, B.K., Anttila, V., Paternoster, L., Gaunt, T.R., Evans, D.M., Neale, B.M., 2017b. LD Hub: a centralized database and web interface to perform LD score regression that maximizes the potential of summary level GWAS data for SNP heritability and genetic correlation analysis. Bioinforma. Oxf. Engl. 33, 272–279. https://doi.org/10.1093/bioinformatics/btw613

Zhu, Z., Zhang, F., Hu, H., Bakshi, A., Robinson, M.R., Powell, J.E., Montgomery, G.W., Goddard, M.E., Wray, N.R., Visscher, P.M., Yang, J., 2016. Integration of summary data from GWAS and eQTL studies predicts complex trait gene targets. Nat. Genet. 48, 481–487. https://doi.org/10.1038/ng.3538

Zuber, V., Grinberg, N.F., Gill, D., Manipur, I., Slob, E.A.W., Patel, A., Wallace, C., Burgess, S., 2022. Combining evidence from Mendelian randomization and colocalization: Review and comparison of approaches. Am. J. Hum. Genet. 109, 767–782. https://doi.org/10.1016/j.ajhg.2022.04.001

Appendix A

Table A.1. GWAS results. Results showing 359 significant associations between circulating cytokine levels and variants in 169 independent loci, including 150 trans-acting and 19 cis-acting loci.

SNP	Allele1	Allele2	Zscore	P-value	Direction	HetISq	HetPVal	EAF	Beta	SE	Chromosome	Position	Cytokine	Locus	Explained variance	acting
rs2179071	t	c	-5,67	1,5E-08	---	13,40	3,15E-01	0,41	-0,04	0,01	6	22114325	bNGF	6p22.3	0,06%	trans
rs35099140	a	t	5,72	1,1E-08	?-+	87,20	5,16E-03	0,23	0,05	0,01	14	106952318	bNGF	14q32.33	0,08%	trans
rs1329424	t	g	5,70	1,2E-08	++	62,40	1,03E-01	0,40	0,04	0,01	1	196646176	CTACK	1q31.3	0,08%	trans
rs7550207	t	c	-6,19	6,0E-10	--	82,50	1,67E-02	0,26	-0,05	0,01	1	159174885	Eotaxin	1q23.2	0,09%	trans
rs116758863	t	g	-5,64	1,7E-08	--	74,40	4,79E-02	0,02	-0,13	0,02	3	39250894	Eotaxin	3p22.2	0,07%	trans
rs77012232	c	g	5,92	3,2E-09	++	51,50	1,51E-01	0,02	0,14	0,02	3	41067877	Eotaxin	3p22.1	0,08%	trans
rs704903	t	c	-10,07	7,8E-24	--	77,90	3,35E-02	0,25	-0,08	0,01	3	43070847	Eotaxin	3p22.1	0,23%	trans
rs11920996	t	c	9,63	5,8E-22	++	94,10	3,73E-05	0,02	0,22	0,02	3	42542761	Eotaxin	3p22.1	0,21%	trans
rs73087348	t	c	8,44	3,2E-17	++	0,00	4,97E-01	0,24	0,07	0,01	3	42811571	Eotaxin	3p22.1	0,16%	trans
rs9810934	a	g	12,57	3,2E-36	++	85,90	7,80E-03	0,29	0,09	0,01	3	45954352	Eotaxin	3p21.31	0,36%	trans
rs78961792	a	g	-5,56	2,7E-08	--	47,20	1,69E-01	0,10	-0,06	0,01	3	66401761	Eotaxin	3p14.1	0,07%	trans
rs7783786	a	g	-5,86	4,7E-09	--	0,00	3,56E-01	0,42	-0,04	0,01	7	75429731	Eotaxin	7q11.23	0,08%	trans
rs140921648	a	c	5,69	1,3E-08	++	76,20	4,02E-02	0,04	0,10	0,02	7	75202900	Eotaxin	7q11.23	0,07%	trans
rs826725	a	g	-6,55	5,7E-11	--	0,00	7,77E-01	0,47	-0,04	0,01	8	59733378	Eotaxin	8q12.1	0,10%	trans
rs11646780	a	t	-5,46	4,9E-08	--	0,00	4,17E-01	0,41	-0,04	0,01	16	80022802	Eotaxin	16q23.2	0,07%	trans
rs10491109	t	g	6,51	7,5E-11	++	0,00	9,34E-01	0,10	0,07	0,01	17	32549026	Eotaxin	17q12	0,10%	trans
rs763781	t	c	-5,83	5,7E-09	--	86,80	5,87E-03	0,2535	-0,05	0,01	17	32488890	Eotaxin	17q12	n/a	cis
rs10402455	a	g	-5,52	3,3E-08	--	37,40	2,06E-01	0,12	-0,06	0,01	19	37728707	Eotaxin	19q13.12	0,07%	trans
rs1671209	c	g	-5,65	1,6E-08	--	0,00	6,29E-01	0,26	-0,04	0,01	19	55551002	Eotaxin	19q13.42	0,07%	trans
rs12239179	t	c	5,59	2,2E-08	++	44,30	1,80E-01	0,25	0,04	0,01	1	198976492	FGF-b	1q32.1	0,07%	trans
rs1344142	t	c	-5,60	2,2E-08	--	61,00	1,09E-01	0,43	-0,04	0,01	3	56857433	FGF-b	3p14.3	0,07%	trans
rs7441142	t	c	6,42	1,4E-10	++	5,30	3,04E-01	0,43	0,04	0,01	4	120008227	FGF-b	4q26	0,10%	trans
rs139369025	a	g	6,09	1,1E-09	++	0,00	9,22E-01	0,02	0,15	0,02	4	119298328	FGF-b	4q26	0,09%	trans
rs76665547	t	c	-25,28	4,8E-141	--	99,30	5,62E-31	0,9314	-0,29	0,01	4	123697294	FGF-b	4q27	n/a	cis

Table A.1 (cont.)

SNP	Allele1	Allele2	Zscore	P-value	Direction	HetISq	HetPVal	EAF	Beta	SE	Chromosome	Position	Cytokine	Locus	Explained variance	acting
rs141091752	c	g	7,51	5,8E-14	-+	95,80	1,02E-06	0,02	0,17	0,02	4	122898197	FGF-b	4q27	0,13%	trans
rs141635731	t	g	6,62	3,7E-11	++	63,80	9,64E-02	0,03	0,13	0,02	4	123439970	FGF-b	4q27	0,10%	trans
rs937355	a	g	6,60	4,1E-11	-+	96,20	3,28E-07	0,31	0,05	0,01	4	121570292	FGF-b	4q27	0,10%	trans
rs6857701	t	c	-5,78	7,5E-09	+-	87,40	4,91E-03	0,14	-0,06	0,01	4	122315742	FGF-b	4q27	0,08%	trans
rs78836533	a	g	5,66	1,5E-08	-+	95,20	5,40E-06	0,05	0,09	0,02	4	121168969	FGF-b	4q27	0,07%	trans
rs115049760	a	g	-5,53	3,2E-08	+-	96,20	2,86E-07	0,03	-0,11	0,02	4	124302061	FGF-b	4q28.1	0,07%	trans
rs60093606	t	g	9,06	1,3E-19	-+	95,10	5,97E-06	0,29	0,07	0,01	4	127266290	FGF-b	4q28.1	0,19%	trans
rs56147474	a	g	5,84	5,2E-09	++	78,10	3,24E-02	0,11	0,06	0,01	3	165798383	G-CSF	3q26.1	0,08%	trans
rs694664	c	g	-5,56	2,8E-08	--	57,30	1,26E-01	0,44	-0,04	0,01	3	165330411	G-CSF	3q26.1	0,07%	trans
rs34939346	t	c	-5,93	3,0E-09	--	86,90	5,70E-03	0,20	-0,05	0,01	19	40421612	G-CSF	19q13.2	0,08%	trans
rs11880654	t	c	-6,64	3,1E-11	+-	95,40	3,48E-06	0,08	-0,08	0,01	19	45745857	G-CSF	19q13.32	0,10%	trans
rs11668536	t	c	-6,59	4,3E-11	+-	96,60	6,65E-08	0,25	-0,05	0,01	19	45328476	G-CSF	19q13.32	0,10%	trans
rs117372248	a	g	5,68	1,3E-08	++	86,20	7,13E-03	0,14	0,05	0,01	19	43361820	G-CSF	19q13.2	0,07%	trans
rs7252448	t	c	-5,63	1,8E-08	--	71,10	6,27E-02	0,31	-0,04	0,01	19	46142053	G-CSF	19q13.32	0,07%	trans
rs16979231	t	c	-5,54	3,1E-08	--	72,80	5,51E-02	0,21	-0,05	0,01	19	45042765	G-CSF	19q13.31	0,07%	trans
rs79924756	a	g	5,46	4,6E-08	-+	85,90	7,78E-03	0,22	0,05	0,01	19	44321973	G-CSF	19q13.31	0,07%	trans
rs2249581	t	c	-5,70	1,2E-08	---	96,60	1,30E-13	0,25	-0,04	0,01	1	159144581	GROa	1q23.2	0,06%	trans
rs784492	t	g	5,52	3,3E-08	-++	50,80	1,31E-01	0,21	0,04	0,01	3	39175576	GROa	3p22.2	0,05%	trans
rs192031641	c	g	-5,55	2,9E-08	-+-	81,20	4,84E-03	0,03	-0,10	0,02	4	64401593	GROa	4q13.1	0,06%	trans
rs114296817	a	c	6,69	2,3E-11	?++	89,20	2,36E-03	0,01	0,21	0,03	4	68310149	GROa	4q13.2	0,09%	trans
rs57619473	a	c	-6,10	1,1E-09	?--	93,60	8,23E-05	0,04	-0,09	0,02	4	69180867	GROa	4q13.2	0,07%	trans
rs2367442	a	g	32,53	3,8E-232	+++	97,10	1,24E-15	0,2187	0,24	0,01	4	74816843	GROa	4q13.3	n/a	cis
rs28624853	a	g	-8,09	5,9E-16	?--	95,90	7,90E-07	0,03	-0,15	0,02	4	72138143	GROa	4q13.3	0,13%	trans
rs10019504	a	g	7,61	2,8E-14	?++	94,60	1,55E-05	0,03	0,15	0,02	4	71486305	GROa	4q13.3	0,12%	trans
rs115275434	t	c	-7,26	4,0E-13	+--	81,90	4,00E-03	0,02	-0,16	0,02	4	71719779	GROa	4q13.3	0,10%	trans
rs114536173	a	t	7,03	2,0E-12	?++	93,90	5,12E-05	0,03	0,13	0,02	4	71538474	GROa	4q13.3	0,10%	trans
rs56042607	a	g	6,81	1,0E-11	?-+	97,10	4,04E-09	0,04	0,11	0,02	4	73005872	GROa	4q13.3	0,09%	trans

Table A.1 (cont.)

SNP	Allele1	Allele2	Zscore	P-value	Direction	HetISq	HetPVal	EAF	Beta	SE	Chromosome	Position	Cytokine	Locus	Explained variance	acting
rs146702741	t	c	6,26	3,9E-10	-++	91,60	6,87E-06	0,01	0,17	0,03	4	72484429	GROa	4q13.3	0,07%	trans
rs377499720	a	g	-5,92	3,1E-09	?--	65,00	9,12E-02	0,02	-0,13	0,02	4	75137124	GROa	4q13.3	0,08%	trans
rs141391108	a	g	5,77	7,8E-09	+++	54,70	1,10E-01	0,02	0,13	0,02	4	73716661	GROa	4q13.3	0,06%	trans
rs78898749	t	c	5,52	3,4E-08	--+	91,60	6,64E-06	0,01	0,18	0,03	4	70831665	GROa	4q13.3	0,06%	trans
rs192437265	t	c	5,86	4,8E-09	--+	91,60	6,67E-06	0,03	0,10	0,02	4	76875335	GROa	4q21.1	0,06%	trans
rs10995445	a	t	-8,61	7,6E-18	---	64,40	6,02E-02	0,50	-0,05	0,01	10	64874754	GROa	10q21.3	0,13%	trans
rs11895352	t	c	-5,46	4,9E-08	---	44,10	1,67E-01	0,44	-0,03	0,01	2	20367135	HGF	2p24.1	0,05%	trans
rs362307	t	c	5,81	6,2E-09	++?	54,20	1,40E-01	0,09	0,09	0,02	4	3241845	HGF	4p16.3	0,14%	trans
rs1793892	t	c	-5,55	2,9E-08	?--	0,00	5,03E-01	0,09	-0,06	0,01	6	31221351	HGF	6p21.33	0,06%	trans
rs17155615	a	g	-8,46	2,8E-17	--?	0,00	3,57E-01	0,0746	-0,12	0,01	7	81515706	HGF	7q21.11	n/a	cis
rs4732401	t	c	-8,05	8,2E-16	---	0,00	3,71E-01	0,15	-0,06	0,01	7	81322168	HGF	7q21.11	0,11%	trans
rs5745692	c	g	-5,49	4,0E-08	---	80,20	6,33E-03	0,05	-0,08	0,01	7	81358266	HGF	7q21.11	0,05%	trans
rs34826779	t	g	-6,01	1,8E-09	---	47,80	1,47E-01	0,22	-0,04	0,01	8	106570964	HGF	8q23.1	0,06%	trans
rs149467613	a	g	7,26	4,0E-13	+++	81,10	5,07E-03	0,06	0,09	0,01	11	72943483	HGF	11q13.4	0,09%	trans
rs7310615	c	g	6,49	8,3E-11	+++	0,00	7,99E-01	0,38	0,04	0,01	12	111865049	HGF	12q24.12	0,07%	trans
rs1421085	t	c	-5,50	3,8E-08	---	0,00	9,05E-01	0,41	-0,03	0,01	16	53800954	HGF	16q12.2	0,05%	trans
rs9898547	t	g	-5,82	5,8E-09	---	41,00	1,84E-01	0,45	-0,03	0,01	17	38136026	HGF	17q21.1	0,06%	trans
rs12127759	t	c	-7,60	2,9E-14	--	83,20	1,48E-02	0,14	-0,07	0,01	1	196648613	IFN-g	1q31.3	0,13%	trans
rs71631848	a	g	6,81	9,7E-12	++	85,20	9,43E-03	0,23	0,06	0,01	1	196186335	IFN-g	1q31.3	0,11%	trans
rs116224050	a	g	6,38	1,8E-10	-+	89,60	1,95E-03	0,03	0,14	0,02	1	196918145	IFN-g	1q31.3	0,09%	trans
rs3106442	t	c	-5,46	4,9E-08	--	54,70	1,38E-01	0,46	-0,04	0,01	3	165363821	IFN-g	3q26.1	0,07%	trans
rs1042663	a	g	8,71	3,1E-18	++	93,00	1,63E-04	0,09	0,10	0,01	6	31905130	IFN-g	6p21.33	0,18%	trans
rs4713470	t	c	-5,48	4,3E-08	--	0,00	9,16E-01	0,33	-0,04	0,01	6	31472821	IFN-g	6p21.33	0,07%	trans
rs1329424	t	g	6,41	1,5E-10	-+	90,50	1,20E-03	0,40	0,04	0,01	1	196646176	IL-10	1q31.3	0,10%	trans
rs7739450	a	g	-8,58	9,7E-18	--	99,40	8,28E-37	0,47	-0,06	0,01	6	43911598	IL-10	6p21.1	0,17%	trans
rs12127759	t	c	-6,83	8,3E-12	+-	90,70	1,03E-03	0,14	-0,07	0,01	1	196648613	IL-13	1q31.3	0,12%	trans
rs71631848	a	g	6,63	3,4E-11	++	0,00	7,51E-01	0,23	0,06	0,01	1	196186335	IL-13	1q31.3	0,11%	trans

Table A.1 (cont.)

SNP	Allele1	Allele2	Zscore	P-value	Direction	HetISq	HetPVal	EAF	Beta	SE	Chromosome	Position	Cytokine	Locus	Explained variance	acting
rs34388368	t	g	-5,51	3,6E-08	---	0,00	6,40E-01	0,24	-0,04	0,01	1	196635470	IL-16	1q31.3	0,05%	trans
rs743862	t	c	-5,86	4,7E-09	+--	25,90	2,59E-01	0,35	-0,04	0,01	6	32381939	IL-16	6p21.32	0,07%	trans
rs72851055	c	g	5,74	9,7E-09	?++	78,20	3,21E-02	0,34	0,04	0,01	6	32502814	IL-16	6p21.32	0,07%	trans
rs79473108	t	c	-5,61	2,0E-08	---	0,00	7,42E-01	0,15	-0,05	0,01	9	95857081	IL-16	9q22.31	0,06%	trans
rs7167790	t	c	5,55	2,9E-08	+++	0,00	4,43E-01	0,24	0,04	0,01	15	70345281	IL-16	15q23	0,05%	trans
rs11072257	t	c	5,45	5,0E-08	-++	65,50	5,52E-02	0,08	0,06	0,01	15	71463600	IL-16	15q23	0,05%	trans
rs12708524	t	c	-5,86	4,6E-09	---	35,50	2,12E-01	0,43	-0,03	0,01	15	78528538	IL-16	15q25.1	0,06%	trans
rs17211644	t	c	5,48	4,2E-08	+-+	90,90	1,70E-05	0,14	0,05	0,01	15	80116362	IL-16	15q25.1	0,05%	trans
rs3848180	t	g	33,78	4,3E-250	+++	84,50	1,60E-03	0,4503	0,20	0,01	15	81596590	IL-16	15q25.1	n/a	cis
rs71404763	a	c	17,78	1,0E-70	+++	89,10	1,06E-04	0,05	0,25	0,01	15	81439371	IL-16	15q25.1	0,57%	trans
rs72744124	c	g	-5,98	2,3E-09	---	0,00	9,00E-01	0,03	-0,11	0,02	15	81467345	IL-16	15q25.1	0,07%	trans
rs138561568	a	c	5,94	2,9E-09	?++	84,90	9,98E-03	0,01	0,20	0,03	15	81806029	IL-16	15q25.2	0,07%	trans
rs139576939	c	g	-14,32	1,7E-46	+--	97,20	1,61E-16	0,05	-0,20	0,01	15	83393723	IL-16	15q25.2	0,38%	trans
rs75156308	a	g	6,37	1,9E-10	+++	85,30	1,09E-03	0,05	0,09	0,01	15	86174098	IL-16	15q25.3	0,07%	trans
rs62143194	c	g	-8,69	3,7E-18	--?	92,10	3,80E-04	0,25	-0,10	0,01	19	54319624	IL-16	19q13.42	0,35%	trans
rs1329424	t	g	5,97	2,3E-09	-+	88,30	3,41E-03	0,40	0,04	0,01	1	196646176	IL-17	1q31.3	0,08%	trans
rs17011356	a	g	-7,12	1,1E-12	--?	n/a	n/a	0,65	-0,07	0,01	2	31588577	IL-18	2p23.1	0,23%	trans
rs149705626	a	g	5,56	2,7E-08	++?	n/a	n/a	0,99	0,28	0,05	2	31905273	IL-18	2p23.1	0,18%	trans
rs72927001	t	c	-5,45	4,9E-08	--?	n/a	n/a	0,70	-0,06	0,01	2	203530332	IL-18	2q33.2	0,13%	trans
rs75084521	a	g	5,65	1,6E-08	++?	n/a	n/a	0,07	0,11	0,02	5	68100579	IL-18	5q13.1	0,16%	trans
rs149612950	a	g	5,62	2,0E-08	++?	n/a	n/a	0,97	0,18	0,03	5	68166499	IL-18	5q13.1	0,17%	trans
rs35257100	t	c	-5,53	3,3E-08	--?	n/a	n/a	0,22	-0,06	0,01	7	26135404	IL-18	7p15.2	0,13%	trans
rs1487888	t	c	5,88	4,2E-09	++?	n/a	n/a	0,18	0,08	0,01	8	144562603	IL-18	8q24.3	0,18%	trans
rs1852138	a	g	7,63	2,4E-14	++-	n/a	n/a	0,4145	0,05	0,01	11	112201569	IL-18	11q23.1	n/a	cis
rs516286	t	g	5,72	1,1E-08	++?	n/a	n/a	0,83	0,07	0,01	11	104894171	IL-18	11q22.3	0,14%	trans
rs3184504	t	c	5,55	2,9E-08	++?	n/a	n/a	0,46	0,06	0,01	12	111884608	IL-18	12q24.12	0,15%	trans
rs4419163	a	t	-6,88	5,9E-12	+-?	n/a	n/a	0,21	-0,08	0,01	19	54327568	IL-18	19q13.42	0,22%	trans

Table A.1 (cont.)

SNP	Allele1	Allele2	Zscore	P-value	Direction	HetISq	HetPVal	EAF	Beta	SE	Chromosome	Position	Cytokine	Locus	Explained variance	acting
rs3859501	a	c	5,91	3,4E-09	-+?	n/a	n/a	0,49	0,06	0,01	19	54291411	IL-18	19q13.42	0,19%	trans
rs56836833	a	t	5,48	4,4E-08	++	58,80	1,19E-01	0,01	0,17	0,03	2	1157438	IL-1B	2p25.3	0,08%	trans
rs77246730	t	c	-18,03	1,1E-72	+-	97,40	6,36E-10	0,01	-0,55	0,03	2	3642756	IL-1B	2p25.3	0,83%	trans
rs143732640	t	c	9,19	3,9E-20	++	70,80	6,42E-02	0,03	0,21	0,02	2	3353632	IL-1B	2p25.3	0,22%	trans
rs75564661	a	g	-6,68	2,5E-11	+-	94,80	1,26E-05	0,04	-0,12	0,02	2	3032487	IL-1B	2p25.3	0,12%	trans
rs4352245	a	g	5,73	1,0E-08	++	39,80	1,97E-01	0,01	0,24	0,04	2	3614546	IL-1B	2p25.3	0,08%	trans
rs79668485	a	g	5,62	1,9E-08	++	0,00	7,83E-01	0,01	0,26	0,05	2	2743107	IL-1B	2p25.3	0,08%	trans
rs698092	a	g	5,48	4,3E-08	++	0,00	4,23E-01	0,37	0,04	0,01	3	186969634	IL-1B	3q27.3	0,08%	trans
rs16997771	t	c	-6,24	4,5E-10	+-	92,30	3,13E-04	0,03	-0,13	0,02	19	10148713	IL-1B	19p13.2	0,10%	trans
rs6743171	c	g	-26,21	2,0E-151	+--	97,10	1,46E-15	0,3966	-0,15	0,01	2	113840058	IL-1ra	2q13	n/a	cis
rs28877112	t	c	5,69	1,3E-08	?++	0,00	5,26E-01	0,20	0,05	0,01	2	114233086	IL-1ra	2q13	0,07%	trans
rs10169524	a	g	-5,57	2,6E-08	+--	81,70	4,29E-03	0,27	-0,04	0,01	2	113528872	IL-1ra	2q13	0,05%	trans
rs74439530	t	g	5,48	4,3E-08	+++	46,00	1,57E-01	0,10	0,06	0,01	2	113360594	IL-1ra	2q13	0,05%	trans
rs7310615	c	g	6,17	6,8E-10	+++	0,00	8,31E-01	0,38	0,04	0,01	12	111865049	IL-1ra	12q24.12	0,07%	trans
rs9937053	a	g	5,52	3,4E-08	+++	58,70	8,88E-02	0,44	0,03	0,01	16	53799507	IL-1ra	16q12.2	0,05%	trans
rs7221894	t	c	-5,47	4,5E-08	--?	66,20	8,55E-02	0,37	-0,06	0,01	17	38165485	IL-1ra	17q21.1	0,14%	trans
rs62143194	c	g	-15,68	2,0E-55	--?	97,20	2,35E-09	0,25	-0,17	0,01	19	54319624	IL-1ra	19q13.42	1,11%	trans
rs4665972	t	c	8,00	1,2E-15	++	72,80	5,51E-02	0,34	0,06	0,01	2	27598097	IL-2	2p23.3	0,16%	trans
rs12331618	a	g	-6,66	2,7E-11	--	0,00	5,36E-01	0,49	-0,05	0,01	4	187139939	IL-2	4q35.2	0,11%	trans
rs4976691	c	g	-6,02	1,8E-09	--	0,00	6,80E-01	0,40	-0,04	0,01	5	176827815	IL-2	5q35.3	0,09%	trans
rs28383314	t	c	-5,63	1,8E-08	--	25,00	2,48E-01	0,36	-0,04	0,01	6	32587213	IL-2	6p21.32	0,08%	trans
rs799169	a	g	5,78	7,4E-09	++	60,50	1,11E-01	0,38	0,04	0,01	7	73050599	IL-2	7q11.23	0,09%	trans
rs2239804	t	c	-5,83	5,5E-09	--	0,00	4,19E-01	0,33	-0,04	0,01	6	32411523	IL-2ra	6p21.32	0,09%	trans
rs56022334	a	g	-7,73	1,1E-14	--	95,20	5,22E-06	0,335	-0,06	0,01	10	6127641	IL-2ra	10p15.1	n/a	cis
rs1329424	t	g	8,00	1,3E-15	-+	96,00	5,49E-07	0,40	0,06	0,01	1	196646176	IL-4	1q31.3	0,15%	trans
rs453821	t	c	5,57	2,6E-08	++	30,40	2,31E-01	0,14	0,06	0,01	6	31935311	IL-4	6p21.33	0,07%	trans
rs7194068	t	g	-5,69	1,3E-08	--	72,60	5,63E-02	0,43	-0,04	0,01	16	17576804	IL-4	16p12.3	0,07%	trans

Table A.1 (cont.)

SNP	Allele1	Allele2	Zscore	P-value	Direction	HetISq	HetPVal	EAF	Beta	SE	Chromosome	Position	Cytokine	Locus	Explained variance	acting
rs1329424	t	g	7,10	1,2E-12	++	56,80	1,28E-01	0,40	0,05	0,01	1	196646176	IL-5	1q31.3	0,13%	trans
rs11265611	a	g	6,70	2,0E-11	+++	95,30	5,36E-10	0,34	0,04	0,01	1	154395125	IL-6	1q21.3	0,08%	trans
rs9267951	t	c	5,47	4,6E-08	?++	61,30	1,08E-01	0,32	0,04	0,01	6	32212655	IL-6	6p21.32	0,06%	trans
rs1329424	t	g	7,68	1,6E-14	++	49,00	1,61E-01	0,40	0,06	0,01	1	196646176	IL-7	1q31.3	0,15%	trans
rs34826779	t	g	-5,47	4,4E-08	--	0,00	7,42E-01	0,22	-0,05	0,01	8	106570964	IL-7	8q23.1	0,08%	trans
rs12075	a	g	10,01	1,3E-23	+++	76,10	1,53E-02	0,42	0,06	0,01	1	159175354	IL-8	1q23.2	0,18%	trans
rs12127759	t	c	-5,96	2,5E-09	-+-	88,50	1,73E-04	0,14	-0,05	0,01	1	196648613	IL-8	1q31.3	0,06%	trans
rs61820876	t	g	-5,85	5,0E-09	---	82,50	3,33E-03	0,28	-0,04	0,01	1	196209945	IL-8	1q31.3	0,07%	trans
rs942053	t	c	5,84	5,2E-09	+++	78,70	9,22E-03	0,04	0,09	0,02	4	74530753	IL-8	4q13.3	0,07%	trans
rs9277379	a	c	-5,58	2,5E-08	?--	48,70	1,63E-01	0,18	-0,04	0,01	6	33050325	IL-8	6p21.32	0,06%	trans
rs41285751	t	g	5,49	4,1E-08	?++	80,10	2,49E-02	0,08	0,07	0,01	6	31899815	IL-8	6p21.33	0,07%	trans
rs6993770	a	t	5,68	1,4E-08	-++	62,00	7,20E-02	0,22	0,04	0,01	8	106581528	IL-8	8q23.1	0,06%	trans
rs9903871	t	c	5,95	2,6E-09	+++	33,10	2,24E-01	0,36	0,04	0,01	17	16131927	IL-8	17p11.2	0,07%	trans
rs4239225	a	g	-6,05	1,5E-09	---	0,00	7,14E-01	0,49	-0,04	0,01	17	38127112	IL-8	17q21.1	0,07%	trans
rs2548977	t	c	5,65	1,6E-08	++	0,00	3,99E-01	0,40	0,04	0,01	5	135463769	IL-9	5q31.1	0,08%	trans
rs11742478	a	c	-5,54	3,0E-08	+-	84,00	1,23E-02	0,07	-0,08	0,01	5	135222840	IL-9	5q31.1	0,08%	trans
rs9399136	t	c	-5,47	4,6E-08	--	0,00	5,91E-01	0,27	-0,04	0,01	6	135402339	IL-9	6q23.3	0,08%	trans
rs7964426	t	c	-6,29	3,2E-10	+-	80,00	2,52E-02	0,34	-0,05	0,01	12	54668471	IL-9	12q13.13	0,10%	trans
rs80136777	a	t	-5,79	7,0E-09	--	0,00	8,42E-01	0,12	-0,06	0,01	3	45931005	IP-10	3p21.31	0,09%	trans
rs113587264	a	g	-5,95	2,6E-09	--	0,00	8,63E-01	0,01	-0,21	0,03	4	72955217	IP-10	4q13.3	0,09%	trans
rs1532985	t	g	7,35	1,9E-13	-+	91,20	7,32E-04	0,0139	0,32	0,04	4	77222245	IP-10	4q21.1	n/a	cis
rs1048381	a	g	5,83	5,7E-09	++	0,00	8,74E-01	0,14	0,06	0,01	6	32610445	IP-10	6p21.32	0,09%	trans
rs4766517	c	g	-5,81	6,1E-09	--	58,90	1,19E-01	0,34	-0,04	0,01	12	111359712	IP-10	12q24.11	0,09%	trans
rs2376263	a	g	5,63	1,9E-08	++	0,00	8,77E-01	0,31	0,04	0,01	17	33763678	IP-10	17q12	0,08%	trans
rs12121864	a	c	-6,14	8,3E-10	---	81,60	4,40E-03	0,12	-0,06	0,01	1	9205332	M-CSF	1p36.22	0,07%	trans
rs61785488	a	g	6,20	5,5E-10	+++	95,30	5,39E-10	0,7654	0,05	0,01	1	110557015	M-CSF	1p13.3	n/a	cis
rs3093044	a	g	5,84	5,2E-09	-++	92,60	1,44E-06	0,08	0,07	0,01	1	110459730	M-CSF	1p13.3	0,06%	trans

Table A.1 (cont.)

SNP	Allele1	Allele2	Zscore	P-value	Direction	HetISq	HetPVal	EAF	Beta	SE	Chromosome	Position	Cytokine	Locus	Explained variance	acting
rs4665972	t	c	-5,45	5,0E-08	+--	82,40	3,38E-03	0,34	-0,03	0,01	2	27598097	M-CSF	2p23.3	0,05%	trans
rs77155840	t	c	10,12	4,5E-24	--+	97,60	4,40E-19	0,02	0,23	0,02	2	134973524	M-CSF	2q21.2	0,19%	trans
rs1257371	a	g	5,48	4,4E-08	+++	82,50	3,32E-03	0,16	0,05	0,01	2	134839539	M-CSF	2q21.2	0,06%	trans
rs3755573	t	c	-9,49	2,4E-21	---	92,20	2,85E-06	0,44	-0,06	0,01	3	98489011	M-CSF	3q12.1	0,17%	trans
rs3804622	a	g	7,35	2,0E-13	+-+	93,70	1,38E-07	0,43	0,05	0,01	3	98303182	M-CSF	3q12.1	0,11%	trans
rs3749260	a	c	5,82	6,0E-09	--+	91,80	5,19E-06	0,10	0,06	0,01	3	98250862	M-CSF	3q11.2	0,07%	trans
rs2237085	a	g	-8,71	3,2E-18	---	92,70	1,13E-06	0,21	-0,07	0,01	5	149465249	M-CSF	5q32	0,15%	trans
rs245056	a	t	5,74	9,4E-09	+-+	92,40	1,78E-06	0,34	0,04	0,01	5	149341038	M-CSF	5q32	0,06%	trans
rs6571186	a	c	-5,54	3,0E-08	+--	68,50	4,19E-02	0,12	-0,05	0,01	6	95921373	M-CSF	6q16.1	0,06%	trans
rs41274009	a	g	5,55	2,9E-08	-++	51,70	1,26E-01	0,09	0,06	0,01	9	33043127	M-CSF	9p21.1	0,06%	trans
rs576123	t	c	-7,38	1,6E-13	?--	69,60	6,97E-02	0,26	-0,06	0,01	9	136144308	M-CSF	9q34.2	0,12%	trans
rs75071241	a	g	-8,23	1,8E-16	---	93,80	1,03E-07	0,06	-0,11	0,01	11	126232186	M-CSF	11q24.2	0,12%	trans
rs10894808	t	c	6,11	1,0E-09	+++	0,00	6,58E-01	0,12	0,06	0,01	11	134256805	M-CSF	11q25	0,07%	trans
rs1265565	t	c	6,19	6,0E-10	-++	62,80	6,82E-02	0,34	0,04	0,01	12	111715197	M-CSF	12q24.12	0,07%	trans
rs17880604	c	g	-7,40	1,3E-13	+--	89,90	4,90E-05	0,02	-0,19	0,03	17	7577644	M-CSF	17p13.1	0,11%	trans
rs41556717	t	c	6,98	2,9E-12	-++	88,10	2,28E-04	0,02	0,16	0,02	17	7399319	M-CSF	17p13.1	0,10%	trans
rs11655829	a	g	5,48	4,2E-08	+++	0,00	4,97E-01	0,04	0,09	0,02	17	6744513	M-CSF	17p13.1	0,06%	trans
rs573764538	t	c	5,47	4,5E-08	?-+	86,20	7,10E-03	0,06	0,08	0,01	17	6962925	M-CSF	17p13.1	0,07%	trans
rs8081395	a	g	5,47	4,5E-08	-++	60,80	7,82E-02	0,46	0,03	0,01	17	57801761	M-CSF	17q23.1	0,05%	trans
rs12940443	t	c	-5,53	3,2E-08	-+-	91,00	1,45E-05	0,34	-0,04	0,01	17	74482559	M-CSF	17q25.1	0,07%	trans
rs679574	c	g	-6,04	1,6E-09	++-	94,70	6,88E-09	0,39	-0,04	0,01	19	49206108	M-CSF	19q13.33	0,07%	trans
rs738409	c	g	-6,70	2,2E-11	+--	84,70	1,42E-03	0,23	-0,05	0,01	22	44324727	M-CSF	22q13.31	0,08%	trans
rs9427342	c	g	5,63	1,8E-08	+++	63,30	6,55E-02	0,31	0,03	0,01	1	159360156	MCP-1	1q23.2	0,05%	trans
rs3026943	a	c	-5,48	4,3E-08	---	34,00	2,20E-01	0,41	-0,03	0,01	1	159131926	MCP-1	1q23.2	0,05%	trans
rs3888652	a	g	6,35	2,2E-10	+++	82,60	3,22E-03	0,26	0,04	0,01	3	42726718	MCP-1	3p22.1	0,06%	trans
rs34901975	a	g	10,25	1,2E-24	+++	87,50	3,39E-04	0,12	0,09	0,01	3	45916786	MCP-1	3p21.31	0,16%	trans
rs62245068	t	c	8,94	4,1E-19	+++	62,60	6,91E-02	0,06	0,10	0,01	3	45840051	MCP-1	3p21.31	0,12%	trans

Table A.1 (cont.)

SNP	Allele1	Allele2	Zscore	P-value	Direction	HetISq	HetPVal	EAF	Beta	SE	Chromosome	Position	Cytokine	Locus	Explained variance	acting
rs2269443	a	g	-8,36	6,4E-17	---	86,90	4,78E-04	0,12	-0,07	0,01	3	46491290	MCP-1	3p21.31	0,11%	trans
rs4857857	a	g	5,60	2,1E-08	+++	87,40	3,60E-04	0,36	0,03	0,01	3	128313880	MCP-1	3q21.3	0,05%	trans
rs2887259	t	c	5,49	4,1E-08	++?	0,00	7,91E-01	0,35	0,05	0,01	17	32590612	MCP-1	17q12	0,10%	trans
rs3845622	a	c	6,09	1,1E-09	++	0,00	7,16E-01	0,12	0,07	0,01	1	159171603	MCP-3	1q23.2	0,10%	trans
rs146903072	a	g	5,53	3,1E-08	++	0,00	8,94E-01	0,04	0,10	0,02	6	31847180	MCP-3	6p21.33	0,08%	trans
rs145274022	a	c	6,06	1,4E-09	-+	62,90	1,01E-01	0,01	0,23	0,04	17	30454415	MCP-3	17q11.2	0,10%	trans
rs17734411	a	g	6,05	1,4E-09	++	0,00	3,23E-01	0,16	0,06	0,01	17	31320630	MCP-3	17q11.2	0,10%	trans
rs74832623	a	g	-35,82	5,9E-281	+-	97,50	2,28E-10	0,9771	-0,94	0,03	17	32535173	MCP-3	17q12	n/a	cis
rs1233653	t	c	9,73	2,2E-22	-+	87,20	5,13E-03	0,06	0,15	0,02	17	32639058	MCP-3	17q12	0,26%	trans
rs117971411	a	g	9,03	1,7E-19	++	0,00	4,26E-01	0,02	0,24	0,03	17	32389429	MCP-3	17q12	0,22%	trans
rs60319976	a	g	6,93	4,2E-12	++	0,00	4,16E-01	0,08	0,10	0,01	17	32678932	MCP-3	17q12	0,13%	trans
rs56949579	a	g	-5,80	6,6E-09	--	0,00	9,39E-01	0,38	-0,04	0,01	8	144646201	MIF	8q24.3	0,09%	trans
rs9620336	c	g	-5,65	1,6E-08	+-	72,90	5,48E-02	0,1998	-0,05	0,01	22	24281620	MIF	22q11.23	n/a	cis
rs6679677	a	c	5,63	1,8E-08	++	91,40	6,68E-04	0,13	0,06	0,01	1	114303808	MIG	1p13.2	0,08%	trans
rs79815064	a	g	5,67	1,4E-08	++	0,00	8,98E-01	0,12	0,06	0,01	3	46277577	MIG	3p21.31	0,08%	trans
rs2135232	t	c	6,01	1,9E-09	++	58,80	1,19E-01	0,28	0,05	0,01	4	76832856	MIG	4q21.1	0,09%	trans
rs6532173	t	c	5,86	4,7E-09	++	0,00	5,34E-01	0,31	0,05	0,01	4	76998583	MIG	4q21.1	0,09%	trans
rs3135338	t	c	5,74	9,3E-09	++	0,00	9,71E-01	0,40	0,04	0,01	6	32401217	MIG	6p21.32	0,08%	trans
rs4252066	a	g	5,57	2,6E-08	++	0,00	6,23E-01	0,27	0,05	0,01	6	161127125	MIG	6q26	0,08%	trans
rs4766517	c	g	-6,41	1,5E-10	--	5,40	3,04E-01	0,34	-0,05	0,01	12	111359712	MIG	12q24.11	0,10%	trans
rs62140208	a	g	-6,02	1,7E-09	---	88,60	1,59E-04	0,42	-0,04	0,01	2	42325560	MIP-1a	2p21	0,06%	trans
rs3924113	t	g	5,50	3,7E-08	++?	0,00	5,67E-01	0,24	0,06	0,01	4	38796255	MIP-1a	4p14	0,13%	trans
rs3129773	t	c	-5,70	1,2E-08	?--	0,00	5,77E-01	0,49	-0,04	0,01	6	32601930	MIP-1a	6p21.32	0,07%	trans
rs12302980	a	g	5,48	4,2E-08	+++	0,00	9,51E-01	0,35	0,03	0,01	12	111360290	MIP-1a	12q24.11	0,05%	trans
rs764872	a	g	14,16	1,5E-45	++?	97,50	3,71E-10	0,6183	0,14	0,01	17	34415272	MIP-1a	17q12	n/a	cis
rs9903158	t	c	-8,00	1,2E-15	++-	98,50	1,62E-30	0,04	-0,12	0,02	17	34312337	MIP-1a	17q12	0,11%	trans
rs113961817	a	c	6,90	5,4E-12	?++	0,00	8,45E-01	0,01	0,25	0,04	17	34108212	MIP-1a	17q12	0,10%	trans

Table A.1 (cont.)

SNP	Allele1	Allele2	Zscore	P-value	Direction	HetISq	HetPVal	EAF	Beta	SE	Chromosome	Position	Cytokine	Locus	Explained variance	acting
rs8066793	t	c	5,62	2,0E-08	+++	0,00	9,04E-01	0,42	0,03	0,01	17	33696096	MIP-1a	17q12	0,06%	trans
rs7412	t	c	5,74	9,4E-09	-++	70,40	3,41E-02	0,06	0,07	0,01	19	45412079	MIP-1a	19q13.32	0,06%	trans
rs73089379	c	g	-9,05	1,4E-19	--	94,30	2,71E-05	0,92	-0,16	0,02	3	45183414	MIP-1b	3p21.31	0,37%	trans
rs62242542	t	c	-7,84	4,5E-15	--	98,20	6,54E-14	0,98	-0,29	0,04	3	45169491	MIP-1b	3p21.31	0,32%	trans
rs2373048	a	t	-6,94	3,9E-12	--	53,90	1,41E-01	0,22	-0,08	0,01	3	45834988	MIP-1b	3p21.31	0,21%	trans
rs10510748	a	g	6,45	1,1E-10	++	84,60	1,08E-02	0,90	0,10	0,01	3	46178538	MIP-1b	3p21.31	0,16%	trans
rs9847395	t	c	5,67	1,4E-08	++	86,00	7,51E-03	0,44	0,05	0,01	3	46724548	MIP-1b	3p21.31	0,13%	trans
rs10023850	a	g	5,46	4,7E-08	++	26,10	2,45E-01	0,18	0,06	0,01	4	38763693	MIP-1b	4p14	0,12%	trans
rs10818069	a	c	-5,47	4,5E-08	--	0,00	8,21E-01	0,08	-0,09	0,02	9	120453971	MIP-1b	9q33.1	0,12%	trans
rs56673427	a	g	-15,36	3,2E-53	--	95,70	1,37E-06	0,1252	-0,24	0,02	17	34471393	MIP-1b	17q12	n/a	cis
rs7217473	t	c	7,13	1,0E-12	++	65,90	8,66E-02	0,06	0,14	0,02	17	34319064	MIP-1b	17q12	0,21%	trans
rs76960253	t	c	5,89	3,8E-09	++	97,90	6,83E-12	0,02	0,22	0,04	17	34088656	MIP-1b	17q12	0,17%	trans
rs140950972	c	g	5,72	1,1E-08	++	51,80	1,50E-01	0,98	0,18	0,03	17	34034912	MIP-1b	17q12	0,15%	trans
rs34437725	t	c	-5,53	3,3E-08	--	83,50	1,39E-02	0,96	-0,13	0,02	17	33826785	MIP-1b	17q12	0,14%	trans
rs11658282	t	c	-5,49	4,1E-08	--	82,50	1,68E-02	0,34	-0,05	0,01	17	33483115	MIP-1b	17q12	0,12%	trans
rs2182760	a	g	-6,03	1,6E-09	---	7,40	3,40E-01	0,06	-0,07	0,01	1	156867990	PDGFbb	1q23.1	0,06%	trans
rs12117194	c	g	-6,24	4,3E-10	---	0,00	3,72E-01	0,50	-0,04	0,01	1	205040943	PDGFbb	1q32.1	0,06%	trans
rs4952071	t	c	6,11	9,8E-10	+++	0,00	8,39E-01	0,40	0,04	0,01	2	31455148	PDGFbb	2p23.1	0,06%	trans
rs4674836	a	g	-6,04	1,6E-09	---	73,10	2,43E-02	0,35	-0,04	0,01	2	224855511	PDGFbb	2q36.1	0,06%	trans
rs10184062	c	g	5,48	4,3E-08	+++	66,50	5,08E-02	0,26	0,04	0,01	2	224867341	PDGFbb	2q36.1	0,05%	trans
rs2064223	t	c	-5,85	5,0E-09	---	0,00	6,68E-01	0,33	-0,04	0,01	6	163794814	PDGFbb	6q26	0,05%	trans
rs10282644	a	g	-5,61	2,1E-08	---	3,70	3,54E-01	0,47	-0,03	0,01	7	80164380	PDGFbb	7q21.11	0,05%	trans
rs302953	t	c	5,67	1,5E-08	-++	86,60	5,75E-04	0,40	0,03	0,01	8	106512481	PDGFbb	8q23.1	0,05%	trans
rs385893	t	c	-5,73	9,9E-09	---	66,90	4,86E-02	0,44	-0,03	0,01	9	4763176	PDGFbb	9p24.1	0,05%	trans
rs6479248	t	g	-6,71	2,0E-11	---	0,00	8,11E-01	0,44	-0,04	0,01	9	99086062	PDGFbb	9q22.32	0,07%	trans
rs73554552	a	c	-5,50	3,8E-08	---	0,00	5,22E-01	0,07	-0,06	0,01	9	135861502	PDGFbb	9q34.13	0,05%	trans
rs34237126	a	c	-5,68	1,4E-08	---	0,00	4,58E-01	0,29	-0,04	0,01	10	64873883	PDGFbb	10q21.3	0,05%	trans

Table A.1 (cont.)

SNP	Allele1	Allele2	Zscore	P-value	Direction	HetISq	HetPVal	EAF	Beta	SE	Chromosome	Position	Cytokine	Locus	Explained variance	acting
rs7075281	a	c	6,98	3,0E-12	+++	0,00	8,30E-01	0,26	0,04	0,01	10	104220301	PDGFbb	10q24.32	0,08%	trans
rs6580980	a	g	-5,71	1,1E-08	---	68,40	4,22E-02	0,44	-0,03	0,01	12	54692061	PDGFbb	12q13.13	0,05%	trans
rs11553699	a	g	-5,57	2,6E-08	---	0,00	4,69E-01	0,14	-0,04	0,01	12	122216910	PDGFbb	12q24.31	0,05%	trans
rs12050334	t	c	5,57	2,6E-08	+++	44,40	1,65E-01	0,41	0,03	0,01	14	70653317	PDGFbb	14q24.2	0,05%	trans
rs2816648	t	c	5,69	1,3E-08	+++	42,10	1,78E-01	0,31	0,04	0,01	14	105708289	PDGFbb	14q32.33	0,05%	trans
rs2643356	t	c	5,82	6,1E-09	+++	84,10	1,86E-03	0,30	0,04	0,01	15	101971388	PDGFbb	15q26.3	0,06%	trans
rs79141987	a	g	5,65	1,6E-08	+++	0,00	7,52E-01	0,16	0,04	0,01	17	56398479	PDGFbb	17q22	0,05%	trans
rs1671226	c	g	-6,42	1,3E-10	---	27,40	2,52E-01	0,22	-0,05	0,01	19	55502846	PDGFbb	19q13.42	0,07%	trans
rs6075493	a	c	-5,49	4,1E-08	---	37,10	2,04E-01	0,30	-0,03	0,01	20	19272791	PDGFbb	20p11.23	0,05%	trans
rs1926231	t	c	-5,52	3,4E-08	--	0,00	3,33E-01	0,44	-0,04	0,01	1	198603279	RANTES	1q31.3	0,08%	trans
rs1354034	t	c	6,60	4,1E-11	++	0,00	4,39E-01	0,38	0,05	0,01	3	56849749	RANTES	3p14.3	0,11%	trans
rs2253294	t	c	5,66	1,5E-08	++	0,00	3,63E-01	0,21	0,05	0,01	10	37706195	RANTES	10p11.21	0,08%	trans
rs4746855	a	g	6,67	2,5E-11	++	62,80	1,01E-01	0,40	0,05	0,01	10	64822828	RANTES	10q21.3	0,11%	trans
rs11650416	a	c	12,41	2,3E-35	++	0,00	8,20E-01	0,826	0,12	0,01	17	34077428	RANTES	17q12	n/a	cis
rs295070	a	g	5,99	2,2E-09	++	0,00	5,98E-01	0,02	0,16	0,03	17	32786927	RANTES	17q12	0,09%	trans
rs12953115	a	g	5,64	1,7E-08	-+	72,40	5,71E-02	0,14	0,06	0,01	17	33797534	RANTES	17q12	0,08%	trans
rs143719578	t	g	5,59	2,3E-08	++	0,00	3,29E-01	0,03	0,12	0,02	17	33779964	RANTES	17q12	0,08%	trans
rs1671152	t	g	-5,54	3,0E-08	--	0,00	3,26E-01	0,15	-0,06	0,01	19	55526345	RANTES	19q13.42	0,08%	trans
rs4634925	c	g	-6,45	1,1E-10	---	86,70	5,58E-04	0,38	-0,04	0,01	1	161189344	SCF	1q23.3	0,07%	trans
rs72704449	t	c	-6,97	3,2E-12	---	0,00	6,22E-01	0,05	-0,10	0,01	1	179473273	SCF	1q25.2	0,08%	trans
rs4846913	a	c	-5,62	2,0E-08	---	58,90	8,78E-02	0,39	-0,03	0,01	1	230294715	SCF	1q42.13	0,05%	trans
rs514230	a	t	-5,49	4,0E-08	+--	87,30	3,82E-04	0,45	-0,03	0,01	1	234858597	SCF	1q42.3	0,05%	trans
rs1585488	t	g	6,11	1,0E-09	-++	74,80	1,90E-02	0,49	0,03	0,01	3	98359663	SCF	3q12.1	0,06%	trans
rs2125787	a	g	-5,53	3,2E-08	+--	87,70	2,99E-04	0,39	-0,03	0,01	4	87996623	SCF	4q21.3	0,05%	trans
rs854562	t	c	6,01	1,8E-09	+++	59,80	8,33E-02	0,27	0,04	0,01	7	94947969	SCF	7q21.3	0,06%	trans
rs6999569	a	g	-6,33	2,4E-10	---	0,00	6,23E-01	0,50	-0,04	0,01	8	126475770	SCF	8q24.13	0,06%	trans
rs675849	t	c	-5,64	1,7E-08	+--	83,00	2,80E-03	0,12	-0,05	0,01	9	15298666	SCF	9p22.3	0,05%	trans

Table A.1 (cont.)

SNP	Allele1	Allele2	Zscore	P-value	Direction	HetISq	HetPVal	EAF	Beta	SE	Chromosome	Position	Cytokine	Locus	Explained variance	acting
rs112853430	t	c	9,01	2,1E-19	?++	65,50	8,88E-02	0,04	0,15	0,02	9	107585213	SCF	9q31.1	0,15%	trans
rs4743764	t	c	7,42	1,2E-13	+++	0,00	9,73E-01	0,38	0,04	0,01	9	107629104	SCF	9q31.1	0,09%	trans
rs7868232	t	c	5,51	3,5E-08	+++	35,10	2,14E-01	0,20	0,04	0,01	9	136042264	SCF	9q34.2	0,05%	trans
rs7304494	t	c	-6,84	7,7E-12	---	57,70	9,43E-02	0,32	-0,04	0,01	12	89363909	SCF	12q21.33	0,08%	trans
rs143875230	a	g	-6,14	8,5E-10	---	47,40	1,49E-01	0,03	-0,10	0,02	15	43278726	SCF	15q15.2	0,06%	trans
rs10468017	t	c	-5,55	2,8E-08	+--	90,30	3,38E-05	0,31	-0,03	0,01	15	58678512	SCF	15q21.3	0,05%	trans
rs77924615	a	g	-6,70	2,1E-11	---	49,50	1,38E-01	0,20	-0,05	0,01	16	20392332	SCF	16p12.3	0,07%	trans
rs9989419	a	g	-7,22	5,1E-13	---	49,80	1,36E-01	0,39	-0,04	0,01	16	56985139	SCF	16q13	0,08%	trans
rs150781363	t	c	6,60	4,2E-11	+++	0,00	4,68E-01	0,03	0,11	0,02	16	67884268	SCF	16q22.1	0,07%	trans
rs28382814	t	c	-5,87	4,3E-09	---	69,20	3,89E-02	0,03	-0,10	0,02	16	66971780	SCF	16q22.1	0,06%	trans
rs12721051	c	g	-5,74	9,3E-09	---	0,20	3,67E-01	0,20	-0,04	0,01	19	45422160	SCF	19q13.32	0,05%	trans
rs389096	a	g	-6,16	7,1E-10	+--	90,70	2,23E-05	0,33	-0,04	0,01	19	54764322	SCF	19q13.42	0,06%	trans
rs148773337	a	c	8,47	2,4E-17	-++	90,40	2,92E-05	0,02	0,18	0,02	20	44539057	SCF	20q13.12	0,11%	trans
rs6032254	a	c	7,66	1,8E-14	-++	87,80	2,84E-04	0,08	0,08	0,01	20	44132654	SCF	20q13.12	0,09%	trans
rs149890864	t	c	6,20	5,5E-10	?++	92,10	3,59E-04	0,00	0,35	0,06	20	43612904	SCF	20q13.12	0,08%	trans
rs12053610	a	g	6,11	1,0E-09	-++	84,00	1,90E-03	0,06	0,07	0,01	20	43963739	SCF	20q13.12	0,06%	trans
rs2741441	t	g	5,89	3,9E-09	-++	74,70	1,92E-02	0,13	0,05	0,01	20	43979887	SCF	20q13.12	0,06%	trans
rs12134724	t	c	5,59	2,3E-08	++	0,00	8,11E-01	0,43	0,04	0,01	1	205039288	SCGF-b	1q32.1	0,08%	trans
rs6662383	t	c	5,59	2,3E-08	++	31,20	2,28E-01	0,09	0,07	0,01	1	236108446	SCGF-b	1q42.3	0,08%	trans
rs10804034	t	c	5,71	1,1E-08	++	0,00	3,88E-01	0,37	0,04	0,01	2	191244826	SCGF-b	2q32.2	0,08%	trans
rs150741051	a	g	5,93	3,0E-09	++	0,00	8,87E-01	0,09	0,07	0,01	3	46660223	SCGF-b	3p21.31	0,09%	trans
rs6782228	c	g	-6,51	7,5E-11	--	0,00	7,82E-01	0,29	-0,05	0,01	3	128323424	SCGF-b	3q21.3	0,11%	trans
rs3797358	t	c	-5,46	4,9E-08	--	0,00	5,80E-01	0,46	-0,04	0,01	5	72168857	SCGF-b	5q13.2	0,08%	trans
rs915654	a	t	5,53	3,2E-08	++	0,00	9,10E-01	0,38	0,04	0,01	6	31538497	SCGF-b	6p21.33	0,08%	trans
rs1873547	a	g	-5,81	6,1E-09	--	0,00	5,29E-01	0,47	-0,04	0,01	8	70724911	SCGF-b	8q13.3	0,09%	trans
rs2012880	c	g	6,03	1,6E-09	++	0,00	5,54E-01	0,14	0,06	0,01	8	130545566	SCGF-b	8q24.21	0,09%	trans
rs2093839	c	g	5,67	1,5E-08	++	0,00	5,38E-01	0,18	0,05	0,01	9	79106652	SCGF-b	9q21.13	0,08%	trans

Table A.1 (cont.)

SNP	Allele1	Allele2	Zscore	P-value	Direction	HetISq	HetPVal	EAF	Beta	SE	Chromosome	Position	Cytokine	Locus	Explained variance	acting
rs11257361	a	t	5,46	4,7E-08	++	19,60	2,65E-01	0,19	0,05	0,01	10	11895507	SCGF-b	10p14	0,08%	trans
rs56086228	a	g	5,89	3,8E-09	++	61,00	1,09E-01	0,02	0,17	0,03	12	101598983	SCGF-b	12q23.1	0,09%	trans
rs11111748	a	g	7,87	3,6E-15	++	0,00	9,75E-01	0,08	0,11	0,01	12	104149022	SCGF-b	12q23.3	0,16%	trans
rs139133040	c	g	7,52	5,5E-14	++	79,30	2,80E-02	0,02	0,19	0,03	12	105084960	SCGF-b	12q23.3	0,14%	trans
rs4981026	a	g	-6,42	1,4E-10	--	81,50	2,02E-02	0,23	-0,05	0,01	12	104152456	SCGF-b	12q23.3	0,11%	trans
rs10861032	t	c	-5,91	3,4E-09	--	0,00	7,30E-01	0,16	-0,06	0,01	12	103912506	SCGF-b	12q23.3	0,09%	trans
rs150179248	a	t	5,73	9,8E-09	++	66,90	8,23E-02	0,02	0,13	0,02	12	103019462	SCGF-b	12q23.2	0,08%	trans
rs483879	t	c	-5,94	2,9E-09	--	0,00	8,93E-01	0,21	-0,05	0,01	13	52127212	SCGF-b	13q14.3	0,09%	trans
rs12878578	a	g	6,26	4,0E-10	++	0,00	3,85E-01	0,13	0,07	0,01	14	25045589	SCGF-b	14q12	0,10%	trans
rs7149169	a	g	-6,16	7,3E-10	--	69,20	7,16E-02	0,32	-0,05	0,01	14	103833065	SCGF-b	14q32.32	0,10%	trans
rs35609972	a	g	6,12	9,5E-10	++	0,00	8,50E-01	0,27	0,05	0,01	15	50324126	SCGF-b	15q21.2	0,10%	trans
rs11864191	t	c	6,88	5,8E-12	++	64,40	9,40E-02	0,08	0,09	0,01	16	545996	SCGF-b	16p13.3	0,12%	trans
rs1698237	t	c	-5,45	5,0E-08	--	0,00	7,68E-01	0,42	-0,04	0,01	16	451306	SCGF-b	16p13.3	0,08%	trans
rs255056	c	g	5,65	1,6E-08	++	4,30	3,07E-01	0,13	0,06	0,01	16	68016185	SCGF-b	16q22.1	0,08%	trans
rs60384564	a	c	5,51	3,6E-08	++	0,00	5,03E-01	0,04	0,10	0,02	17	55421435	SCGF-b	17q22	0,08%	trans
rs7246004	t	g	10,98	5,0E-28	++	18,80	2,67E-01	0,341	0,08	0,01	19	51216909	SCGF-b	19q13.33	n/a	cis
rs144686073	a	g	9,89	4,5E-23	++	88,10	3,81E-03	0,01	0,39	0,04	19	51053661	SCGF-b	19q13.33	0,25%	trans
rs77578935	a	g	7,88	3,2E-15	-+	92,30	3,20E-04	0,03	0,18	0,02	19	50414185	SCGF-b	19q13.33	0,16%	trans
rs75256967	a	g	7,49	7,1E-14	++	79,70	2,64E-02	0,01	0,34	0,04	19	50901551	SCGF-b	19q13.33	0,14%	trans
rs144724875	t	c	6,22	4,8E-10	++	95,70	1,56E-06	0,02	0,16	0,03	19	51195936	SCGF-b	19q13.33	0,10%	trans
rs80226314	t	c	5,72	1,1E-08	-+	78,60	3,05E-02	0,02	0,14	0,02	19	50829530	SCGF-b	19q13.33	0,08%	trans
rs4813271	a	c	-5,75	9,1E-09	--	0,00	3,38E-01	0,21	-0,05	0,01	20	17546574	SCGF-b	20p12.1	0,08%	trans
rs72683129	a	g	-5,89	3,9E-09	--	79,10	2,87E-02	0,13	-0,06	0,01	1	66069781	SDF-1a	1p31.3	0,08%	trans
rs6733162	c	g	-5,58	2,4E-08	--	61,60	1,07E-01	0,41	-0,04	0,01	2	162913498	SDF-1a	2q24.2	0,07%	trans
rs28595399	t	c	5,72	1,1E-08	++	54,60	1,38E-01	0,29	0,04	0,01	3	12500065	SDF-1a	3p25.2	0,08%	trans
rs56013261	t	c	5,50	3,8E-08	++	0,00	6,74E-01	0,39	0,04	0,01	3	47224014	SDF-1a	3p21.31	0,07%	trans
rs17404060	t	c	6,18	6,3E-10	++	87,30	5,02E-03	0,12	0,06	0,01	5	115319911	SDF-1a	5q23.1	0,09%	trans

Table A.1 (cont.)

SNP	Allele1	Allele2	Zscore	P-value	Direction	HetISq	HetPVal	EAF	Beta	SE	Chromosome	Position	Cytokine	Locus	Explained variance	acting
rs115841185	t	c	5,49	4,0E-08	++	30,20	2,31E-01	0,03	0,11	0,02	7	153655480	SDF-1a	7q36.2	0,07%	trans
rs10123570	t	c	5,49	3,9E-08	++	51,40	1,51E-01	0,48	0,04	0,01	9	89356766	SDF-1a	9q21.33	0,07%	trans
rs17391002	a	g	-6,43	1,3E-10	+-	94,80	1,09E-05	0,7734	-0,06	0,01	10	44855927	SDF-1a	10q11.21	n/a	cis
rs180738147	t	c	6,38	1,8E-10	++	83,20	1,48E-02	0,03	0,13	0,02	10	44925153	SDF-1a	10q11.21	0,09%	trans
rs2279555	a	g	5,64	1,7E-08	-+	91,30	6,91E-04	0,18	0,05	0,01	10	44476596	SDF-1a	10q11.21	0,07%	trans
rs10822145	t	c	5,58	2,5E-08	++	0,00	9,77E-01	0,48	0,04	0,01	10	64934548	SDF-1a	10q21.3	0,07%	trans
rs7310615	c	g	5,94	2,8E-09	++	0,00	3,33E-01	0,38	0,04	0,01	12	111865049	SDF-1a	12q24.12	0,08%	trans
rs4147990	t	c	10,04	1,0E-23	++	86,30	6,85E-03	0,06	0,15	0,01	17	66913936	SDF-1a	17q24.2	0,26%	trans
rs1468512	t	c	5,59	2,3E-08	++	0,00	3,77E-01	0,15	0,05	0,01	17	67219768	SDF-1a	17q24.3	0,07%	trans
rs1329424	t	g	6,35	2,1E-10	-+	83,30	1,45E-02	0,40	0,05	0,01	1	196646176	TNF-a	1q31.3	0,10%	trans
rs1329424	t	g	8,43	3,3E-17	-+	93,30	1,16E-04	0,40	0,06	0,01	1	196646176	TNF-b	1q31.3	0,19%	trans
rs4850046	t	c	-6,04	1,5E-09	--	0,00	8,56E-01	0,12	-0,07	0,01	2	3634606	TNF-b	2p25.3	0,10%	trans
rs1329424	t	g	7,93	2,2E-15	+-+	96,30	2,11E-12	0,40	0,05	0,01	1	196646176	TRAIL	1q31.3	0,11%	trans
rs6542680	t	c	-5,70	1,2E-08	++-	95,30	6,81E-10	0,18	-0,04	0,01	2	3640142	TRAIL	2p25.3	0,05%	trans
rs73169285	a	t	10,44	1,6E-25	++?	71,90	5,92E-02	0,7435	0,12	0,01	3	172216957	TRAIL	3q26.31	n/a	cis
rs562416	a	c	-5,68	1,3E-08	---	91,80	5,26E-06	0,14	-0,05	0,01	3	172161842	TRAIL	3q26.31	0,05%	trans
rs59724749	a	g	-7,64	2,1E-14	+-?	98,40	6,25E-15	0,18	-0,09	0,01	3	186408443	TRAIL	3q27.3	0,25%	trans
rs41285751	t	g	6,20	5,6E-10	?++	51,60	1,51E-01	0,08	0,08	0,01	6	31899815	TRAIL	6p21.33	0,09%	trans
rs45505795	c	g	5,91	3,5E-09	+++	97,00	4,51E-15	0,02	0,12	0,02	14	94756943	TRAIL	14q32.13	0,06%	trans
rs2901364	t	g	-10,13	4,0E-24	--?	99,10	4,23E-26	0,02	-0,36	0,04	18	29569416	TRAIL	18q12.1	0,51%	trans
rs140103836	t	c	-6,51	7,7E-11	--+	99,20	1,18E-53	0,02	-0,14	0,02	18	28811450	TRAIL	18q12.1	0,08%	trans
rs74778900	t	c	6,07	1,3E-09	+++	97,70	8,47E-20	0,01	0,15	0,03	18	28086266	TRAIL	18q12.1	0,06%	trans
rs117618570	t	g	-5,88	4,2E-09	---	98,40	2,73E-28	0,02	-0,13	0,02	18	29008594	TRAIL	18q12.1	0,06%	trans
rs78186881	a	t	-5,65	1,6E-08	---	97,70	9,97E-20	0,06	-0,07	0,01	18	29382112	TRAIL	18q12.1	0,05%	trans
rs77121181	a	g	6,60	4,0E-11	-+?	98,60	9,80E-17	0,04	0,16	0,02	19	44072655	TRAIL	19q13.31	0,21%	trans
rs145243487	a	t	-5,46	4,8E-08	---	49,20	1,40E-01	0,08	-0,06	0,01	5	88035532	VEGF	5q14.3	0,05%	trans
rs74556053	a	g	-15,31	6,3E-53	---	86,30	6,65E-04	0,0716	-0,17	0,01	6	43934340	VEGF	6p21.1	n/a	cis

Table A.1 (cont.)

SNP	Allele1	Allele2	Zscore	P-value	Direction	HetISq	HetPVal	EAF	Beta	SE	Chromosome	Position	Cytokine	Locus	Explained variance	acting
rs6914863	c	g	-7,12	1,1E-12	---	93,10	4,72E-07	0,02	-0,14	0,02	6	43961813	VEGF	6p21.1	0,09%	trans
rs62401205	a	c	-7,09	1,4E-12	---	89,20	9,45E-05	0,03	-0,13	0,02	6	43855489	VEGF	6p21.1	0,09%	trans
rs13202103	t	c	-6,56	5,3E-11	---	54,80	1,10E-01	0,03	-0,11	0,02	6	43883984	VEGF	6p21.1	0,08%	trans
rs35703624	t	c	6,42	1,4E-10	-++	73,90	2,17E-02	0,03	0,12	0,02	6	43968412	VEGF	6p21.1	0,08%	trans
rs833065	a	g	5,70	1,2E-08	+++	0,00	4,63E-01	0,16	0,05	0,01	6	43683804	VEGF	6p21.1	0,06%	trans
rs7692	a	c	-5,46	4,9E-08	+--	78,20	1,02E-02	0,28	-0,04	0,01	6	43304007	VEGF	6p21.1	0,05%	trans
rs302953	t	c	6,41	1,4E-10	+++	89,60	6,78E-05	0,40	0,04	0,01	8	106512481	VEGF	8q23.1	0,07%	trans
rs10967571	t	c	-11,30	1,3E-29	---	83,60	2,25E-03	0,45	-0,07	0,01	9	2694834	VEGF	9p24.2	0,22%	trans
rs34881325	t	c	-6,11	1,0E-09	--?	85,50	8,56E-03	0,39	-0,06	0,01	9	2622134	VEGF	9p24.2	0,19%	trans
rs4746855	a	g	5,52	3,4E-08	+++	68,20	4,29E-02	0,40	0,03	0,01	10	64822828	VEGF	10q21.3	0,05%	trans
rs12444373	c	g	-7,03	2,1E-12	---	31,20	2,34E-01	0,03	-0,12	0,02	16	88564585	VEGF	16q24.2	0,09%	trans

Table A.2. GWAS heterogeneity results. Results, restricted to heterogenous variant (heterogeneity p-value < 0.1), showing 174 significant associations between circulating cytokine levels and variants.

SNP	Allele1	Allele2	Zscore	P-value	Direction	HetISq	HetPVal	EAF	Beta	SE	Chromosome	Position	Cytokine	Locus	Explained variance
rs35099140	a	t	5,72	1,1E-08	?-+	87,20	5,16E-03	0,23	0,05	0,01	14	106952318	bNGF	14q32.33	0,08%
rs116758863	t	g	-5,64	1,7E-08	--	74,40	4,79E-02	0,02	-0,13	0,02	3	39250894	Eotaxin	3p22.2	0,07%
rs11920996	t	c	9,63	5,8E-22	++	94,10	3,73E-05	0,02	0,22	0,02	3	42542761	Eotaxin	3p22.1	0,21%
rs140921648	a	c	5,69	1,3E-08	++	76,20	4,02E-02	0,04	0,10	0,02	7	75202900	Eotaxin	7q11.23	0,07%
rs704903	t	c	-10,07	7,8E-24	--	77,90	3,35E-02	0,25	-0,08	0,01	3	43070847	Eotaxin	3p22.1	0,23%
rs7550207	t	c	-6,19	6,0E-10	--	82,50	1,67E-02	0,26	-0,05	0,01	1	159174885	Eotaxin	1q23.2	0,09%
rs9810934	a	g	12,57	3,2E-36	++	85,90	7,80E-03	0,29	0,09	0,01	3	45954352	Eotaxin	3p21.31	0,36%
rs78836533	a	g	5,66	1,5E-08	-+	95,20	5,40E-06	0,05	0,09	0,02	4	121168969	FGF-b	4q27	0,07%
rs937355	a	g	6,60	4,1E-11	-+	96,20	3,28E-07	0,31	0,05	0,01	4	121570292	FGF-b	4q27	0,10%
rs6857701	t	c	-5,78	7,5E-09	+-	87,40	4,91E-03	0,14	-0,06	0,01	4	122315742	FGF-b	4q27	0,08%
rs141091752	c	g	7,51	5,8E-14	-+	95,80	1,02E-06	0,02	0,17	0,02	4	122898197	FGF-b	4q27	0,13%
rs141635731	t	g	6,62	3,7E-11	++	63,80	9,64E-02	0,03	0,13	0,02	4	123439970	FGF-b	4q27	0,10%
rs115049760	a	g	-5,53	3,2E-08	+-	96,20	2,86E-07	0,03	-0,11	0,02	4	124302061	FGF-b	4q28.1	0,07%
rs60093606	t	g	9,06	1,3E-19	-+	95,10	5,97E-06	0,29	0,07	0,01	4	127266290	FGF-b	4q28.1	0,19%
rs11668536	t	c	-6,59	4,3E-11	+-	96,60	6,65E-08	0,25	-0,05	0,01	19	45328476	G-CSF	19q13.32	0,10%
rs117372248	a	g	5,68	1,3E-08	++	86,20	7,13E-03	0,14	0,05	0,01	19	43361820	G-CSF	19q13.2	0,07%
rs11880654	t	c	-6,64	3,1E-11	+-	95,40	3,48E-06	0,08	-0,08	0,01	19	45745857	G-CSF	19q13.32	0,10%
rs16979231	t	c	-5,54	3,1E-08	--	72,80	5,51E-02	0,21	-0,05	0,01	19	45042765	G-CSF	19q13.31	0,07%
rs34939346	t	c	-5,93	3,0E-09	--	86,90	5,70E-03	0,20	-0,05	0,01	19	40421612	G-CSF	19q13.2	0,08%
rs56147474	a	g	5,84	5,2E-09	++	78,10	3,24E-02	0,11	0,06	0,01	3	165798383	G-CSF	3q26.1	0,08%
rs7252448	t	c	-5,63	1,8E-08	--	71,10	6,27E-02	0,31	-0,04	0,01	19	46142053	G-CSF	19q13.32	0,07%
rs79924756	a	g	5,46	4,6E-08	-+	85,90	7,78E-03	0,22	0,05	0,01	19	44321973	G-CSF	19q13.31	0,07%
rs10019504	a	g	7,61	2,8E-14	?++	94,60	1,55E-05	0,03	0,15	0,02	4	71486305	GROa	4q13.3	0,12%
rs10995445	a	t	-8,61	7,6E-18	---	64,40	6,02E-02	0,50	-0,05	0,01	10	64874754	GROa	10q21.3	0,13%
rs114296817	a	c	6,69	2,3E-11	?++	89,20	2,36E-03	0,01	0,21	0,03	4	68310149	GROa	4q13.2	0,09%

Table A.2 (cont.)

SNP	Allele1	Allele2	Zscore	P-value	Direction	HetISq	HetPVal	EAF	Beta	SE	Chromosome	Position	Cytokine	Locus	Explained variance
rs114536173	a	t	7,03	2,0E-12	?++	93,90	5,12E-05	0,03	0,13	0,02	4	71538474	GROa	4q13.3	0,10%
rs115275434	t	c	-7,26	4,0E-13	+--	81,90	4,00E-03	0,02	-0,16	0,02	4	71719779	GROa	4q13.3	0,10%
rs146702741	t	c	6,26	3,9E-10	-++	91,60	6,87E-06	0,01	0,17	0,03	4	72484429	GROa	4q13.3	0,07%
rs192031641	c	g	-5,55	2,9E-08	-+-	81,20	4,84E-03	0,03	-0,10	0,02	4	64401593	GROa	4q13.1	0,06%
rs192437265	t	c	5,86	4,8E-09	--+	91,60	6,67E-06	0,03	0,10	0,02	4	76875335	GROa	4q21.1	0,06%
rs2249581	t	c	-5,70	1,2E-08	---	96,60	1,30E-13	0,25	-0,04	0,01	1	159144581	GROa	1q23.2	0,06%
rs28624853	a	g	-8,09	5,9E-16	?--	95,90	7,90E-07	0,03	-0,15	0,02	4	72138143	GROa	4q13.3	0,13%
rs377499720	a	g	-5,92	3,1E-09	?--	65,00	9,12E-02	0,02	-0,13	0,02	4	75137124	GROa	4q13.3	0,08%
rs56042607	a	g	6,81	1,0E-11	?-+	97,10	4,04E-09	0,04	0,11	0,02	4	73005872	GROa	4q13.3	0,09%
rs57619473	a	c	-6,10	1,1E-09	?--	93,60	8,23E-05	0,04	-0,09	0,02	4	69180867	GROa	4q13.2	0,07%
rs78898749	t	c	5,52	3,4E-08	--+	91,60	6,64E-06	0,01	0,18	0,03	4	70831665	GROa	4q13.3	0,06%
rs149467613	a	g	7,26	4,0E-13	+++	81,10	5,07E-03	0,06	0,09	0,01	11	72943483	HGF	11q13.4	0,09%
rs5745692	c	g	-5,49	4,0E-08	---	80,20	6,33E-03	0,05	-0,08	0,01	7	81358266	HGF	7q21.11	0,05%
rs1042663	a	g	8,71	3,1E-18	++	93,00	1,63E-04	0,09	0,10	0,01	6	31905130	IFN-g	6p21.33	0,18%
rs116224050	a	g	6,38	1,8E-10	-+	89,60	1,95E-03	0,03	0,14	0,02	1	196918145	IFN-g	1q31.3	0,09%
rs12127759	t	c	-7,60	2,9E-14	--	83,20	1,48E-02	0,14	-0,07	0,01	1	196648613	IFN-g	1q31.3	0,13%
rs71631848	a	g	6,81	9,7E-12	++	85,20	9,43E-03	0,23	0,06	0,01	1	196186335	IFN-g	1q31.3	0,11%
rs1329424	t	g	6,41	1,5E-10	-+	90,50	1,20E-03	0,40	0,04	0,01	1	196646176	IL-10	1q31.3	0,10%
rs7739450	a	g	-8,58	9,7E-18	--	99,40	8,28E-37	0,47	-0,06	0,01	6	43911598	IL-10	6p21.1	0,17%
rs12127759	t	c	-6,83	8,3E-12	+-	90,70	1,03E-03	0,14	-0,07	0,01	1	196648613	IL-13	1q31.3	0,12%
rs11072257	t	c	5,45	5,0E-08	-++	65,50	5,52E-02	0,08	0,06	0,01	15	71463600	IL-16	15q23	0,05%
rs138561568	a	c	5,94	2,9E-09	?++	84,90	9,98E-03	0,01	0,20	0,03	15	81806029	IL-16	15q25.2	0,07%
rs139576939	c	g	-14,32	1,7E-46	+--	97,20	1,61E-16	0,05	-0,20	0,01	15	83393723	IL-16	15q25.2	0,38%
rs17211644	t	c	5,48	4,2E-08	+-+	90,90	1,70E-05	0,14	0,05	0,01	15	80116362	IL-16	15q25.1	0,05%
rs62143194	c	g	-8,69	3,7E-18	--?	92,10	3,80E-04	0,25	-0,10	0,01	19	54319624	IL-16	19q13.42	0,35%
rs71404763	a	c	17,78	1,0E-70	+++	89,10	1,06E-04	0,05	0,25	0,01	15	81439371	IL-16	15q25.1	0,57%
rs72851055	c	g	5,74	9,7E-09	?++	78,20	3,21E-02	0,34	0,04	0,01	6	32502814	IL-16	6p21.32	0,07%

Table A.2 (cont.)

SNP	Allele1	Allele2	Zscore	P-value	Direction	HetISq	HetPVal	EAF	Beta	SE	Chromosome	Position	Cytokine	Locus	Explained variance
rs75156308	a	g	6,37	1,9E-10	+++	85,30	1,09E-03	0,05	0,09	0,01	15	86174098	IL-16	15q25.3	0,07%
rs1329424	t	g	5,97	2,3E-09	-+	88,30	3,41E-03	0,40	0,04	0,01	1	196646176	IL-17	1q31.3	0,08%
rs143732640	t	c	9,19	3,9E-20	++	70,80	6,42E-02	0,03	0,21	0,02	2	3353632	IL-1B	2p25.3	0,22%
rs16997771	t	c	-6,24	4,5E-10	+-	92,30	3,13E-04	0,03	-0,13	0,02	19	10148713	IL-1B	19p13.2	0,10%
rs75564661	a	g	-6,68	2,5E-11	+-	94,80	1,26E-05	0,04	-0,12	0,02	2	3032487	IL-1B	2p25.3	0,12%
rs77246730	t	c	-18,03	1,1E-72	+-	97,40	6,36E-10	0,01	-0,55	0,03	2	3642756	IL-1B	2p25.3	0,83%
rs7221894	t	c	-5,47	4,5E-08	--?	66,20	8,55E-02	0,37	-0,06	0,01	17	38165485	IL-1ra	17q21.1	0,14%
rs9937053	a	g	5,52	3,4E-08	+++	58,70	8,88E-02	0,44	0,03	0,01	16	53799507	IL-1ra	16q12.2	0,05%
rs62143194	c	g	-15,68	2,0E-55	--?	97,20	2,35E-09	0,25	-0,17	0,01	19	54319624	IL-1ra	19q13.42	1,11%
rs10169524	a	g	-5,57	2,6E-08	+--	81,70	4,29E-03	0,27	-0,04	0,01	2	113528872	IL-1ra	2q13	0,05%
rs4665972	t	c	8,00	1,2E-15	++	72,80	5,51E-02	0,34	0,06	0,01	2	27598097	IL-2	2p23.3	0,16%
rs1329424	t	g	8,00	1,3E-15	-+	96,00	5,49E-07	0,40	0,06	0,01	1	196646176	IL-4	1q31.3	0,15%
rs7194068	t	g	-5,69	1,3E-08	--	72,60	5,63E-02	0,43	-0,04	0,01	16	17576804	IL-4	16p12.3	0,07%
rs11265611	a	g	6,70	2,0E-11	+++	95,30	5,36E-10	0,34	0,04	0,01	1	154395125	IL-6	1q21.3	0,08%
rs12075	a	g	10,01	1,3E-23	+++	76,10	1,53E-02	0,42	0,06	0,01	1	159175354	IL-8	1q23.2	0,18%
rs12127759	t	c	-5,96	2,5E-09	-+-	88,50	1,73E-04	0,14	-0,05	0,01	1	196648613	IL-8	1q31.3	0,06%
rs41285751	t	g	5,49	4,1E-08	?++	80,10	2,49E-02	0,08	0,07	0,01	6	31899815	IL-8	6p21.33	0,07%
rs61820876	t	g	-5,85	5,0E-09	---	82,50	3,33E-03	0,28	-0,04	0,01	1	196209945	IL-8	1q31.3	0,07%
rs6993770	a	t	5,68	1,4E-08	-++	62,00	7,20E-02	0,22	0,04	0,01	8	106581528	IL-8	8q23.1	0,06%
rs942053	t	c	5,84	5,2E-09	+++	78,70	9,22E-03	0,04	0,09	0,02	4	74530753	IL-8	4q13.3	0,07%
rs11742478	a	c	-5,54	3,0E-08	+-	84,00	1,23E-02	0,07	-0,08	0,01	5	135222840	IL-9	5q31.1	0,08%
rs7964426	t	c	-6,29	3,2E-10	+-	80,00	2,52E-02	0,34	-0,05	0,01	12	54668471	IL-9	12q13.13	0,10%
rs573764538	t	c	5,47	4,5E-08	?-+	86,20	7,10E-03	0,06	0,08	0,01	17	6962925	M-CSF	17p13.1	0,07%
rs41556717	t	c	6,98	2,9E-12	-++	88,10	2,28E-04	0,02	0,16	0,02	17	7399319	M-CSF	17p13.1	0,10%
rs17880604	c	g	-7,40	1,3E-13	+--	89,90	4,90E-05	0,02	-0,19	0,03	17	7577644	M-CSF	17p13.1	0,11%
rs12121864	a	c	-6,14	8,3E-10	---	81,60	4,40E-03	0,12	-0,06	0,01	1	9205332	M-CSF	1p36.22	0,07%
rs4665972	t	c	-5,45	5,0E-08	+--	82,40	3,38E-03	0,34	-0,03	0,01	2	27598097	M-CSF	2p23.3	0,05%

Table A.2 (cont.)

SNP	Allele1	Allele2	Zscore	P-value	Direction	HetISq	HetPVal	EAF	Beta	SE	Chromosome	Position	Cytokine	Locus	Explained variance
rs738409	c	g	-6,70	2,2E-11	+--	84,70	1,42E-03	0,23	-0,05	0,01	22	44324727	M-CSF	22q13.31	0,08%
rs679574	c	g	-6,04	1,6E-09	++-	94,70	6,88E-09	0,39	-0,04	0,01	19	49206108	M-CSF	19q13.33	0,07%
rs8081395	a	g	5,47	4,5E-08	-++	60,80	7,82E-02	0,46	0,03	0,01	17	57801761	M-CSF	17q23.1	0,05%
rs12940443	t	c	-5,53	3,2E-08	-+-	91,00	1,45E-05	0,34	-0,04	0,01	17	74482559	M-CSF	17q25.1	0,07%
rs6571186	a	c	-5,54	3,0E-08	+--	68,50	4,19E-02	0,12	-0,05	0,01	6	95921373	M-CSF	6q16.1	0,06%
rs3749260	a	c	5,82	6,0E-09	--+	91,80	5,19E-06	0,10	0,06	0,01	3	98250862	M-CSF	3q11.2	0,07%
rs3804622	a	g	7,35	2,0E-13	+-+	93,70	1,38E-07	0,43	0,05	0,01	3	98303182	M-CSF	3q12.1	0,11%
rs3755573	t	c	-9,49	2,4E-21	---	92,20	2,85E-06	0,44	-0,06	0,01	3	98489011	M-CSF	3q12.1	0,17%
rs3093044	a	g	5,84	5,2E-09	-++	92,60	1,44E-06	0,08	0,07	0,01	1	110459730	M-CSF	1p13.3	0,06%
rs1265565	t	c	6,19	6,0E-10	-++	62,80	6,82E-02	0,34	0,04	0,01	12	111715197	M-CSF	12q24.12	0,07%
rs75071241	a	g	-8,23	1,8E-16	---	93,80	1,03E-07	0,06	-0,11	0,01	11	126232186	M-CSF	11q24.2	0,12%
rs1257371	a	g	5,48	4,4E-08	+++	82,50	3,32E-03	0,16	0,05	0,01	2	134839539	M-CSF	2q21.2	0,06%
rs77155840	t	c	10,12	4,5E-24	--+	97,60	4,40E-19	0,02	0,23	0,02	2	134973524	M-CSF	2q21.2	0,19%
rs576123	t	c	-7,38	1,6E-13	?--	69,60	6,97E-02	0,26	-0,06	0,01	9	136144308	M-CSF	9q34.2	0,12%
rs245056	a	t	5,74	9,4E-09	+-+	92,40	1,78E-06	0,34	0,04	0,01	5	149341038	M-CSF	5q32	0,06%
rs2237085	a	g	-8,71	3,2E-18	---	92,70	1,13E-06	0,21	-0,07	0,01	5	149465249	M-CSF	5q32	0,15%
rs2269443	a	g	-8,36	6,4E-17	---	86,90	4,78E-04	0,12	-0,07	0,01	3	46491290	MCP-1	3p21.31	0,11%
rs34901975	a	g	10,25	1,2E-24	+++	87,50	3,39E-04	0,12	0,09	0,01	3	45916786	MCP-1	3p21.31	0,16%
rs3888652	a	g	6,35	2,2E-10	+++	82,60	3,22E-03	0,26	0,04	0,01	3	42726718	MCP-1	3p22.1	0,06%
rs4857857	a	g	5,60	2,1E-08	+++	87,40	3,60E-04	0,36	0,03	0,01	3	128313880	MCP-1	3q21.3	0,05%
rs62245068	t	c	8,94	4,1E-19	+++	62,60	6,91E-02	0,06	0,10	0,01	3	45840051	MCP-1	3p21.31	0,12%
rs9427342	c	g	5,63	1,8E-08	+++	63,30	6,55E-02	0,31	0,03	0,01	1	159360156	MCP-1	1q23.2	0,05%
rs1233653	t	c	9,73	2,2E-22	-+	87,20	5,13E-03	0,06	0,15	0,02	17	32639058	MCP-3	17q12	0,26%
rs6679677	a	c	5,63	1,8E-08	++	91,40	6,68E-04	0,13	0,06	0,01	1	114303808	MIG	1p13.2	0,08%
rs9903158	t	c	-8,00	1,2E-15	++-	98,50	1,62E-30	0,04	-0,12	0,02	17	34312337	MIP-1a	17q12	0,11%
rs62140208	a	g	-6,02	1,7E-09	---	88,60	1,59E-04	0,42	-0,04	0,01	2	42325560	MIP-1a	2p21	0,06%
rs7412	t	c	5,74	9,4E-09	-++	70,40	3,41E-02	0,06	0,07	0,01	19	45412079	MIP-1a	19q13.32	0,06%

Table A.2 (cont.)

SNP	Allele1	Allele2	Zscore	P-value	Direction	HetISq	HetPVal	EAF	Beta	SE	Chromosome	Position	Cytokine	Locus	Explained variance
rs11658282	t	c	-5,49	4,1E-08	--	82,50	1,68E-02	0,34	-0,05	0,01	17	33483115	MIP-1b	17q12	0,12%
rs34437725	t	c	-5,53	3,3E-08	--	83,50	1,39E-02	0,96	-0,13	0,02	17	33826785	MIP-1b	17q12	0,14%
rs76960253	t	c	5,89	3,8E-09	++	97,90	6,83E-12	0,02	0,22	0,04	17	34088656	MIP-1b	17q12	0,17%
rs7217473	t	c	7,13	1,0E-12	++	65,90	8,66E-02	0,06	0,14	0,02	17	34319064	MIP-1b	17q12	0,21%
rs62242542	t	c	-7,84	4,5E-15	--	98,20	6,54E-14	0,98	-0,29	0,04	3	45169491	MIP-1b	3p21.31	0,32%
rs73089379	c	g	-9,05	1,4E-19	--	94,30	2,71E-05	0,92	-0,16	0,02	3	45183414	MIP-1b	3p21.31	0,37%
rs10510748	a	g	6,45	1,1E-10	++	84,60	1,08E-02	0,90	0,10	0,01	3	46178538	MIP-1b	3p21.31	0,16%
rs9847395	t	c	5,67	1,4E-08	++	86,00	7,51E-03	0,44	0,05	0,01	3	46724548	MIP-1b	3p21.31	0,13%
rs10184062	c	g	5,48	4,3E-08	+++	66,50	5,08E-02	0,26	0,04	0,01	2	224867341	PDGFbb	2q36.1	0,05%
rs2643356	t	c	5,82	6,1E-09	+++	84,10	1,86E-03	0,30	0,04	0,01	15	101971388	PDGFbb	15q26.3	0,06%
rs302953	t	c	5,67	1,5E-08	-++	86,60	5,75E-04	0,40	0,03	0,01	8	106512481	PDGFbb	8q23.1	0,05%
rs385893	t	c	-5,73	9,9E-09	---	66,90	4,86E-02	0,44	-0,03	0,01	9	4763176	PDGFbb	9p24.1	0,05%
rs4674836	a	g	-6,04	1,6E-09	---	73,10	2,43E-02	0,35	-0,04	0,01	2	224855511	PDGFbb	2q36.1	0,06%
rs6580980	a	g	-5,71	1,1E-08	---	68,40	4,22E-02	0,44	-0,03	0,01	12	54692061	PDGFbb	12q13.13	0,05%
rs12953115	a	g	5,64	1,7E-08	-+	72,40	5,71E-02	0,14	0,06	0,01	17	33797534	RANTES	17q12	0,08%
rs10468017	t	c	-5,55	2,8E-08	+--	90,30	3,38E-05	0,31	-0,03	0,01	15	58678512	SCF	15q21.3	0,05%
rs112853430	t	c	9,01	2,1E-19	?++	65,50	8,88E-02	0,04	0,15	0,02	9	107585213	SCF	9q31.1	0,15%
rs12053610	a	g	6,11	1,0E-09	-++	84,00	1,90E-03	0,06	0,07	0,01	20	43963739	SCF	20q13.12	0,06%
rs148773337	a	c	8,47	2,4E-17	-++	90,40	2,92E-05	0,02	0,18	0,02	20	44539057	SCF	20q13.12	0,11%
rs149890864	t	c	6,20	5,5E-10	?++	92,10	3,59E-04	0,00	0,35	0,06	20	43612904	SCF	20q13.12	0,08%
rs1585488	t	g	6,11	1,0E-09	-++	74,80	1,90E-02	0,49	0,03	0,01	3	98359663	SCF	3q12.1	0,06%
rs2125787	a	g	-5,53	3,2E-08	+--	87,70	2,99E-04	0,39	-0,03	0,01	4	87996623	SCF	4q21.3	0,05%
rs2741441	t	g	5,89	3,9E-09	-++	74,70	1,92E-02	0,13	0,05	0,01	20	43979887	SCF	20q13.12	0,06%
rs28382814	t	c	-5,87	4,3E-09	---	69,20	3,89E-02	0,03	-0,10	0,02	16	66971780	SCF	16q22.1	0,06%
rs389096	a	g	-6,16	7,1E-10	+--	90,70	2,23E-05	0,33	-0,04	0,01	19	54764322	SCF	19q13.42	0,06%
rs4634925	c	g	-6,45	1,1E-10	---	86,70	5,58E-04	0,38	-0,04	0,01	1	161189344	SCF	1q23.3	0,07%
rs4846913	a	c	-5,62	2,0E-08	---	58,90	8,78E-02	0,39	-0,03	0,01	1	230294715	SCF	1q42.13	0,05%

Table A.2 (cont.)

SNP	Allele1	Allele2	Zscore	P-value	Direction	HetISq	HetPVal	EAF	Beta	SE	Chromosome	Position	Cytokine	Locus	Explained variance
rs514230	a	t	-5,49	4,0E-08	+--	87,30	3,82E-04	0,45	-0,03	0,01	1	234858597	SCF	1q42.3	0,05%
rs6032254	a	c	7,66	1,8E-14	-++	87,80	2,84E-04	0,08	0,08	0,01	20	44132654	SCF	20q13.12	0,09%
rs675849	t	c	-5,64	1,7E-08	+--	83,00	2,80E-03	0,12	-0,05	0,01	9	15298666	SCF	9p22.3	0,05%
rs7304494	t	c	-6,84	7,7E-12	---	57,70	9,43E-02	0,32	-0,04	0,01	12	89363909	SCF	12q21.33	0,08%
rs854562	t	c	6,01	1,8E-09	+++	59,80	8,33E-02	0,27	0,04	0,01	7	94947969	SCF	7q21.3	0,06%
rs11864191	t	c	6,88	5,8E-12	++	64,40	9,40E-02	0,08	0,09	0,01	16	545996	SCGF-b	16p13.3	0,12%
rs77578935	a	g	7,88	3,2E-15	-+	92,30	3,20E-04	0,03	0,18	0,02	19	50414185	SCGF-b	19q13.33	0,16%
rs80226314	t	c	5,72	1,1E-08	-+	78,60	3,05E-02	0,02	0,14	0,02	19	50829530	SCGF-b	19q13.33	0,08%
rs75256967	a	g	7,49	7,1E-14	++	79,70	2,64E-02	0,01	0,34	0,04	19	50901551	SCGF-b	19q13.33	0,14%
rs144686073	a	g	9,89	4,5E-23	++	88,10	3,81E-03	0,01	0,39	0,04	19	51053661	SCGF-b	19q13.33	0,25%
rs144724875	t	c	6,22	4,8E-10	++	95,70	1,56E-06	0,02	0,16	0,03	19	51195936	SCGF-b	19q13.33	0,10%
rs150179248	a	t	5,73	9,8E-09	++	66,90	8,23E-02	0,02	0,13	0,02	12	103019462	SCGF-b	12q23.2	0,08%
rs7149169	a	g	-6,16	7,3E-10	--	69,20	7,16E-02	0,32	-0,05	0,01	14	103833065	SCGF-b	14q32.32	0,10%
rs4981026	a	g	-6,42	1,4E-10	--	81,50	2,02E-02	0,23	-0,05	0,01	12	104152456	SCGF-b	12q23.3	0,11%
rs139133040	c	g	7,52	5,5E-14	++	79,30	2,80E-02	0,02	0,19	0,03	12	105084960	SCGF-b	12q23.3	0,14%
rs17404060	t	c	6,18	6,3E-10	++	87,30	5,02E-03	0,12	0,06	0,01	5	115319911	SDF-1a	5q23.1	0,09%
rs180738147	t	c	6,38	1,8E-10	++	83,20	1,48E-02	0,03	0,13	0,02	10	44925153	SDF-1a	10q11.21	0,09%
rs2279555	a	g	5,64	1,7E-08	-+	91,30	6,91E-04	0,18	0,05	0,01	10	44476596	SDF-1a	10q11.21	0,07%
rs4147990	t	c	10,04	1,0E-23	++	86,30	6,85E-03	0,06	0,15	0,01	17	66913936	SDF-1a	17q24.2	0,26%
rs72683129	a	g	-5,89	3,9E-09	--	79,10	2,87E-02	0,13	-0,06	0,01	1	66069781	SDF-1a	1p31.3	0,08%
rs1329424	t	g	6,35	2,1E-10	-+	83,30	1,45E-02	0,40	0,05	0,01	1	196646176	TNF-a	1q31.3	0,10%
rs1329424	t	g	8,43	3,3E-17	-+	93,30	1,16E-04	0,40	0,06	0,01	1	196646176	TNF-b	1q31.3	0,19%
rs6542680	t	c	-5,70	1,2E-08	++-	95,30	6,81E-10	0,18	-0,04	0,01	2	3640142	TRAIL	2p25.3	0,05%
rs74778900	t	c	6,07	1,3E-09	+++	97,70	8,47E-20	0,01	0,15	0,03	18	28086266	TRAIL	18q12.1	0,06%
rs140103836	t	c	-6,51	7,7E-11	--+	99,20	1,18E-53	0,02	-0,14	0,02	18	28811450	TRAIL	18q12.1	0,08%
rs117618570	t	g	-5,88	4,2E-09	---	98,40	2,73E-28	0,02	-0,13	0,02	18	29008594	TRAIL	18q12.1	0,06%
rs78186881	a	t	-5,65	1,6E-08	---	97,70	9,97E-20	0,06	-0,07	0,01	18	29382112	TRAIL	18q12.1	0,05%

Table A.2 (cont.)

SNP	Allele1	Allele2	Zscore	P-value	Direction	HetISq	HetPVal	EAF	Beta	SE	Chromosome	Position	Cytokine	Locus	Explained variance
rs2901364	t	g	-10,13	4,0E-24	--?	99,10	4,23E-26	0,02	-0,36	0,04	18	29569416	TRAIL	18q12.1	0,51%
rs77121181	a	g	6,60	4,0E-11	-+?	98,60	9,80E-17	0,04	0,16	0,02	19	44072655	TRAIL	19q13.31	0,21%
rs45505795	c	g	5,91	3,5E-09	+++	97,00	4,51E-15	0,02	0,12	0,02	14	94756943	TRAIL	14q32.13	0,06%
rs562416	a	c	-5,68	1,3E-08	---	91,80	5,26E-06	0,14	-0,05	0,01	3	172161842	TRAIL	3q26.31	0,05%
rs59724749	a	g	-7,64	2,1E-14	+-?	98,40	6,25E-15	0,18	-0,09	0,01	3	186408443	TRAIL	3q27.3	0,25%
rs1329424	t	g	7,93	2,2E-15	+-+	96,30	2,11E-12	0,40	0,05	0,01	1	196646176	TRAIL	1q31.3	0,11%
rs34881325	t	c	-6,11	1,0E-09	--?	85,50	8,56E-03	0,39	-0,06	0,01	9	2622134	VEGF	9p24.2	0,19%
rs10967571	t	c	-11,30	1,3E-29	---	83,60	2,25E-03	0,45	-0,07	0,01	9	2694834	VEGF	9p24.2	0,22%
rs7692	a	c	-5,46	4,9E-08	+--	78,20	1,02E-02	0,28	-0,04	0,01	6	43304007	VEGF	6p21.1	0,05%
rs62401205	a	c	-7,09	1,4E-12	---	89,20	9,45E-05	0,03	-0,13	0,02	6	43855489	VEGF	6p21.1	0,09%
rs6914863	c	g	-7,12	1,1E-12	---	93,10	4,72E-07	0,02	-0,14	0,02	6	43961813	VEGF	6p21.1	0,09%
rs35703624	t	c	6,42	1,4E-10	-++	73,90	2,17E-02	0,03	0,12	0,02	6	43968412	VEGF	6p21.1	0,08%
rs4746855	a	g	5,52	3,4E-08	+++	68,20	4,29E-02	0,40	0,03	0,01	10	64822828	VEGF	10q21.3	0,05%
rs302953	t	c	6,41	1,4E-10	+++	89,60	6,78E-05	0,40	0,04	0,01	8	106512481	VEGF	8q23.1	0,07%

Table A.3. GWAS catalog associations. GWAS catalogue continuous trait variants associated with circulating cytokine concentration within the discovered loci. 13 loci showed associations with circulating cytokine concentrations in previous GWAS's.

SNP	Trait	Trait (details)
rs6679677	monokine induced by gamma interferon measurement	Monokine induced by gamma interferon levels
rs12075	blood protein measurement	Serum levels of protein CXCL8
rs12075	C-C motif chemokine 7 measurement	C-C motif chemokine 7 levels
rs12075	CCL11 measurement	Serum levels of protein CCL11
rs12075	CCL2 measurement	Inflammatory biomarkers
rs12075	CCL2 measurement	Monocyte chemoattractant protein-1 levels
rs12075	CCL2 measurement	Monocyte chemoattractant protein-1 levels
rs12075	CCL2 measurement	Monocyte chemoattractant protein-1 levels
rs12075	CCL2 measurement	Monocyte chemoattractant protein-1 levels
rs12075	CCL2 measurement	Monocyte chemoattractant protein-1 levels
rs12075	CCL2 measurement	Obesity-related traits
rs12075	CCL2 measurement	Serum levels of protein CCL2
rs12075	CXCL1 measurement	Serum levels of protein CXCL1
rs12075	eotaxin measurement	Eotaxin levels
rs12075	eotaxin measurement	Eotaxin levels
rs12075	eotaxin measurement	Eotaxin levels
rs12075	eotaxin measurement	Eotaxin levels (CCL11.5301.7.3)
rs12075	growth-regulated alpha protein measurement	Growth-regulated protein alpha levels
rs12075	interleukin-8 measurement	Interleukin-8 levels
rs12075	level of C-C motif chemokine 2 in blood serum	Monocyte chemoattractant protein-1 levels
rs12075	level of growth-regulated alpha protein in blood serum	C-X-C motif chemokine 1 levels
rs6542680	interleukin-1 beta measurement	Interleukin-1 beta levels
rs6542680	macrophage colony-stimulating factor 1 measurement	Macrophage colony-stimulating factor 1 levels
rs62242542	macrophage inflammatory protein 1b measurement	Macrophage inflammatory protein 1b levels
rs79815064	C-C motif chemokine 3 measurement	C-C motif chemokine 3 levels

Table A.3 (cont.)

SNP	Trait	Trait (details)
rs79815064	macrophage inflammatory protein 1b measurement	Macrophage inflammatory protein 1b levels
rs80136777	CCL4 measurement	CCL4 levels
rs1354034	lymphotoxin-alpha measurement	Lymphotoxin-alpha levels
rs1354034	protein measurement	Acidic fibroblast growth factor intracellular-binding protein levels
rs6993770	fibroblast growth factor basic measurement,granulocyte colony-stimulating factor measurement,interferon gamma measurement,interleukin 10 measurement,interleukin 12 measurement,interleukin 17 measurement,interleukin 4 measurement,interleukin-6 measurement,platelet-derived growth factor BB measurement,stromal cell-derived factor 1 alpha measurement,vascular endothelial growth factor measurement	Cytokine network levels (multivariate analysis)
rs6993770	platelet-derived growth factor subunit b measurement	Platelet-derived growth factor subunit B levels (PDGFB.4149.8.2)
rs6993770	protein measurement	Isoform L-VEGF165 levels
rs6993770	vascular endothelial growth factor A measurement	Serum levels of protein VEGFA
rs6993770	vascular endothelial growth factor A measurement	Vascular endothelial growth factor A levels
rs6993770	vascular endothelial growth factor A measurement	Vascular endothelial growth factor A levels
rs6993770	vascular endothelial growth factor A, isoform 121 measurement	Vascular endothelial growth factor A, isoform 121 levels
rs6993770	vascular endothelial growth factor measurement	Vascular endothelial growth factor levels
rs6993770	vascular endothelial growth factor measurement	Vascular endothelial growth factor levels
rs6993770	vascular endothelial growth factor measurement	Vascular endothelial growth factor levels
rs34881325	vascular endothelial growth factor A measurement	Serum levels of protein VEGFA
rs34881325	vascular endothelial growth factor A measurement	Serum levels of protein VEGFA
rs34881325	vascular endothelial growth factor measurement	Vascular endothelial growth factor levels
rs75071241	macrophage colony-stimulating factor 1 receptor measurement	Macrophage colony-stimulating factor 1 receptor levels
rs3184504	C-C motif chemokine 3 measurement	C-C motif chemokine 3 levels
rs3184504	C-X-C motif chemokine 10 measurement	C-X-C motif chemokine 10 levels
rs3184504	C-X-C motif chemokine 9 measurement	C-X-C motif chemokine 9 levels
rs3184504	protein measurement	Fibroblast growth factor-binding protein 1 levels
rs3184504	tumor necrosis factor measurement	Tumor necrosis factor levels
rs7310615	lymphotoxin-alpha measurement	TNF-beta levels
rs7310615	lymphotoxin-alpha measurement	TNF-beta levels

Table A.3 (cont.)

SNP	Trait	Trait (details)
rs7310615	lymphotoxin-alpha measurement	TNF-beta levels
rs7217473	blood protein measurement	Serum levels of protein CCL4L1
rs76960253	macrophage inflammatory protein 1b measurement	Macrophage inflammatory protein 1b levels
rs117618570	TNF-related apoptosis-inducing ligand measurement	TRAIL levels
rs74778900	TNF-related apoptosis-inducing ligand measurement	TRAIL levels
rs7412	blood protein measurement	Serum levels of protein IFI16
rs62143194	interleukin 1 receptor antagonist measurement	Interleukin-1-receptor antagonist levels
rs62143194	interleukin 1 receptor antagonist measurement	Interleukin-1-receptor antagonist levels

Table A.4. MAGMA functional analysis. Results from MAGMA gene-based analysis showing 829 significant associations with the levels of circulating cytokines. MAGMA mapped 626 uniquely genes, each associated with at least one cytokine.

Cytokine	Z-score	P-value	HGNC symbol	HGNC description
CTACK	6,09	5,70E-10	CFH	complement factor H [HGNC id: 4883]
Eotaxin	4,72	1,16E-06	BCL2A1	BCL2-related protein A1 [HGNC id: 991]
Eotaxin	6,79	5,68E-12	CCR3	chemokine (C-C motif) receptor 3 [HGNC id: 1604]
Eotaxin	5,46	2,41E-08	CCR5	chemokine (C-C motif) receptor 5 (gene/pseudogene) [HGNC id: 1606]
Eotaxin	7,64	1,12E-14	ACKR2	atypical chemokine receptor 2 [HGNC id: 1565]
Eotaxin	6,11	5,00E-10	CYP8B1	cytochrome P450, family 8, subfamily B, polypeptide 1 [HGNC id: 2653]
Eotaxin	5,02	2,55E-07	CYP21A2	cytochrome P450, family 21, subfamily A, polypeptide 2 [HGNC id: 2600]
Eotaxin	7,42	5,72E-14	DARC	Duffy blood group, atypical chemokine receptor [HGNC id: 4035]
Eotaxin	7,39	7,17E-14	HIP1	huntingtin interacting protein 1 [HGNC id: 4913]
Eotaxin	5,84	2,64E-09	POR	P450 (cytochrome) oxidoreductase [HGNC id: 9208]
Eotaxin	5,39	3,62E-08	CCL2	chemokine (C-C motif) ligand 2 [HGNC id: 10618]
Eotaxin	6,29	1,61E-10	CCL7	chemokine (C-C motif) ligand 7 [HGNC id: 10634]
Eotaxin	8,26	7,54E-17	CCL11	chemokine (C-C motif) ligand 11 [HGNC id: 10610]
Eotaxin	6,72	8,93E-12	CCL24	chemokine (C-C motif) ligand 24 [HGNC id: 10623]
Eotaxin	7,04	9,37E-13	VIPR1	vasoactive intestinal peptide receptor 1 [HGNC id: 12694]
Eotaxin	5,60	1,05E-08	CCRL2	chemokine (C-C motif) receptor-like 2 [HGNC id: 1612]
Eotaxin	5,37	3,89E-08	SEC22C	SEC22 vesicle trafficking protein homolog C (S. cerevisiae) [HGNC id: 16828]
Eotaxin	5,69	6,51E-09	CCL26	chemokine (C-C motif) ligand 26 [HGNC id: 10625]
Eotaxin	6,58	2,41E-11	CXCR6	chemokine (C-X-C motif) receptor 6 [HGNC id: 16647]
Eotaxin	5,36	4,19E-08	CCR9	chemokine (C-C motif) receptor 9 [HGNC id: 1610]
Eotaxin	5,78	3,71E-09	ZFP30	ZFP30 zinc finger protein [HGNC id: 29555]
Eotaxin	6,11	5,00E-10	HIGD1A	HIG1 hypoxia inducible domain family, member 1A [HGNC id: 29527]
Eotaxin	4,84	6,38E-07	SS18L2	synovial sarcoma translocation gene on chromosome 18-like 2 [HGNC id: 15593]
Eotaxin	6,12	4,74E-10	ZNF571	zinc finger protein 571 [HGNC id: 25000]
Eotaxin	7,76	4,22E-15	LZTFL1	leucine zipper transcription factor-like 1 [HGNC id: 6741]
Eotaxin	4,95	3,64E-07	RHBDD2	rhomboid domain containing 2 [HGNC id: 23082]
Eotaxin	7,92	1,18E-15	HHATL	hedgehog acyltransferase-like [HGNC id: 13242]
Eotaxin	4,97	3,40E-07	CADM3	cell adhesion molecule 3 [HGNC id: 17601]
Eotaxin	5,52	1,70E-08	CDCP1	CUB domain containing protein 1 [HGNC id: 24357]
Eotaxin	7,32	1,22E-13	FYCO1	FYVE and coiled-coil domain containing 1 [HGNC id: 14673]
Eotaxin	5,60	1,06E-08	WDR87	WD repeat domain 87 [HGNC id: 29934]
Eotaxin	6,13	4,52E-10	ZNF527	zinc finger protein 527 [HGNC id: 29385]
Eotaxin	5,95	1,34E-09	ZNF607	zinc finger protein 607 [HGNC id: 28192]
Eotaxin	7,27	1,80E-13	POMGNT2	protein O-linked mannose N-acetylglucosaminyltransferase 2 (beta 1,4-) [HGNC id: 25902]
Eotaxin	4,90	4,71E-07	ZNF585B	zinc finger protein 585B [HGNC id: 30948]
Eotaxin	6,60	2,05E-11	ZBTB47	zinc finger and BTB domain containing 47 [HGNC id: 26955]
Eotaxin	5,27	6,82E-08	RDH13	retinol dehydrogenase 13 (all-trans/9-cis) [HGNC id: 19978]
Eotaxin	5,88	2,06E-09	ZNF573	zinc finger protein 573 [HGNC id: 26420]
Eotaxin	7,95	9,38E-16	KLHL40	kelch-like family member 40 [HGNC id: 30372]
Eotaxin	6,08	5,95E-10	ZNF569	zinc finger protein 569 [HGNC id: 24737]
Eotaxin	5,91	1,68E-09	ZNF570	zinc finger protein 570 [HGNC id: 26416]

Table A.4 (cont.)

Cytokine	Z-score	P-value	HGNC symbol	HGNC description
Eotaxin	6,94	1,95E-12	CCDC13	coiled-coil domain containing 13 [HGNC id: 26358]
Eotaxin	5,80	3,32E-09	ZNF781	zinc finger protein 781 [HGNC id: 26745]
Eotaxin	6,15	3,85E-10	ZNF540	zinc finger protein 540 [HGNC id: 25331]
Eotaxin	4,71	1,23E-06	ZNF585A	zinc finger protein 585A [HGNC id: 26305]
Eotaxin	6,04	7,90E-10	HKR1	HKR1, GLI-Kruppel zinc finger family member [HGNC id: 4928]
Eotaxin	5,41	3,10E-08	ZNF662	zinc finger protein 662 [HGNC id: 31930]
Eotaxin	6,60	2,02E-11	ZNF793	zinc finger protein 793 [HGNC id: 33115]
Eotaxin	6,11	5,00E-10	FAM198A	family with sequence similarity 198, member A [HGNC id: 24485]
Eotaxin	7,06	8,22E-13	CCR2	chemokine (C-C motif) receptor 2 [HGNC id: 1603]
Eotaxin	5,23	8,63E-08	n/a	n/a
Eotaxin	5,11	1,61E-07	KRBOX1	KRAB box domain containing 1 [HGNC id: 38708]
FGF-b	5,86	2,30E-09	CCNA2	cyclin A2 [HGNC id: 1578]
FGF-b	8,24	8,42E-17	FGF2	fibroblast growth factor 2 (basic) [HGNC id: 3676]
FGF-b	6,16	3,68E-10	IL2	interleukin 2 [HGNC id: 6001]
FGF-b	5,15	1,31E-07	EXOSC9	exosome component 9 [HGNC id: 9137]
FGF-b	7,14	4,67E-13	TRPC3	transient receptor potential cation channel, subfamily C, member 3 [HGNC id: 12335]
FGF-b	6,23	2,32E-10	SPRY1	sprouty homolog 1, antagonist of FGF signaling (Drosophila) [HGNC id: 11269]
FGF-b	6,52	3,63E-11	PRDM5	PR domain containing 5 [HGNC id: 9349]
FGF-b	6,11	5,00E-10	NUDT6	nudix (nucleoside diphosphate linked moiety X)-type motif 6 [HGNC id: 8053]
FGF-b	6,21	2,70E-10	BBS7	Bardet-Biedl syndrome 7 [HGNC id: 18758]
FGF-b	6,11	5,00E-10	IL21	interleukin 21 [HGNC id: 6005]
FGF-b	8,02	5,10E-16	KIAA1109	KIAA1109 [HGNC id: 26953]
FGF-b	6,34	1,17E-10	TMEM155	transmembrane protein 155 [HGNC id: 26418]
FGF-b	7,70	7,04E-15	ADAD1	adenosine deaminase domain containing 1 (testis-specific) [HGNC id: 30713]
FGF-b	8,45	1,47E-17	SPATA5	spermatogenesis associated 5 [HGNC id: 18119]
FGF-b	6,21	2,57E-10	BBS12	Bardet-Biedl syndrome 12 [HGNC id: 26648]
FGF-b	4,87	5,54E-07	SYNPO2	synaptopodin 2 [HGNC id: 17732]
G-CSF	7,90	1,43E-15	APOC1	apolipoprotein C-I [HGNC id: 607]
G-CSF	8,04	4,52E-16	APOC2	apolipoprotein C-II [HGNC id: 609]
G-CSF	6,11	5,00E-10	APOC4	apolipoprotein C-IV [HGNC id: 611]
G-CSF	7,99	6,54E-16	APOE	apolipoprotein E [HGNC id: 613]
G-CSF	7,31	1,34E-13	BCHE	butyrylcholinesterase [HGNC id: 983]
G-CSF	7,70	6,99E-15	BCL3	B-cell CLL/lymphoma 3 [HGNC id: 998]
G-CSF	6,22	2,47E-10	CKM	creatine kinase, muscle [HGNC id: 1994]
G-CSF	7,53	2,57E-14	CLPTM1	cleft lip and palate associated transmembrane protein 1 [HGNC id: 2087]
G-CSF	4,93	4,05E-07	CSF3R	colony stimulating factor 3 receptor (granulocyte) [HGNC id: 2439]
G-CSF	6,11	5,00E-10	ERCC1	excision repair cross-complementing rodent repair deficiency, complementation group 1 (includes overlapping antisense sequence) [HGNC id: 3433]
G-CSF	7,33	1,17E-13	FOSB	FBJ murine osteosarcoma viral oncogene homolog B [HGNC id: 3797]
G-CSF	4,99	3,10E-07	GIPR	gastric inhibitory polypeptide receptor [HGNC id: 4271]
G-CSF	5,42	3,03E-08	KCNN4	potassium intermediate/small conductance calcium-activated channel, subfamily N, member 4 [HGNC id: 6293]
G-CSF	4,82	7,35E-07	PSG1	pregnancy specific beta-1-glycoprotein 1 [HGNC id: 9514]
G-CSF	4,81	7,48E-07	PSG6	pregnancy specific beta-1-glycoprotein 6 [HGNC id: 9523]
G-CSF	5,48	2,18E-08	PSG7	pregnancy specific beta-1-glycoprotein 7 (gene/pseudogene) [HGNC id: 9524]

Table A.4 (cont.)

Cytokine	Z-score	P-value	HGNC symbol	HGNC description
G-CSF	4,62	1,90E-06	PSMD3	proteasome (prosome, macropain) 26S subunit, non-ATPase, 3 [HGNC id: 9560]
G-CSF	6,99	1,40E-12	PVR	poliovirus receptor [HGNC id: 9705]
G-CSF	7,31	1,31E-13	PVRL2	poliovirus receptor-related 2 (herpesvirus entry mediator B) [HGNC id: 9707]
G-CSF	6,11	5,00E-10	RELB	v-rel avian reticuloendotheliosis viral oncogene homolog B [HGNC id: 9956]
G-CSF	5,39	3,54E-08	RTN2	reticulon 2 [HGNC id: 10468]
G-CSF	5,95	1,37E-09	VASP	vasodilator-stimulated phosphoprotein [HGNC id: 12652]
G-CSF	4,81	7,40E-07	MED24	mediator complex subunit 24 [HGNC id: 22963]
G-CSF	6,11	5,00E-10	TOMM40	translocase of outer mitochondrial membrane 40 homolog (yeast) [HGNC id: 18001]
G-CSF	6,33	1,21E-10	PPP1R13L	protein phosphatase 1, regulatory subunit 13 like [HGNC id: 18838]
G-CSF	7,35	1,03E-13	CLASRP	CLK4-associating serine/arginine rich protein [HGNC id: 17731]
G-CSF	4,61	1,98E-06	FBXO46	F-box protein 46 [HGNC id: 25069]
G-CSF	5,15	1,27E-07	STRN4	striatin, calmodulin binding protein 4 [HGNC id: 15721]
G-CSF	5,90	1,87E-09	QPCTL	glutaminyl-peptide cyclotransferase-like [HGNC id: 25952]
G-CSF	7,70	6,94E-15	TRAPPC6A	trafficking protein particle complex 6A [HGNC id: 23069]
G-CSF	7,87	1,71E-15	GEMIN7	gem (nuclear organelle) associated protein 7 [HGNC id: 20045]
G-CSF	6,95	1,83E-12	EXOC3L2	exocyst complex component 3-like 2 [HGNC id: 30162]
G-CSF	5,18	1,10E-07	n/a	n/a
G-CSF	4,64	1,72E-06	PPM1N	protein phosphatase, Mg2+/Mn2+ dependent, 1N (putative) [HGNC id: 26845]
G-CSF	5,66	7,59E-09	IGSF23	immunoglobulin superfamily, member 23 [HGNC id: 40040]
G-CSF	4,82	7,01E-07	ZNF420	zinc finger protein 420 [HGNC id: 20649]
G-CSF	6,87	3,14E-12	ZNF296	zinc finger protein 296 [HGNC id: 15981]
G-CSF	4,76	9,72E-07	ZNF283	zinc finger protein 283 [HGNC id: 13077]
G-CSF	7,00	1,24E-12	PPP1R37	protein phosphatase 1, regulatory subunit 37 [HGNC id: 27607]
G-CSF	7,94	1,03E-15	NKPD1	NTPase, KAP family P-loop domain containing 1 [HGNC id: 24739]
G-CSF	6,97	1,62E-12	BLOC1S3	biogenesis of lysosomal organelles complex-1, subunit 3 [HGNC id: 20914]
GROa	7,41	6,47E-14	AFM	afamin [HGNC id: 316]
GROa	6,11	5,00E-10	AFP	alpha-fetoprotein [HGNC id: 317]
GROa	6,99	1,35E-12	ALB	albumin [HGNC id: 399]
GROa	5,75	4,52E-09	AMBN	ameloblastin (enamel matrix protein) [HGNC id: 452]
GROa	5,01	2,69E-07	CSN1S1	casein alpha s1 [HGNC id: 2445]
GROa	4,62	1,90E-06	EPHA5	EPH receptor A5 [HGNC id: 3389]
GROa	6,93	2,13E-12	EREG	epiregulin [HGNC id: 3443]
GROa	5,07	1,95E-07	GC	group-specific component (vitamin D binding protein) [HGNC id: 4187]
GROa	6,11	5,00E-10	CXCL1	chemokine (C-X-C motif) ligand 1 (melanoma growth stimulating activity, alpha) [HGNC id: 4602]
GROa	6,94	2,00E-12	CXCL2	chemokine (C-X-C motif) ligand 2 [HGNC id: 4603]
GROa	7,33	1,16E-13	CXCL3	chemokine (C-X-C motif) ligand 3 [HGNC id: 4604]
GROa	4,62	1,87E-06	CFH	complement factor H [HGNC id: 4883]
GROa	6,22	2,56E-10	HTN1	histatin 1 [HGNC id: 5283]
GROa	5,05	2,21E-07	HTN3	histatin 3 [HGNC id: 5284]
GROa	6,11	5,00E-10	PF4	platelet factor 4 [HGNC id: 8861]
GROa	6,11	5,00E-10	PF4V1	platelet factor 4 variant 1 [HGNC id: 8862]
GROa	7,68	7,73E-15	PPEF2	protein phosphatase, EF-hand calcium binding domain 2 [HGNC id: 9244]
GROa	6,11	5,00E-10	PPBP	pro-platelet basic protein (chemokine (C-X-C motif) ligand 7) [HGNC id: 9240]

Table A.4 (cont.)

Cytokine	Z-score	P-value	HGNC symbol	HGNC description
GROa	6,51	3,81E-11	CXCL5	chemokine (C-X-C motif) ligand 5 [HGNC id: 10642]
GROa	6,71	9,66E-12	STATH	statherin [HGNC id: 11369]
GROa	5, 86	2,26E-09	SULT1E1	sulfotransferase family 1E, estrogen-preferring, member 1 [HGNC id: 11377]
GROa	7,28	1,63E-13	SLC4A4	solute carrier family 4 (sodium bicarbonate cotransporter), member 4 [HGNC id: 11030]
GROa	9,23	1,32E-20	ADAMTS3	ADAM metallopeptidase with thrombospondin type 1 motif, 3 [HGNC id: 219]
GROa	5,82	3,00E-09	CXCL13	chemokine (C-X-C motif) ligand 13 [HGNC id: 10639]
GROa	5,50	1,85E-08	SMR3B	submaxillary gland androgen regulated protein 3B [HGNC id: 17326]
GROa	4,79	8,28E-07	PARM1	prostate androgen-regulated mucin-like protein 1 [HGNC id: 24536]
GROa	4,80	8,10E-07	RCHY1	ring finger and CHY zinc finger domain containing 1, E3 ubiquitin protein ligase [HGNC id: 17479]
GROa	7,28	1,70E-13	ANKRD17	ankyrin repeat domain 17 [HGNC id: 23575]
GROa	5,08	1,86E-07	TMPRSS11E	transmembrane protease, serine 11E [HGNC id: 24465]
GROa	7,28	1,72E-13	NRBF2	nuclear receptor binding factor 2 [HGNC id: 19692]
GROa	5,35	4,51E-08	SDAD1	SDA1 domain containing 1 [HGNC id: 25537]
GROa	4,66	1,56E-06	CADM3	cell adhesion molecule 3 [HGNC id: 17601]
GROa	4,92	4,41E-07	CSRNP1	cysteine-serine-rich nuclear protein 1 [HGNC id: 14300]
GROa	5,71	5,57E-09	FRAS1	Fraser syndrome 1 [HGNC id: 19185]
GROa	5,39	3,52E-08	THAP6	THAP domain containing 6 [HGNC id: 23189]
GROa	5,55	1,44E-08	C4orf26	chromosome 4 open reading frame 26 [HGNC id: 26300]
GROa	8,07	3,58E-16	RASSF6	Ras association (RalGDS/AF-6) domain family member 6 [HGNC id: 20796]
GROa	5,02	2,62E-07	TTC21A	tetratricopeptide repeat domain 21A [HGNC id: 30761]
GROa	7,50	3,27E-14	REEP3	receptor accessory protein 3 [HGNC id: 23711]
GROa	7,62	1,28E-14	JMJD1C	jumonji domain containing 1C [HGNC id: 12313]
GROa	7,93	1,12E-15	EPGN	epithelial mitogen [HGNC id: 17470]
GROa	7,93	1,11E-15	COX18	COX18 cytochrome C oxidase assembly factor [HGNC id: 26801]
GROa	7,87	1,82E-15	MTHFD2L	methylenetetrahydrofolate dehydrogenase (NADP+ dependent) 2-like [HGNC id: 31865]
GROa	5,73	5,10E-09	FAM47E	family with sequence similarity 47, member E [HGNC id: 34343]
HGF	6,11	5,00E-10	HGF	hepatocyte growth factor (hepapoietin A; scatter factor) [HGNC id: 4893]
HGF	6,11	5,00E-10	HGFAC	HGF activator [HGNC id: 4894]
HGF	4,95	3,70E-07	HIP1	huntingtin interacting protein 1 [HGNC id: 4913]
HGF	4,77	9,34E-07	LRPAP1	low density lipoprotein receptor-related protein associated protein 1 [HGNC id: 6701]
HGF	7,01	1,19E-12	P2RY2	purinergic receptor P2Y, G-protein coupled, 2 [HGNC id: 8541]
HGF	4,75	1,02E-06	PCSK6	proprotein convertase subtilisin/kexin type 6 [HGNC id: 8569]
HGF	5,83	2,81E-09	PSMD3	proteasome (prosome, macropain) 26S subunit, non-ATPase, 3 [HGNC id: 9560]
HGF	6,06	6,74E-10	RGS12	regulator of G-protein signaling 12 [HGNC id: 9994]
HGF	5,83	2,76E-09	MED24	mediator complex subunit 24 [HGNC id: 22963]
HGF	4,86	5,97E-07	GSDMA	gasdermin A [HGNC id: 13311]
HGF	7,46	4,37E-14	DOK7	docking protein 7 [HGNC id: 26594]
IFN-g	6,48	4,68E-11	BCHE	butyrylcholinesterase [HGNC id: 983]
IFN-g	6,11	5,00E-10	CFB	complement factor B [HGNC id: 1037]
IFN-g	7,53	2,51E-14	C2	complement component 2 [HGNC id: 1248]
IFN-g	6,35	1,10E-10	C4A	complement component 4A (Rodgers blood group) [HGNC id: 1323]
IFN-g	5,61	9,94E-09	CYP21A2	cytochrome P450, family 21, subfamily A, polypeptide 2 [HGNC id: 2600]
IFN-g	5,04	2,39E-07	DXO	decapping exoribonuclease [HGNC id: 2992]

Table A.4 (cont.)

Cytokine	Z-score	P-value	HGNC symbol	HGNC description
IFN-g	7,35	9,88E-14	F13B	coagulation factor XIII, B polypeptide [HGNC id: 3534]
IFN-g	8,19	1,34E-16	CFH	complement factor H [HGNC id: 4883]
IFN-g	7,80	3,00E-15	CFHR1	complement factor H-related 1 [HGNC id: 4888]
IFN-g	6,11	5,00E-10	CFHR2	complement factor H-related 2 [HGNC id: 4890]
IFN-g	5,20	1,02E-07	MICB	MHC class I polypeptide-related sequence B [HGNC id: 7091]
IFN-g	7,90	1,43E-15	SKIV2L	superkiller viralicidic activity 2-like (S. cerevisiae) [HGNC id: 10898]
IFN-g	6,91	2,44E-12	TNXB	tenascin XB [HGNC id: 11976]
IFN-g	5,77	4,01E-09	VARS	valyl-tRNA synthetase [HGNC id: 12651]
IFN-g	7,26	1,89E-13	NELFE	negative elongation factor complex member E [HGNC id: 13974]
IFN-g	7,99	6,80E-16	STK19	serine/threonine kinase 19 [HGNC id: 11398]
IFN-g	6,11	5,00E-10	CFHR4	complement factor H-related 4 [HGNC id: 16979]
IFN-g	7,80	3,04E-15	CFHR3	complement factor H-related 3 [HGNC id: 16980]
IFN-g	7,10	6,27E-13	CRB1	crumbs homolog 1 (Drosophila) [HGNC id: 2343]
IFN-g	7,75	4,59E-15	CFHR5	complement factor H-related 5 [HGNC id: 24668]
IFN-g	6,11	4,85E-10	ASPM	asp (abnormal spindle) homolog, microcephaly associated (Drosophila) [HGNC id: 19048]
IFN-g	6,30	1,52E-10	ZBTB41	zinc finger and BTB domain containing 41 [HGNC id: 24819]
IFN-g	5,12	1,56E-07	MUC21	mucin 21, cell surface associated [HGNC id: 21661]
IFN-g	4,56	2,57E-06	MUC22	mucin 22 [HGNC id: 39755]
IL-10	6,43	6,24E-11	CFH	complement factor H [HGNC id: 4883]
IL-13	6,24	2,17E-10	F13B	coagulation factor XIII, B polypeptide [HGNC id: 3534]
IL-13	7,92	1,16E-15	CFH	complement factor H [HGNC id: 4883]
IL-13	7,70	6,69E-15	CFHR1	complement factor H-related 1 [HGNC id: 4888]
IL-13	7,28	1,61E-13	CFHR2	complement factor H-related 2 [HGNC id: 4890]
IL-13	7,94	9,95E-16	CFHR4	complement factor H-related 4 [HGNC id: 16979]
IL-13	7,95	9,29E-16	CFHR3	complement factor H-related 3 [HGNC id: 16980]
IL-13	5,88	2,02E-09	CRB1	crumbs homolog 1 (Drosophila) [HGNC id: 2343]
IL-13	7,28	1,65E-13	CFHR5	complement factor H-related 5 [HGNC id: 24668]
IL-13	5,16	1,24E-07	ASPM	asp (abnormal spindle) homolog, microcephaly associated (Drosophila) [HGNC id: 19048]
IL-13	5,00	2,81E-07	ZBTB41	zinc finger and BTB domain containing 41 [HGNC id: 24819]
IL-16	5,04	2,28E-07	HLA-DRA	major histocompatibility complex, class II, DR alpha [HGNC id: 4947]
IL-16	6,91	2,40E-12	IL16	interleukin 16 [HGNC id: 5980]
IL-16	4,62	1,96E-06	LTA	lymphotoxin alpha [HGNC id: 6709]
IL-16	7,52	2,69E-14	NINJ1	ninjurin 1 [HGNC id: 7824]
IL-16	5,47	2,26E-08	NTRK3	neurotrophic tyrosine kinase, receptor, type 3 [HGNC id: 8033]
IL-16	14,13	1,26E-45	RPS17	ribosomal protein S17 [HGNC id: 10397]
IL-16	8,70	1,61E-18	SH3GL3	SH3-domain GRB2-like 3 [HGNC id: 10832]
IL-16	4,62	1,91E-06	TLE3	transducin-like enhancer of split 3 (E(sp1) homolog, Drosophila) [HGNC id: 11839]
IL-16	6,90	2,65E-12	AP3B2	adaptor-related protein complex 3, beta 2 subunit [HGNC id: 567]
IL-16	7,01	1,20E-12	SLC28A1	solute carrier family 28 (concentrative nucleoside transporter), member 1 [HGNC id: 11001]
IL-16	4,67	1,49E-06	ARNT2	aryl-hydrocarbon receptor nuclear translocator 2 [HGNC id: 16876]
IL-16	5,71	5,64E-09	MTHFS	5,10-methenyltetrahydrofolate synthetase (5-formyltetrahydrofolate cyclo-ligase) [HGNC id: 7437]
IL-16	4,73	1,14E-06	FAM120A	family with sequence similarity 120A [HGNC id: 13247]
IL-16	5,37	4,02E-08	BTBD1	BTB (POZ) domain containing 1 [HGNC id: 1120]
IL-16	5,39	3,62E-08	ADAMTSL3	ADAMTS-like 3 [HGNC id: 14633]

Table A.4 (cont.)

Cytokine	Z-score	P-value	HGNC symbol	HGNC description
IL-16	8,44	1,53E-17	KIAA1199	KIAA1199 [HGNC id: 29213]
IL-16	7,71	6,23E-15	CPEB1	cytoplasmic polyadenylation element binding protein 1 [HGNC id: 21744]
IL-16	5,36	4,05E-08	WNK2	WNK lysine deficient protein kinase 2 [HGNC id: 14542]
IL-16	7,40	6,66E-14	EFTUD1	elongation factor Tu GTP binding domain containing 1 [HGNC id: 25789]
IL-16	4,95	3,69E-07	C6orf25	chromosome 6 open reading frame 25 [HGNC id: 13937]
IL-16	4,69	1,34E-06	LY6G6C	lymphocyte antigen 6 complex, locus G6C [HGNC id: 13936]
IL-16	6,11	5,00E-10	STARD5	StAR-related lipid transfer (START) domain containing 5 [HGNC id: 18065]
IL-16	6,13	4,43E-10	MEX3B	mex-3 RNA binding family member B [HGNC id: 25297]
IL-16	4,87	5,49E-07	NLRP12	NLR family, pyrin domain containing 12 [HGNC id: 22938]
IL-16	5,57	1,25E-08	AGBL1	ATP/GTP binding protein-like 1 [HGNC id: 26504]
IL-16	6,36	1,04E-10	C15orf26	chromosome 15 open reading frame 26 [HGNC id: 26782]
IL-16	6,75	7,22E-12	FAM154B	family with sequence similarity 154, member B [HGNC id: 33727]
IL-16	7,58	1,78E-14	TMC3	transmembrane channel-like 3 [HGNC id: 22995]
IL-16	4,99	3,07E-07	ST20-MTHFS	ST20-MTHFS readthrough [HGNC id: 44655]
IL-17	5,78	3,79E-09	CFH	complement factor H [HGNC id: 4883]
IL-17	4,77	9,15E-07	NELFE	negative elongation factor complex member E [HGNC id: 13974]
IL-17	4,63	1,79E-06	STK19	serine/threonine kinase 19 [HGNC id: 11398]
IL-18	5,57	1,29E-08	CCNB1	cyclin B1 [HGNC id: 1579]
IL-18	5,79	3,57E-09	CDK7	cyclin-dependent kinase 7 [HGNC id: 1778]
IL-18	4,99	2,98E-07	EEF1D	eukaryotic translation elongation factor 1 delta (guanine nucleotide exchange protein) [HGNC id: 3211]
IL-18	4,57	2,46E-06	CFH	complement factor H [HGNC id: 4883]
IL-18	6,11	5,00E-10	IL18	interleukin 18 (interferon-gamma-inducing factor) [HGNC id: 5986]
IL-18	6,86	3,35E-12	SPAST	spastin [HGNC id: 11233]
IL-18	7,79	3,24E-15	n/a	n/a
IL-18	4,85	6,29E-07	TCF19	transcription factor 19 [HGNC id: 11629]
IL-18	6,78	5,94E-12	XDH	xanthine dehydrogenase [HGNC id: 12805]
IL-18	4,92	4,41E-07	ZC3H3	zinc finger CCCH-type containing 3 [HGNC id: 28972]
IL-18	6,70	1,04E-11	MEMO1	mediator of cell motility 1 [HGNC id: 14014]
IL-18	5,53	1,61E-08	TTC27	tetratricopeptide repeat domain 27 [HGNC id: 25986]
IL-18	6,11	5,00E-10	SLC30A6	solute carrier family 30 (zinc transporter), member 6 [HGNC id: 19305]
IL-18	7,32	1,24E-13	TEX12	testis expressed 12 [HGNC id: 11734]
IL-18	6,92	2,29E-12	BIRC6	baculoviral IAP repeat containing 6 [HGNC id: 13516]
IL-18	6,11	5,00E-10	NLRC4	NLR family, CARD domain containing 4 [HGNC id: 16412]
IL-18	5,75	4,36E-09	CENPH	centromere protein H [HGNC id: 17268]
IL-18	6,89	2,79E-12	GSDMD	gasdermin D [HGNC id: 25697]
IL-18	6,11	5,00E-10	BCO2	beta-carotene oxygenase 2 [HGNC id: 18503]
IL-18	7,96	8,65E-16	YIPF4	Yip1 domain family, member 4 [HGNC id: 28145]
IL-18	7,12	5,40E-13	DPY30	dpy-30 homolog (C. elegans) [HGNC id: 24590]
IL-18	5,67	7,04E-09	TIGD5	tigger transposable element derived 5 [HGNC id: 18336]
IL-18	7,62	1,23E-14	NLRP12	NLR family, pyrin domain containing 12 [HGNC id: 22938]
IL-18	5,38	3,68E-08	MRPS36	mitochondrial ribosomal protein S36 [HGNC id: 16631]
IL-18	7,02	1,15E-12	NAPRT1	nicotinate phosphoribosyltransferase domain containing 1 [HGNC id: 30450]
IL-18	4,58	2,33E-06	FAM117B	family with sequence similarity 117, member B [HGNC id: 14440]
IL-18	4,95	3,63E-07	PSORS1C1	Psoriasis susceptibility 1 candidate 1 [HGNC id: 17202]

Table A.4 (cont.)

Cytokine	Z-score	P-value	HGNC symbol	HGNC description
IL-18	6,95	1,83E-12	MROH6	maestro heat-like repeat family member 6 [HGNC id: 27814]
IL-1B	6,11	5,00E-10	RPS7	ribosomal protein S7 [HGNC id: 10440]
IL-1B	4,72	1,21E-06	DDX42	DEAD (Asp-Glu-Ala-Asp) box helicase 42 [HGNC id: 18676]
IL-1B	4,98	3,13E-07	TRAPPC12	trafficking protein particle complex 12 [HGNC id: 24284]
IL-1B	4,75	1,03E-06	CCDC47	coiled-coil domain containing 47 [HGNC id: 24856]
IL-1B	6,21	2,66E-10	COLEC11	collectin sub-family member 11 [HGNC id: 17213]
IL-1B	4,69	1,35E-06	STRADA	STE20-related kinase adaptor alpha [HGNC id: 30172]
IL-1B	4,68	1,42E-06	FTSJ3	FtsJ homolog 3 (E. coli) [HGNC id: 17136]
IL-1B	7,95	9,20E-16	RNASEH1	ribonuclease H1 [HGNC id: 18466]
IL-1B	4,61	2,01E-06	DCDC2C	doublecortin domain containing 2C [HGNC id: 32696]
IL-1ra	4,81	7,70E-07	APOE	apolipoprotein E [HGNC id: 613]
IL-1ra	7,50	3,24E-14	IL1B	interleukin 1, beta [HGNC id: 5992]
IL-1ra	7,18	3,46E-13	IL1RN	interleukin 1 receptor antagonist [HGNC id: 6000]
IL-1ra	8,39	2,44E-17	PAX8	paired box 8 [HGNC id: 8622]
IL-1ra	7,62	1,28E-14	PSD4	pleckstrin and Sec7 domain containing 4 [HGNC id: 19096]
IL-1ra	7,84	2,23E-15	IL36RN	interleukin 36 receptor antagonist [HGNC id: 15561]
IL-1ra	7,32	1,26E-13	IL36B	interleukin 36, beta [HGNC id: 15564]
IL-1ra	7,88	1,70E-15	IL37	interleukin 37 [HGNC id: 15563]
IL-1ra	6,11	5,00E-10	IL36A	interleukin 36, alpha [HGNC id: 15562]
IL-1ra	6,11	5,00E-10	IL36G	interleukin 36, gamma [HGNC id: 15741]
IL-1ra	5,81	3,05E-09	POLR1B	polymerase (RNA) I polypeptide B, 128kDa [HGNC id: 20454]
IL-1ra	6,11	5,00E-10	IL1F10	interleukin 1 family, member 10 (theta) [HGNC id: 15552]
IL-1ra	6,44	5,96E-11	NLRP12	NLR family, pyrin domain containing 12 [HGNC id: 22938]
IL-1ra	7,13	5,08E-13	CKAP2L	cytoskeleton associated protein 2-like [HGNC id: 26877]
IL-1ra	5,77	4,07E-09	CBWD1	COBW domain containing 1 [HGNC id: 17134]
IL-1ra	6,08	6,00E-10	FOXD4L1	forkhead box D4-like 1 [HGNC id: 18521]
IL-2	6,28	1,70E-10	F12	coagulation factor XII (Hageman factor) [HGNC id: 3530]
IL-2	5,00	2,85E-07	GCKR	glucokinase (hexokinase 4) regulator [HGNC id: 4196]
IL-2	6,47	4,88E-11	KLKB1	kallikrein B, plasma (Fletcher factor) 1 [HGNC id: 6371]
IL-2	4,57	2,49E-06	TBL2	transducin (beta)-like 2 [HGNC id: 11586]
IL-2	4,78	8,84E-07	MLXIPL	MLX interacting protein-like [HGNC id: 12744]
IL-2	4,98	3,19E-07	C2orf16	chromosome 2 open reading frame 16 [HGNC id: 25275]
IL-2	6,52	3,50E-11	ZNF512	zinc finger protein 512 [HGNC id: 29380]
IL-2ra	6,56	2,62E-11	HLA-DRA	major histocompatibility complex, class II, DR alpha [HGNC id: 4947]
IL-2ra	4,65	1,64E-06	HLA-DRB1	major histocompatibility complex, class II, DR beta 1 [HGNC id: 4948]
IL-2ra	6,11	5,00E-10	IL2RA	interleukin 2 receptor, alpha [HGNC id: 6008]
IL-2ra	5,77	3,98E-09	IL15RA	interleukin 15 receptor, alpha [HGNC id: 5978]
IL-2ra	4,67	1,53E-06	STK19	serine/threonine kinase 19 [HGNC id: 11398]
IL-2ra	5,50	1,89E-08	RBM17	RNA binding motif protein 17 [HGNC id: 16944]
IL-4	4,62	1,87E-06	C2	complement component 2 [HGNC id: 1248]
IL-4	8,35	3,46E-17	CFH	complement factor H [HGNC id: 4883]
IL-4	4,97	3,35E-07	SKIV2L	superkiller viralicidic activity 2-like (S. cerevisiae) [HGNC id: 10898]
IL-4	4,81	7,67E-07	NELFE	negative elongation factor complex member E [HGNC id: 13974]
IL-4	4,98	3,11E-07	STK19	serine/threonine kinase 19 [HGNC id: 11398]
IL-4	4,59	2,23E-06	CFHR3	complement factor H-related 3 [HGNC id: 16980]

Table A.4 (cont.)

Cytokine	Z-score	P-value	HGNC symbol	HGNC description
IL-4	4,82	7,22E-07	CFHR5	complement factor H-related 5 [HGNC id: 24668]
IL-5	7,52	2,70E-14	CFH	complement factor H [HGNC id: 4883]
IL-5	4,58	2,37E-06	CFHR2	complement factor H-related 2 [HGNC id: 4890]
IL-5	4,53	3,00E-06	CFHR4	complement factor H-related 4 [HGNC id: 16979]
IL-5	4,55	2,64E-06	CFHR5	complement factor H-related 5 [HGNC id: 24668]
IL-6	4,63	1,80E-06	ADAR	adenosine deaminase, RNA-specific [HGNC id: 225]
IL-6	8,05	4,12E-16	IL6R	interleukin 6 receptor [HGNC id: 6019]
IL-6	4,56	2,62E-06	MICB	MHC class I polypeptide-related sequence B [HGNC id: 7091]
IL-6	4,67	1,51E-06	GPANK1	G patch domain and ankyrin repeats 1 [HGNC id: 13920]
IL-6	4,72	1,20E-06	C6orf10	chromosome 6 open reading frame 10 [HGNC id: 13922]
IL-6	4,73	1,10E-06	EHMT2	euchromatic histone-lysine N-methyltransferase 2 [HGNC id: 14129]
IL-6	6,38	9,03E-11	TDRD10	tudor domain containing 10 [HGNC id: 25316]
IL-6	6,80	5,33E-12	SHE	Src homology 2 domain containing E [HGNC id: 27004]
IL-7	8,39	2,44E-17	CFH	complement factor H [HGNC id: 4883]
IL-7	4,58	2,29E-06	CFHR1	complement factor H-related 1 [HGNC id: 4888]
IL-7	4,65	1,65E-06	CFHR2	complement factor H-related 2 [HGNC id: 4890]
IL-7	4,90	4,69E-07	CFHR4	complement factor H-related 4 [HGNC id: 16979]
IL-7	5,45	2,55E-08	CFHR3	complement factor H-related 3 [HGNC id: 16980]
IL-8	5,30	5,92E-08	CFB	complement factor B [HGNC id: 1037]
IL-8	4,67	1,47E-06	C2	complement component 2 [HGNC id: 1248]
IL-8	4,61	1,98E-06	C4A	complement component 4A (Rodgers blood group) [HGNC id: 1323]
IL-8	5,19	1,07E-07	F13B	coagulation factor XIII, B polypeptide [HGNC id: 3534]
IL-8	7,57	1,85E-14	DARC	Duffy blood group, atypical chemokine receptor [HGNC id: 4035]
IL-8	7,63	1,16E-14	CFH	complement factor H [HGNC id: 4883]
IL-8	6,54	3,05E-11	CFHR1	complement factor H-related 1 [HGNC id: 4888]
IL-8	7,55	2,19E-14	CFHR2	complement factor H-related 2 [HGNC id: 4890]
IL-8	5,25	7,63E-08	HLA-DPB1	major histocompatibility complex, class II, DP beta 1 [HGNC id: 4940]
IL-8	4,85	6,05E-07	IL8	interleukin 8 [HGNC id: 6025]
IL-8	5,45	2,57E-08	PSMD3	proteasome (prosome, macropain) 26S subunit, non-ATPase, 3 [HGNC id: 9560]
IL-8	4,94	3,87E-07	RING1	ring finger protein 1 [HGNC id: 10018]
IL-8	4,68	1,41E-06	SKIV2L	superkiller viralicidic activity 2-like (S. cerevisiae) [HGNC id: 10898]
IL-8	4,70	1,27E-06	SMARCD2	SWI/SNF related, matrix associated, actin dependent regulator of chromatin, subfamily d, member 2 [HGNC id: 11107]
IL-8	5,08	1,89E-07	NELFE	negative elongation factor complex member E [HGNC id: 13974]
IL-8	5,12	1,52E-07	STK19	serine/threonine kinase 19 [HGNC id: 11398]
IL-8	5,07	2,03E-07	PIGL	phosphatidylinositol glycan anchor biosynthesis, class L [HGNC id: 8966]
IL-8	5,73	4,90E-09	MED24	mediator complex subunit 24 [HGNC id: 22963]
IL-8	7,68	8,02E-15	CFHR4	complement factor H-related 4 [HGNC id: 16979]
IL-8	7,01	1,20E-12	CFHR3	complement factor H-related 3 [HGNC id: 16980]
IL-8	4,58	2,32E-06	DDX42	DEAD (Asp-Glu-Ala-Asp) box helicase 42 [HGNC id: 18676]
IL-8	4,74	1,08E-06	GSDMB	gasdermin B [HGNC id: 23690]
IL-8	4,64	1,72E-06	CCDC47	coiled-coil domain containing 47 [HGNC id: 24856]
IL-8	5,12	1,54E-07	CADM3	cell adhesion molecule 3 [HGNC id: 17601]
IL-8	7,57	1,94E-14	CFHR5	complement factor H-related 5 [HGNC id: 24668]
IL-8	4,74	1,09E-06	STRADA	STE20-related kinase adaptor alpha [HGNC id: 30172]

Table A.4 (cont.)

Cytokine	Z-score	P-value	HGNC symbol	HGNC description
IL-8	4,78	8,64E-07	FTSJ3	FtsJ homolog 3 (E. coli) [HGNC id: 17136]
IL-8	4,65	1,66E-06	ASPM	asp (abnormal spindle) homolog, microcephaly associated (Drosophila) [HGNC id: 19048]
IL-8	5,54	1,55E-08	GSDMA	gasdermin A [HGNC id: 13311]
IL-8	4,68	1,41E-06	RUFY4	RUN and FYVE domain containing 4 [HGNC id: 24804]
IL-8	4,91	4,60E-07	n/a	n/a
IL-9	4,82	7,14E-07	CFH	complement factor H [HGNC id: 4883]
IL-9	5,34	4,71E-08	HNRNPA1	heterogeneous nuclear ribonucleoprotein A1 [HGNC id: 5031]
IL-9	6,11	5,00E-10	SMAD5	SMAD family member 5 [HGNC id: 6771]
IL-9	6,56	2,76E-11	NFE2	nuclear factor, erythroid 2 [HGNC id: 7780]
IL-9	4,63	1,85E-06	PTGES3	prostaglandin E synthase 3 (cytosolic) [HGNC id: 16049]
IL-9	5,44	2,62E-08	COPZ1	coatomer protein complex, subunit zeta 1 [HGNC id: 2243]
IP-10	4,85	6,31E-07	ALDH2	aldehyde dehydrogenase 2 family (mitochondrial) [HGNC id: 404]
IP-10	8,17	1,48E-16	ART3	ADP-ribosyltransferase 3 [HGNC id: 725]
IP-10	4,56	2,61E-06	TNFSF8	tumor necrosis factor (ligand) superfamily, member 8 [HGNC id: 11938]
IP-10	4,66	1,58E-06	HLA-DQA1	major histocompatibility complex, class II, DQ alpha 1 [HGNC id: 4942]
IP-10	6,11	5,00E-10	CXCL10	chemokine (C-X-C motif) ligand 10 [HGNC id: 10637]
IP-10	7,37	8,61E-14	CXCL9	chemokine (C-X-C motif) ligand 9 [HGNC id: 7098]
IP-10	5,06	2,13E-07	PTH1R	parathyroid hormone 1 receptor [HGNC id: 9608]
IP-10	5,15	1,30E-07	PTPN11	protein tyrosine phosphatase, non-receptor type 11 [HGNC id: 9644]
IP-10	5,41	3,19E-08	RPL6	ribosomal protein L6 [HGNC id: 10362]
IP-10	6,40	8,03E-11	ATXN2	ataxin 2 [HGNC id: 10555]
IP-10	7,84	2,25E-15	CXCL11	chemokine (C-X-C motif) ligand 11 [HGNC id: 10638]
IP-10	4,66	1,57E-06	STAT4	signal transducer and activator of transcription 4 [HGNC id: 11365]
IP-10	4,57	2,42E-06	PRRC2A	proline-rich coiled-coil 2A [HGNC id: 13918]
IP-10	5,81	3,16E-09	BAG6	BCL2-associated athanogene 6 [HGNC id: 13919]
IP-10	5,69	6,33E-09	BRAP	BRCA1 associated protein [HGNC id: 1099]
IP-10	6,03	8,42E-10	CCRL2	chemokine (C-C motif) receptor-like 2 [HGNC id: 1612]
IP-10	6,42	6,89E-11	SH2B3	SH2B adaptor protein 3 [HGNC id: 29605]
IP-10	4,91	4,49E-07	SCAP	SREBF chaperone [HGNC id: 30634]
IP-10	5,42	2,92E-08	NBEAL2	neurobeachin-like 2 [HGNC id: 31928]
IP-10	4,76	9,86E-07	KLHL18	kelch-like family member 18 [HGNC id: 29120]
IP-10	5,14	1,36E-07	CUX2	cut-like homeobox 2 [HGNC id: 19347]
IP-10	4,75	1,03E-06	PTPN23	protein tyrosine phosphatase, non-receptor type 23 [HGNC id: 14406]
IP-10	5,38	3,71E-08	NAAA	N-acylethanolamine acid amidase [HGNC id: 736]
IP-10	5,63	9,09E-09	SETD2	SET domain containing 2 [HGNC id: 18420]
IP-10	4,56	2,52E-06	ELP6	elongator acetyltransferase complex subunit 6 [HGNC id: 25976]
IP-10	7,31	1,30E-13	SDAD1	SDA1 domain containing 1 [HGNC id: 25537]
IP-10	5,00	2,93E-07	KIF9	kinesin family member 9 [HGNC id: 16666]
IP-10	5,16	1,21E-07	ACAD10	acyl-CoA dehydrogenase family, member 10 [HGNC id: 21597]
IP-10	5,04	2,32E-07	SLFN11	schlafen family member 11 [HGNC id: 26633]
IP-10	5,13	1,48E-07	FAM109A	family with sequence similarity 109, member A [HGNC id: 26509]
IP-10	5,50	1,94E-08	CCDC12	coiled-coil domain containing 12 [HGNC id: 28332]
M-CSF	4,93	4,21E-07	AANAT	aralkylamine N-acetyltransferase [HGNC id: 19]
M-CSF	6,02	8,61E-10	ACADVL	acyl-CoA dehydrogenase, very long chain [HGNC id: 92]
M-CSF	4,73	1,14E-06	ADH4	alcohol dehydrogenase 4 (class II), pi polypeptide [HGNC id: 252]

Table A.4 (cont.)

Cytokine	Z-score	P-value	HGNC symbol	HGNC description
M-CSF	7,55	2,14E-14	ALX3	ALX homeobox 3 [HGNC id: 449]
M-CSF	7,82	2,71E-15	ASGR1	asialoglycoprotein receptor 1 [HGNC id: 742]
M-CSF	7,04	9,77E-13	ASGR2	asialoglycoprotein receptor 2 [HGNC id: 743]
M-CSF	5,45	2,46E-08	CLDN7	claudin 7 [HGNC id: 2049]
M-CSF	5,78	3,83E-09	CPOX	coproporphyrinogen oxidase [HGNC id: 2321]
M-CSF	7,66	9,63E-15	CSF1	colony stimulating factor 1 (macrophage) [HGNC id: 2432]
M-CSF	6,11	5,00E-10	CSF1R	colony stimulating factor 1 receptor [HGNC id: 2433]
M-CSF	5,88	2,00E-09	DLG4	discs, large homolog 4 (Drosophila) [HGNC id: 2903]
M-CSF	6,50	3,95E-11	SLC26A2	solute carrier family 26 (anion exchanger), member 2 [HGNC id: 10994]
M-CSF	6,88	2,98E-12	DVL2	dishevelled segment polarity protein 2 [HGNC id: 3086]
M-CSF	5,41	3,09E-08	FUT2	fucosyltransferase 2 (secretor status included) [HGNC id: 4013]
M-CSF	6,54	3,01E-11	B4GALT1	UDP-Gal:betaGlcNAc beta 1,4- galactosyltransferase, polypeptide 1 [HGNC id: 924]
M-CSF	4,98	3,23E-07	GPR15	G protein-coupled receptor 15 [HGNC id: 4469]
M-CSF	9,20	1,85E-20	MGAT5	mannosyl (alpha-1,6-)-glycoprotein beta-1,6-N-acetyl-glucosaminyltransferase [HGNC id: 7049]
M-CSF	5,88	2,10E-09	RPS6KB1	ribosomal protein S6 kinase, 70kDa, polypeptide 1 [HGNC id: 10436]
M-CSF	7,50	3,23E-14	ST3GAL4	ST3 beta-galactoside alpha-2,3-sialyltransferase 4 [HGNC id: 10864]
M-CSF	7,41	6,51E-14	ST3GAL6	ST3 beta-galactoside alpha-2,3-sialyltransferase 6 [HGNC id: 18080]
M-CSF	5,22	9,08E-08	CLEC10A	C-type lectin domain family 10, member A [HGNC id: 16916]
M-CSF	4,66	1,59E-06	AHCYL1	adenosylhomocysteinase-like 1 [HGNC id: 344]
M-CSF	5,17	1,15E-07	HMGXB3	HMG box domain containing 3 [HGNC id: 28982]
M-CSF	4,84	6,46E-07	CUX2	cut-like homeobox 2 [HGNC id: 19347]
M-CSF	6,37	9,43E-11	B3GAT1	beta-1,3-glucuronyltransferase 1 (glucuronosyltransferase P) [HGNC id: 921]
M-CSF	5,73	5,01E-09	RNFT1	ring finger protein, transmembrane 1 [HGNC id: 30206]
M-CSF	5,60	1,07E-08	TUBD1	tubulin, delta 1 [HGNC id: 16811]
M-CSF	4,63	1,85E-06	UBE2O	ubiquitin-conjugating enzyme E2O [HGNC id: 29554]
M-CSF	5,26	7,21E-08	RHBDF2	rhomboid 5 homolog 2 (Drosophila) [HGNC id: 20788]
M-CSF	4,70	1,29E-06	CTC1	CTS telomere maintenance complex component 1 [HGNC id: 26169]
M-CSF	5,41	3,20E-08	PNPLA3	patatin-like phospholipase domain containing 3 [HGNC id: 18590]
M-CSF	5,65	7,99E-09	TIGD6	tigger transposable element derived 6 [HGNC id: 18332]
M-CSF	6,17	3,42E-10	STRIP1	striatin interacting protein 1 [HGNC id: 25916]
M-CSF	4,95	3,63E-07	SPPL3	signal peptide peptidase like 3 [HGNC id: 30424]
M-CSF	7,89	1,46E-15	DCBLD2	discoidin, CUB and LCCL domain containing 2 [HGNC id: 24627]
M-CSF	4,79	8,52E-07	DNAH2	dynein, axonemal, heavy chain 2 [HGNC id: 2948]
M-CSF	4,57	2,40E-06	MAMSTR	MEF2 activating motif and SAP domain containing transcriptional regulator [HGNC id: 26689]
MCP-1	6,85	3,69E-12	CCR1	chemokine (C-C motif) receptor 1 [HGNC id: 1602]
MCP-1	6,11	5,00E-10	CCR3	chemokine (C-C motif) receptor 3 [HGNC id: 1604]
MCP-1	6,11	5,00E-10	CCR5	chemokine (C-C motif) receptor 5 (gene/pseudogene) [HGNC id: 1606]
MCP-1	7,93	1,07E-15	ACKR2	atypical chemokine receptor 2 [HGNC id: 1565]
MCP-1	5,65	8,23E-09	CYP8B1	cytochrome P450, family 8, subfamily B, polypeptide 1 [HGNC id: 2653]
MCP-1	7,17	3,80E-13	FCER1A	Fc fragment of IgE, high affinity I, receptor for; alpha polypeptide [HGNC id: 3609]
MCP-1	6,11	5,00E-10	DARC	Duffy blood group, atypical chemokine receptor [HGNC id: 4035]
MCP-1	7,86	1,85E-15	XCR1	chemokine (C motif) receptor 1 [HGNC id: 1625]
MCP-1	6,11	5,00E-10	LTF	lactotransferrin [HGNC id: 6720]
MCP-1	5,47	2,27E-08	CCL11	chemokine (C-C motif) ligand 11 [HGNC id: 10610]

Table A.4 (cont.)

Cytokine	Z-score	P-value	HGNC symbol	HGNC description
MCP-1	7,91	1,29E-15	CCRL2	chemokine (C-C motif) receptor-like 2 [HGNC id: 1612]
MCP-1	7,84	2,18E-15	CXCR6	chemokine (C-X-C motif) receptor 6 [HGNC id: 16647]
MCP-1	7,36	8,91E-14	CCR9	chemokine (C-C motif) receptor 9 [HGNC id: 1610]
MCP-1	7,23	2,37E-13	HIGD1A	HIG1 hypoxia inducible domain family, member 1A [HGNC id: 29527]
MCP-1	7,03	1,04E-12	OR10J1	olfactory receptor, family 10, subfamily J, member 1 [HGNC id: 8175]
MCP-1	7,59	1,54E-14	LZTFL1	leucine zipper transcription factor-like 1 [HGNC id: 6741]
MCP-1	5,47	2,29E-08	SLC6A20	solute carrier family 6 (proline IMINO transporter), member 20 [HGNC id: 30927]
MCP-1	4,95	3,72E-07	HHATL	hedgehog acyltransferase-like [HGNC id: 13242]
MCP-1	7,83	2,37E-15	CADM3	cell adhesion molecule 3 [HGNC id: 17601]
MCP-1	6,57	2,52E-11	LRRC2	leucine rich repeat containing 2 [HGNC id: 14676]
MCP-1	8,36	3,24E-17	FYCO1	FYVE and coiled-coil domain containing 1 [HGNC id: 14673]
MCP-1	5,62	9,63E-09	RTP3	receptor (chemosensory) transporter protein 3 [HGNC id: 15572]
MCP-1	6,24	2,13E-10	CCDC13	coiled-coil domain containing 13 [HGNC id: 26358]
MCP-1	4,77	9,08E-07	ALS2CL	ALS2 C-terminal like [HGNC id: 20605]
MCP-1	7,52	2,77E-14	CCR2	chemokine (C-C motif) receptor 2 [HGNC id: 1603]
MCP-1	5,29	5,97E-08	PRSS45	protease, serine, 45 [HGNC id: 30717]
MCP-3	10,92	4,91E-28	ASIC2	acid-sensing (proton-gated) ion channel 2 [HGNC id: 99]
MCP-3	4,58	2,35E-06	CFB	complement factor B [HGNC id: 1037]
MCP-3	7,92	1,17E-15	DARC	Duffy blood group, atypical chemokine receptor [HGNC id: 4035]
MCP-3	7,62	1,25E-14	LIG3	ligase III, DNA, ATP-dependent [HGNC id: 6600]
MCP-3	5,08	1,86E-07	MICB	MHC class I polypeptide-related sequence B [HGNC id: 7091]
MCP-3	5,22	8,86E-08	MYO1D	myosin ID [HGNC id: 7598]
MCP-3	7,13	5,04E-13	RAD51D	RAD51 paralog D [HGNC id: 9823]
MCP-3	6,86	3,46E-12	CCL1	chemokine (C-C motif) ligand 1 [HGNC id: 10609]
MCP-3	6,15	3,78E-10	CCL2	chemokine (C-C motif) ligand 2 [HGNC id: 10618]
MCP-3	6,11	5,00E-10	CCL7	chemokine (C-C motif) ligand 7 [HGNC id: 10634]
MCP-3	14,93	1,00E-50	CCL8	chemokine (C-C motif) ligand 8 [HGNC id: 10635]
MCP-3	6,11	5,00E-10	CCL11	chemokine (C-C motif) ligand 11 [HGNC id: 10610]
MCP-3	6,72	9,16E-12	CCL13	chemokine (C-C motif) ligand 13 [HGNC id: 10611]
MCP-3	4,79	8,34E-07	SKIV2L	superkiller viralicidic activity 2-like (S. cerevisiae) [HGNC id: 10898]
MCP-3	4,61	1,98E-06	TNXB	tenascin XB [HGNC id: 11976]
MCP-3	4,68	1,47E-06	NELFE	negative elongation factor complex member E [HGNC id: 13974]
MCP-3	5,32	5,12E-08	STK19	serine/threonine kinase 19 [HGNC id: 11398]
MCP-3	5,85	2,47E-09	CCT6B	chaperonin containing TCP1, subunit 6B (zeta 2) [HGNC id: 1621]
MCP-3	4,96	3,57E-07	CADM3	cell adhesion molecule 3 [HGNC id: 17601]
MCP-3	7,28	1,72E-13	SLFN11	schlafen family member 11 [HGNC id: 26633]
MCP-3	6,56	2,73E-11	RFFL	ring finger and FYVE-like domain containing E3 ubiquitin protein ligase [HGNC id: 24821]
MCP-3	6,99	1,41E-12	TMEM132E	transmembrane protein 132E [HGNC id: 26991]
MCP-3	6,79	5,52E-12	C17orf102	chromosome 17 open reading frame 102 [HGNC id: 34412]
MIF	6,29	1,59E-10	DDT	D-dopachrome tautomerase [HGNC id: 2732]
MIF	5,62	9,41E-09	EEF1D	eukaryotic translation elongation factor 1 delta (guanine nucleotide exchange protein) [HGNC id: 3211]
MIF	6,11	5,00E-10	GSTT2	glutathione S-transferase theta 2 [HGNC id: 4642]
MIF	4,98	3,21E-07	PYCRL	pyrroline-5-carboxylate reductase-like [HGNC id: 25846]
MIF	6,51	3,71E-11	TIGD5	tigger transposable element derived 5 [HGNC id: 18336]

Table A.4 (cont.)

Cytokine	Z-score	P-value	HGNC symbol	HGNC description
MIF	6,14	4,19E-10	NAPRT1	nicotinate phosphoribosyltransferase domain containing 1 [HGNC id: 30450]
MIF	4,92	4,37E-07	MROH6	maestro heat-like repeat family member 6 [HGNC id: 27814]
MIF	8,57	5,26E-18	GSTT2B	glutathione S-transferase theta 2B (gene/pseudogene) [HGNC id: 33437]
MIF	6,74	8,19E-12	DDT	D-dopachrome tautomerase [HGNC id: 2732]
MIF	7,56	2,07E-14	n/a	n/a
MIG	4,91	4,52E-07	ART3	ADP-ribosyltransferase 3 [HGNC id: 725]
MIG	6,72	9,19E-12	CXCL9	chemokine (C-X-C motif) ligand 9 [HGNC id: 7098]
MIG	5,25	7,64E-08	PLG	plasminogen [HGNC id: 9071]
MIG	4,88	5,20E-07	ATXN2	ataxin 2 [HGNC id: 10555]
MIG	4,60	2,15E-06	PRRC2A	proline-rich coiled-coil 2A [HGNC id: 13918]
MIG	4,62	1,88E-06	BRAP	BRCA1 associated protein [HGNC id: 1099]
MIG	4,80	7,94E-07	SH2B3	SH2B adaptor protein 3 [HGNC id: 29605]
MIG	7,14	4,55E-13	NAAA	N-acylethanolamine acid amidase [HGNC id: 736]
MIG	7,44	5,11E-14	SDAD1	SDA1 domain containing 1 [HGNC id: 25537]
MIP-1a	6,11	5,00E-10	CCL3	chemokine (C-C motif) ligand 3 [HGNC id: 10627]
MIP-1a	6,14	4,09E-10	CCL4	chemokine (C-C motif) ligand 4 [HGNC id: 10630]
MIP-1a	7,01	1,16E-12	CCL14	chemokine (C-C motif) ligand 14 [HGNC id: 10612]
MIP-1a	4,85	6,25E-07	CCL15	chemokine (C-C motif) ligand 15 [HGNC id: 10613]
MIP-1a	7,97	7,91E-16	CCL18	chemokine (C-C motif) ligand 18 (pulmonary and activation-regulated) [HGNC id: 10616]
MIP-1a	6,66	1,40E-11	CCL23	chemokine (C-C motif) ligand 23 [HGNC id: 10622]
MIP-1a	4,79	8,53E-07	TLR1	toll-like receptor 1 [HGNC id: 11847]
MIP-1a	4,65	1,69E-06	VARS	valyl-tRNA synthetase [HGNC id: 12651]
MIP-1a	4,77	9,26E-07	MED24	mediator complex subunit 24 [HGNC id: 22963]
MIP-1b	5,51	1,80E-08	RHOA	ras homolog family member A [HGNC id: 667]
MIP-1b	5,38	3,81E-08	SLC25A20	solute carrier family 25 (carnitine/acylcarnitine translocase), member 20 [HGNC id: 1421]
MIP-1b	7,37	8,61E-14	CDC25A	cell division cycle 25A [HGNC id: 1725]
MIP-1b	6,13	4,36E-10	CCR1	chemokine (C-C motif) receptor 1 [HGNC id: 1602]
MIP-1b	8,08	3,36E-16	CCR3	chemokine (C-C motif) receptor 3 [HGNC id: 1604]
MIP-1b	7,87	1,79E-15	CCR5	chemokine (C-C motif) receptor 5 (gene/pseudogene) [HGNC id: 1606]
MIP-1b	5,48	2,07E-08	COL7A1	collagen, type VII, alpha 1 [HGNC id: 2214]
MIP-1b	4,63	1,82E-06	DAG1	dystroglycan 1 (dystrophin-associated glycoprotein 1) [HGNC id: 2666]
MIP-1b	5,00	2,85E-07	XCR1	chemokine (C motif) receptor 1 [HGNC id: 1625]
MIP-1b	5,20	1,02E-07	GRM2	glutamate receptor, metabotropic 2 [HGNC id: 4594]
MIP-1b	7,57	1,86E-14	LTF	lactotransferrin [HGNC id: 6720]
MIP-1b	7,29	1,56E-13	MAP4	microtubule-associated protein 4 [HGNC id: 6862]
MIP-1b	7,53	2,53E-14	MST1	macrophage stimulating 1 (hepatocyte growth factor-like) [HGNC id: 7380]
MIP-1b	5,77	3,88E-09	MST1R	macrophage stimulating 1 receptor (c-met-related tyrosine kinase) [HGNC id: 7381]
MIP-1b	4,90	4,79E-07	PFKFB4	6-phosphofructo-2-kinase/fructose-2,6-biphosphatase 4 [HGNC id: 8875]
MIP-1b	6,29	1,62E-10	PRKAR2A	protein kinase, cAMP-dependent, regulatory, type II, alpha [HGNC id: 9391]
MIP-1b	7,77	3,86E-15	PTH1R	parathyroid hormone 1 receptor [HGNC id: 9608]
MIP-1b	5,79	3,61E-09	QARS	glutaminyl-tRNA synthetase [HGNC id: 9751]
MIP-1b	4,93	4,19E-07	CCL3	chemokine (C-C motif) ligand 3 [HGNC id: 10627]
MIP-1b	4,61	2,00E-06	CCL4	chemokine (C-C motif) ligand 4 [HGNC id: 10630]

Table A.4 (cont.)

Cytokine	Z-score	P-value	HGNC symbol	HGNC description
MIP-1b	5,02	2,56E-07	CCL5	chemokine (C-C motif) ligand 5 [HGNC id: 10632]
MIP-1b	4,87	5,59E-07	CCL14	chemokine (C-C motif) ligand 14 [HGNC id: 10612]
MIP-1b	5,04	2,34E-07	CCL15	chemokine (C-C motif) ligand 15 [HGNC id: 10613]
MIP-1b	4,89	5,15E-07	CCL16	chemokine (C-C motif) ligand 16 [HGNC id: 10614]
MIP-1b	6,48	4,54E-11	CCL18	chemokine (C-C motif) ligand 18 (pulmonary and activation-regulated) [HGNC id: 10616]
MIP-1b	6,77	6,44E-12	CCL23	chemokine (C-C motif) ligand 23 [HGNC id: 10622]
MIP-1b	7,15	4,45E-13	SMARCC1	SWI/SNF related, matrix associated, actin dependent regulator of chromatin, subfamily c, member 1 [HGNC id: 11104]
MIP-1b	6,51	3,85E-11	TDGF1	teratocarcinoma-derived growth factor 1 [HGNC id: 11701]
MIP-1b	6,36	9,82E-11	TLR1	toll-like receptor 1 [HGNC id: 11847]
MIP-1b	5,38	3,81E-08	TLR4	toll-like receptor 4 [HGNC id: 11850]
MIP-1b	4,89	4,93E-07	USP4	ubiquitin specific peptidase 4 (proto-oncogene) [HGNC id: 12627]
MIP-1b	5,48	2,07E-08	TAF15	TAF15 RNA polymerase II, TATA box binding protein (TBP)-associated factor, 68kDa [HGNC id: 11547]
MIP-1b	4,75	1,02E-06	BSN	bassoon presynaptic cytomatrix protein [HGNC id: 1117]
MIP-1b	5,90	1,76E-09	LIMD1	LIM domains containing 1 [HGNC id: 6612]
MIP-1b	6,11	5,00E-10	CCRL2	chemokine (C-C motif) receptor-like 2 [HGNC id: 1612]
MIP-1b	6,11	5,00E-10	ZNHIT3	zinc finger, HIT-type containing 3 [HGNC id: 12309]
MIP-1b	7,15	4,49E-13	RBM6	RNA binding motif protein 6 [HGNC id: 9903]
MIP-1b	6,66	1,38E-11	RBM5	RNA binding motif protein 5 [HGNC id: 9902]
MIP-1b	4,78	8,72E-07	NME6	NME/NM23 nucleoside diphosphate kinase 6 [HGNC id: 20567]
MIP-1b	5,54	1,55E-08	ARIH2	ariadne RBR E3 ubiquitin protein ligase 2 [HGNC id: 690]
MIP-1b	6,11	5,00E-10	CXCR6	chemokine (C-X-C motif) receptor 6 [HGNC id: 16647]
MIP-1b	7,60	1,48E-14	CSPG5	chondroitin sulfate proteoglycan 5 (neuroglycan C) [HGNC id: 2467]
MIP-1b	4,76	9,45E-07	CCT6B	chaperonin containing TCP1, subunit 6B (zeta 2) [HGNC id: 1621]
MIP-1b	6,11	5,00E-10	CCR9	chemokine (C-C motif) receptor 9 [HGNC id: 1610]
MIP-1b	4,85	6,12E-07	USP19	ubiquitin specific peptidase 19 [HGNC id: 12617]
MIP-1b	5,67	7,21E-09	TMEM115	transmembrane protein 115 [HGNC id: 30055]
MIP-1b	4,56	2,57E-06	WDR6	WD repeat domain 6 [HGNC id: 12758]
MIP-1b	5,03	2,47E-07	TREX1	three prime repair exonuclease 1 [HGNC id: 12269]
MIP-1b	7,41	6,44E-14	DHX30	DEAH (Asp-Glu-Ala-His) box helicase 30 [HGNC id: 16716]
MIP-1b	7,04	9,39E-13	SACM1L	SAC1 suppressor of actin mutations 1-like (yeast) [HGNC id: 17059]
MIP-1b	6,66	1,37E-11	SCAP	SREBF chaperone [HGNC id: 30634]
MIP-1b	6,05	7,18E-10	NBEAL2	neurobeachin-like 2 [HGNC id: 31928]
MIP-1b	6,02	8,73E-10	KLHL18	kelch-like family member 18 [HGNC id: 29120]
MIP-1b	5,19	1,03E-07	ABHD14A	abhydrolase domain containing 14A [HGNC id: 24538]
MIP-1b	5,15	1,33E-07	POC1A	POC1 centriolar protein A [HGNC id: 24488]
MIP-1b	5,95	1,30E-09	PTPN23	protein tyrosine phosphatase, non-receptor type 23 [HGNC id: 14406]
MIP-1b	6,58	2,38E-11	SETD2	SET domain containing 2 [HGNC id: 18420]
MIP-1b	7,35	1,03E-13	PRSS50	protease, serine, 50 [HGNC id: 17910]
MIP-1b	5,26	7,15E-08	ZNF589	zinc finger protein 589 [HGNC id: 16747]
MIP-1b	6,11	5,00E-10	LZTFL1	leucine zipper transcription factor-like 1 [HGNC id: 6741]
MIP-1b	5,77	4,06E-09	P4HTM	prolyl 4-hydroxylase, transmembrane (endoplasmic reticulum) [HGNC id: 28858]
MIP-1b	6,11	5,00E-10	SLC6A20	solute carrier family 6 (proline IMINO transporter), member 20 [HGNC id: 30927]
MIP-1b	5,96	1,28E-09	ELP6	elongator acetyltransferase complex subunit 6 [HGNC id: 25976]
MIP-1b	4,88	5,43E-07	QRICH1	glutamine-rich 1 [HGNC id: 24713]

Table A.4 (cont.)

Cytokine	Z-score	P-value	HGNC symbol	HGNC description
MIP-1b	6,69	1,12E-11	LYZL6	lysozyme-like 6 [HGNC id: 29614]
MIP-1b	6,82	4,69E-12	KIF9	kinesin family member 9 [HGNC id: 16666]
MIP-1b	5,74	4,62E-09	CCDC71	coiled-coil domain containing 71 [HGNC id: 25760]
MIP-1b	5,72	5,25E-09	CAMKV	CaM kinase-like vesicle-associated [HGNC id: 28788]
MIP-1b	8,14	1,96E-16	DHRS11	dehydrogenase/reductase (SDR family) member 11 [HGNC id: 28639]
MIP-1b	7,65	9,91E-15	LRRC2	leucine rich repeat containing 2 [HGNC id: 14676]
MIP-1b	6,11	5,00E-10	FYCO1	FYVE and coiled-coil domain containing 1 [HGNC id: 14673]
MIP-1b	7,16	4,01E-13	GGNBP2	gametogenetin binding protein 2 [HGNC id: 19357]
MIP-1b	7,14	4,62E-13	MRM1	mitochondrial rRNA methyltransferase 1 homolog (S. cerevisiae) [HGNC id: 26202]
MIP-1b	7,07	7,57E-13	MYO19	myosin XIX [HGNC id: 26234]
MIP-1b	6,11	5,00E-10	RTP3	receptor (chemosensory) transporter protein 3 [HGNC id: 15572]
MIP-1b	4,77	9,00E-07	NICN1	nicolin 1 [HGNC id: 18317]
MIP-1b	6,07	6,59E-10	MON1A	MON1 secretory trafficking family member A [HGNC id: 28207]
MIP-1b	5,11	1,63E-07	C17orf50	chromosome 17 open reading frame 50 [HGNC id: 29581]
MIP-1b	5,35	4,49E-08	UNC45B	unc-45 homolog B (C. elegans) [HGNC id: 14304]
MIP-1b	6,70	1,03E-11	CCDC12	coiled-coil domain containing 12 [HGNC id: 28332]
MIP-1b	4,85	6,12E-07	RDM1	RAD52 motif 1 [HGNC id: 19950]
MIP-1b	5,41	3,11E-08	C17orf66	chromosome 17 open reading frame 66 [HGNC id: 26548]
MIP-1b	7,71	6,37E-15	ALS2CL	ALS2 C-terminal like [HGNC id: 20605]
MIP-1b	5,06	2,09E-07	TMIE	transmembrane inner ear [HGNC id: 30800]
MIP-1b	6,11	5,00E-10	PIGW	phosphatidylinositol glycan anchor biosynthesis, class W [HGNC id: 23213]
MIP-1b	6,04	7,62E-10	CCDC36	coiled-coil domain containing 36 [HGNC id: 27945]
MIP-1b	5,54	1,48E-08	CDHR4	cadherin-related family member 4 [HGNC id: 34527]
MIP-1b	6,29	1,59E-10	TMEM89	transmembrane protein 89 [HGNC id: 32372]
MIP-1b	5,10	1,69E-07	SPINK8	serine peptidase inhibitor, Kazal type 8 (putative) [HGNC id: 33160]
MIP-1b	5,30	5,74E-08	C3orf84	chromosome 3 open reading frame 84 [HGNC id: 44666]
MIP-1b	6,11	5,00E-10	CCR2	chemokine (C-C motif) receptor 2 [HGNC id: 1603]
MIP-1b	7,77	3,99E-15	n/a	n/a
PDGFbb	5,40	3,37E-08	ARL3	ADP-ribosylation factor-like 3 [HGNC id: 694]
PDGFbb	6,83	4,27E-12	CD36	CD36 molecule (thrombospondin receptor) [HGNC id: 1663]
PDGFbb	5,66	7,38E-09	BRF1	BRF1, RNA polymerase III transcription initiation factor 90 kDa subunit [HGNC id: 11551]
PDGFbb	7,78	3,56E-15	PCSK6	proprotein convertase subtilisin/kexin type 6 [HGNC id: 8569]
PDGFbb	9,26	1,02E-20	SERPINE2	serpin peptidase inhibitor, clade E (nexin, plasminogen activator inhibitor type 1), member 2 [HGNC id: 8951]
PDGFbb	5,29	6,20E-08	RBBP5	retinoblastoma binding protein 5 [HGNC id: 9888]
PDGFbb	5,19	1,04E-07	BZRAP1	benzodiazepine receptor (peripheral) associated protein 1 [HGNC id: 16831]
PDGFbb	5,35	4,28E-08	QKI	QKI, KH domain containing, RNA binding [HGNC id: 21100]
PDGFbb	5,85	2,52E-09	TMCC2	transmembrane and coiled-coil domain family 2 [HGNC id: 24239]
PDGFbb	5,40	3,30E-08	ACTR1A	ARP1 actin-related protein 1 homolog A, centractin alpha (yeast) [HGNC id: 167]
PDGFbb	6,27	1,76E-10	RCL1	RNA terminal phosphate cyclase-like 1 [HGNC id: 17687]
PDGFbb	7,86	1,86E-15	ZFPM2	zinc finger protein, FOG family member 2 [HGNC id: 16700]
PDGFbb	4,58	2,38E-06	DSTYK	dual serine/threonine and tyrosine protein kinase [HGNC id: 29043]
PDGFbb	7,86	1,97E-15	NRBF2	nuclear receptor binding factor 2 [HGNC id: 19692]
PDGFbb	6,70	1,05E-11	EHD3	EH-domain containing 3 [HGNC id: 3244]
PDGFbb	7,23	2,48E-13	GP6	glycoprotein VI (platelet) [HGNC id: 14388]

Table A.4 (cont.)

Cytokine	Z-score	P-value	HGNC symbol	HGNC description
PDGFbb	7,26	1,87E-13	SUFU	suppressor of fused homolog (Drosophila) [HGNC id: 16466]
PDGFbb	4,82	7,06E-07	WBP1L	WW domain binding protein 1-like [HGNC id: 23510]
PDGFbb	4,70	1,30E-06	DOCK10	dedicator of cytokinesis 10 [HGNC id: 23479]
PDGFbb	6,61	1,96E-11	TMEM180	transmembrane protein 180 [HGNC id: 26196]
PDGFbb	6,43	6,29E-11	TRIM8	tripartite motif containing 8 [HGNC id: 15579]
PDGFbb	5,19	1,05E-07	BTBD6	BTB (POZ) domain containing 6 [HGNC id: 19897]
PDGFbb	6,26	1,96E-10	RDH13	retinol dehydrogenase 13 (all-trans/9-cis) [HGNC id: 19978]
PDGFbb	5,50	1,95E-08	SFXN2	sideroflexin 2 [HGNC id: 16086]
PDGFbb	8,34	3,82E-17	REEP3	receptor accessory protein 3 [HGNC id: 23711]
PDGFbb	7,44	5,10E-14	JMJD1C	jumonji domain containing 1C [HGNC id: 12313]
PDGFbb	5,28	6,31E-08	PEAR1	platelet endothelial aggregation receptor 1 [HGNC id: 33631]
RANTES	6,46	5,18E-11	AP2B1	adaptor-related protein complex 2, beta 1 subunit [HGNC id: 563]
RANTES	5,58	1,23E-08	PEX12	peroxisomal biogenesis factor 12 [HGNC id: 8854]
RANTES	6,11	5,00E-10	CCL5	chemokine (C-C motif) ligand 5 [HGNC id: 10632]
RANTES	4,77	9,05E-07	ZNF33A	zinc finger protein 33A [HGNC id: 13096]
RANTES	6,20	2,76E-10	ZNF37A	zinc finger protein 37A [HGNC id: 13102]
RANTES	6,11	5,00E-10	TAF15	TAF15 RNA polymerase II, TATA box binding protein (TBP)-associated factor, 68kDa [HGNC id: 11547]
RANTES	4,76	9,54E-07	RCL1	RNA terminal phosphate cyclase-like 1 [HGNC id: 17687]
RANTES	7,87	1,71E-15	NRBF2	nuclear receptor binding factor 2 [HGNC id: 19692]
RANTES	5,49	2,01E-08	GP6	glycoprotein VI (platelet) [HGNC id: 14388]
RANTES	5,54	1,53E-08	FAM46C	family with sequence similarity 46, member C [HGNC id: 24712]
RANTES	6,11	5,00E-10	LYZL6	lysozyme-like 6 [HGNC id: 29614]
RANTES	6,11	5,00E-10	MMP28	matrix metallopeptidase 28 [HGNC id: 14366]
RANTES	8,20	1,24E-16	RASL10B	RAS-like, family 10, member B [HGNC id: 30295]
RANTES	5,42	3,06E-08	RDH13	retinol dehydrogenase 13 (all-trans/9-cis) [HGNC id: 19978]
RANTES	6,19	3,01E-10	C17orf50	chromosome 17 open reading frame 50 [HGNC id: 29581]
RANTES	6,11	5,00E-10	RDM1	RAD52 motif 1 [HGNC id: 19950]
RANTES	4,62	1,96E-06	ZNF25	zinc finger protein 25 [HGNC id: 13043]
RANTES	7,15	4,25E-13	REEP3	receptor accessory protein 3 [HGNC id: 23711]
RANTES	6,73	8,52E-12	JMJD1C	jumonji domain containing 1C [HGNC id: 12313]
RANTES	8,10	2,76E-16	GAS2L2	growth arrest-specific 2 like 2 [HGNC id: 24846]
RANTES	6,11	5,00E-10	C17orf66	chromosome 17 open reading frame 66 [HGNC id: 26548]
RANTES	5,35	4,50E-08	SLFN14	schlafen family member 14 [HGNC id: 32689]
RANTES	6,09	5,64E-10	MTRNR2L7	MT-RNR2-like 7 [HGNC id: 37164]
RANTES	5,46	2,43E-08	SLFN12L	schlafen family member 12-like [HGNC id: 33920]
SCF	11,00	1,93E-28	ABCA1	ATP-binding cassette, sub-family A (ABC1), member 1 [HGNC id: 29]
SCF	5,29	6,15E-08	ABO	ABO blood group (transferase A, alpha 1-3-N-acetylgalactosaminyltransferase; transferase B, alpha 1-3-galactosyltransferase) [HGNC id: 79]
SCF	4,89	4,98E-07	APOC1	apolipoprotein C-I [HGNC id: 607]
SCF	4,71	1,25E-06	BCKDHA	branched chain keto acid dehydrogenase E1, alpha polypeptide [HGNC id: 986]
SCF	4,63	1,83E-06	CBFB	core-binding factor, beta subunit [HGNC id: 1539]
SCF	6,11	5,00E-10	CD40	CD40 molecule, TNF receptor superfamily member 5 [HGNC id: 11919]
SCF	6,11	5,00E-10	CETP	cholesteryl ester transfer protein, plasma [HGNC id: 1869]
SCF	4,93	4,18E-07	CKMT1A	creatine kinase, mitochondrial 1A [HGNC id: 31736]
SCF	5,92	1,62E-09	CTRL	chymotrypsin-like [HGNC id: 2524]

Table A.4 (cont.)

Cytokine	Z-score	P-value	HGNC symbol	HGNC description
SCF	5,09	1,83E-07	E2F4	E2F transcription factor 4, p107/p130-binding [HGNC id: 3118]
SCF	6,87	3,24E-12	LCAT	lecithin-cholesterol acyltransferase [HGNC id: 6522]
SCF	5,20	9,72E-08	LIPC	lipase, hepatic [HGNC id: 6619]
SCF	4,89	5,16E-07	MAP1A	microtubule-associated protein 1A [HGNC id: 6835]
SCF	4,76	9,70E-07	MFAP1	microfibrillar-associated protein 1 [HGNC id: 7032]
SCF	5,00	2,89E-07	AFF1	AF4/FMR2 family, member 1 [HGNC id: 7135]
SCF	6,11	5,00E-10	MMP9	matrix metallopeptidase 9 (gelatinase B, 92kDa gelatinase, 92kDa type IV collagenase) [HGNC id: 7176]
SCF	8,03	4,73E-16	NFATC3	nuclear factor of activated T-cells, cytoplasmic, calcineurin-dependent 3 [HGNC id: 7777]
SCF	8,08	3,30E-16	PLTP	phospholipid transfer protein [HGNC id: 9093]
SCF	5,04	2,30E-07	PON1	paraoxonase 1 [HGNC id: 9204]
SCF	8,00	6,23E-16	CTSA	cathepsin A [HGNC id: 9251]
SCF	7,60	1,48E-14	PSKH1	protein serine kinase H1 [HGNC id: 9529]
SCF	6,49	4,36E-11	PSMB10	proteasome (prosome, macropain) subunit, beta type, 10 [HGNC id: 9538]
SCF	4,74	1,05E-06	SLC9A5	solute carrier family 9, subfamily A (NHE5, cation proton antiporter 5), member 5 [HGNC id: 11078]
SCF	6,63	1,67E-11	SLC12A4	solute carrier family 12 (potassium/chloride transporter), member 4 [HGNC id: 10913]
SCF	5,70	6,07E-09	MED22	mediator complex subunit 22 [HGNC id: 11477]
SCF	4,98	3,22E-07	HNF1A	HNF1 homeobox A [HGNC id: 11621]
SCF	8,29	5,75E-17	TNNC2	troponin C type 2 (fast) [HGNC id: 11944]
SCF	5,00	2,89E-07	TP53BP1	tumor protein p53 binding protein 1 [HGNC id: 11999]
SCF	4,92	4,31E-07	NOL3	nucleolar protein 3 (apoptosis repressor with CARD domain) [HGNC id: 7869]
SCF	5,38	3,62E-08	SLC7A6	solute carrier family 7 (amino acid transporter light chain, y+L system), member 6 [HGNC id: 11064]
SCF	5,24	8,16E-08	LCMT2	leucine carboxyl methyltransferase 2 [HGNC id: 17558]
SCF	6,98	1,43E-12	ACOT8	acyl-CoA thioesterase 8 [HGNC id: 15919]
SCF	6,11	5,00E-10	NUTF2	nuclear transport factor 2 [HGNC id: 13722]
SCF	5,56	1,37E-08	LILRB2	leukocyte immunoglobulin-like receptor, subfamily B (with TM and ITIM domains), member 2 [HGNC id: 6606]
SCF	7,87	1,76E-15	WFDC2	WAP four-disulfide core domain 2 [HGNC id: 15939]
SCF	7,12	5,53E-13	CTCF	CCCTC-binding factor (zinc finger protein) [HGNC id: 13723]
SCF	5,32	5,07E-08	SPINT3	serine peptidase inhibitor, Kunitz type, 3 [HGNC id: 11248]
SCF	7,81	2,85E-15	LILRA3	leukocyte immunoglobulin-like receptor, subfamily A (without TM domain), member 3 [HGNC id: 6604]
SCF	5,21	9,36E-08	CACFD1	calcium channel flower domain containing 1 [HGNC id: 1365]
SCF	5,37	3,91E-08	EDC4	enhancer of mRNA decapping 4 [HGNC id: 17157]
SCF	7,75	4,74E-15	PLA2G15	phospholipase A2, group XV [HGNC id: 17163]
SCF	5,42	2,94E-08	TUBGCP4	tubulin, gamma complex associated protein 4 [HGNC id: 16691]
SCF	5,51	1,84E-08	TP53TG5	TP53 target 5 [HGNC id: 15856]
SCF	5,59	1,16E-08	PIGT	phosphatidylinositol glycan anchor biosynthesis, class T [HGNC id: 14938]
SCF	5,68	6,70E-09	PRMT7	protein arginine methyltransferase 7 [HGNC id: 25557]
SCF	7,58	1,67E-14	DUS2	dihydrouridine synthase 2 [HGNC id: 26014]
SCF	6,13	4,39E-10	DDX28	DEAD (Asp-Glu-Ala-Asp) box polypeptide 28 [HGNC id: 17330]
SCF	7,32	1,21E-13	TSNAXIP1	translin-associated factor X interacting protein 1 [HGNC id: 18586]
SCF	7,18	3,56E-13	DBNDD2	dysbindin (dystrobrevin binding protein 1) domain containing 2 [HGNC id: 15881]
SCF	7,81	2,77E-15	SLC12A5	solute carrier family 12 (potassium/chloride transporter), member 5 [HGNC id: 13818]
SCF	7,06	8,28E-13	RANBP10	RAN binding protein 10 [HGNC id: 29285]

Table A.4 (cont.)

Cytokine	Z-score	P-value	HGNC symbol	HGNC description
SCF	6,68	1,19E-11	NCOA5	nuclear receptor coactivator 5 [HGNC id: 15909]
SCF	6,11	5,00E-10	ZNF335	zinc finger protein 335 [HGNC id: 15807]
SCF	6,11	5,00E-10	PCIF1	PDX1 C-terminal inhibiting factor 1 [HGNC id: 16200]
SCF	6,11	5,00E-10	DPEP2	dipeptidase 2 [HGNC id: 23028]
SCF	6,81	5,03E-12	DPEP3	dipeptidase 3 [HGNC id: 23029]
SCF	7,40	6,62E-14	CDH22	cadherin 22, type 2 [HGNC id: 13251]
SCF	4,93	4,12E-07	C12orf43	chromosome 12 open reading frame 43 [HGNC id: 25719]
SCF	8,03	4,90E-16	ACD	adrenocortical dysplasia homolog (mouse) [HGNC id: 25070]
SCF	6,94	1,99E-12	FAM65A	family with sequence similarity 65, member A [HGNC id: 25836]
SCF	4,99	2,95E-07	ELMO3	engulfment and cell motility 3 [HGNC id: 17289]
SCF	4,72	1,18E-06	WDR76	WD repeat domain 76 [HGNC id: 25773]
SCF	8,11	2,45E-16	ESRP2	epithelial splicing regulatory protein 2 [HGNC id: 26152]
SCF	6,02	8,76E-10	CENPT	centromere protein T [HGNC id: 25787]
SCF	4,56	2,60E-06	ELL3	elongation factor RNA polymerase II-like 3 [HGNC id: 23113]
SCF	7,59	1,58E-14	GFOD2	glucose-fructose oxidoreductase domain containing 2 [HGNC id: 28159]
SCF	4,93	4,07E-07	ENKD1	enkurin domain containing 1 [HGNC id: 25246]
SCF	5,35	4,39E-08	TOMM40L	translocase of outer mitochondrial membrane 40 homolog (yeast)-like [HGNC id: 25756]
SCF	6,92	2,29E-12	SLC7A6OS	solute carrier family 7, member 6 opposite strand [HGNC id: 25807]
SCF	7,27	1,84E-13	FRMD5	FERM domain containing 5 [HGNC id: 28214]
SCF	4,61	2,03E-06	DOCK7	dedicator of cytokinesis 7 [HGNC id: 19190]
SCF	5,00	2,86E-07	SYS1	SYS1 Golgi-localized integral membrane protein homolog (S. cerevisiae) [HGNC id: 16162]
SCF	5,97	1,17E-09	WFDC8	WAP four-disulfide core domain 8 [HGNC id: 16163]
SCF	7,54	2,42E-14	SNX21	sorting nexin family member 21 [HGNC id: 16154]
SCF	7,87	1,75E-15	ZSWIM1	zinc finger, SWIM-type containing 1 [HGNC id: 16155]
SCF	7,40	6,85E-14	DNTTIP1	deoxynucleotidyltransferase, terminal, interacting protein 1 [HGNC id: 16160]
SCF	4,59	2,20E-06	TGM7	transglutaminase 7 [HGNC id: 30790]
SCF	6,11	5,00E-10	NRN1L	neuritin 1-like [HGNC id: 29811]
SCF	7,69	7,08E-15	SPATA25	spermatogenesis associated 25 [HGNC id: 16158]
SCF	7,96	8,68E-16	NEURL2	neuralized E3 ubiquitin protein ligase 2 [HGNC id: 16156]
SCF	7,38	7,74E-14	ZSWIM3	zinc finger, SWIM-type containing 3 [HGNC id: 16157]
SCF	4,57	2,41E-06	WFDC10A	WAP four-disulfide core domain 10A [HGNC id: 16139]
SCF	6,17	3,34E-10	WFDC6	WAP four-disulfide core domain 6 [HGNC id: 16164]
SCF	7,74	4,97E-15	RLTPR	RGD motif, leucine rich repeats, tropomodulin domain and proline-rich containing [HGNC id: 27089]
SCF	4,90	4,70E-07	STRC	stereocilin [HGNC id: 16035]
SCF	5,31	5,55E-08	ADAL	adenosine deaminase-like [HGNC id: 31853]
SCF	7,05	8,90E-13	WFDC13	WAP four-disulfide core domain 13 [HGNC id: 16131]
SCF	6,30	1,46E-10	WFDC9	WAP four-disulfide core domain 9 [HGNC id: 20380]
SCF	4,71	1,22E-06	WFDC10B	WAP four-disulfide core domain 10B [HGNC id: 20479]
SCF	4,64	1,74E-06	CES4A	carboxylesterase 4A [HGNC id: 26741]
SCF	4,65	1,65E-06	EXOC3L1	exocyst complex component 3-like 1 [HGNC id: 27540]
SCF	6,91	2,44E-12	LILRA5	leukocyte immunoglobulin-like receptor, subfamily A (with TM domain), member 5 [HGNC id: 16309]
SCF	4,76	9,45E-07	B3GNT8	UDP-GlcNAc:betaGal beta-1,3-N-acetylglucosaminyltransferase 8 [HGNC id: 24139]
SCF	4,87	5,64E-07	CKMT1A	creatine kinase, mitochondrial 1A [HGNC id: 31736]
SCF	4,83	6,86E-07	KIAA0895L	KIAA0895-like [HGNC id: 34408]

Table A.4 (cont.)

Cytokine	Z-score	P-value	HGNC symbol	HGNC description
SCGF-b	5,34	4,56E-08	CKB	creatine kinase, brain [HGNC id: 1991]
SCGF-b	5,66	7,79E-09	CFH	complement factor H [HGNC id: 4883]
SCGF-b	4,58	2,33E-06	CFHR1	complement factor H-related 1 [HGNC id: 4888]
SCGF-b	5,04	2,27E-07	TNPO1	transportin 1 [HGNC id: 6401]
SCGF-b	5,45	2,55E-08	MARK3	MAP/microtubule affinity-regulating kinase 3 [HGNC id: 6897]
SCGF-b	5,82	3,01E-09	NFATC3	nuclear factor of activated T-cells, cytoplasmic, calcineurin-dependent 3 [HGNC id: 7777]
SCGF-b	5,36	4,25E-08	RBBP5	retinoblastoma binding protein 5 [HGNC id: 9888]
SCGF-b	5,35	4,49E-08	RPN1	ribophorin I [HGNC id: 10381]
SCGF-b	5,85	2,40E-09	RRBP1	ribosome binding protein 1 [HGNC id: 10448]
SCGF-b	7,89	1,46E-15	CLEC11A	C-type lectin domain family 11, member A [HGNC id: 10576]
SCGF-b	6,43	6,58E-11	CAPN15	calpain 15 [HGNC id: 11182]
SCGF-b	6,82	4,61E-12	HSP90B1	heat shock protein 90kDa beta (Grp94), member 1 [HGNC id: 12028]
SCGF-b	8,34	3,67E-17	RAB11FIP3	RAB11 family interacting protein 3 (class II) [HGNC id: 17224]
SCGF-b	4,89	4,97E-07	TMCC2	transmembrane and coiled-coil domain family 2 [HGNC id: 24239]
SCGF-b	4,62	1,94E-06	CLEC4M	C-type lectin domain family 4, member M [HGNC id: 13523]
SCGF-b	4,67	1,49E-06	KLHL18	kelch-like family member 18 [HGNC id: 29120]
SCGF-b	5,58	1,23E-08	PLA2G15	phospholipase A2, group XV [HGNC id: 17163]
SCGF-b	7,08	7,06E-13	DECR2	2,4-dienoyl CoA reductase 2, peroxisomal [HGNC id: 2754]
SCGF-b	7,95	9,07E-16	CHST11	carbohydrate (chondroitin 4) sulfotransferase 11 [HGNC id: 17422]
SCGF-b	7,79	3,33E-15	SHANK1	SH3 and multiple ankyrin repeat domains 1 [HGNC id: 15474]
SCGF-b	6,18	3,13E-10	MFSD6	major facilitator superfamily domain containing 6 [HGNC id: 24711]
SCGF-b	5,48	2,15E-08	DUS2	dihydrouridine synthase 2 [HGNC id: 26014]
SCGF-b	5,92	1,60E-09	KLK15	kallikrein-related peptidase 15 [HGNC id: 20453]
SCGF-b	8,60	4,03E-18	STAB2	stabilin 2 [HGNC id: 18629]
SCGF-b	5,34	4,73E-08	DDX28	DEAD (Asp-Glu-Ala-Asp) box polypeptide 28 [HGNC id: 17330]
SCGF-b	5,08	1,94E-07	DPEP2	dipeptidase 2 [HGNC id: 23028]
SCGF-b	5,38	3,79E-08	DHRS12	dehydrogenase/reductase (SDR family) member 12 [HGNC id: 25832]
SCGF-b	6,56	2,64E-11	ATP8B4	ATPase, class I, type 8B, member 4 [HGNC id: 13536]
SCGF-b	6,18	3,12E-10	ESRP2	epithelial splicing regulatory protein 2 [HGNC id: 26152]
SCGF-b	6,03	8,22E-10	GLT8D2	glycosyltransferase 8 domain containing 2 [HGNC id: 24890]
SCGF-b	4,85	6,32E-07	SYT3	synaptotagmin III [HGNC id: 11511]
SCGF-b	5,61	9,84E-09	TRMT61A	tRNA methyltransferase 61 homolog A (S. cerevisiae) [HGNC id: 23790]
SCGF-b	5,30	5,91E-08	WDFY2	WD repeat and FYVE domain containing 2 [HGNC id: 20482]
SCGF-b	4,63	1,82E-06	NRN1L	neuritin 1-like [HGNC id: 29811]
SCGF-b	4,78	8,64E-07	PROSER2	proline and serine-rich protein 2 [HGNC id: 23728]
SCGF-b	4,86	5,93E-07	C2orf74	chromosome 2 open reading frame 74 [HGNC id: 34439]
SCGF-b	5,95	1,36E-09	C12orf73	chromosome 12 open reading frame 73 [HGNC id: 34450]
SCGF-b	4,72	1,16E-06	TMEM194B	transmembrane protein 194B [HGNC id: 33700]
SDF-1a	7,50	3,13E-14	CXCL12	chemokine (C-X-C motif) ligand 12 [HGNC id: 10672]
SDF-1a	4,80	7,92E-07	NBEAL2	neurobeachin-like 2 [HGNC id: 31928]
SDF-1a	4,90	4,91E-07	MKRN2	makorin ring finger protein 2 [HGNC id: 7113]
SDF-1a	4,99	2,97E-07	SETD2	SET domain containing 2 [HGNC id: 18420]
SDF-1a	5,95	1,33E-09	C10orf54	chromosome 10 open reading frame 54 [HGNC id: 30085]
SDF-1a	4,90	4,82E-07	TSEN2	TSEN2 tRNA splicing endonuclease subunit [HGNC id: 28422]

Table A.4 (cont.)

Cytokine	Z-score	P-value	HGNC symbol	HGNC description
SDF-1a	6,06	6,85E-10	0	Aminopeptidase Q [Source:UniProtKB/Swiss-Prot;Acc:Q6Q4G3]
SDF-1a	5,61	1,01E-08	REEP3	receptor accessory protein 3 [HGNC id: 23711]
SDF-1a	5,18	1,13E-07	JMJD1C	jumonji domain containing 1C [HGNC id: 12313]
TNF-a	6,10	5,20E-10	CFH	complement factor H [HGNC id: 4883]
TNF-b	6,11	5,00E-10	CFH	complement factor H [HGNC id: 4883]
TNF-b	4,80	7,76E-07	CFHR2	complement factor H-related 2 [HGNC id: 4890]
TNF-b	4,95	3,78E-07	CFHR4	complement factor H-related 4 [HGNC id: 16979]
TRAIL	4,85	6,04E-07	C2	complement component 2 [HGNC id: 1248]
TRAIL	5,42	2,96E-08	C4A	complement component 4A (Rodgers blood group) [HGNC id: 1323]
TRAIL	7,62	1,26E-14	CFH	complement factor H [HGNC id: 4883]
TRAIL	6,53	3,23E-11	KNG1	kininogen 1 [HGNC id: 6383]
TRAIL	4,87	5,54E-07	MEP1B	meprin A, beta [HGNC id: 7020]
TRAIL	5,19	1,08E-07	SKIV2L	superkiller viralicidic activity 2-like (S. cerevisiae) [HGNC id: 10898]
TRAIL	5,15	1,32E-07	TNXB	tenascin XB [HGNC id: 11976]
TRAIL	4,91	4,67E-07	VARS	valyl-tRNA synthetase [HGNC id: 12651]
TRAIL	5,11	1,61E-07	NELFE	negative elongation factor complex member E [HGNC id: 13974]
TRAIL	6,65	1,46E-11	TNFSF10	tumor necrosis factor (ligand) superfamily, member 10 [HGNC id: 11925]
TRAIL	5,52	1,68E-08	STK19	serine/threonine kinase 19 [HGNC id: 11398]
TRAIL	4,69	1,37E-06	PPT2	palmitoyl-protein thioesterase 2 [HGNC id: 9326]
TRAIL	4,82	7,27E-07	CFHR3	complement factor H-related 3 [HGNC id: 16980]
TRAIL	5,20	9,92E-08	CRB1	crumbs homolog 1 (Drosophila) [HGNC id: 2343]
TRAIL	4,62	1,96E-06	ZNF428	zinc finger protein 428 [HGNC id: 20804]
TRAIL	5,14	1,36E-07	CADM4	cell adhesion molecule 4 [HGNC id: 30825]
VEGF	4,98	3,15E-07	SLC29A1	solute carrier family 29 (equilibrative nucleoside transporter), member 1 [HGNC id: 11003]
VEGF	4,83	6,95E-07	GRIN2B	glutamate receptor, ionotropic, N-methyl D-aspartate 2B [HGNC id: 4586]
VEGF	4,69	1,39E-06	HSP90AB1	heat shock protein 90kDa alpha (cytosolic), class B member 1 [HGNC id: 5258]
VEGF	5,14	1,38E-07	ORM1	orosomucoid 1 [HGNC id: 8498]
VEGF	5,55	1,47E-08	VEGFA	vascular endothelial growth factor A [HGNC id: 12680]
VEGF	4,97	3,43E-07	KIAA0020	KIAA0020 [HGNC id: 29676]
VEGF	5,03	2,39E-07	SLC22A7	solute carrier family 22 (organic anion transporter), member 7 [HGNC id: 10971]
VEGF	5,12	1,51E-07	CAPN11	calpain 11 [HGNC id: 1478]
VEGF	7,75	4,43E-15	ZFPM2	zinc finger protein, FOG family member 2 [HGNC id: 16700]
VEGF	4,62	1,93E-06	ZNF318	zinc finger protein 318 [HGNC id: 13578]
VEGF	7,01	1,21E-12	NRBF2	nuclear receptor binding factor 2 [HGNC id: 19692]
VEGF	7,25	2,05E-13	TMEM63B	transmembrane protein 63B [HGNC id: 17735]
VEGF	7,21	2,78E-13	MRPL14	mitochondrial ribosomal protein L14 [HGNC id: 14279]
VEGF	4,67	1,53E-06	DLK2	delta-like 2 homolog (Drosophila) [HGNC id: 21113]
VEGF	4,64	1,72E-06	ABCC10	ATP-binding cassette, sub-family C (CFTR/MRP), member 10 [HGNC id: 52]
VEGF	5,62	9,74E-09	ZFPM1	zinc finger protein, FOG family member 1 [HGNC id: 19762]
VEGF	8,16	1,65E-16	REEP3	receptor accessory protein 3 [HGNC id: 23711]
VEGF	7,68	8,11E-15	JMJD1C	jumonji domain containing 1C [HGNC id: 12313]
VEGF	7,91	1,27E-15	C6orf223	chromosome 6 open reading frame 223 [HGNC id: 28692]
VEGF	5,52	1,73E-08	CRIP3	cysteine-rich protein 3 [HGNC id: 17751]

Table A.5. TWAS-MR functional analysis. Results from inverse-variance weighted TWAS-MR analysis showing 245 significant associations between cis-eQTL's and circulating cytokine levels.

Exposure	Outcome	n_{snp}	Beta	SE	P-value	FDR-corrected p-value
IGHV4-28	bNGF	2	-0,16	0,03	3,07E-08	2,07E-04
LCMT2	bNGF	10	-0,06	0,01	2,53E-06	7,98E-03
NKTR	bNGF	4	0,10	0,02	2,51E-05	4,34E-02
FCER1A	Eotaxin	7	0,06	0,01	2,07E-05	3,80E-02
RAPGEF6	Eotaxin	3	-0,21	0,05	2,80E-05	4,51E-02
CCR1	Eotaxin	17	0,12	0,03	6,89E-06	1,67E-02
CCR3	Eotaxin	11	-0,10	0,02	3,13E-06	9,42E-03
FLT1P1	Eotaxin	7	-0,23	0,05	1,39E-06	5,12E-03
CTD-3064H18.6	Eotaxin	2	-0,31	0,06	5,86E-08	3,56E-04
FCGR2B	Eotaxin	22	0,04	0,01	1,45E-06	5,23E-03
ZNRD1	Eotaxin	6	0,10	0,02	8,17E-06	1,86E-02
ZNF573	Eotaxin	2	-0,11	0,02	4,73E-07	2,24E-03
DARC	Eotaxin	2	0,22	0,02	2,42E-19	9,78E-15
ZNF790-AS1	Eotaxin	3	-0,21	0,04	1,07E-06	4,11E-03
SNHG8	FGF-b	4	-0,09	0,02	3,27E-05	4,92E-02
IGFBP2	G-CSF	4	-0,06	0,01	3,88E-06	1,08E-02
PVR	G-CSF	2	0,27	0,04	9,76E-10	8,89E-06
RTN2	G-CSF	2	0,20	0,04	7,06E-07	2,92E-03
HLA-DRB5	G-CSF	16	-0,03	0,01	1,40E-07	7,51E-04
PPP1R37	G-CSF	3	-0,32	0,03	4,63E-21	2,41E-16
HCG22	GROa	6	0,11	0,02	5,21E-07	2,36E-03
FCER1A	GROa	10	0,07	0,02	1,09E-05	2,31E-02
RP11-453E17.1	GROa	4	-0,08	0,02	3,65E-08	2,42E-04
WDR48	GROa	13	-0,05	0,01	6,61E-07	2,77E-03
DARC	GROa	2	0,14	0,02	6,89E-11	8,37E-07
ZNF696	HGF	8	0,06	0,01	5,06E-07	2,33E-03
PDE2A	HGF	4	-0,21	0,03	3,38E-12	4,92E-08
HIP1	HGF	19	0,03	0,01	1,45E-05	2,84E-02
AIF1	IFN-g	3	-0,15	0,04	1,34E-05	2,71E-02
SKIV2L	IFN-g	5	0,18	0,02	4,49E-20	2,04E-15
IGFBP2	IFN-g	4	-0,06	0,01	1,98E-05	3,65E-02
TCEA3	IFN-g	3	0,12	0,03	5,01E-06	1,30E-02
NELFE	IFN-g	2	-0,48	0,07	2,10E-13	3,82E-09
HLA-DRB5	IFN-g	17	-0,04	0,01	2,27E-05	4,08E-02
SKIV2L	IL-10	5	0,08	0,02	3,28E-05	4,92E-02
ATL3	IL-10	3	-0,10	0,02	2,61E-05	4,37E-02
HLA-DQB1	IL-10	16	0,04	0,01	8,10E-06	1,86E-02
NELFE	IL-10	2	-0,25	0,06	2,79E-05	4,51E-02
TCEA3	IL-13	3	0,12	0,03	2,42E-05	4,24E-02
HLA-DRB1	IL-16	10	0,08	0,02	5,03E-07	2,33E-03
CHD7	IL-16	4	-0,11	0,02	1,06E-05	2,27E-02
PHOSPHO2	IL-16	10	-0,05	0,01	5,32E-06	1,36E-02
SPTBN1	IL-16	8	-0,07	0,02	5,04E-06	1,30E-02
SKIV2L	IL-17	5	0,10	0,02	6,98E-08	4,12E-04

Table A.5 (cont.)

Exposure	Outcome	n_{snp}	Beta	SE	P-value	FDR-corrected p-value
NOD2	IL-17	17	0,04	0,01	1,97E-05	3,64E-02
NELFE	IL-17	2	-0,26	0,05	3,02E-08	2,07E-04
TIGD5	IL-18	4	0,19	0,04	1,97E-06	6,53E-03
NLRC4	IL-18	3	0,78	0,12	5,16E-11	6,49E-07
AC092295.7	IL-18	5	0,13	0,03	2,51E-05	4,34E-02
FAM117B	IL-18	29	-0,04	0,01	4,16E-06	1,12E-02
NFE2L3	IL-18	5	0,12	0,02	1,31E-08	9,94E-05
HLA-DRB5	IL-18	23	0,04	0,01	4,70E-08	2,90E-04
HLA-DQA1	IL-1B	9	0,05	0,01	7,19E-07	2,94E-03
RP11-510J16.3	IL-1ra	3	0,29	0,05	5,76E-09	4,77E-05
IL1RN	IL-1ra	2	0,36	0,04	2,46E-18	8,14E-14
ABO	IL-1ra	8	0,08	0,02	2,11E-05	3,84E-02
TCEB3	IL-1ra	4	0,08	0,02	3,22E-06	9,61E-03
RARS	IL-1ra	3	-0,18	0,04	9,85E-06	2,14E-02
DDAH2	IL-1ra	4	-0,06	0,01	1,59E-05	3,04E-02
HLA-DRB5	IL-1ra	20	-0,03	0,01	2,57E-10	2,68E-06
MRPL33	IL-2	2	0,22	0,05	3,36E-05	4,99E-02
HLA-S	IL-2	8	0,09	0,02	2,54E-06	7,98E-03
SSPO	IL-2	8	0,07	0,02	4,25E-06	1,13E-02
HLA-DRB5	IL-2	15	-0,04	0,01	1,22E-08	9,46E-05
TAGAP	IL-2ra	2	-0,19	0,04	1,61E-06	5,53E-03
HLA-DQA2	IL-2ra	11	0,06	0,01	1,59E-08	1,18E-04
SPTLC2	IL-2ra	8	0,07	0,02	5,50E-06	1,37E-02
MICA	IL-2ra	14	0,06	0,01	4,08E-06	1,11E-02
NELFE	IL-2ra	2	-0,21	0,05	2,86E-05	4,58E-02
HTATIP2	IL-2ra	11	0,07	0,02	1,05E-05	2,26E-02
HLA-DRB5	IL-2ra	16	-0,05	0,01	5,58E-07	2,45E-03
SKIV2L	IL-4	5	0,11	0,02	4,32E-08	2,76E-04
NELFE	IL-4	2	-0,28	0,07	3,19E-05	4,84E-02
HLA-DRB5	IL-4	17	-0,03	0,01	8,61E-06	1,94E-02
NOD2	IL-5	17	0,04	0,01	1,10E-05	2,31E-02
HLA-C	IL-6	24	-0,03	0,01	1,73E-06	5,87E-03
ALOX15	IL-6	5	-0,07	0,02	1,75E-05	3,29E-02
HLA-S	IL-6	9	0,07	0,01	1,59E-06	5,53E-03
AKIP1	IL-6	13	-0,04	0,01	3,19E-05	4,84E-02
HLA-DRB5	IL-6	20	-0,03	0,01	2,21E-07	1,12E-03
SKIV2L	IL-7	5	0,09	0,02	9,51E-06	2,08E-02
SYK	IL-7	12	-0,06	0,01	2,89E-05	4,58E-02
NCOR1	IL-8	2	-0,11	0,02	2,30E-08	1,64E-04
TNXB	IL-8	3	-0,11	0,03	3,05E-05	4,74E-02
CXCR1	IL-8	7	-0,07	0,02	5,38E-06	1,36E-02
LSMD1	IL-8	6	0,09	0,02	2,97E-05	4,65E-02
CASC3	IL-8	6	-0,10	0,02	2,16E-05	3,90E-02
CENPV	IL-8	6	-0,07	0,02	1,56E-05	3,00E-02
DARC	IL-8	2	0,22	0,02	3,51E-21	2,13E-16

Table A.5 (cont.)

Exposure	Outcome	n_{snp}	Beta	SE	P-value	FDR-corrected p-value
RP11-378A13.1	IL-8	12	-0,07	0,01	9,94E-08	5,57E-04
PLCL2	IL-8	9	0,05	0,01	2,58E-05	4,37E-02
UQCC	IL-8	12	-0,05	0,01	7,71E-06	1,81E-02
MED24	IL-8	2	0,24	0,04	3,09E-09	2,61E-05
NELFE	IL-8	3	-0,23	0,05	3,75E-06	1,08E-02
PNKD	IL-8	11	-0,07	0,01	9,68E-08	5,51E-04
LCMT2	IL-8	10	-0,07	0,01	1,37E-07	7,51E-04
HLA-DQA1	IL-8	12	0,04	0,01	3,08E-05	4,75E-02
ASAP3	IL-9	2	0,21	0,05	2,74E-05	4,48E-02
SMAD5	IL-9	17	0,11	0,01	1,82E-14	4,41E-10
TYK2	IP-10	5	-0,14	0,03	3,93E-07	1,91E-03
ATF6B	IP-10	3	0,17	0,04	1,70E-05	3,21E-02
TRAFD1	IP-10	2	0,94	0,06	7,42E-55	1,35E-49
NEU1	IP-10	2	-0,28	0,05	8,23E-09	6,66E-05
FKBPL	IP-10	3	-0,23	0,05	2,67E-05	4,42E-02
WRB	IP-10	11	-0,05	0,01	2,68E-05	4,42E-02
LCMT2	IP-10	10	-0,07	0,02	1,46E-05	2,84E-02
KLRC3	M-CSF	14	0,04	0,01	2,63E-05	4,37E-02
RP11-627G23.1	M-CSF	4	-0,12	0,02	2,50E-10	2,68E-06
KANSL1-AS1	M-CSF	11	-0,04	0,01	2,92E-06	8,94E-03
FAM69A	M-CSF	3	0,05	0,01	5,79E-07	2,48E-03
CDC42SE2	M-CSF	7	0,05	0,01	2,96E-05	4,64E-02
ASB16-AS1	M-CSF	13	0,06	0,01	1,27E-05	2,59E-02
CSF1R	M-CSF	5	0,21	0,03	3,14E-13	5,20E-09
HMGXB3	M-CSF	2	-0,18	0,03	3,52E-13	5,57E-09
RP3-473L9.4	M-CSF	2	-0,21	0,05	6,42E-06	1,58E-02
TIRAP	M-CSF	2	0,23	0,05	3,88E-06	1,08E-02
MGAT5	M-CSF	4	-0,18	0,04	1,60E-06	5,53E-03
KIRREL3	M-CSF	3	0,18	0,04	4,53E-07	2,17E-03
RP11-704M14.1	M-CSF	4	0,10	0,02	2,73E-05	4,48E-02
AURKB	M-CSF	2	0,15	0,03	8,05E-07	3,26E-03
UBE2O	M-CSF	2	0,15	0,03	9,37E-06	2,06E-02
B3GAT1	M-CSF	6	-0,09	0,01	2,45E-09	2,13E-05
FCHO1	MCP-1	5	-0,08	0,02	3,27E-05	4,92E-02
KIAA0101	MCP-1	2	0,11	0,03	2,55E-05	4,37E-02
FCER1A	MCP-1	10	0,12	0,02	9,86E-07	3,86E-03
KDELR2	MCP-1	20	0,03	0,01	1,69E-05	3,20E-02
DARC	MCP-1	2	0,37	0,02	1,19E-75	4,33E-70
FLT1P1	MCP-1	7	-0,20	0,02	3,57E-18	1,08E-13
NOTCH4	MCP-1	4	0,21	0,04	1,09E-08	8,67E-05
CCR2	MCP-1	4	-0,27	0,04	5,49E-10	5,13E-06
FCER1A	MCP-3	4	-0,10	0,02	1,64E-07	8,54E-04
TRAFD1	MCP-3	2	0,41	0,06	9,09E-11	1,03E-06
SKIV2L	MCP-3	4	0,11	0,02	7,08E-06	1,70E-02
MADD	MCP-3	5	0,06	0,01	1,41E-05	2,83E-02

Table A.5 (cont.)

Exposure	Outcome	n_{snp}	Beta	SE	P-value	FDR-corrected p-value
DARC	MCP-3	2	-0,36	0,03	4,74E-30	4,32E-25
DDT	MIF	16	-0,05	0,01	1,65E-05	3,14E-02
TIGD5	MIF	4	0,14	0,02	4,12E-10	4,05E-06
AP000350.4	MIF	7	-0,15	0,02	1,16E-13	2,35E-09
AP000351.10	MIF	6	-0,13	0,02	1,92E-08	1,40E-04
GSTT1	MIF	14	-0,05	0,01	8,10E-06	1,86E-02
ATF6B	MIG	3	0,13	0,03	2,35E-05	4,16E-02
CCR1	MIG	17	0,06	0,01	3,12E-05	4,80E-02
TRAFD1	MIG	2	0,78	0,06	5,81E-38	7,05E-33
FKBPL	MIG	3	-0,24	0,05	1,01E-05	2,17E-02
RNF5	MIG	5	-0,18	0,04	1,23E-06	4,61E-03
C4B	MIG	6	0,06	0,01	2,74E-07	1,37E-03
PTPN11	MIG	2	-0,21	0,05	2,33E-05	4,16E-02
MAP3K5	MIG	2	-0,12	0,03	3,79E-06	1,08E-02
C4A	MIG	6	-0,06	0,01	5,31E-07	2,36E-03
DHCR24	MIG	3	-0,11	0,02	2,69E-06	8,30E-03
RP11-128A6.2	MIG	2	-0,38	0,08	3,97E-06	1,10E-02
FCRL3	MIP-1a	16	0,04	0,01	6,98E-06	1,68E-02
CCL4	MIP-1a	4	0,41	0,06	2,96E-13	5,13E-09
HLA-DQA2	MIP-1a	15	0,04	0,01	2,54E-06	7,98E-03
MSH5	MIP-1a	3	-0,29	0,06	1,22E-06	4,61E-03
MAP3K8	MIP-1a	5	0,11	0,02	7,77E-06	1,81E-02
LY6G5C	MIP-1a	11	-0,09	0,02	1,49E-05	2,90E-02
EML4	MIP-1a	9	0,05	0,01	1,84E-05	3,43E-02
PRDX1	MIP-1a	4	0,08	0,02	2,56E-05	4,37E-02
FAM114A1	MIP-1a	2	0,15	0,03	1,42E-05	2,83E-02
HLA-DRB5	MIP-1a	20	-0,03	0,01	1,11E-05	2,33E-02
GZMB	MIP-1b	6	0,11	0,02	9,25E-06	2,04E-02
CCL4L2	MIP-1b	4	1,23	0,11	8,59E-29	6,26E-24
RP11-981P6.1	MIP-1b	3	0,15	0,03	8,90E-06	1,98E-02
ACTA2	MIP-1b	26	-0,05	0,01	1,30E-06	4,84E-03
AC069363.1	MIP-1b	2	-0,25	0,03	4,92E-16	1,28E-11
MLF1IP	MIP-1b	4	-0,12	0,03	8,04E-06	1,86E-02
NDUFAF3	MIP-1b	2	0,21	0,05	1,16E-05	2,39E-02
TOX	MIP-1b	5	0,17	0,04	8,25E-06	1,87E-02
IP6K2	MIP-1b	6	-0,19	0,03	8,12E-12	1,10E-07
FAM114A1	MIP-1b	2	0,30	0,06	1,39E-07	7,51E-04
TEN1-CDK3	MIP-1b	3	-0,12	0,03	2,88E-05	4,58E-02
GS1-124K5.3	PDGFbb	2	0,37	0,09	2,91E-05	4,59E-02
TMEM194B	PDGFbb	6	0,06	0,01	1,41E-05	2,83E-02
LINC00304	PDGFbb	3	0,13	0,03	6,15E-06	1,53E-02
SERPINE2	PDGFbb	12	-0,08	0,01	1,85E-13	3,56E-09
TRIM5	PDGFbb	9	0,05	0,01	3,00E-05	4,67E-02
AC034220.3	PDGFbb	4	-0,08	0,02	5,68E-07	2,47E-03
RABGEF1	PDGFbb	6	-0,08	0,02	6,72E-06	1,64E-02

Table A.5 (cont.)

Exposure	Outcome	n_{snp}	Beta	SE	P-value	FDR-corrected p-value
SLC8A3	PDGFbb	3	-0,14	0,02	7,89E-11	9,28E-07
TRIM8	PDGFbb	5	0,14	0,03	3,56E-06	1,04E-02
RP11-18I14.7	PDGFbb	8	-0,09	0,01	2,83E-10	2,87E-06
JAK2	PDGFbb	4	-0,08	0,02	3,36E-05	4,99E-02
BTBD6	PDGFbb	5	-0,11	0,02	4,70E-08	2,90E-04
HABP4	PDGFbb	2	-0,13	0,03	1,13E-05	2,36E-02
ELOVL7	PDGFbb	2	0,11	0,02	4,31E-06	1,13E-02
LCMT2	PDGFbb	10	-0,06	0,01	3,83E-06	1,08E-02
AL133216.1	RANTES	2	-0,45	0,07	4,83E-12	6,77E-08
ADHFE1	RANTES	25	0,03	0,01	2,39E-05	4,20E-02
AC069363.1	RANTES	2	-0,17	0,03	2,23E-09	1,98E-05
GNAI1	RANTES	3	-0,22	0,05	3,16E-05	4,83E-02
HSD17B7P2	RANTES	6	-0,13	0,02	1,13E-13	2,35E-09
LILRA5	SCF	5	-0,11	0,01	1,24E-18	4,50E-14
IFT46	SCF	2	-0,14	0,03	5,35E-06	1,36E-02
AC008984.7	SCF	3	-0,15	0,02	1,46E-12	2,22E-08
ABO	SCF	8	0,14	0,03	4,28E-06	1,13E-02
DDX39B	SCF	3	-0,14	0,03	1,04E-06	4,03E-03
BCKDHA	SCF	2	0,11	0,02	2,17E-06	7,05E-03
DOCK7	SCF	2	-0,13	0,03	3,55E-06	1,04E-02
SPPL3	SCF	3	0,10	0,02	1,56E-06	5,53E-03
ACD	SCF	2	-0,31	0,05	2,11E-10	2,33E-06
ADAL	SCF	4	0,14	0,02	4,74E-10	4,55E-06
PRMT7	SCF	4	0,14	0,03	5,49E-06	1,37E-02
LILRA3	SCF	11	-0,05	0,01	5,26E-07	2,36E-03
PRAM1	SCF	2	0,12	0,03	2,48E-05	4,33E-02
STARD10	SCF	7	-0,06	0,01	8,32E-07	3,33E-03
SURF6	SCF	4	-0,06	0,01	4,27E-06	1,13E-02
LCAT	SCF	4	0,24	0,03	2,07E-17	5,81E-13
DPEP3	SCF	7	-0,15	0,03	1,62E-07	8,54E-04
WDFY2	SCGF-b	10	0,07	0,02	2,30E-06	7,40E-03
MFSD6	SCGF-b	15	0,05	0,01	1,74E-06	5,87E-03
ABTB1	SCGF-b	8	-0,07	0,01	6,32E-07	2,68E-03
KCTD11	SCGF-b	2	0,11	0,02	4,01E-06	1,10E-02
HIATL1	SCGF-b	14	-0,05	0,01	7,34E-06	1,75E-02
DECR2	SCGF-b	8	0,10	0,02	3,01E-08	2,07E-04
NPDC1	SCGF-b	4	-0,08	0,02	2,16E-06	7,05E-03
MARK3	SCGF-b	9	-0,11	0,02	4,14E-08	2,69E-04
AL359314.1	SCGF-b	2	-0,16	0,03	3,00E-06	9,10E-03
SIGLEC16	SCGF-b	3	-0,12	0,03	7,64E-06	1,81E-02
POU5F1P6	SCGF-b	5	-0,12	0,02	1,42E-06	5,16E-03
MEF2C	SCGF-b	5	-0,22	0,05	2,57E-05	4,37E-02
CTSG	SCGF-b	10	0,09	0,01	9,16E-14	2,09E-09
CTD-3018O17.3	SCGF-b	5	0,09	0,02	8,74E-06	1,95E-02
TNPO1	SCGF-b	2	0,33	0,08	2,61E-05	4,37E-02

Table A.5 (cont.)

Exposure	Outcome	n_{snp}	Beta	SE	P-value	FDR-corrected p-value
MAP3K5	SCGF-b	2	-0,11	0,03	2,35E-05	4,16E-02
AC016747.3	SCGF-b	4	0,15	0,03	8,08E-08	4,67E-04
LCAT	SCGF-b	4	0,17	0,03	7,02E-08	4,12E-04
ASB16-AS1	SDF-1a	11	0,07	0,02	1,46E-05	2,84E-02
MAP3K8	SDF-1a	5	0,12	0,03	1,17E-05	2,41E-02
PHF11	SDF-1a	9	-0,09	0,02	2,65E-06	8,26E-03
SND1	SDF-1a	2	0,12	0,03	2,79E-05	4,51E-02
DPP4	SDF-1a	2	0,30	0,06	3,70E-06	1,07E-02
SKIV2L	TNF-a	5	0,10	0,02	9,44E-07	3,74E-03
BET1L	TNF-b	3	0,08	0,02	1,45E-05	2,84E-02
TRAFD1	TNF-b	2	0,32	0,06	2,81E-07	1,39E-03
SKIV2L	TNF-b	4	0,10	0,02	3,44E-06	1,02E-02
STK19P	TNF-b	3	0,25	0,05	1,83E-06	6,11E-03
SKIV2L	TRAIL	5	0,09	0,02	1,66E-07	8,54E-04
TNFSF10	TRAIL	2	0,12	0,03	2,59E-05	4,37E-02
NELFE	TRAIL	3	-0,23	0,05	2,89E-05	4,58E-02
HLA-DQA1	TRAIL	12	0,04	0,01	1,77E-05	3,31E-02
SIRT1	VEGF	6	0,06	0,01	1,25E-05	2,55E-02
ORM2	VEGF	8	0,06	0,01	1,57E-06	5,53E-03
VEGFA	VEGF	6	0,19	0,03	1,16E-11	1,50E-07
ENPP5	VEGF	2	0,16	0,04	2,14E-05	3,87E-02

Table A.6. Cytokine interconnections MR analysis. Cross-cytokine inverse-variance weighted MR analysis showing 65 significant associations between cis-variants and circulating cytokine levels.

Exposure	Outcome	LDSC R^2	LDSC p-value	MR Beta	MR FDR-corrected p-value	MR log-transformed, FDR-corrected p-value
GROa	bNGF	0,02	9,40E-01	-0,04	0,020	1,7
SCGFb	bNGF	0,36	1,21E-01	0,07	0,020	1,7
TNF-b	bNGF	0,46	2,41E-01	0,61	0,000	8,1
MIP1a	FGF-b	0,15	3,85E-01	0,13	0,013	1,9
IL-9	GROa	0,30	1,21E-02	0,34	0,000	5,5
TNF-b	GROa	0,30	1,66E-02	0,34	0,002	2,7
VEGF	GROa	0,63	2,01E-02	0,04	0,017	1,8
G-CSF	HGF	n/a	n/a	0,86	0,028	1,6
IL-1ra	HGF	0,37	8,54E-02	-0,09	0,003	2,6
VEGF	HGF	0,51	1,95E-02	0,05	0,006	2,2
G-CSF	IL-16	n/a	n/a	0,57	0,001	3,3
TNF-b	IL-16	0,25	5,75E-02	0,31	0,018	1,8
G-CSF	IL-18	0,20	9,40E-01	0,70	0,023	1,6
G-CSF	IL-1ra	n/a	n/a	0,58	0,025	1,6
TNF-b	IL-1ra	0,29	2,43E-01	0,33	0,004	2,4
VEGF	IL-1ra	0,31	2,63E-01	0,05	0,039	1,4
TNF-b	IL-2ra	0,99	9,52E-04	0,70	0,000	8,5
G-CSF	IL-8	n/a	n/a	-0,91	0,000	6,8
VEGF	IL-8	0,53	2,40E-02	0,06	0,004	2,4
IL-1ra	IL-9	0,20	1,45E-01	-0,07	0,037	1,4
TNF-b	IL-9	0,66	8,11E-09	0,62	0,000	6,7
SDF-1a	IP-10	0,37	7,15E-05	0,20	0,003	2,5
Eotaxin	MCP-1	0,38	1,84E-06	0,24	0,000	3,3
MIF	MCP-1	n/a	n/a	0,19	0,032	1,5
VEGF	MCP-1	0,22	2,51E-01	0,04	0,032	1,5
Eotaxin	MCP-3	0,38	9,58E-04	1,37	0,021	1,7
IL-1ra	MCP-3	0,15	3,11E-01	-0,09	0,006	2,2
IL-9	MCP-3	0,70	6,09E-07	0,36	0,000	3,6
TNF-b	MCP-3	0,77	3,70E-09	0,92	0,000	14,0
VEGF	MCP-3	1,23	4,81E-02	0,07	0,006	2,2
GROa	M-CSF	0,02	8,54E-01	-0,03	0,035	1,5
IL-2ra	M-CSF	0,29	1,41E-01	-0,12	0,035	1,5
VEGF	M-CSF	-0,10	6,26E-01	0,05	0,023	1,6
SDF-1a	MIG	0,29	7,86E-03	0,18	0,007	2,2
TNF-b	MIG	0,51	1,29E-04	0,41	0,003	2,6
G-CSF	MIP1a	n/a	n/a	0,62	0,000	4,2
HGF	MIP1a	0,40	1,88E-04	0,14	0,041	1,4
IL-1ra	MIP1a	0,29	2,11E-01	-0,10	0,000	5,0
TNF-b	MIP1a	0,51	4,04E-04	0,75	0,000	14,4
G-CSF	MIP1b	n/a	n/a	0,99	0,000	4,4
IL-18	MIP1b	0,68	9,71E-02	0,28	0,034	1,5
RANTES	MIP1b	0,25	4,80E-01	0,50	0,010	2,0
IL-9	PDGFbb	0,37	3,15E-05	0,28	0,000	3,8
MIP1a	PDGFbb	0,25	1,29E-02	0,07	0,032	1,5

Table A.6 (cont.)

Exposure	Outcome	LDSC R^2	LDSC p-value	MR Beta	MR FDR-corrected p-value	MR log-transformed, FDR-corrected p-value
HGF	RANTES	0,14	9,68E-02	0,22	0,019	1,7
IL-2ra	RANTES	0,15	4,49E-01	0,14	0,035	1,5
IL-9	RANTES	0,32	8,77E-03	0,42	0,000	6,0
SDF-1a	RANTES	0,28	4,33E-02	0,15	0,035	1,5
VEGF	RANTES	0,61	4,07E-02	0,06	0,035	1,5
TNF-b	SCGFb	0,35	4,10E-03	0,80	0,000	11,4
IL-9	SDF-1a	0,50	9,32E-07	0,28	0,003	2,6
IL-1ra	TNF-a	0,29	1,83E-01	-0,11	0,000	3,9
IL-9	TNF-a	0,80	2,95E-24	0,32	0,000	3,5
MCP-3	TNF-a	0,93	9,79E-16	0,03	0,046	1,3
TNF-b	TNF-a	0,96	7,49E-39	0,71	0,000	8,6
VEGF	TNF-a	0,98	1,12E-02	0,08	0,001	3,3
IL-1ra	TNF-b	0,29	2,43E-01	-0,10	0,013	1,9
MCP-3	TNF-b	0,77	3,70E-09	0,06	0,021	1,7
MCP-3	TRAIL	0,68	2,53E-03	0,04	0,008	2,1
TNF-b	TRAIL	0,59	5,29E-03	0,63	0,000	10,6
GROa	VEGF	0,63	2,01E-02	-0,03	0,026	1,6
IL-1ra	VEGF	0,31	2,63E-01	-0,05	0,034	1,5
IL-9	VEGF	0,70	3,79E-02	0,17	0,034	1,5
RANTES	VEGF	0,61	4,07E-02	0,11	0,006	2,2
TNF-b	VEGF	0,88	1,41E-01	0,34	0,002	2,6

Table A.7. Drug-target two-sample MR analysis. Drug-target inverse-variance weighted MR analysis showing 24 significant associations between cis-variants and allergic and Autoimmune, cardiometabolic, and cancer outcomes.

Disease group	Exposure	Outcome	n_{snp}	Beta	SE	P-value	FDR-corrected p-value
Autoimmune	Eotaxin	Asthma	10	0,02	0,05	7,59E-01	8,77E-01
Autoimmune	FGF-b	Asthma	41	0,06	0,02	**1,84E-02**	1,24E-01
Autoimmune	G-CSF	Asthma	2	1,71	0,47	2,91E-04	**9,33E-03**
Autoimmune	GROa	Asthma	45	-0,03	0,01	**1,99E-02**	1,29E-01
Autoimmune	HGF	Asthma	9	0,01	0,05	8,51E-01	9,40E-01
Autoimmune	IL-16	Asthma	44	0,02	0,01	1,69E-01	4,18E-01
Autoimmune	IL-18	Asthma	8	0,05	0,06	4,38E-01	6,45E-01
Autoimmune	IL-1ra	Asthma	29	-0,04	0,02	6,05E-02	2,55E-01
Autoimmune	IL-2ra	Asthma	12	0,00	0,05	9,78E-01	9,78E-01
Autoimmune	IL-8	Asthma	3	0,02	0,16	8,89E-01	9,53E-01
Autoimmune	IL-9	Asthma	8	0,04	0,05	4,50E-01	6,45E-01
Autoimmune	IP-10	Asthma	4	-0,11	0,07	1,15E-01	3,58E-01
Autoimmune	M-CSF	Asthma	4	0,13	0,07	8,66E-02	3,15E-01
Autoimmune	MCP-1	Asthma	3	-0,17	0,17	3,24E-01	5,87E-01
Autoimmune	MCP-3	Asthma	39	0,01	0,01	3,58E-01	5,87E-01
Autoimmune	MIF	Asthma	6	0,05	0,07	5,06E-01	6,91E-01
Autoimmune	MIG	Asthma	8	0,07	0,06	2,24E-01	4,76E-01
Autoimmune	MIP-1a	Asthma	27	0,00	0,02	9,76E-01	9,78E-01
Autoimmune	MIP-1b	Asthma	15	0,01	0,03	6,27E-01	7,72E-01
Autoimmune	RANTES	Asthma	11	0,06	0,03	**4,88E-02**	2,35E-01
Autoimmune	SCGF-b	Asthma	22	-0,03	0,02	1,06E-01	3,42E-01
Autoimmune	SDF-1a	Asthma	15	-0,01	0,05	9,08E-01	9,53E-01
Autoimmune	TNF-b	Asthma	4	0,21	0,30	4,81E-01	6,69E-01
Autoimmune	TRAIL	Asthma	5	0,04	0,08	6,06E-01	7,59E-01
Autoimmune	VEGF	Asthma	52	0,02	0,02	2,11E-01	4,74E-01
Autoimmune	Eotaxin	Crohn's disease	11	-0,13	0,36	7,13E-01	8,44E-01
Autoimmune	FGF-b	Crohn's disease	48	0,08	0,07	2,37E-01	4,89E-01
Autoimmune	G-CSF	Crohn's disease	2	-2,64	0,79	8,16E-04	**1,52E-02**
Autoimmune	GROa	Crohn's disease	57	-0,06	0,04	2,13E-01	4,74E-01
Autoimmune	HGF	Crohn's disease	12	0,13	0,20	5,03E-01	6,91E-01
Autoimmune	IL-16	Crohn's disease	58	0,05	0,06	3,35E-01	5,87E-01
Autoimmune	IL-18	Crohn's disease	8	0,21	0,25	4,02E-01	6,11E-01
Autoimmune	IL-1ra	Crohn's disease	33	-0,24	0,08	2,88E-03	**2,68E-02**
Autoimmune	IL-2ra	Crohn's disease	14	0,64	0,17	1,45E-04	**7,19E-03**
Autoimmune	IL-8	Crohn's disease	3	0,09	0,42	8,29E-01	9,29E-01
Autoimmune	IL-9	Crohn's disease	8	-0,34	0,35	3,33E-01	5,87E-01
Autoimmune	IP-10	Crohn's disease	8	-0,67	0,22	2,10E-03	**2,24E-02**
Autoimmune	M-CSF	Crohn's disease	4	0,49	0,36	1,74E-01	4,18E-01
Autoimmune	MCP-1	Crohn's disease	3	-3,43	1,53	**2,48E-02**	1,31E-01
Autoimmune	MCP-3	Crohn's disease	51	-0,06	0,07	3,58E-01	5,87E-01
Autoimmune	MIF	Crohn's disease	6	0,06	0,33	8,52E-01	9,40E-01
Autoimmune	MIG	Crohn's disease	8	0,78	0,26	2,74E-03	**2,68E-02**
Autoimmune	MIP-1a	Crohn's disease	33	-0,11	0,09	2,45E-01	4,93E-01

Table A.7 (cont.)

Disease group	Exposure	Outcome	n_{snp}	Beta	SE	P-value	FDR-corrected p-value
Autoimmune	MIP-1b	Crohn's disease	20	-0,13	0,12	2,65E-01	5,26E-01
Autoimmune	RANTES	Crohn's disease	12	0,09	0,15	5,28E-01	6,96E-01
Autoimmune	SCGF-b	Crohn's disease	27	-0,11	0,08	1,56E-01	4,07E-01
Autoimmune	SDF-1a	Crohn's disease	17	0,57	0,18	1,37E-03	**2,24E-02**
Autoimmune	TNF-b	Crohn's disease	2	0,46	0,64	4,71E-01	6,68E-01
Autoimmune	TRAIL	Crohn's disease	6	-0,45	0,17	**7,46E-03**	5,56E-02
Autoimmune	VEGF	Crohn's disease	64	0,03	0,07	6,25E-01	7,72E-01
Autoimmune	Eotaxin	Multiple sclerosis	10	-0,01	0,21	9,62E-01	9,77E-01
Autoimmune	FGF-b	Multiple sclerosis	34	-0,05	0,05	2,87E-01	5,58E-01
Autoimmune	G-CSF	Multiple sclerosis	2	-0,47	0,62	4,46E-01	6,45E-01
Autoimmune	GROa	Multiple sclerosis	33	-0,02	0,04	5,41E-01	7,07E-01
Autoimmune	HGF	Multiple sclerosis	11	-0,25	0,17	1,33E-01	3,83E-01
Autoimmune	IL-16	Multiple sclerosis	44	0,04	0,05	4,48E-01	6,45E-01
Autoimmune	IL-18	Multiple sclerosis	6	-0,19	0,21	3,53E-01	5,87E-01
Autoimmune	IL-1ra	Multiple sclerosis	30	-0,16	0,07	**2,42E-02**	1,31E-01
Autoimmune	IL-2ra	Multiple sclerosis	13	2,11	0,45	2,47E-06	**3,68E-04**
Autoimmune	IL-8	Multiple sclerosis	3	0,73	0,44	1,01E-01	3,35E-01
Autoimmune	IL-9	Multiple sclerosis	6	0,02	0,24	9,49E-01	9,75E-01
Autoimmune	IP-10	Multiple sclerosis	7	0,42	0,17	**1,09E-02**	7,72E-02
Autoimmune	M-CSF	Multiple sclerosis	4	0,88	0,39	**2,18E-02**	1,31E-01
Autoimmune	MCP-1	Multiple sclerosis	2	0,64	0,47	1,77E-01	4,18E-01
Autoimmune	MCP-3	Multiple sclerosis	50	-0,09	0,05	**4,71E-02**	2,34E-01
Autoimmune	MIF	Multiple sclerosis	5	-0,24	0,29	4,02E-01	6,11E-01
Autoimmune	MIG	Multiple sclerosis	7	-0,19	0,21	3,60E-01	5,87E-01
Autoimmune	MIP-1a	Multiple sclerosis	25	0,00	0,07	9,64E-01	9,77E-01
Autoimmune	MIP-1b	Multiple sclerosis	16	0,10	0,10	3,48E-01	5,87E-01
Autoimmune	RANTES	Multiple sclerosis	10	-0,43	0,12	3,92E-04	**9,74E-03**
Autoimmune	SCGF-b	Multiple sclerosis	23	0,05	0,05	3,61E-01	5,87E-01
Autoimmune	SDF-1a	Multiple sclerosis	17	-0,28	0,15	6,13E-02	2,55E-01
Autoimmune	TNF-b	Multiple sclerosis	4	-2,18	0,60	3,13E-04	**9,33E-03**
Autoimmune	TRAIL	Multiple sclerosis	6	0,18	0,12	1,34E-01	3,83E-01
Autoimmune	VEGF	Multiple sclerosis	59	-0,05	0,05	3,62E-01	5,87E-01
Autoimmune	Eotaxin	Psoriasis	11	0,08	0,20	6,83E-01	8,27E-01
Autoimmune	FGF-b	Psoriasis	48	0,15	0,05	5,55E-03	**4,60E-02**
Autoimmune	G-CSF	Psoriasis	2	-0,89	0,50	7,22E-02	2,76E-01
Autoimmune	GROa	Psoriasis	57	-0,06	0,04	1,11E-01	3,53E-01
Autoimmune	HGF	Psoriasis	12	-0,13	0,16	3,98E-01	6,11E-01
Autoimmune	IL-16	Psoriasis	57	0,07	0,04	8,96E-02	3,18E-01
Autoimmune	IL-18	Psoriasis	8	0,94	0,22	2,35E-05	**1,75E-03**
Autoimmune	IL-1ra	Psoriasis	33	0,02	0,09	8,27E-01	9,29E-01
Autoimmune	IL-2ra	Psoriasis	13	-0,13	0,16	4,21E-01	6,27E-01
Autoimmune	IL-8	Psoriasis	3	0,74	0,55	1,81E-01	4,21E-01
Autoimmune	IL-9	Psoriasis	7	-0,12	0,26	6,57E-01	8,02E-01
Autoimmune	IP-10	Psoriasis	8	-0,47	0,21	**2,56E-02**	1,31E-01
Autoimmune	M-CSF	Psoriasis	4	-0,08	0,34	8,03E-01	9,13E-01

Table A.7 (cont.)

Disease group	Exposure	Outcome	n_{snp}	Beta	SE	P-value	FDR-corrected p-value
Autoimmune	MCP-1	Psoriasis	3	-0,09	0,51	8,66E-01	9,48E-01
Autoimmune	MCP-3	Psoriasis	49	0,06	0,04	1,51E-01	4,03E-01
Autoimmune	MIF	Psoriasis	4	0,53	0,35	1,30E-01	3,83E-01
Autoimmune	MIG	Psoriasis	8	0,43	0,32	1,76E-01	4,18E-01
Autoimmune	MIP-1a	Psoriasis	28	-0,11	0,08	1,64E-01	4,18E-01
Autoimmune	MIP-1b	Psoriasis	16	-0,01	0,11	9,45E-01	9,75E-01
Autoimmune	RANTES	Psoriasis	12	-0,23	0,12	5,39E-02	2,51E-01
Autoimmune	SCGF-b	Psoriasis	27	-0,10	0,06	8,43E-02	3,14E-01
Autoimmune	SDF-1a	Psoriasis	17	0,50	0,16	1,61E-03	**2,24E-02**
Autoimmune	TNF-b	Psoriasis	4	2,10	2,49	3,98E-01	6,11E-01
Autoimmune	TRAIL	Psoriasis	6	-0,25	0,17	1,37E-01	3,83E-01
Autoimmune	VEGF	Psoriasis	63	-0,12	0,05	**7,26E-03**	5,56E-02
Autoimmune	Eotaxin	Rheumatoid arteritis	9	0,02	0,15	8,92E-01	9,53E-01
Autoimmune	FGF-b	Rheumatoid arteritis	35	0,04	0,06	4,75E-01	6,68E-01
Autoimmune	GROa	Rheumatoid arteritis	22	0,01	0,08	9,02E-01	9,53E-01
Autoimmune	HGF	Rheumatoid arteritis	10	-0,05	0,18	7,92E-01	9,07E-01
Autoimmune	IL-16	Rheumatoid arteritis	28	0,12	0,07	1,01E-01	3,35E-01
Autoimmune	IL-18	Rheumatoid arteritis	4	0,39	0,28	1,74E-01	4,18E-01
Autoimmune	IL-1ra	Rheumatoid arteritis	28	-0,29	0,08	5,39E-04	**1,15E-02**
Autoimmune	IL-2ra	Rheumatoid arteritis	13	0,08	0,25	7,34E-01	8,61E-01
Autoimmune	IL-8	Rheumatoid arteritis	3	0,56	0,38	1,42E-01	3,84E-01
Autoimmune	IL-9	Rheumatoid arteritis	5	-0,12	0,32	7,06E-01	8,41E-01
Autoimmune	IP-10	Rheumatoid arteritis	4	0,40	0,48	4,06E-01	6,12E-01
Autoimmune	M-CSF	Rheumatoid arteritis	4	0,52	0,50	2,95E-01	5,63E-01
Autoimmune	MCP-1	Rheumatoid arteritis	2	-0,15	0,50	7,55E-01	8,77E-01
Autoimmune	MCP-3	Rheumatoid arteritis	37	-0,02	0,04	5,60E-01	7,17E-01
Autoimmune	MIF	Rheumatoid arteritis	2	0,24	0,63	7,03E-01	8,41E-01
Autoimmune	MIG	Rheumatoid arteritis	7	-0,53	0,28	6,42E-02	2,55E-01
Autoimmune	MIP-1a	Rheumatoid arteritis	14	0,11	0,10	2,88E-01	5,58E-01
Autoimmune	MIP-1b	Rheumatoid arteritis	9	-0,07	0,12	5,55E-01	7,17E-01
Autoimmune	RANTES	Rheumatoid arteritis	8	-0,02	0,14	8,91E-01	9,53E-01
Autoimmune	SCGF-b	Rheumatoid arteritis	18	-0,06	0,10	5,20E-01	6,96E-01
Autoimmune	SDF-1a	Rheumatoid arteritis	14	-0,08	0,14	5,85E-01	7,38E-01
Autoimmune	TNF-b	Rheumatoid arteritis	4	3,11	1,63	5,57E-02	2,52E-01
Autoimmune	TRAIL	Rheumatoid arteritis	5	-0,16	0,17	3,64E-01	5,87E-01
Autoimmune	VEGF	Rheumatoid arteritis	39	-0,09	0,05	6,18E-02	2,55E-01
Autoimmune	Eotaxin	Ulcerative colitis	11	-0,29	0,19	1,37E-01	3,83E-01
Autoimmune	FGF-b	Ulcerative colitis	48	0,08	0,07	2,16E-01	4,74E-01
Autoimmune	G-CSF	Ulcerative colitis	2	-2,80	1,24	**2,34E-02**	1,31E-01
Autoimmune	GROa	Ulcerative colitis	57	-0,06	0,05	2,32E-01	4,88E-01
Autoimmune	HGF	Ulcerative colitis	12	0,12	0,18	5,16E-01	6,96E-01
Autoimmune	IL-16	Ulcerative colitis	58	-0,05	0,05	3,55E-01	5,87E-01
Autoimmune	IL-18	Ulcerative colitis	8	0,84	0,29	3,82E-03	**3,35E-02**
Autoimmune	IL-1ra	Ulcerative colitis	33	-0,14	0,07	6,50E-02	2,55E-01
Autoimmune	IL-2ra	Ulcerative colitis	14	0,49	0,22	**2,53E-02**	1,31E-01

Table A.7 (cont.)

Disease group	Exposure	Outcome	n_{snp}	Beta	SE	P-value	FDR-corrected p-value
Autoimmune	IL-8	Ulcerative colitis	3	0,41	0,40	3,15E-01	5,87E-01
Autoimmune	IL-9	Ulcerative colitis	8	0,23	0,26	3,70E-01	5,87E-01
Autoimmune	IP-10	Ulcerative colitis	8	-0,64	0,21	1,82E-03	**2,24E-02**
Autoimmune	M-CSF	Ulcerative colitis	4	0,58	0,35	9,41E-02	3,26E-01
Autoimmune	MCP-1	Ulcerative colitis	3	-1,62	0,52	1,81E-03	**2,24E-02**
Autoimmune	MCP-3	Ulcerative colitis	51	0,00	0,05	9,14E-01	9,53E-01
Autoimmune	MIF	Ulcerative colitis	6	-0,45	0,47	3,36E-01	5,87E-01
Autoimmune	MIG	Ulcerative colitis	8	0,32	0,36	3,71E-01	5,87E-01
Autoimmune	MIP-1a	Ulcerative colitis	33	-0,26	0,08	1,96E-03	**2,24E-02**
Autoimmune	MIP-1b	Ulcerative colitis	20	0,01	0,11	9,10E-01	9,53E-01
Autoimmune	RANTES	Ulcerative colitis	12	-0,09	0,15	5,63E-01	7,17E-01
Autoimmune	SCGF-b	Ulcerative colitis	27	0,10	0,07	1,39E-01	3,83E-01
Autoimmune	SDF-1a	Ulcerative colitis	17	-0,26	0,20	1,95E-01	4,46E-01
Autoimmune	TNF-b	Ulcerative colitis	2	1,69	1,44	2,40E-01	4,89E-01
Autoimmune	TRAIL	Ulcerative colitis	6	0,10	0,16	5,28E-01	6,96E-01
Autoimmune	VEGF	Ulcerative colitis	66	0,07	0,05	2,21E-01	4,76E-01
Cancer	Eotaxin	Breast cancer	11	0,07	0,17	6,72E-01	9,46E-01
Cancer	FGF-b	Breast cancer	48	0,05	0,04	2,39E-01	7,95E-01
Cancer	G-CSF	Breast cancer	2	0,11	0,58	8,44E-01	9,51E-01
Cancer	GROa	Breast cancer	57	-0,01	0,03	7,23E-01	9,51E-01
Cancer	HGF	Breast cancer	12	0,01	0,15	9,28E-01	9,51E-01
Cancer	IL-16	Breast cancer	56	0,01	0,05	9,04E-01	9,51E-01
Cancer	IL-18	Breast cancer	8	0,44	0,20	**3,25E-02**	4,07E-01
Cancer	IL-1ra	Breast cancer	33	-0,06	0,06	3,30E-01	8,09E-01
Cancer	IL-2ra	Breast cancer	14	0,04	0,13	7,52E-01	9,51E-01
Cancer	IL-8	Breast cancer	3	-0,36	0,35	3,12E-01	7,95E-01
Cancer	IL-9	Breast cancer	8	0,96	0,22	1,70E-05	**2,12E-03**
Cancer	IP-10	Breast cancer	8	-0,34	0,22	1,19E-01	5,36E-01
Cancer	M-CSF	Breast cancer	4	0,53	0,29	7,23E-02	5,36E-01
Cancer	MCP-1	Breast cancer	3	0,43	0,51	3,99E-01	8,71E-01
Cancer	MCP-3	Breast cancer	51	-0,03	0,04	3,92E-01	8,71E-01
Cancer	MIF	Breast cancer	6	-0,36	0,25	1,52E-01	6,19E-01
Cancer	MIG	Breast cancer	8	-0,10	0,29	7,29E-01	9,51E-01
Cancer	MIP-1a	Breast cancer	33	-0,07	0,07	3,51E-01	8,28E-01
Cancer	MIP-1b	Breast cancer	20	0,03	0,09	7,03E-01	9,51E-01
Cancer	RANTES	Breast cancer	12	0,12	0,11	2,76E-01	7,95E-01
Cancer	SCGF-b	Breast cancer	27	0,00	0,07	9,94E-01	9,94E-01
Cancer	SDF-1a	Breast cancer	17	0,24	0,14	8,77E-02	5,36E-01
Cancer	TNF-b	Breast cancer	4	0,05	0,30	8,53E-01	9,51E-01
Cancer	TRAIL	Breast cancer	6	-0,20	0,19	3,05E-01	7,95E-01
Cancer	VEGF	Breast cancer	65	-0,06	0,04	1,83E-01	7,17E-01
Cancer	Eotaxin	Colorectal cancer	11	0,00	0,00	8,60E-01	9,51E-01
Cancer	FGF-b	Colorectal cancer	46	0,00	0,00	4,69E-01	8,71E-01
Cancer	G-CSF	Colorectal cancer	2	0,01	0,01	8,40E-02	5,36E-01
Cancer	GROa	Colorectal cancer	55	0,00	0,00	1,20E-01	5,36E-01

Table A.7 (cont.)

Disease group	Exposure	Outcome	n_{snp}	Beta	SE	P-value	FDR-corrected p-value
Cancer	HGF	Colorectal cancer	12	0,00	0,00	7,70E-01	9,51E-01
Cancer	IL-16	Colorectal cancer	55	0,00	0,00	3,75E-01	8,56E-01
Cancer	IL-18	Colorectal cancer	5	-0,02	0,00	6,05E-05	**3,78E-03**
Cancer	IL-1ra	Colorectal cancer	30	0,00	0,00	1,47E-01	6,19E-01
Cancer	IL-2ra	Colorectal cancer	11	0,01	0,00	**5,14E-03**	2,13E-01
Cancer	IL-8	Colorectal cancer	3	0,01	0,01	1,18E-01	5,36E-01
Cancer	IL-9	Colorectal cancer	7	0,00	0,00	8,50E-01	9,51E-01
Cancer	IP-10	Colorectal cancer	8	0,00	0,00	4,35E-01	8,71E-01
Cancer	M-CSF	Colorectal cancer	4	0,00	0,00	4,62E-01	8,71E-01
Cancer	MCP-1	Colorectal cancer	2	0,00	0,01	8,13E-01	9,51E-01
Cancer	MCP-3	Colorectal cancer	47	0,00	0,00	1,17E-01	5,36E-01
Cancer	MIF	Colorectal cancer	6	0,00	0,00	9,24E-01	9,51E-01
Cancer	MIG	Colorectal cancer	8	0,01	0,00	**2,44E-02**	4,07E-01
Cancer	MIP-1a	Colorectal cancer	32	0,00	0,00	8,20E-01	9,51E-01
Cancer	MIP-1b	Colorectal cancer	19	0,00	0,00	5,11E-01	8,83E-01
Cancer	RANTES	Colorectal cancer	12	0,00	0,00	4,81E-01	8,71E-01
Cancer	SCGF-b	Colorectal cancer	24	0,00	0,00	9,89E-01	9,94E-01
Cancer	SDF-1a	Colorectal cancer	17	0,00	0,00	1,02E-01	5,36E-01
Cancer	TNF-b	Colorectal cancer	4	0,00	0,00	3,41E-01	8,19E-01
Cancer	TRAIL	Colorectal cancer	5	0,00	0,00	5,30E-01	8,83E-01
Cancer	VEGF	Colorectal cancer	62	0,00	0,00	6,23E-01	9,35E-01
Cancer	Eotaxin	Lung cancer	9	0,13	0,13	3,30E-01	8,09E-01
Cancer	FGF-b	Lung cancer	38	-0,01	0,03	6,28E-01	9,35E-01
Cancer	G-CSF	Lung cancer	2	-0,30	0,28	2,83E-01	7,95E-01
Cancer	GROa	Lung cancer	40	0,01	0,03	6,72E-01	9,46E-01
Cancer	HGF	Lung cancer	12	0,02	0,10	8,37E-01	9,51E-01
Cancer	IL-16	Lung cancer	51	-0,02	0,03	4,67E-01	8,71E-01
Cancer	IL-18	Lung cancer	8	-0,39	0,15	**6,82E-03**	2,13E-01
Cancer	IL-1ra	Lung cancer	30	-0,07	0,04	8,92E-02	5,36E-01
Cancer	IL-2ra	Lung cancer	12	-0,11	0,09	2,41E-01	7,95E-01
Cancer	IL-8	Lung cancer	3	-0,16	0,22	4,69E-01	8,71E-01
Cancer	IL-9	Lung cancer	7	0,15	0,15	3,07E-01	7,95E-01
Cancer	IP-10	Lung cancer	7	0,13	0,13	2,90E-01	7,95E-01
Cancer	M-CSF	Lung cancer	3	-0,18	0,22	4,06E-01	8,71E-01
Cancer	MCP-1	Lung cancer	3	-0,46	0,41	2,60E-01	7,95E-01
Cancer	MCP-3	Lung cancer	49	-0,03	0,02	2,14E-01	7,85E-01
Cancer	MIF	Lung cancer	5	-0,27	0,19	1,54E-01	6,19E-01
Cancer	MIG	Lung cancer	8	0,12	0,14	3,76E-01	8,56E-01
Cancer	MIP-1a	Lung cancer	26	-0,01	0,06	9,28E-01	9,51E-01
Cancer	MIP-1b	Lung cancer	16	-0,03	0,06	6,73E-01	9,46E-01
Cancer	RANTES	Lung cancer	12	0,03	0,08	7,27E-01	9,51E-01
Cancer	SCGF-b	Lung cancer	24	0,05	0,04	2,76E-01	7,95E-01
Cancer	SDF-1a	Lung cancer	16	-0,04	0,09	6,47E-01	9,43E-01
Cancer	TNF-b	Lung cancer	2	-0,69	0,32	**3,07E-02**	4,07E-01
Cancer	TRAIL	Lung cancer	6	-0,05	0,11	6,23E-01	9,35E-01

Table A.7 (cont.)

Disease group	Exposure	Outcome	n_{snp}	Beta	SE	P-value	FDR-corrected p-value
Cancer	VEGF	Lung cancer	59	-0,01	0,03	8,48E-01	9,51E-01
Cancer	Eotaxin	Non-Hodgkins lymphoma	9	0,09	0,27	7,39E-01	9,51E-01
Cancer	FGF-b	Non-Hodgkins lymphoma	44	-0,04	0,06	5,26E-01	8,83E-01
Cancer	G-CSF	Non-Hodgkins lymphoma	2	-0,20	0,74	7,84E-01	9,51E-01
Cancer	GROa	Non-Hodgkins lymphoma	43	-0,04	0,05	4,75E-01	8,71E-01
Cancer	HGF	Non-Hodgkins lymphoma	12	0,04	0,21	8,40E-01	9,51E-01
Cancer	IL-16	Non-Hodgkins lymphoma	46	-0,02	0,07	8,08E-01	9,51E-01
Cancer	IL-18	Non-Hodgkins lymphoma	6	-0,18	0,32	5,73E-01	9,07E-01
Cancer	IL-1ra	Non-Hodgkins lymphoma	28	0,11	0,10	2,71E-01	7,95E-01
Cancer	IL-2ra	Non-Hodgkins lymphoma	10	0,54	0,24	**2,22E-02**	4,07E-01
Cancer	IL-8	Non-Hodgkins lymphoma	2	0,07	0,59	9,11E-01	9,51E-01
Cancer	IL-9	Non-Hodgkins lymphoma	7	-0,62	0,35	7,47E-02	5,36E-01
Cancer	IP-10	Non-Hodgkins lymphoma	7	-0,31	0,29	3,00E-01	7,95E-01
Cancer	M-CSF	Non-Hodgkins lymphoma	3	0,85	0,49	8,39E-02	5,36E-01
Cancer	MCP-1	Non-Hodgkins lymphoma	3	-0,11	0,69	8,70E-01	9,51E-01
Cancer	MCP-3	Non-Hodgkins lymphoma	43	0,01	0,06	8,77E-01	9,51E-01
Cancer	MIF	Non-Hodgkins lymphoma	3	-0,31	0,53	5,63E-01	9,07E-01
Cancer	MIG	Non-Hodgkins lymphoma	7	0,15	0,48	7,52E-01	9,51E-01
Cancer	MIP-1a	Non-Hodgkins lymphoma	23	-0,08	0,12	5,29E-01	8,83E-01
Cancer	MIP-1b	Non-Hodgkins lymphoma	12	0,07	0,16	6,49E-01	9,43E-01
Cancer	RANTES	Non-Hodgkins lymphoma	11	-0,37	0,18	**3,64E-02**	4,14E-01
Cancer	SCGF-b	Non-Hodgkins lymphoma	18	0,06	0,09	5,04E-01	8,83E-01
Cancer	SDF-1a	Non-Hodgkins lymphoma	16	0,12	0,22	5,71E-01	9,07E-01
Cancer	TNF-b	Non-Hodgkins lymphoma	2	-1,43	0,84	8,75E-02	5,36E-01
Cancer	TRAIL	Non-Hodgkins lymphoma	6	-0,07	0,20	7,21E-01	9,51E-01
Cancer	VEGF	Non-Hodgkins lymphoma	44	0,15	0,09	1,19E-01	5,36E-01
Cancer	Eotaxin	Skin cancer	11	0,00	0,01	5,02E-01	8,83E-01
Cancer	FGF-b	Skin cancer	46	0,00	0,00	2,73E-01	7,95E-01
Cancer	G-CSF	Skin cancer	2	0,01	0,01	2,92E-01	7,95E-01
Cancer	GROa	Skin cancer	55	0,00	0,00	**2,52E-02**	4,07E-01
Cancer	HGF	Skin cancer	12	-0,01	0,00	**4,99E-02**	5,20E-01
Cancer	IL-16	Skin cancer	55	0,00	0,00	5,62E-01	9,07E-01
Cancer	IL-18	Skin cancer	5	0,01	0,01	6,28E-01	9,35E-01
Cancer	IL-1ra	Skin cancer	30	0,00	0,00	**2,69E-02**	4,07E-01
Cancer	IL-2ra	Skin cancer	11	0,00	0,01	5,94E-01	9,28E-01
Cancer	IL-8	Skin cancer	3	-0,02	0,01	8,23E-02	5,36E-01
Cancer	IL-9	Skin cancer	7	0,00	0,01	8,62E-01	9,51E-01
Cancer	IP-10	Skin cancer	8	-0,01	0,01	1,92E-01	7,29E-01
Cancer	M-CSF	Skin cancer	4	0,01	0,01	1,09E-01	5,36E-01
Cancer	MCP-1	Skin cancer	2	0,01	0,02	4,63E-01	8,71E-01
Cancer	MCP-3	Skin cancer	47	0,00	0,00	8,21E-01	9,51E-01
Cancer	MIF	Skin cancer	6	0,00	0,01	9,13E-01	9,51E-01
Cancer	MIG	Skin cancer	8	0,00	0,01	4,72E-01	8,71E-01
Cancer	MIP-1a	Skin cancer	32	0,00	0,00	8,95E-01	9,51E-01
Cancer	MIP-1b	Skin cancer	19	0,00	0,00	2,54E-01	7,95E-01

Table A.7 (cont.)

Disease group	Exposure	Outcome	n_{snp}	Beta	SE	P-value	FDR-corrected p-value
Cancer	RANTES	Skin cancer	12	0,00	0,00	8,16E-01	9,51E-01
Cancer	SCGF-b	Skin cancer	24	0,00	0,00	1,01E-01	5,36E-01
Cancer	SDF-1a	Skin cancer	17	0,00	0,00	7,88E-01	9,51E-01
Cancer	TNF-b	Skin cancer	4	-0,01	0,02	4,62E-01	8,71E-01
Cancer	TRAIL	Skin cancer	5	0,00	0,01	4,29E-01	8,71E-01
Cancer	VEGF	Skin cancer	62	0,00	0,00	9,76E-01	9,91E-01
Cardiometabolic	Eotaxin	Diabetes mellitus type II	10	0,00	0,04	9,41E-01	9,51E-01
Cardiometabolic	FGF-b	Diabetes mellitus type II	48	0,03	0,01	8,23E-05	**4,12E-03**
Cardiometabolic	G-CSF	Diabetes mellitus type II	2	0,06	0,20	7,43E-01	8,85E-01
Cardiometabolic	GROa	Diabetes mellitus type II	55	-0,01	0,01	8,53E-02	4,18E-01
Cardiometabolic	HGF	Diabetes mellitus type II	12	-0,04	0,03	2,87E-01	6,38E-01
Cardiometabolic	IL-16	Diabetes mellitus type II	57	0,00	0,01	6,61E-01	8,48E-01
Cardiometabolic	IL-18	Diabetes mellitus type II	8	0,09	0,04	**1,83E-02**	1,83E-01
Cardiometabolic	IL-1ra	Diabetes mellitus type II	33	0,04	0,01	**2,98E-03**	5,96E-02
Cardiometabolic	IL-2ra	Diabetes mellitus type II	14	-0,06	0,03	5,24E-02	3,76E-01
Cardiometabolic	IL-8	Diabetes mellitus type II	3	0,03	0,07	7,09E-01	8,57E-01
Cardiometabolic	IL-9	Diabetes mellitus type II	8	0,00	0,06	9,88E-01	9,88E-01
Cardiometabolic	IP-10	Diabetes mellitus type II	8	0,03	0,06	5,63E-01	8,06E-01
Cardiometabolic	M-CSF	Diabetes mellitus type II	4	0,05	0,10	6,12E-01	8,16E-01
Cardiometabolic	MCP-1	Diabetes mellitus type II	2	0,06	0,11	5,64E-01	8,06E-01
Cardiometabolic	MCP-3	Diabetes mellitus type II	51	-0,01	0,01	1,08E-01	4,34E-01
Cardiometabolic	MIF	Diabetes mellitus type II	4	0,06	0,11	5,94E-01	8,16E-01
Cardiometabolic	MIG	Diabetes mellitus type II	8	0,13	0,07	7,87E-02	4,18E-01
Cardiometabolic	MIP-1a	Diabetes mellitus type II	31	0,02	0,02	3,50E-01	6,49E-01
Cardiometabolic	MIP-1b	Diabetes mellitus type II	20	0,01	0,02	4,72E-01	7,29E-01
Cardiometabolic	RANTES	Diabetes mellitus type II	11	0,02	0,02	3,29E-01	6,38E-01
Cardiometabolic	SCGF-b	Diabetes mellitus type II	26	0,01	0,02	6,96E-01	8,57E-01
Cardiometabolic	SDF-1a	Diabetes mellitus type II	17	0,01	0,04	7,07E-01	8,57E-01
Cardiometabolic	TNF-b	Diabetes mellitus type II	4	0,09	0,09	3,22E-01	6,38E-01
Cardiometabolic	TRAIL	Diabetes mellitus type II	6	0,05	0,03	6,94E-02	4,08E-01
Cardiometabolic	VEGF	Diabetes mellitus type II	66	0,02	0,01	2,51E-01	6,13E-01
Cardiometabolic	Eotaxin	Coronary artery disease	11	0,06	0,08	4,31E-01	7,07E-01
Cardiometabolic	FGF-b	Coronary artery disease	42	0,02	0,02	3,21E-01	6,38E-01
Cardiometabolic	G-CSF	Coronary artery disease	2	0,49	0,20	**1,21E-02**	1,35E-01
Cardiometabolic	GROa	Coronary artery disease	46	-0,03	0,02	1,00E-01	4,18E-01
Cardiometabolic	HGF	Coronary artery disease	12	-0,05	0,06	4,22E-01	7,03E-01
Cardiometabolic	IL-16	Coronary artery disease	47	-0,01	0,02	7,08E-01	8,57E-01
Cardiometabolic	IL-18	Coronary artery disease	8	0,02	0,09	8,17E-01	9,18E-01
Cardiometabolic	IL-1ra	Coronary artery disease	33	0,15	0,03	4,27E-07	**4,27E-05**
Cardiometabolic	IL-2ra	Coronary artery disease	14	-0,05	0,06	4,67E-01	7,29E-01
Cardiometabolic	IL-8	Coronary artery disease	3	0,15	0,13	2,51E-01	6,13E-01
Cardiometabolic	IL-9	Coronary artery disease	7	0,05	0,10	6,12E-01	8,16E-01
Cardiometabolic	IP-10	Coronary artery disease	8	0,04	0,07	5,37E-01	8,06E-01
Cardiometabolic	M-CSF	Coronary artery disease	4	0,35	0,14	**9,11E-03**	1,30E-01
Cardiometabolic	MCP-1	Coronary artery disease	3	-0,21	0,20	2,97E-01	6,38E-01

Table A.7 (cont.)

Disease group	Exposure	Outcome	n_{snp}	Beta	SE	P-value	FDR-corrected p-value
Cardiometabolic	MCP-3	Coronary artery disease	50	-0,03	0,02	8,95E-02	4,18E-01
Cardiometabolic	MIF	Coronary artery disease	6	0,06	0,15	7,12E-01	8,57E-01
Cardiometabolic	MIG	Coronary artery disease	8	0,21	0,10	**4,15E-02**	3,76E-01
Cardiometabolic	MIP-1a	Coronary artery disease	26	-0,05	0,03	1,69E-01	5,13E-01
Cardiometabolic	MIP-1b	Coronary artery disease	15	0,00	0,05	9,17E-01	9,51E-01
Cardiometabolic	RANTES	Coronary artery disease	10	0,00	0,05	9,36E-01	9,51E-01
Cardiometabolic	SCGF-b	Coronary artery disease	24	-0,03	0,03	3,14E-01	6,38E-01
Cardiometabolic	SDF-1a	Coronary artery disease	17	0,38	0,13	**4,30E-03**	7,16E-02
Cardiometabolic	TNF-b	Coronary artery disease	4	0,14	0,15	3,39E-01	6,40E-01
Cardiometabolic	TRAIL	Coronary artery disease	6	0,20	0,06	1,40E-03	**3,49E-02**
Cardiometabolic	VEGF	Coronary artery disease	54	0,00	0,02	8,93E-01	9,50E-01
Cardiometabolic	Eotaxin	Peripheral vascular disease	11	-0,13	0,09	1,53E-01	4,94E-01
Cardiometabolic	FGF-b	Peripheral vascular disease	47	-0,04	0,02	6,23E-02	3,91E-01
Cardiometabolic	G-CSF	Peripheral vascular disease	2	0,37	0,22	9,24E-02	4,18E-01
Cardiometabolic	GROa	Peripheral vascular disease	53	0,02	0,02	3,93E-01	6,71E-01
Cardiometabolic	HGF	Peripheral vascular disease	11	-0,01	0,08	8,90E-01	9,50E-01
Cardiometabolic	IL-16	Peripheral vascular disease	52	0,00	0,02	9,30E-01	9,51E-01
Cardiometabolic	IL-18	Peripheral vascular disease	7	0,09	0,10	3,88E-01	6,71E-01
Cardiometabolic	IL-1ra	Peripheral vascular disease	31	0,07	0,05	1,00E-01	4,18E-01
Cardiometabolic	IL-2ra	Peripheral vascular disease	13	0,06	0,07	3,93E-01	6,71E-01
Cardiometabolic	IL-8	Peripheral vascular disease	3	-0,22	0,18	2,27E-01	6,04E-01
Cardiometabolic	IL-9	Peripheral vascular disease	5	0,38	0,15	**1,17E-02**	1,35E-01
Cardiometabolic	IP-10	Peripheral vascular disease	8	0,05	0,10	6,12E-01	8,16E-01
Cardiometabolic	M-CSF	Peripheral vascular disease	3	0,19	0,22	3,96E-01	6,71E-01
Cardiometabolic	MCP-1	Peripheral vascular disease	3	-0,06	0,22	7,79E-01	8,91E-01
Cardiometabolic	MCP-3	Peripheral vascular disease	47	0,01	0,02	5,55E-01	8,06E-01
Cardiometabolic	MIF	Peripheral vascular disease	4	0,01	0,17	9,32E-01	9,51E-01
Cardiometabolic	MIG	Peripheral vascular disease	6	0,17	0,12	1,33E-01	4,58E-01
Cardiometabolic	MIP-1a	Peripheral vascular disease	26	0,04	0,04	3,03E-01	6,38E-01
Cardiometabolic	MIP-1b	Peripheral vascular disease	18	-0,08	0,05	6,25E-02	3,91E-01
Cardiometabolic	RANTES	Peripheral vascular disease	11	-0,02	0,06	7,57E-01	8,85E-01
Cardiometabolic	SCGF-b	Peripheral vascular disease	23	0,05	0,09	5,60E-01	8,06E-01
Cardiometabolic	SDF-1a	Peripheral vascular disease	16	0,15	0,08	8,00E-02	4,18E-01
Cardiometabolic	TNF-b	Peripheral vascular disease	3	-0,38	0,24	1,18E-01	4,35E-01
Cardiometabolic	TRAIL	Peripheral vascular disease	6	0,11	0,08	1,90E-01	5,44E-01
Cardiometabolic	VEGF	Peripheral vascular disease	62	-0,03	0,03	2,83E-01	6,38E-01
Cardiometabolic	Eotaxin	Largery artery stroke	11	0,22	0,24	3,71E-01	6,71E-01
Cardiometabolic	FGF-b	Largery artery stroke	45	0,03	0,06	6,23E-01	8,19E-01
Cardiometabolic	G-CSF	Largery artery stroke	2	-0,42	0,58	4,74E-01	7,29E-01
Cardiometabolic	GROa	Largery artery stroke	54	0,07	0,05	1,63E-01	5,09E-01
Cardiometabolic	HGF	Largery artery stroke	12	0,06	0,21	7,61E-01	8,85E-01
Cardiometabolic	IL-16	Largery artery stroke	51	0,11	0,07	1,16E-01	4,35E-01
Cardiometabolic	IL-18	Largery artery stroke	8	-0,41	0,39	2,99E-01	6,38E-01
Cardiometabolic	IL-1ra	Largery artery stroke	33	-0,02	0,09	7,84E-01	8,91E-01
Cardiometabolic	IL-2ra	Largery artery stroke	14	0,04	0,20	8,60E-01	9,45E-01

Table A.7 (cont.)

Disease group	Exposure	Outcome	n_{snp}	Beta	SE	P-value	FDR-corrected p-value
Cardiometabolic	IL-8	Largery artery stroke	3	-0,62	0,51	2,21E-01	6,04E-01
Cardiometabolic	IL-9	Largery artery stroke	7	-0,37	0,32	2,43E-01	6,13E-01
Cardiometabolic	IP-10	Largery artery stroke	7	-0,35	0,27	1,88E-01	5,44E-01
Cardiometabolic	M-CSF	Largery artery stroke	4	0,70	0,48	1,44E-01	4,81E-01
Cardiometabolic	MCP-1	Largery artery stroke	3	-0,97	1,00	3,32E-01	6,38E-01
Cardiometabolic	MCP-3	Largery artery stroke	50	0,08	0,07	2,30E-01	6,04E-01
Cardiometabolic	MIF	Largery artery stroke	6	-1,03	0,53	5,26E-02	3,76E-01
Cardiometabolic	MIG	Largery artery stroke	8	0,20	0,28	4,68E-01	7,29E-01
Cardiometabolic	MIP-1a	Largery artery stroke	28	0,17	0,11	1,32E-01	4,58E-01
Cardiometabolic	MIP-1b	Largery artery stroke	16	-0,15	0,14	2,77E-01	6,38E-01
Cardiometabolic	RANTES	Largery artery stroke	12	-0,51	0,16	1,16E-03	**3,49E-02**
Cardiometabolic	SCGF-b	Largery artery stroke	27	0,18	0,09	**4,56E-02**	3,76E-01
Cardiometabolic	SDF-1a	Largery artery stroke	17	0,12	0,23	6,00E-01	8,16E-01
Cardiometabolic	TNF-b	Largery artery stroke	2	0,35	0,77	6,52E-01	8,46E-01
Cardiometabolic	TRAIL	Largery artery stroke	6	-0,04	0,21	8,50E-01	9,44E-01
Cardiometabolic	VEGF	Largery artery stroke	62	0,01	0,07	8,82E-01	9,50E-01

Figure A.1. Manhattan plots. Manhattan plots showing GWAS results for each of the 40 cytokines.

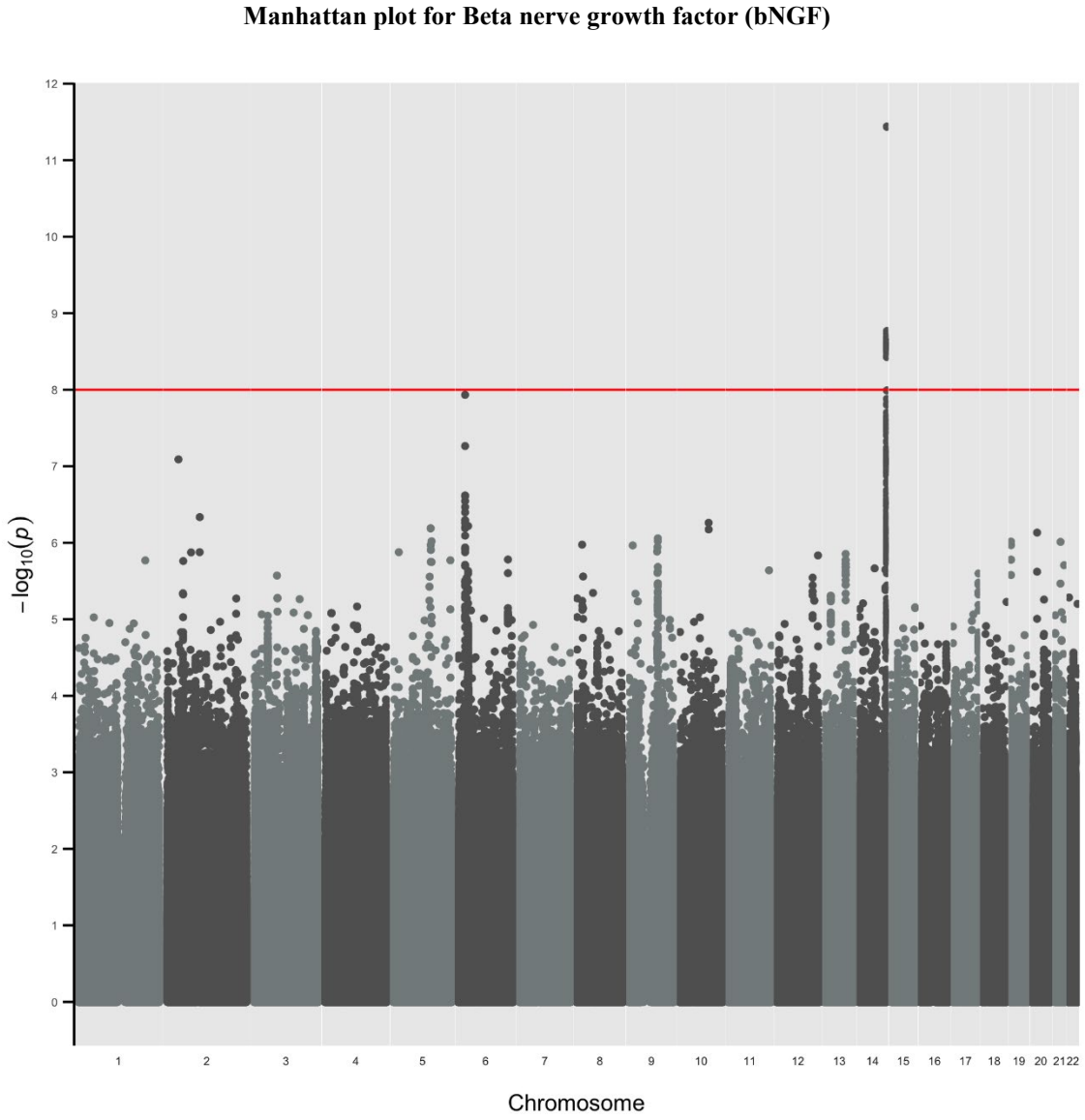

Figure A.1 (cont.)

Manhattan plot for Cutaneous T-cell attracting (CCL27/CTACK)

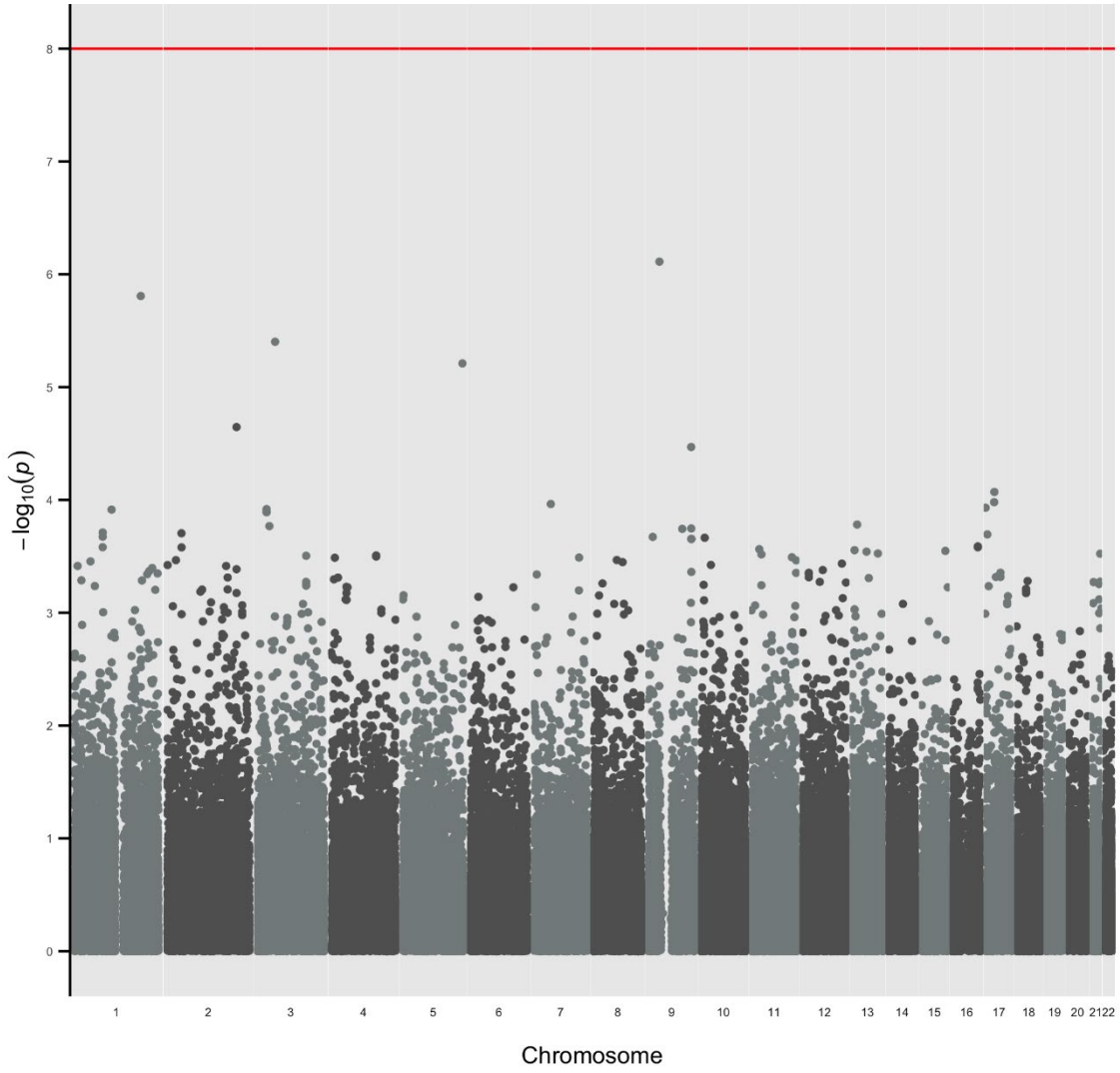

Figure A.1 (cont.)

Manhattan plot for Eotaxin (CCL11/eotaxin-1)

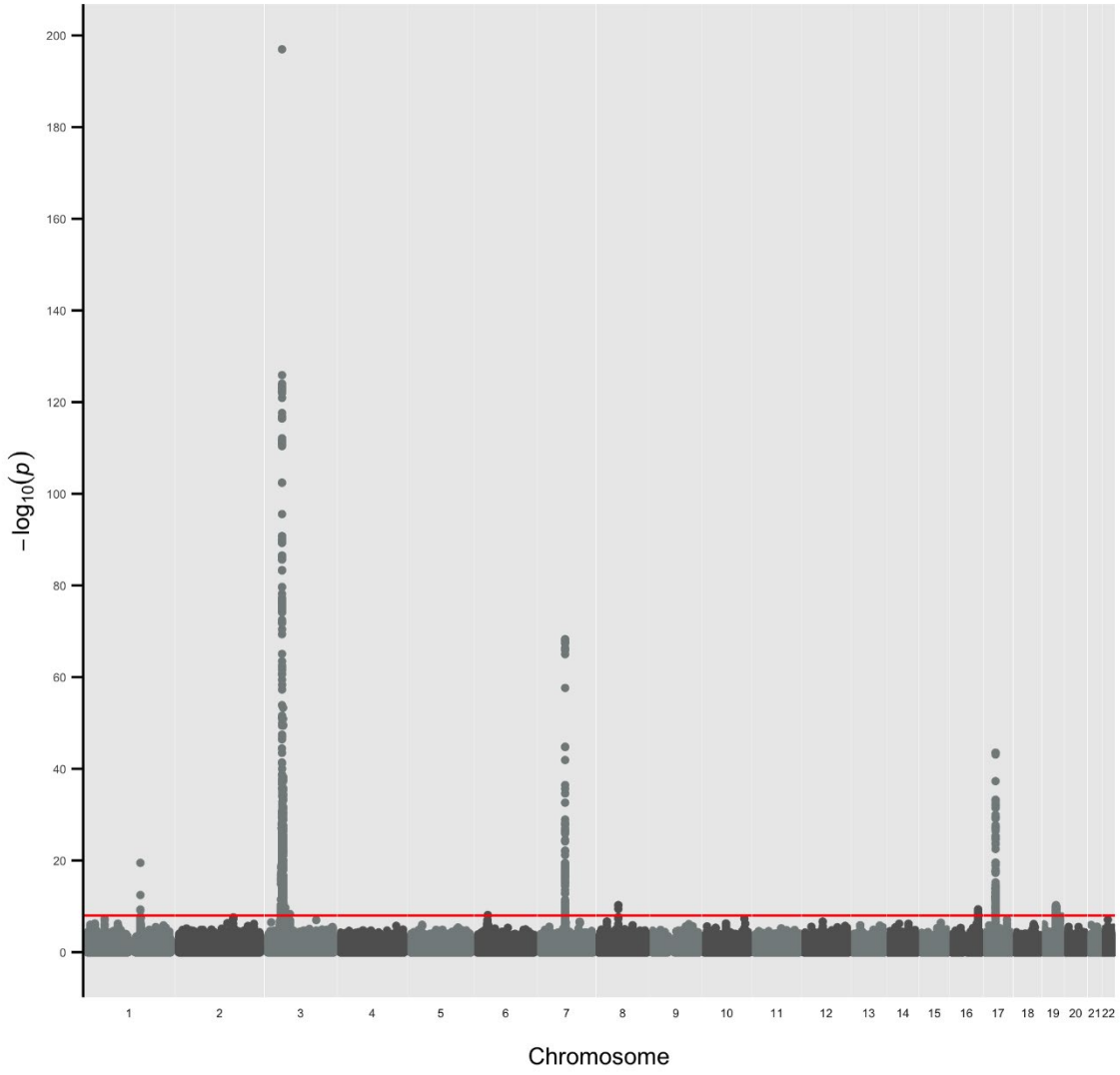

Figure A.1 (cont.)

Manhattan plot for Basic fibroblast growth factor (FGF-b)

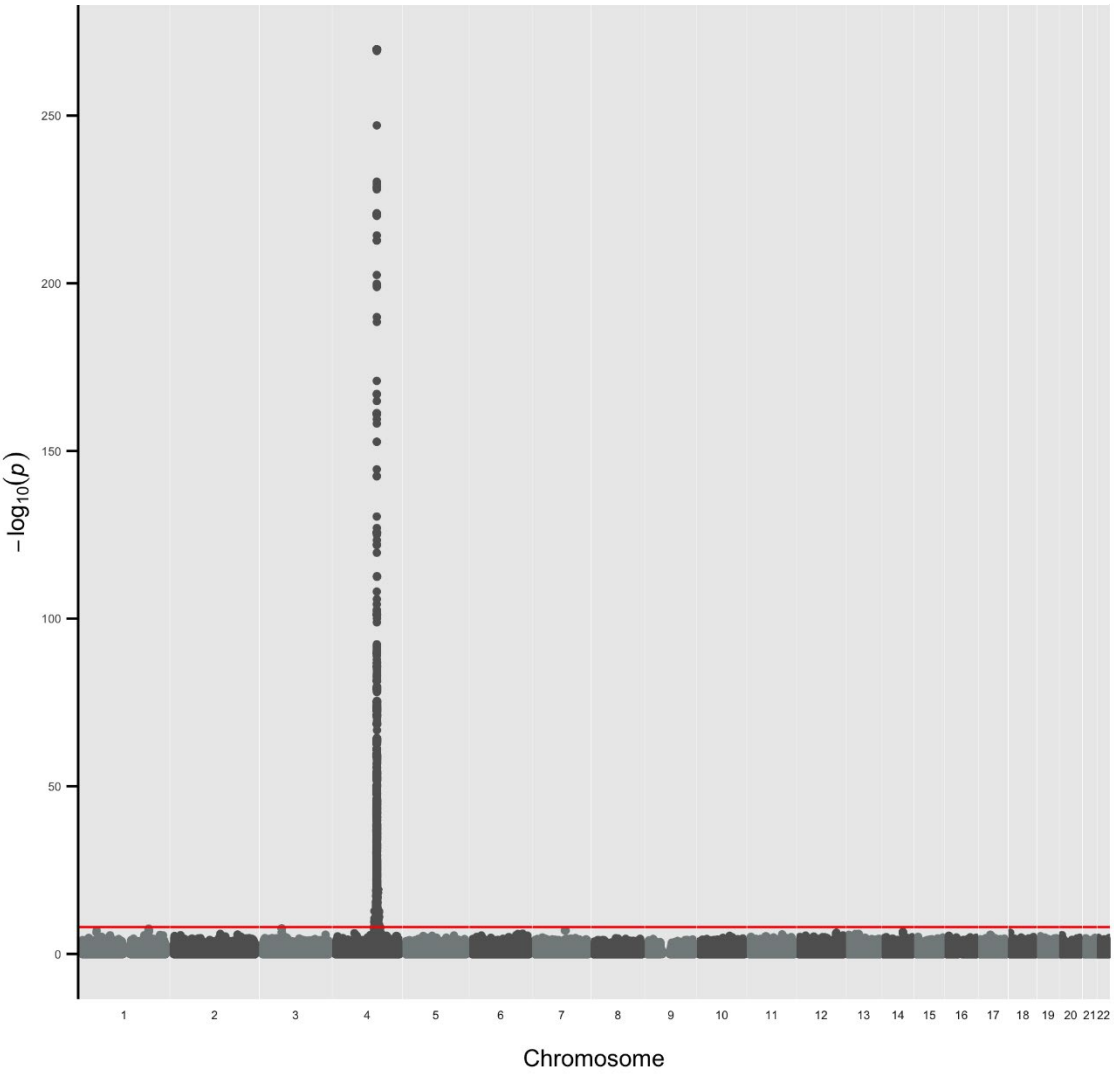

Figure A.1 (cont.)

Manhattan plot for Granulocyte colony-stimulating factor (G-CSF/CSF-3)

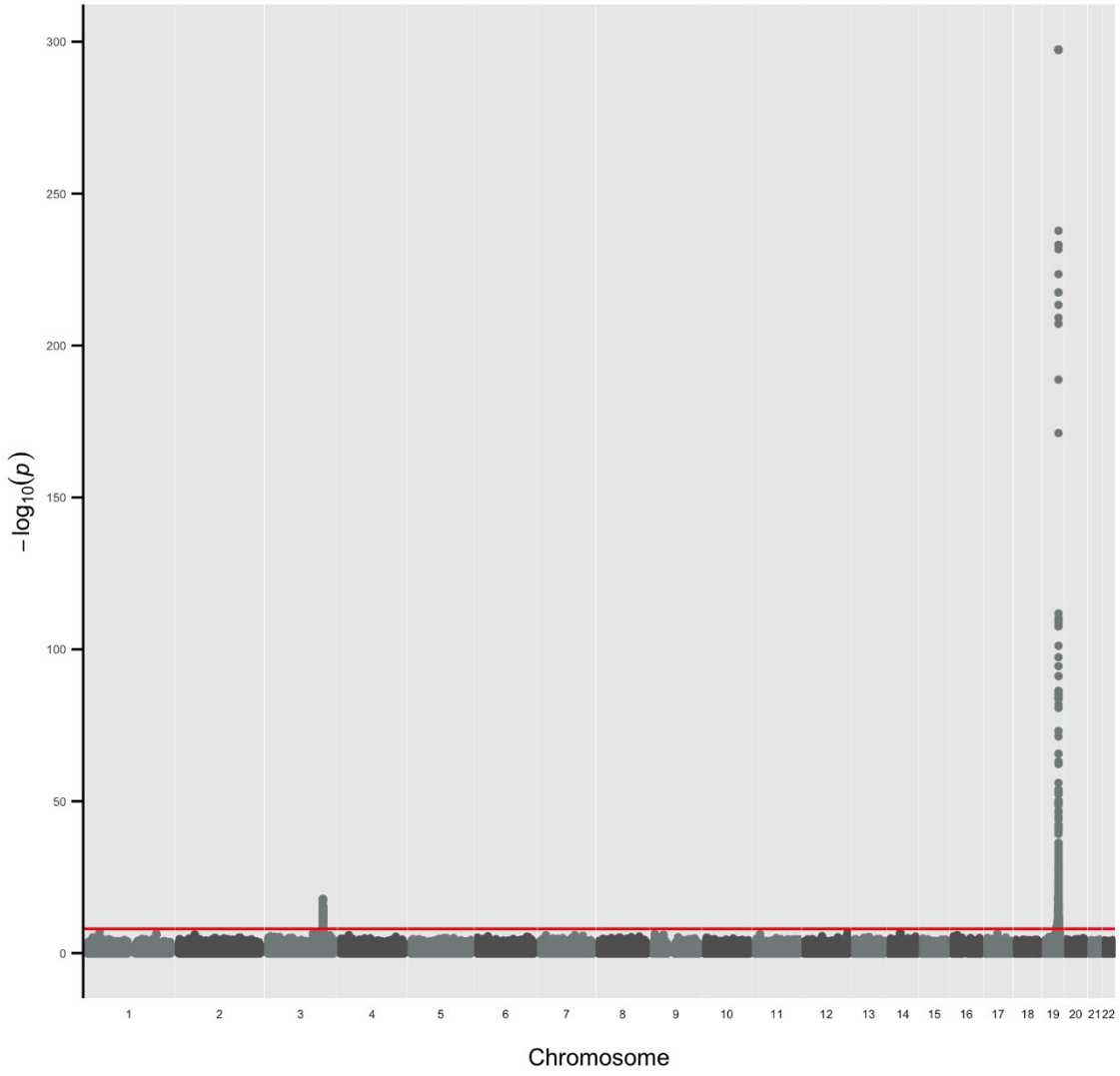

Figure A.1 (cont.)

Manhattan plot for Growth regulated oncogene-alpha (CXCL1/GROa)

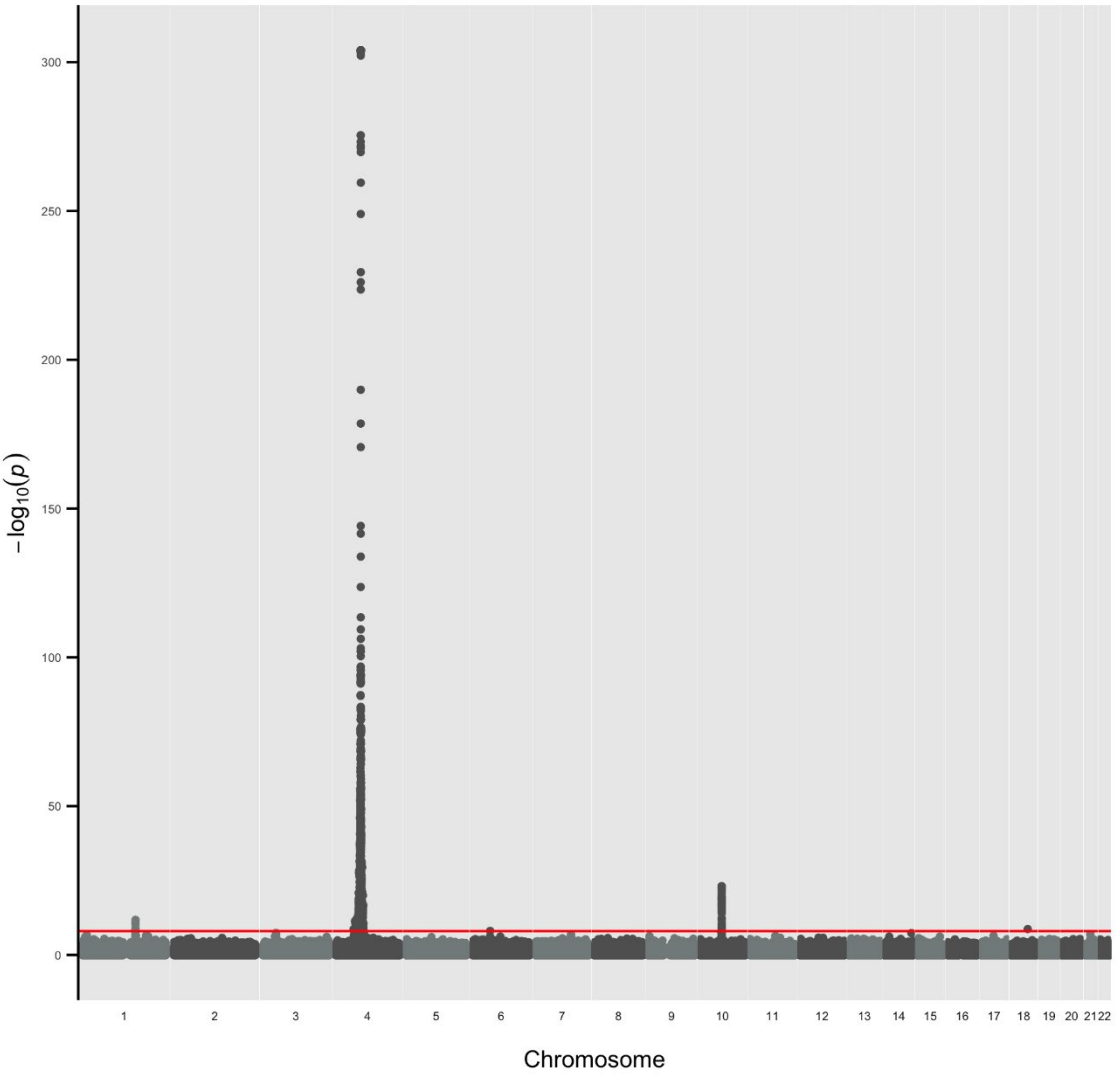

Figure A.1 (cont.)

Manhattan plot for Hepatocyte growth factor (HGF)

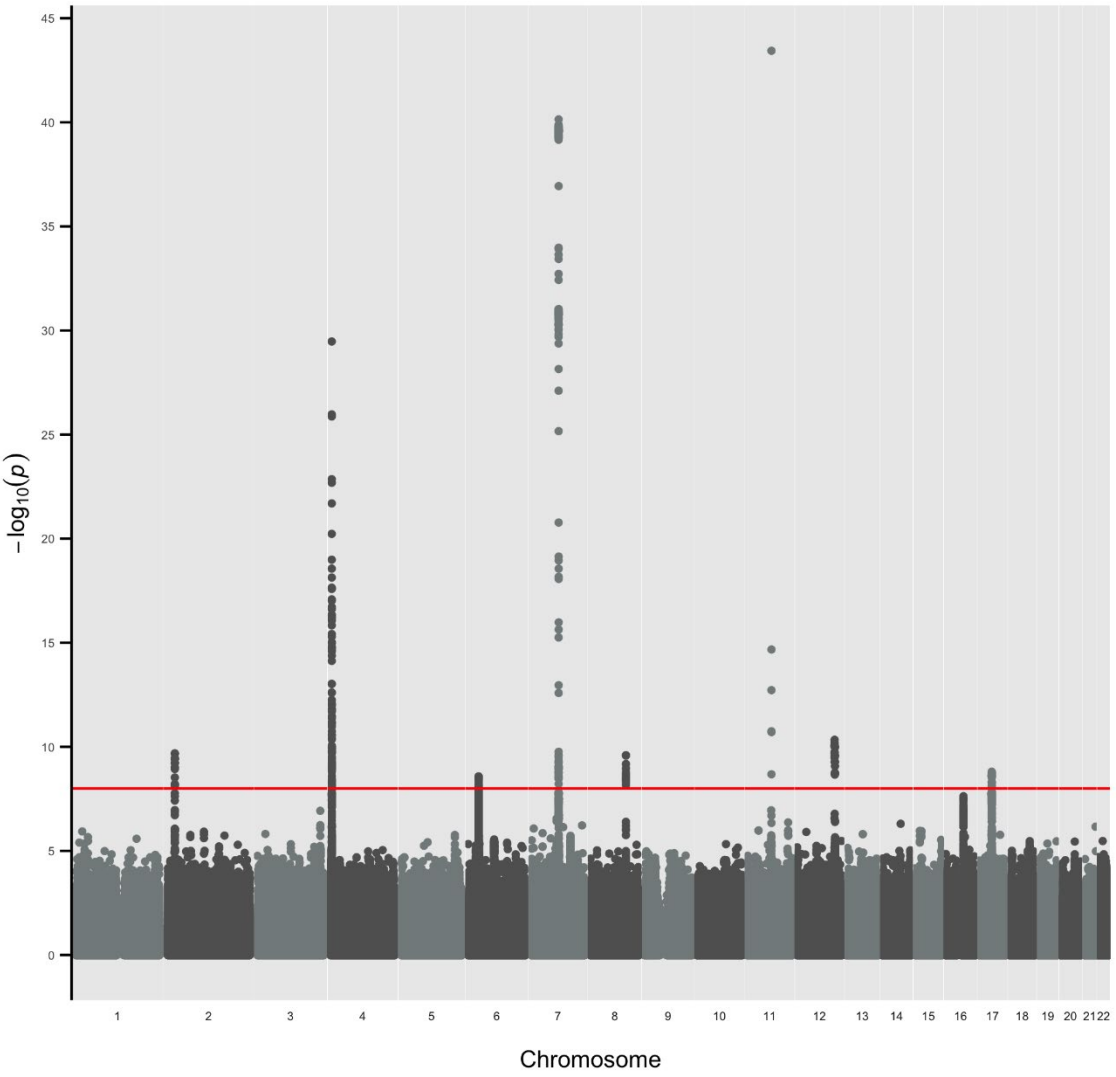

Figure A.1 (cont.)

Manhattan plot for Interferon-gamma (IFN-g)

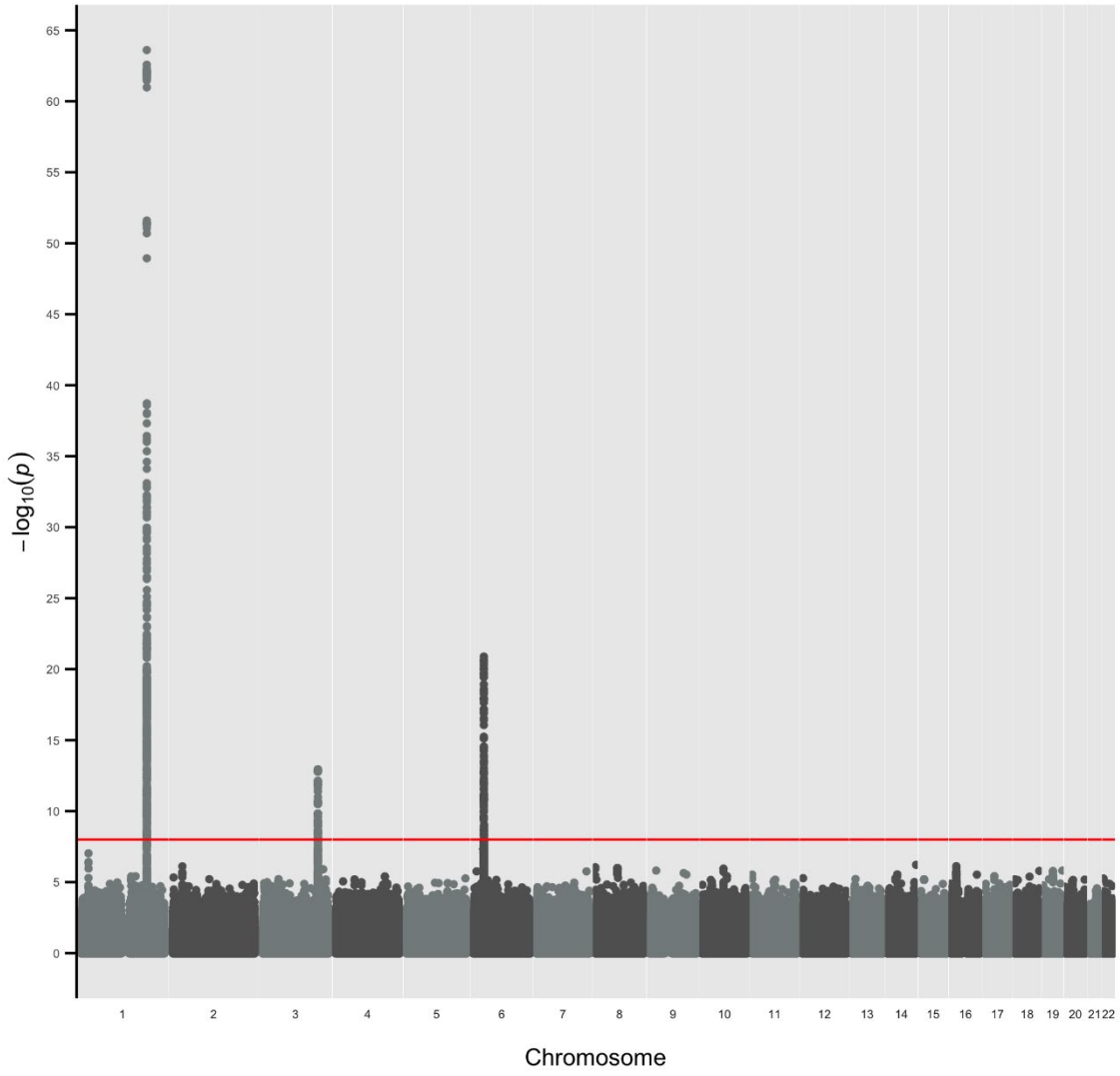

Figure A.1 (cont.)

Manhattan plot for Interleukin-10 (IL-10)

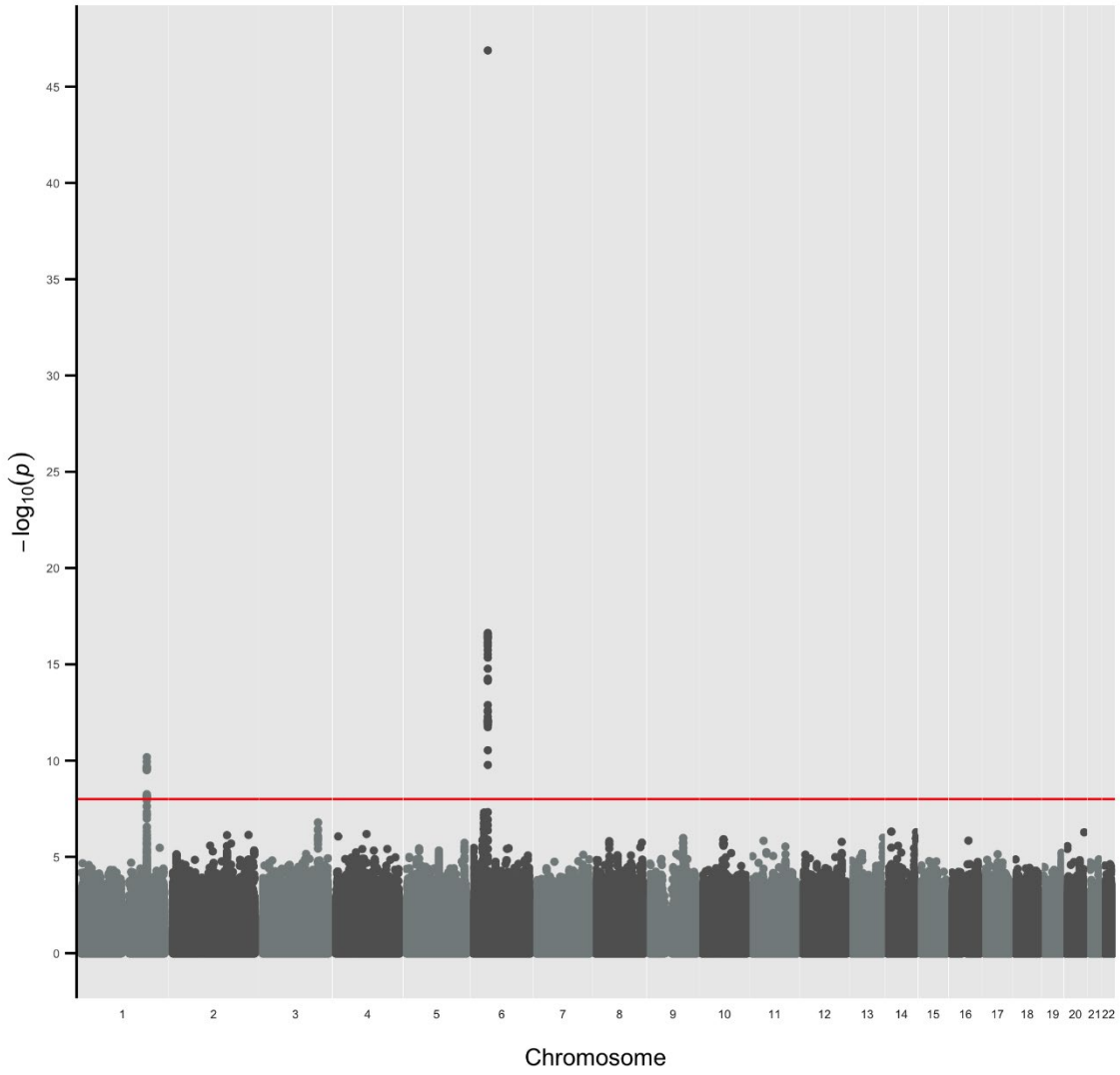

Figure A.1 (cont.)

Manhattan plot for Interleukin-13 (IL-13)

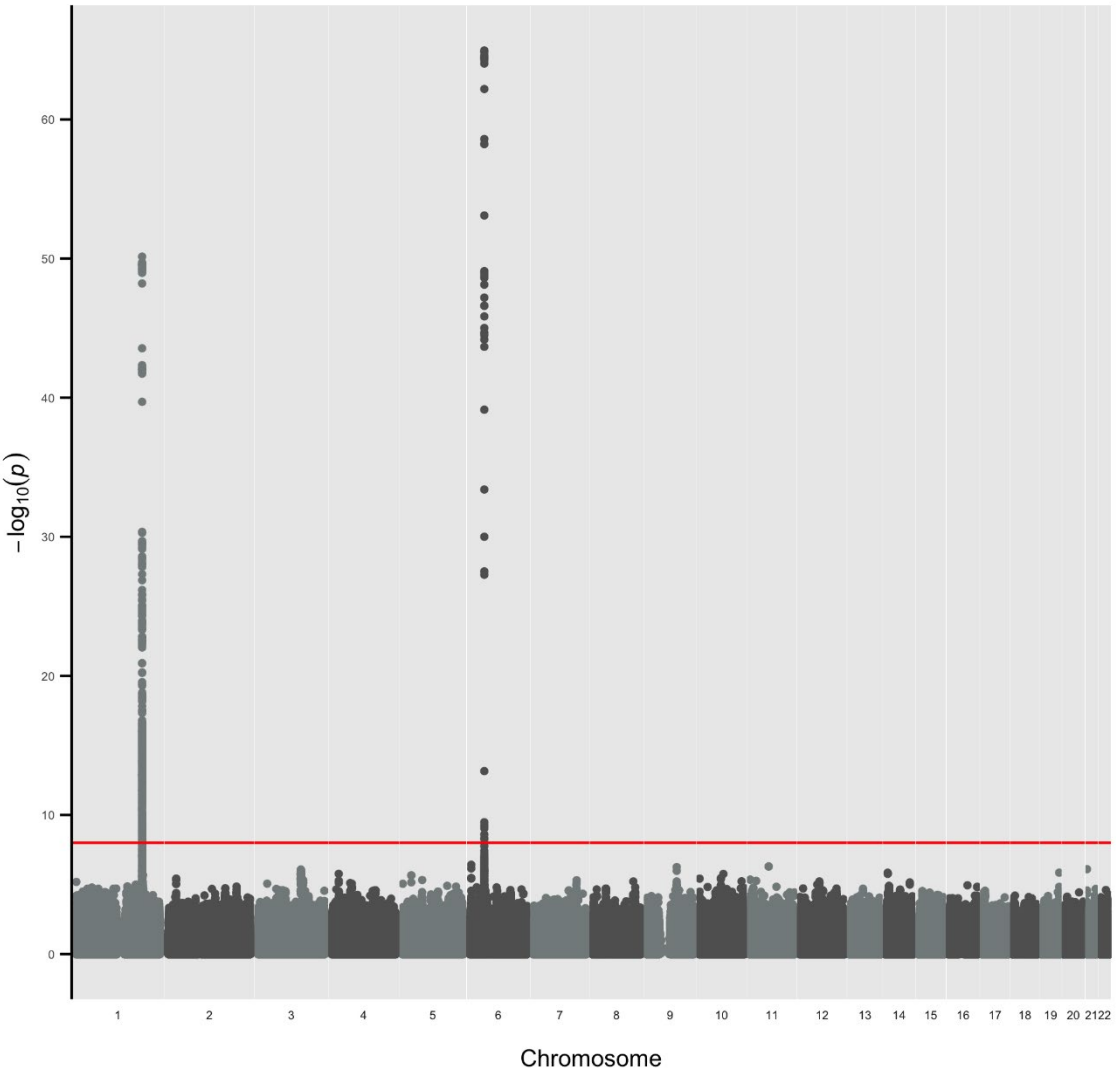

Figure A.1 (cont.)

Manhattan plot for Interleukin-16 (IL-16)

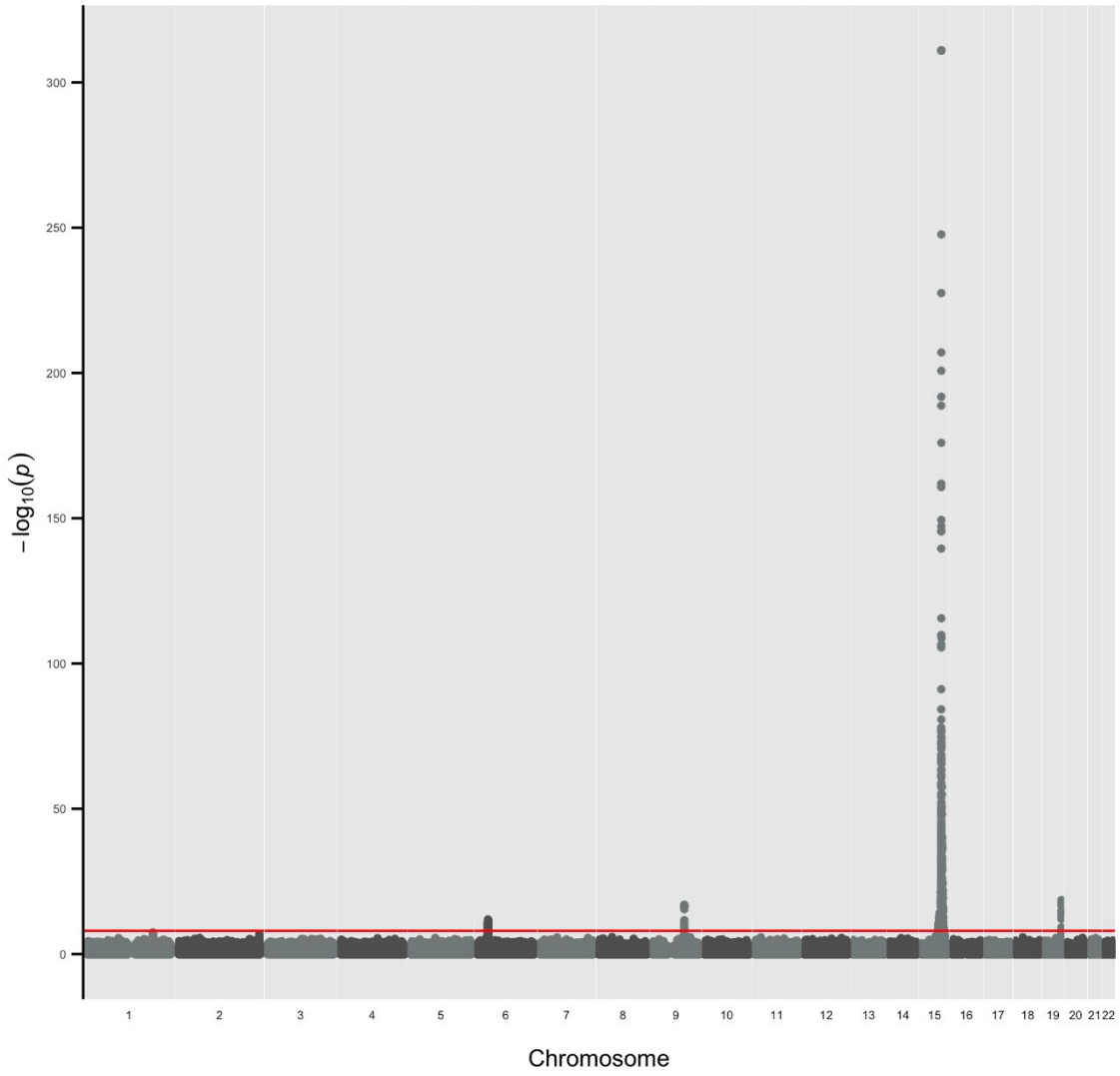

Figure A.1 (cont.)

Manhattan plot for Interleukin-17 (IL-17)

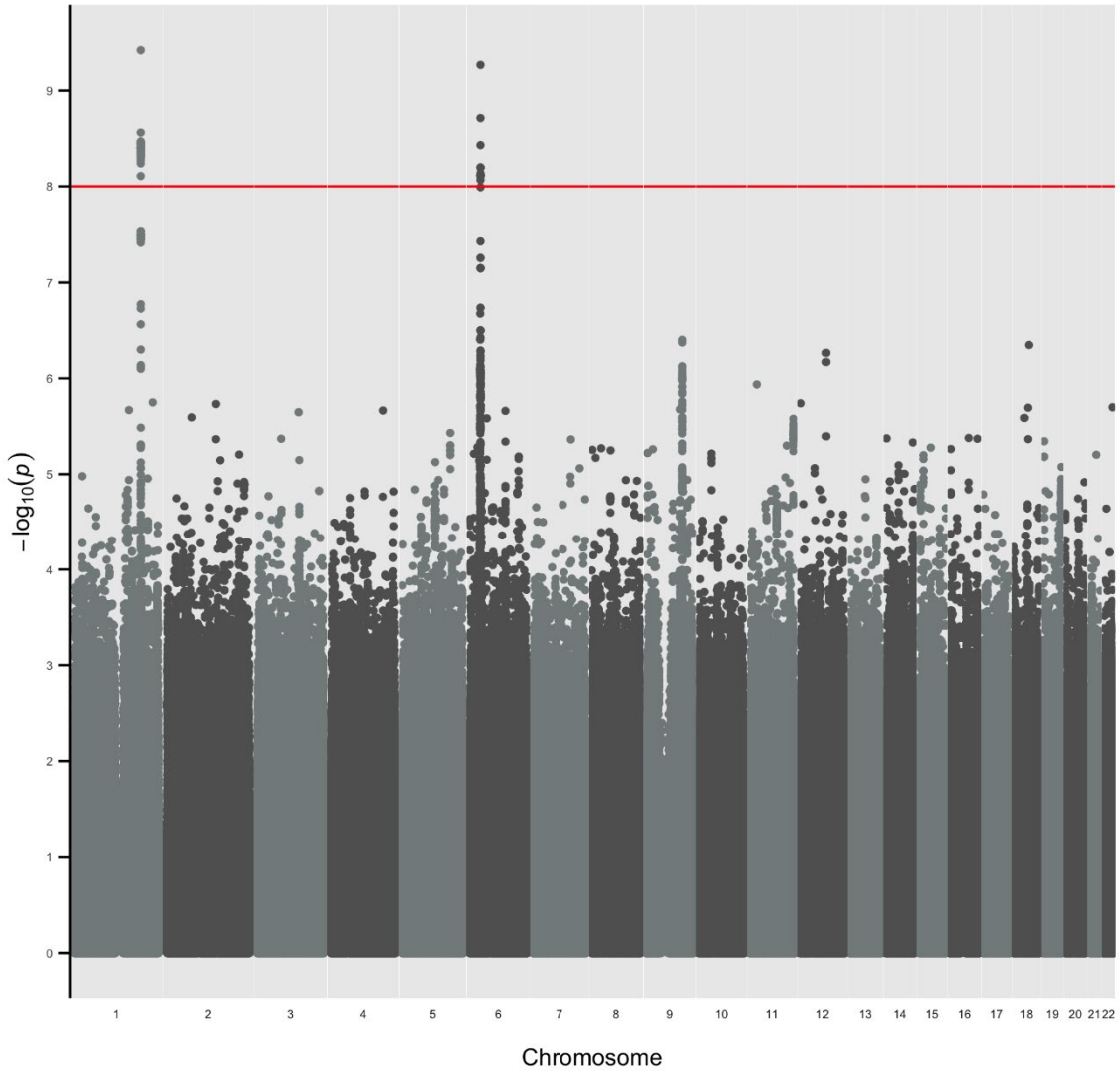

Figure A.1 (cont.)

Manhattan plot for Interleukin-18 (IL-18)

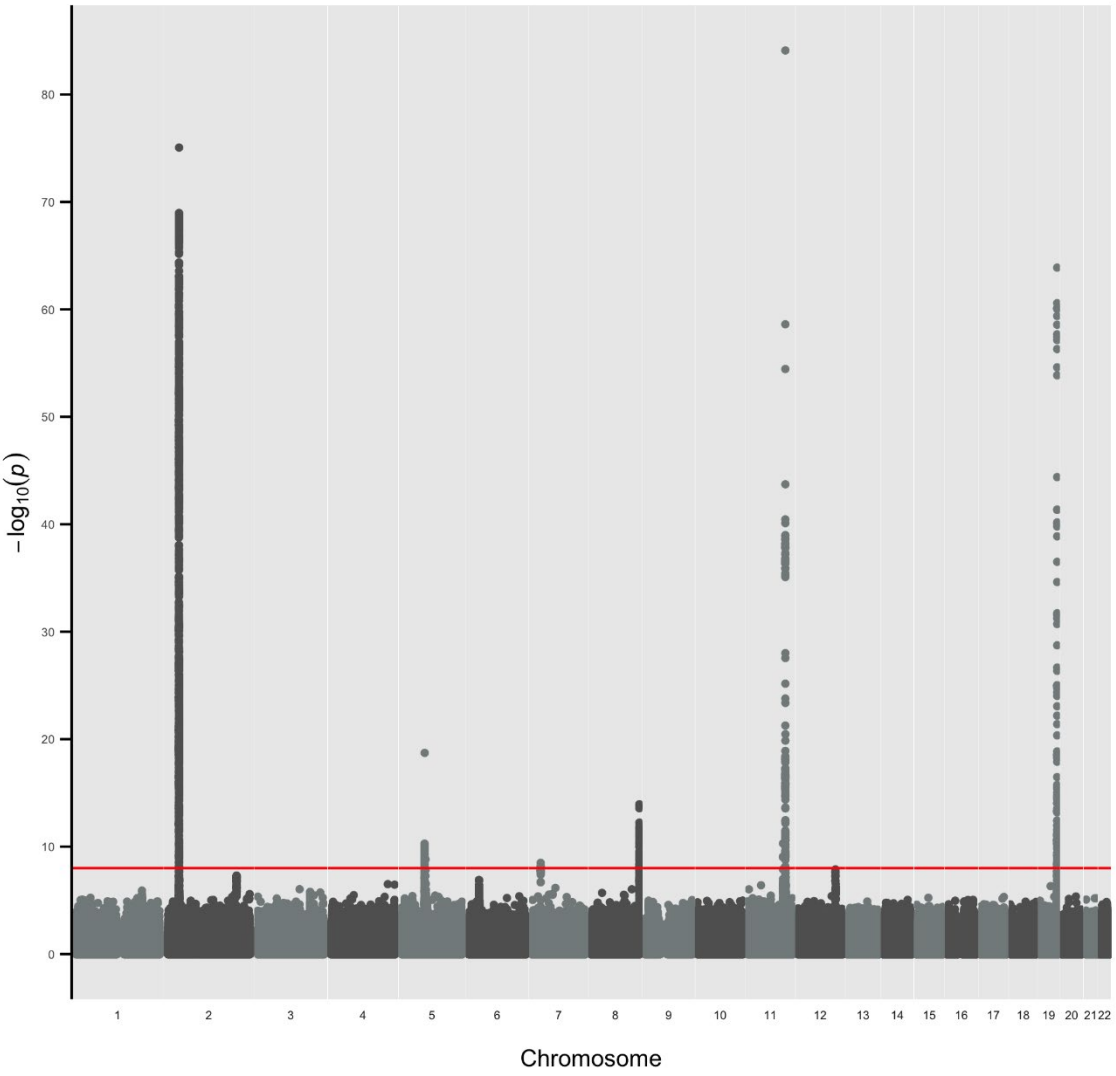

Figure A.1 (cont.)

Manhattan plot for Interleukin-1-beta (IL-1b)

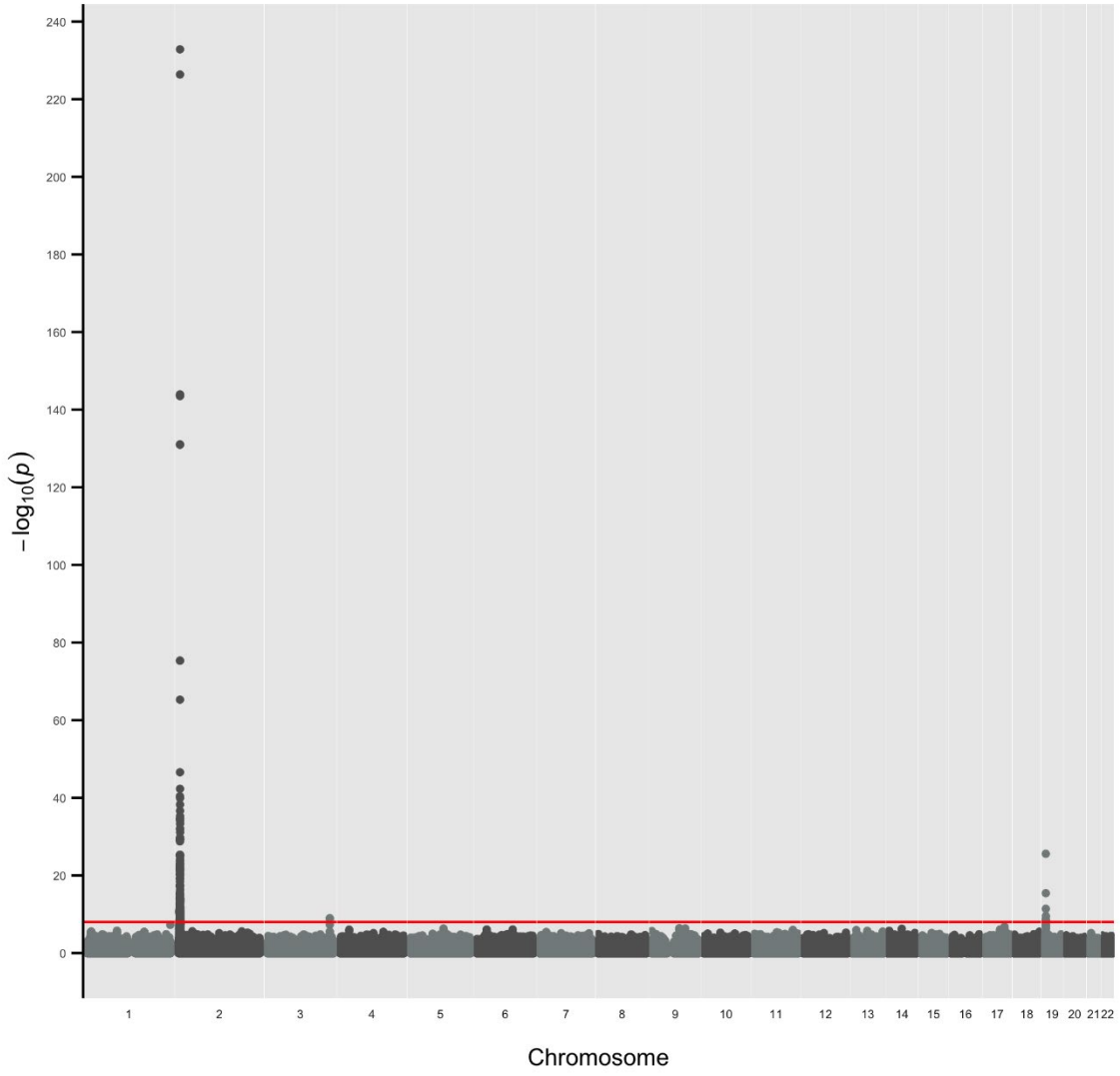

Figure A.1 (cont.)

Manhattan plot for Interleukin-1 receptor antagonist (IL-1ra)

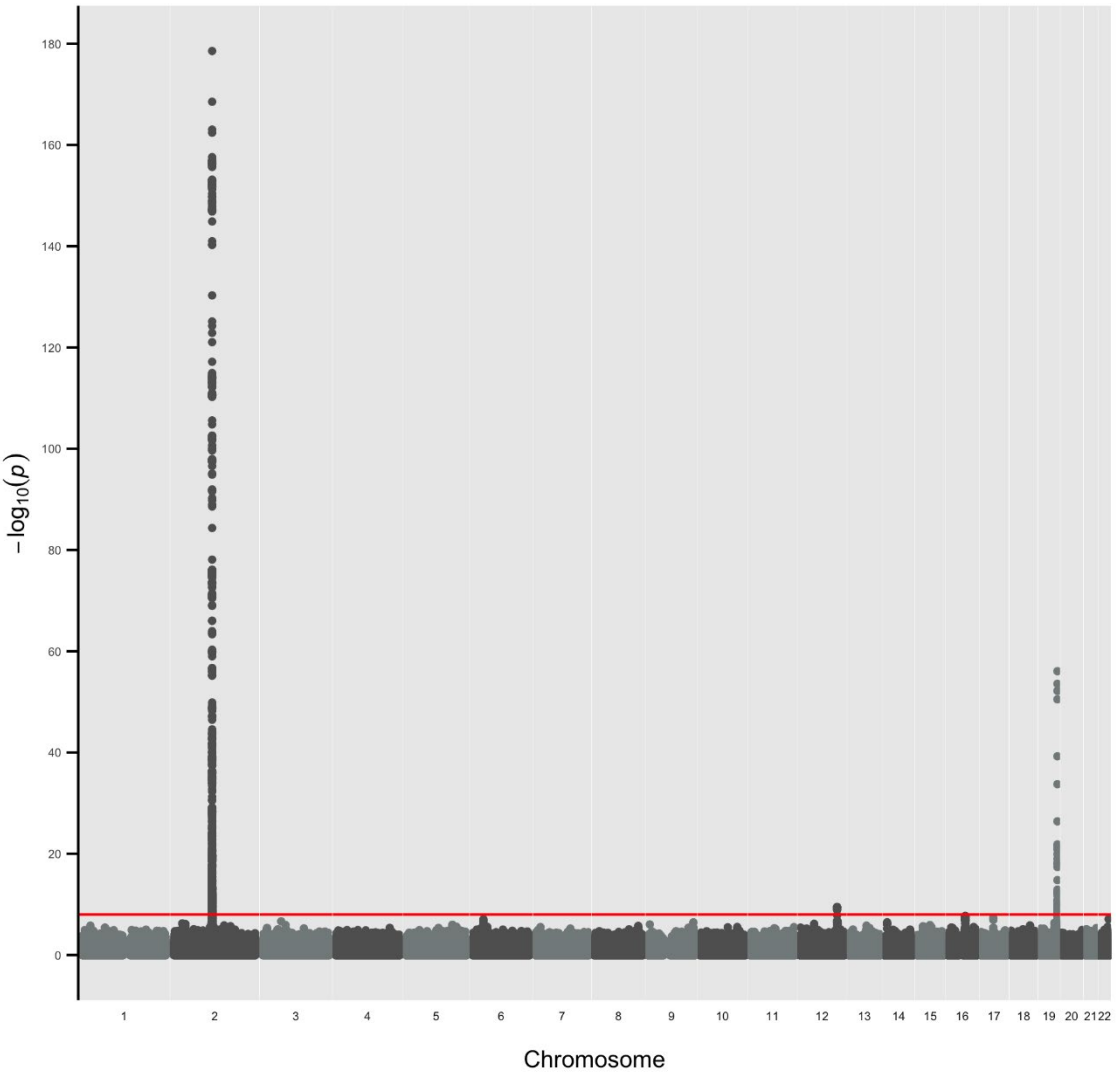

Figure A.1 (cont.)

Manhattan plot for Interleukin-2 (IL-2)

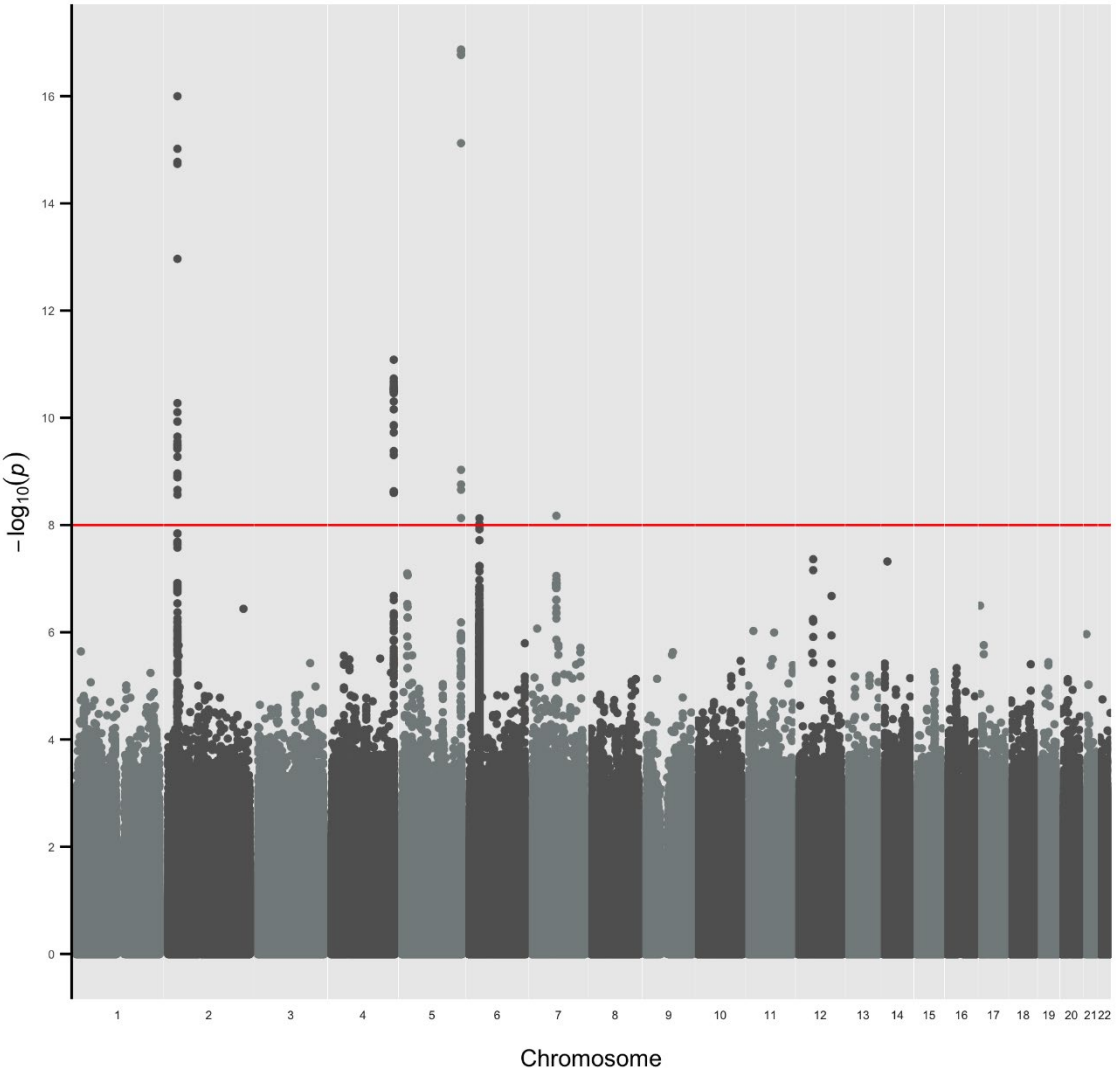

Figure A.1 (cont.)

Manhattan plot for Interleukin-2 receptor, alpha subunit (IL-2ra)

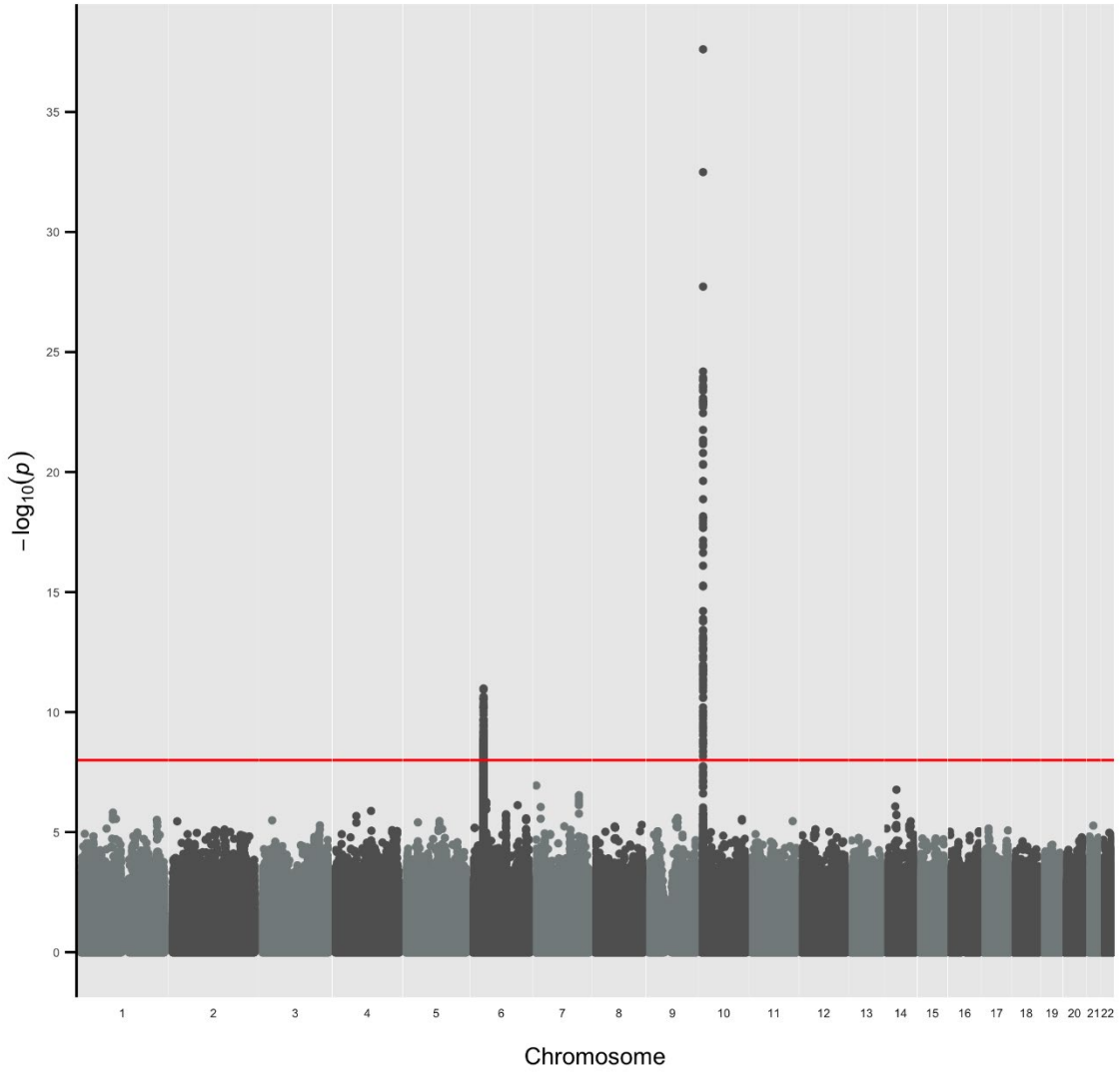

Figure A.1 (cont.)

Manhattan plot for Interleukin-4 (IL-4)

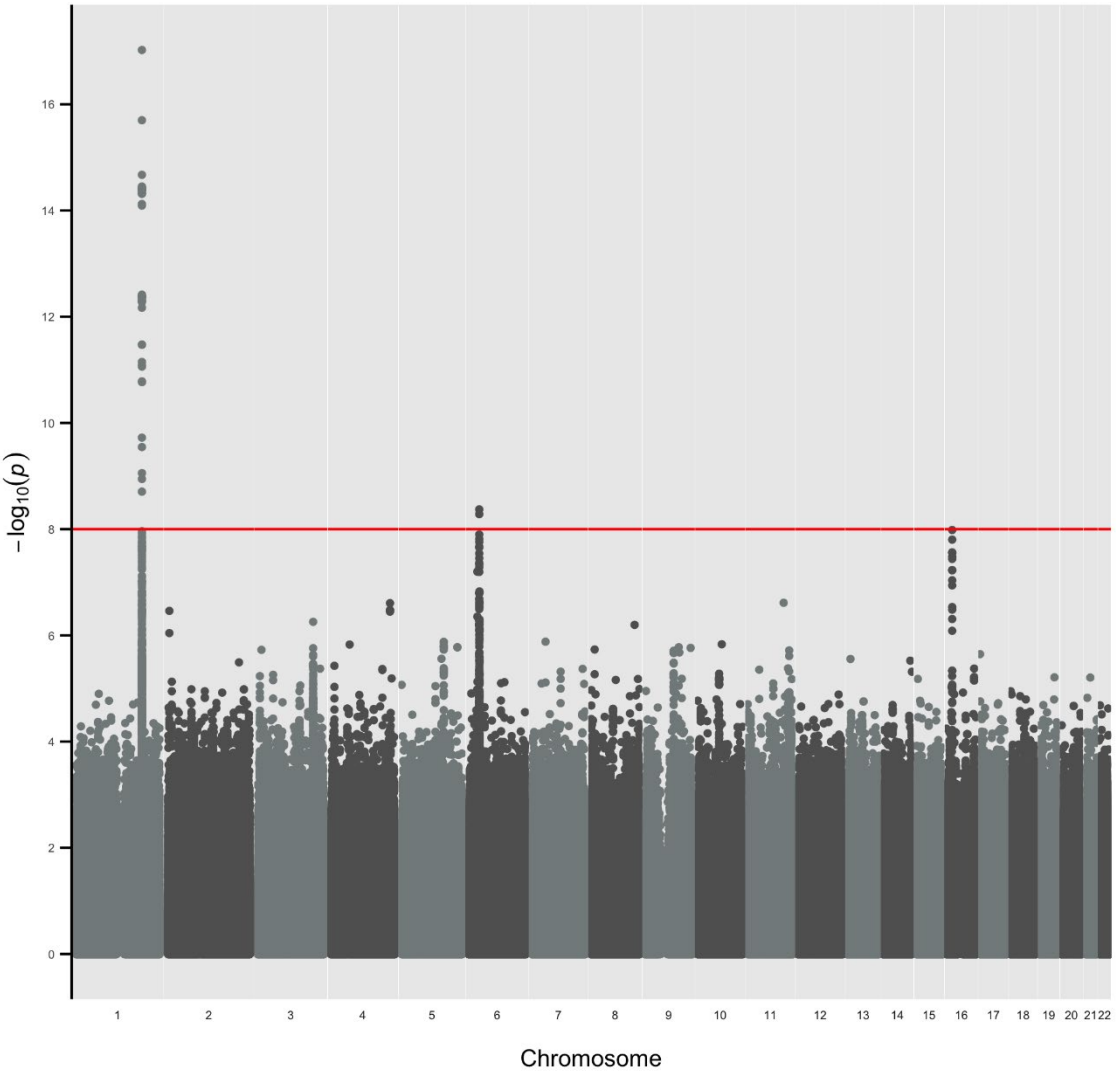

Figure A.1 (cont.)

Manhattan plot for Interleukin-5 (IL-5)

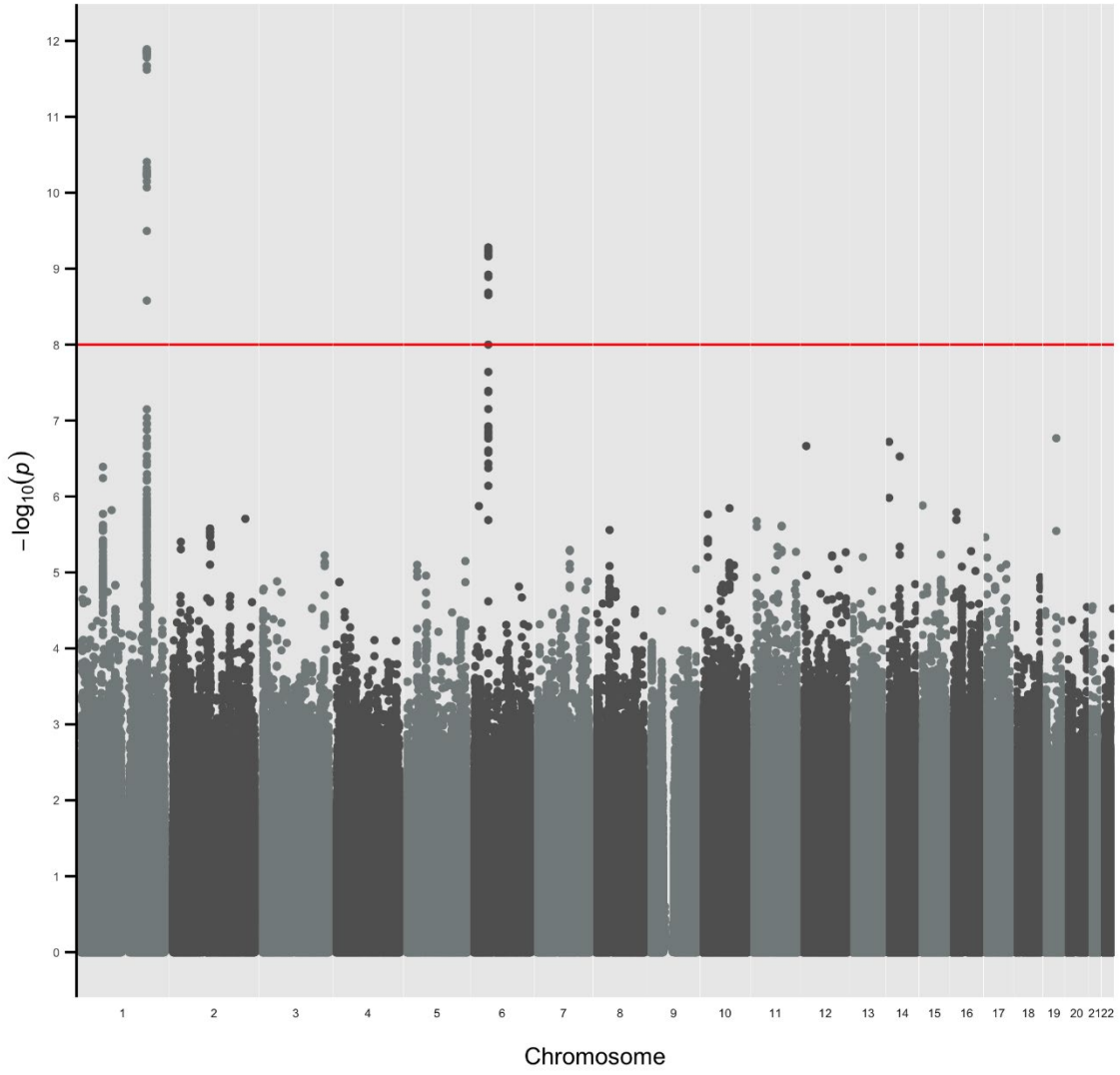

Figure A.1 (cont.)

Manhattan plot for Interleukin-6 (IL-6)

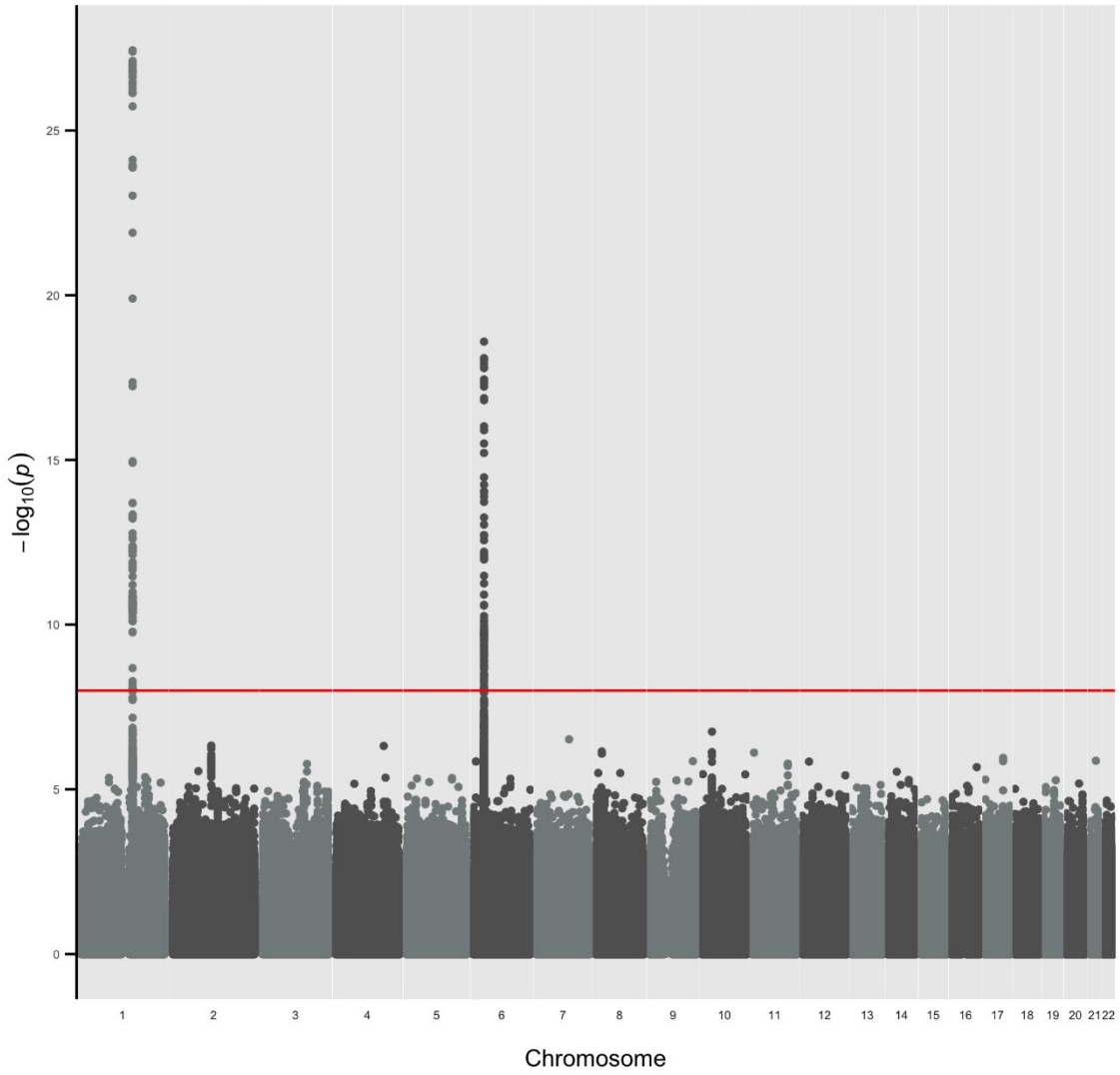

Figure A.1 (cont.)

Manhattan plot for Interleukin-7 (IL-7)

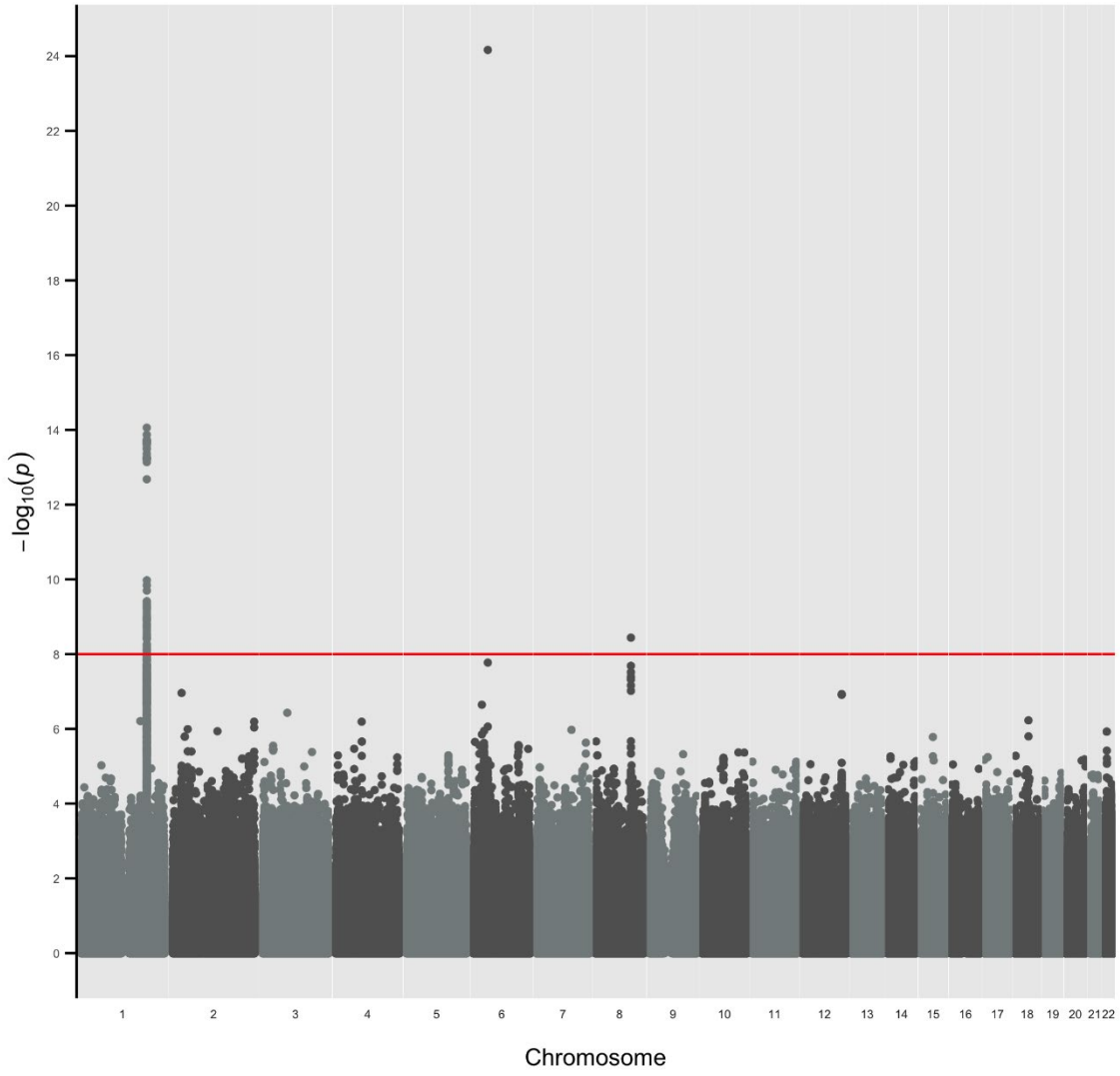

Figure A.1 (cont.)

Manhattan plot for Interleukin-8 (CXCL8/IL-8)

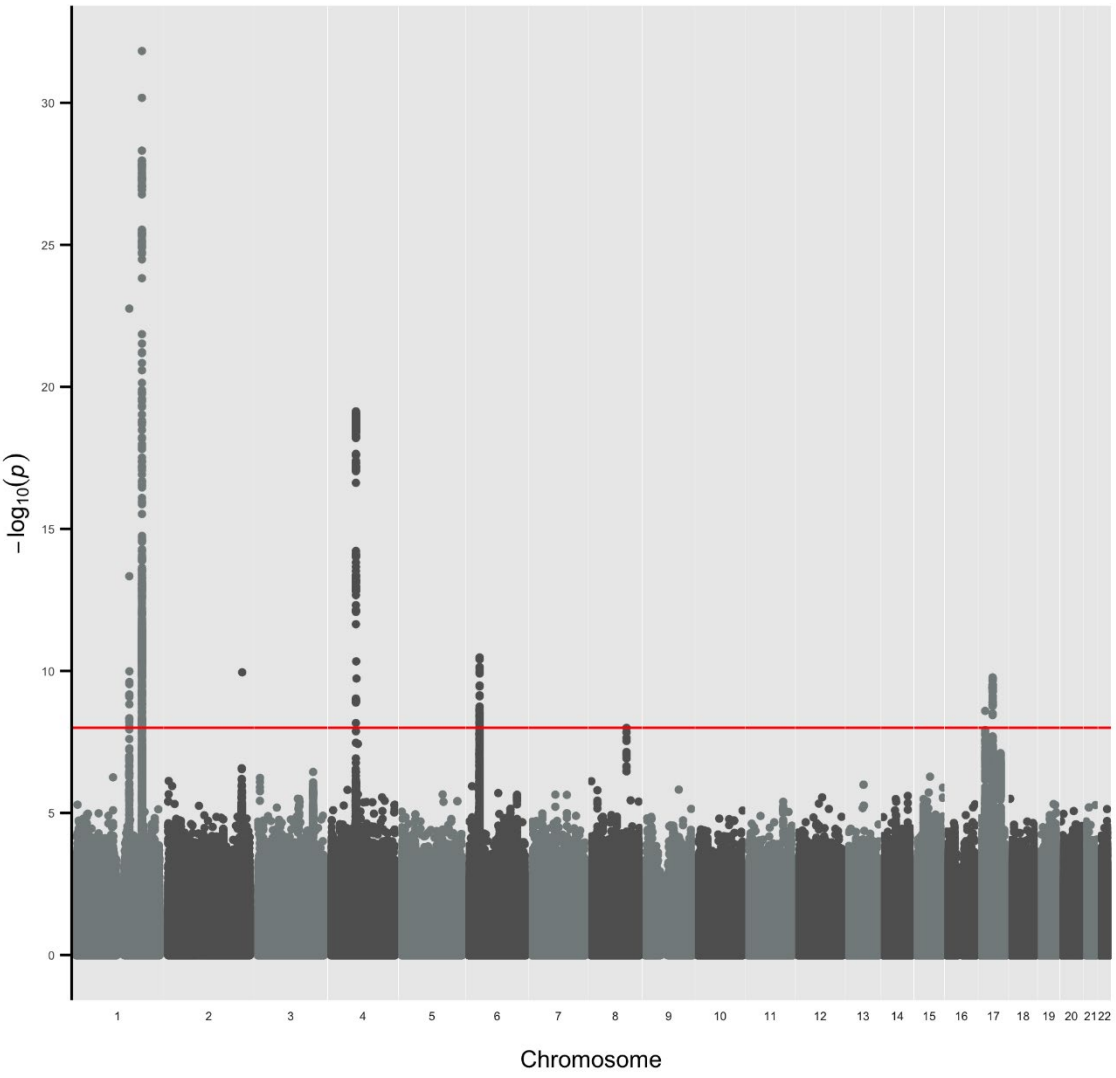

Figure A.1 (cont.)

Manhattan plot for Interleukin-9 (IL-9)

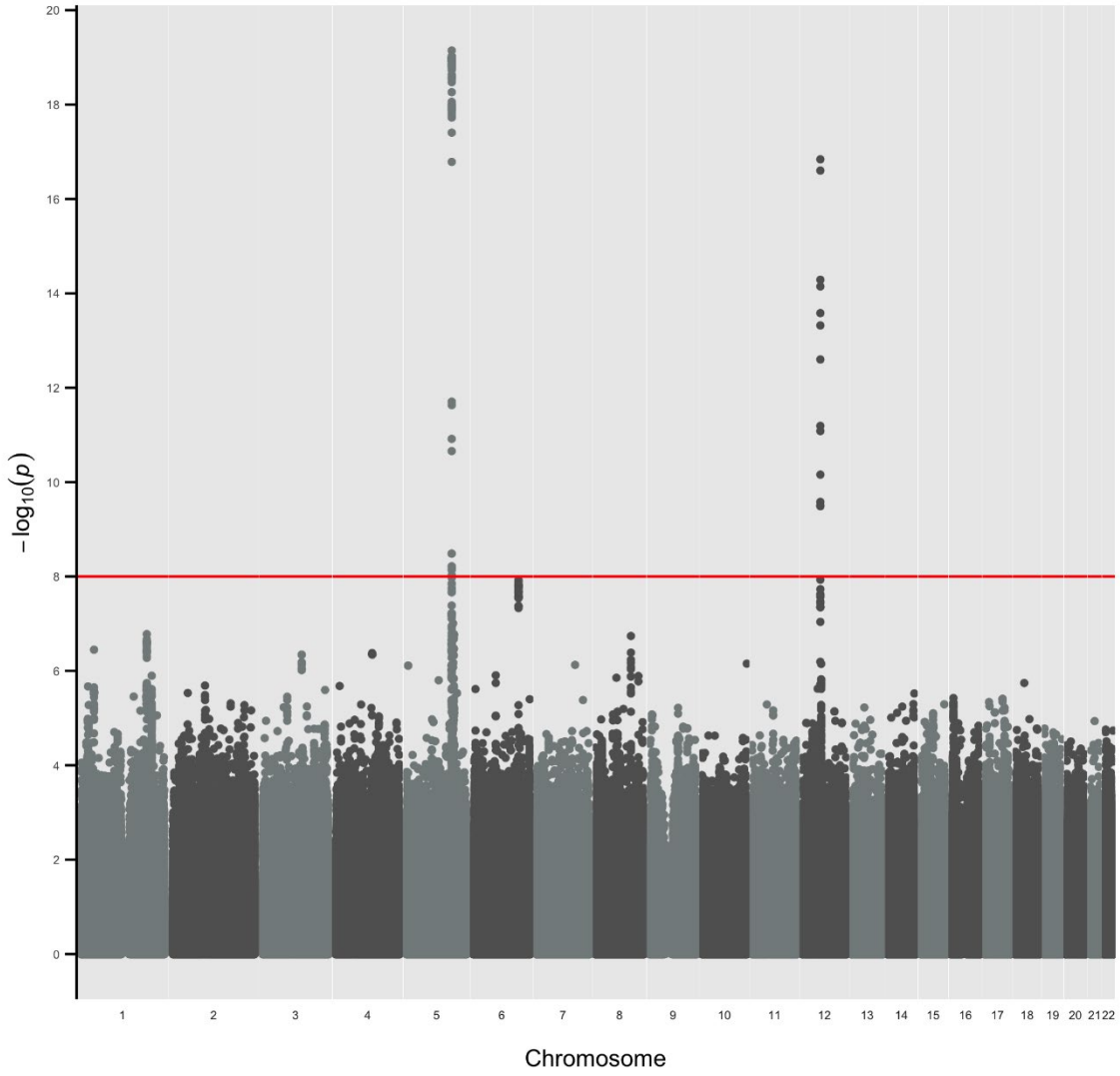

Figure A.1 (cont.)

Manhattan plot for Interferon gamma-induced protein 10 (CXCL10/IP-10)

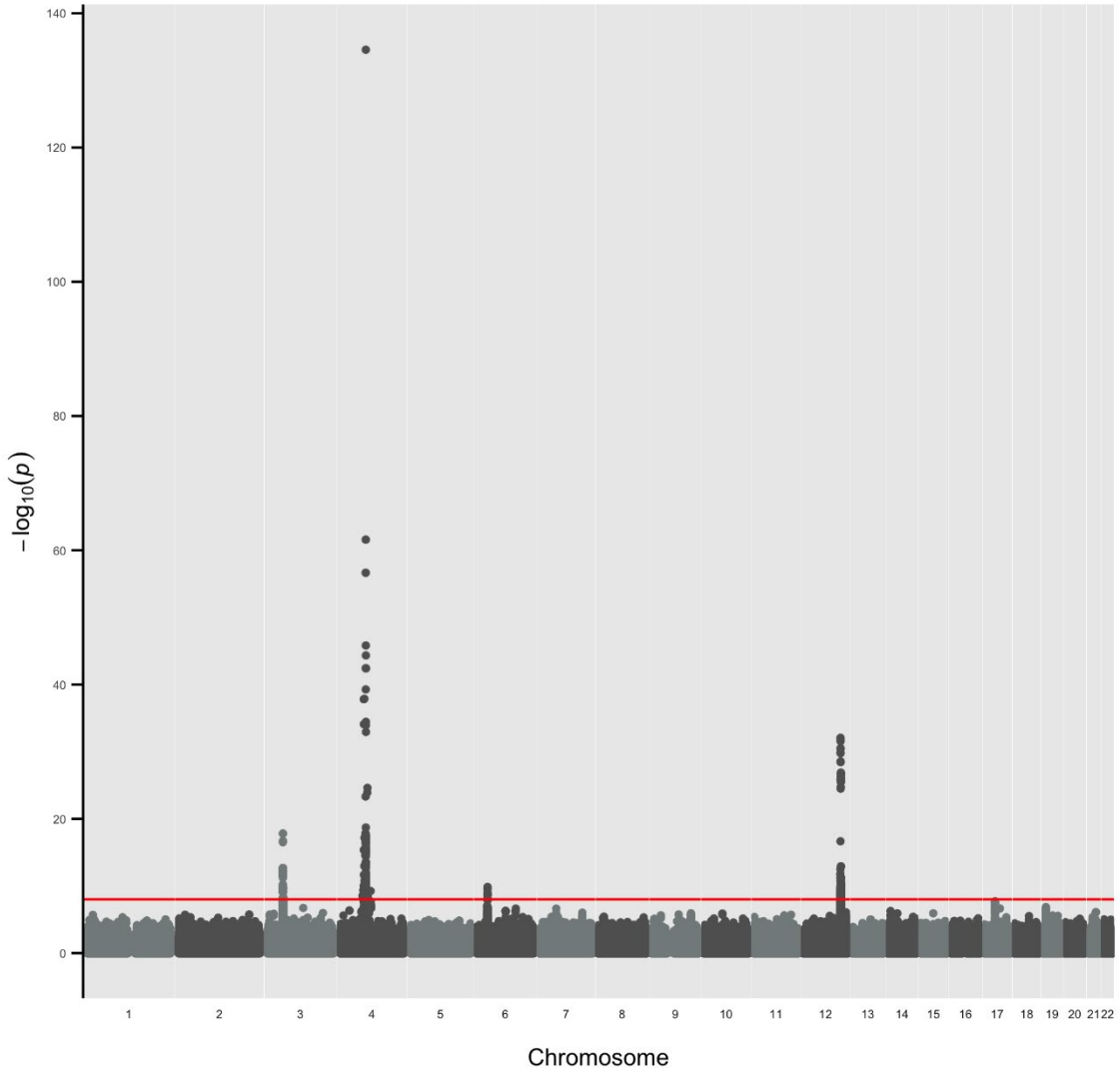

Figure A.1 (cont.)

Manhattan plot for Monocyte chemotactic protein-1 (CCL2/MCP-1)

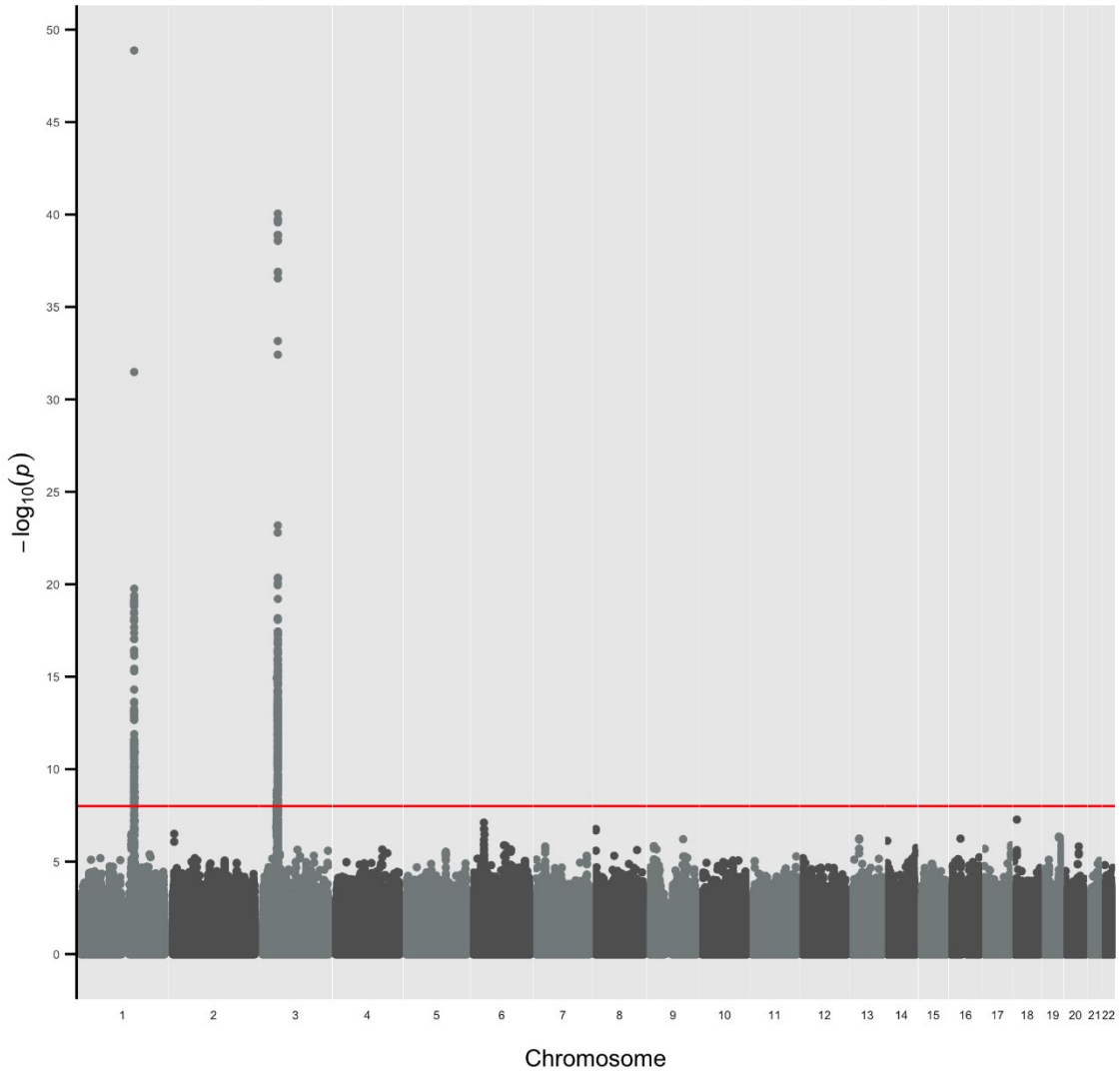

Figure A.1 (cont.)

Manhattan plot for Monocyte specific chemokine 3 (CCL7/MCP-3)

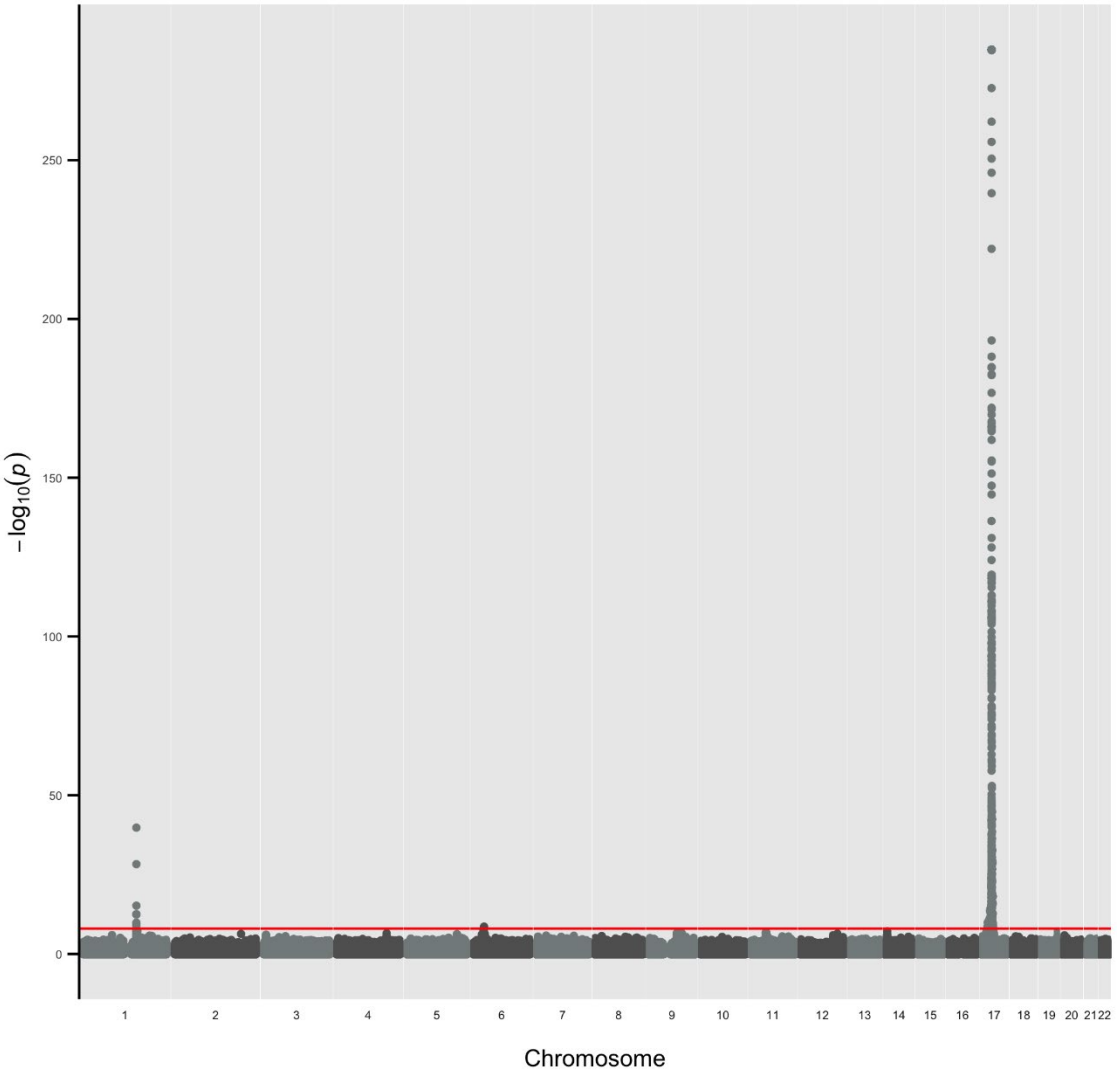

Figure A.1 (cont.)

Manhattan plot for Macrophage colony-stimulating factor (M-CSF/CSF-1)

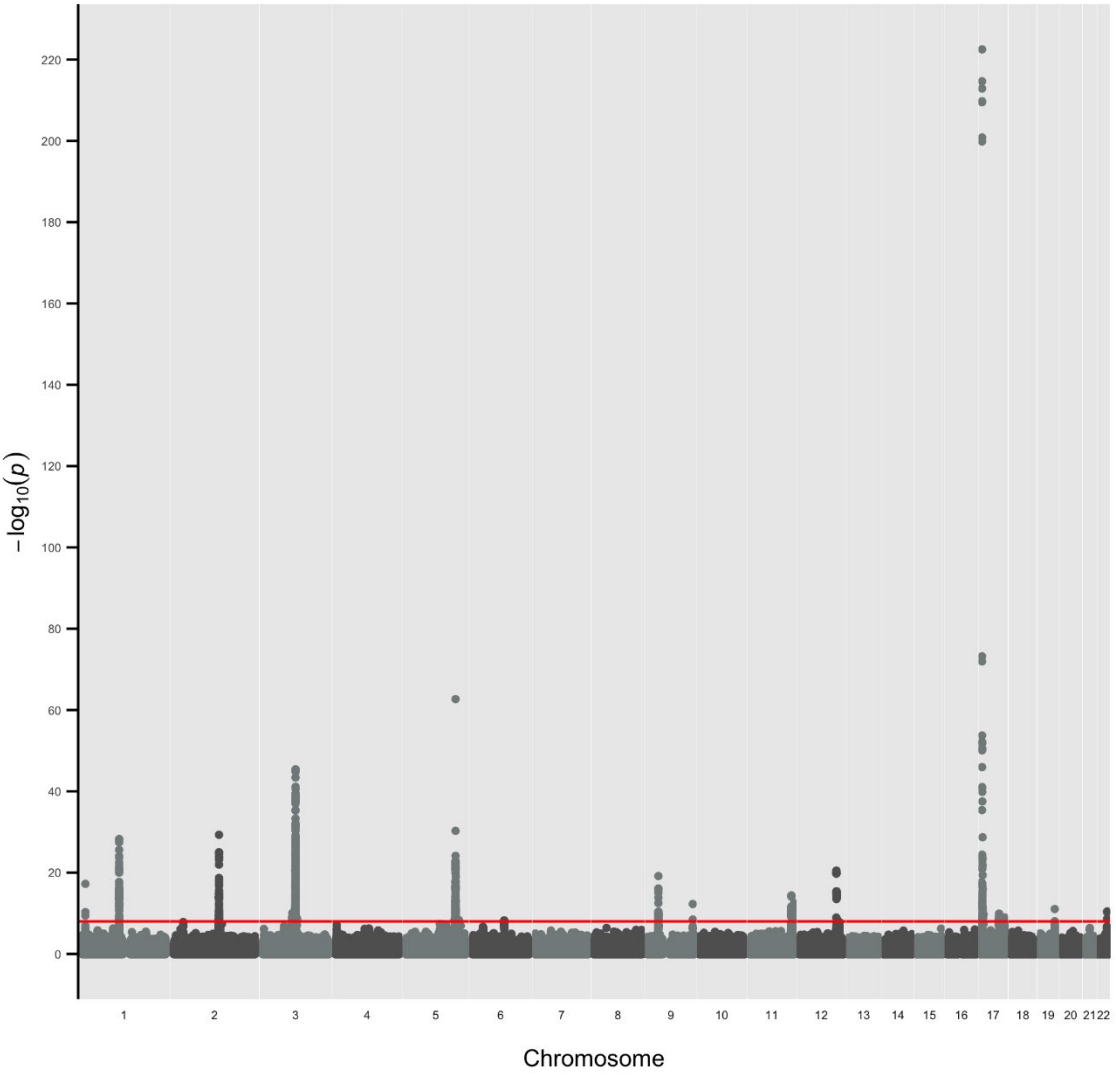

Figure A.1 (cont.)

Manhattan plot for Macrophage migration inhibitory factor (MIF)

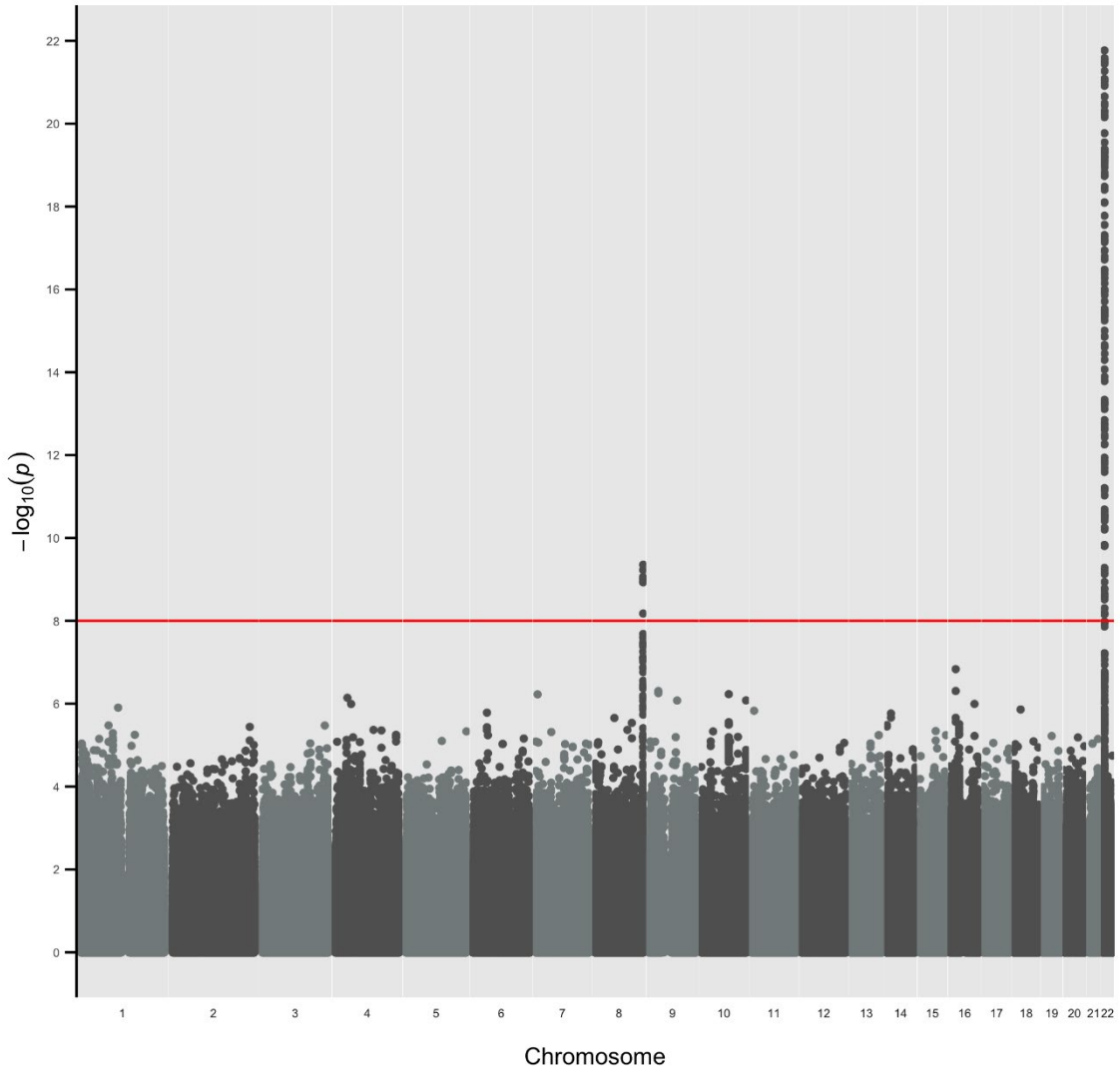

Figure A.1 (cont.)

Manhattan plot for Monokine induced by interferon-gamma (CXCL9/MIG)

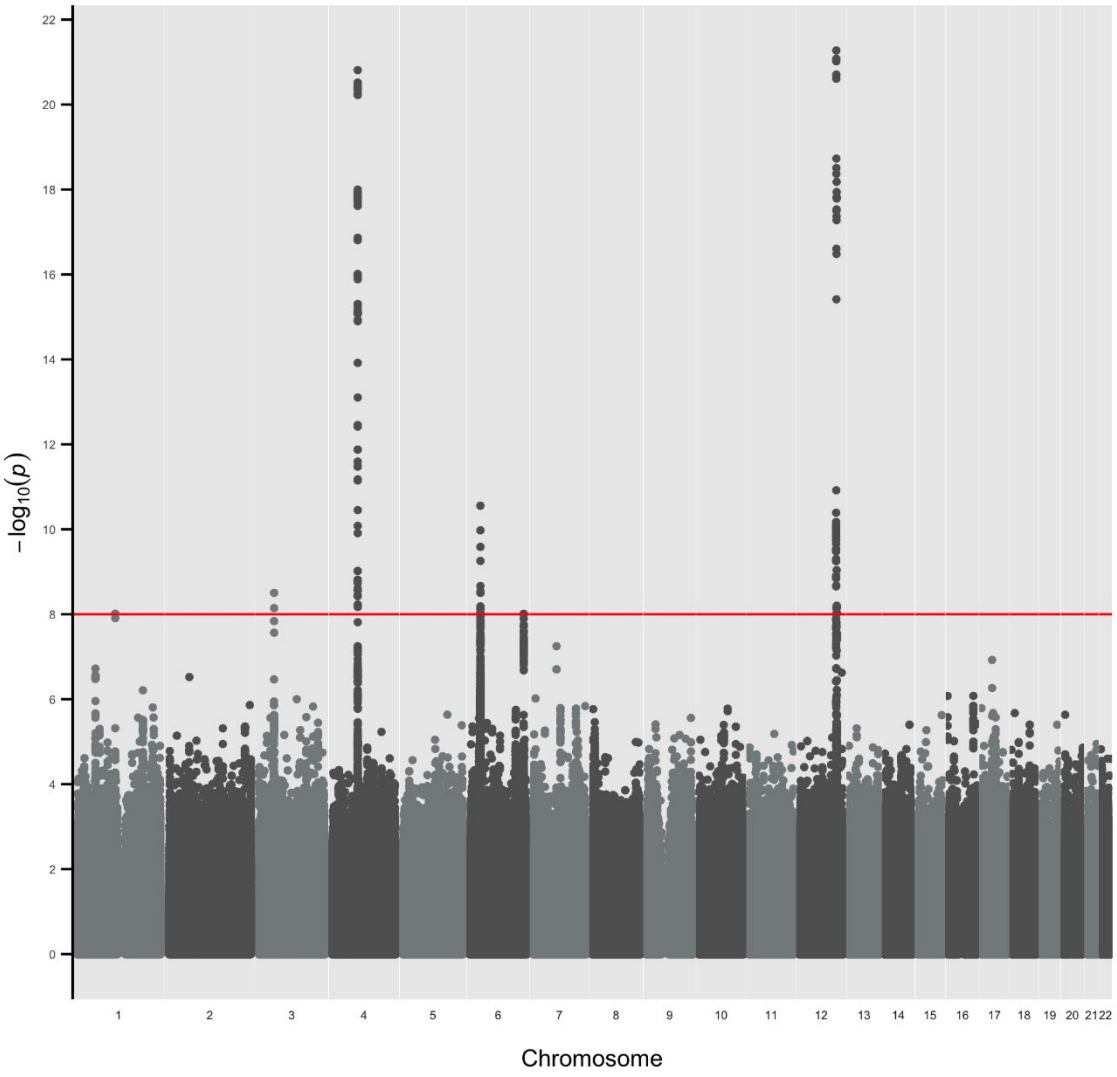

Figure A.1 (cont.)

Manhattan plot for Macrophage inflammatory protein-1 alpha (CCL3/MIP-1a)

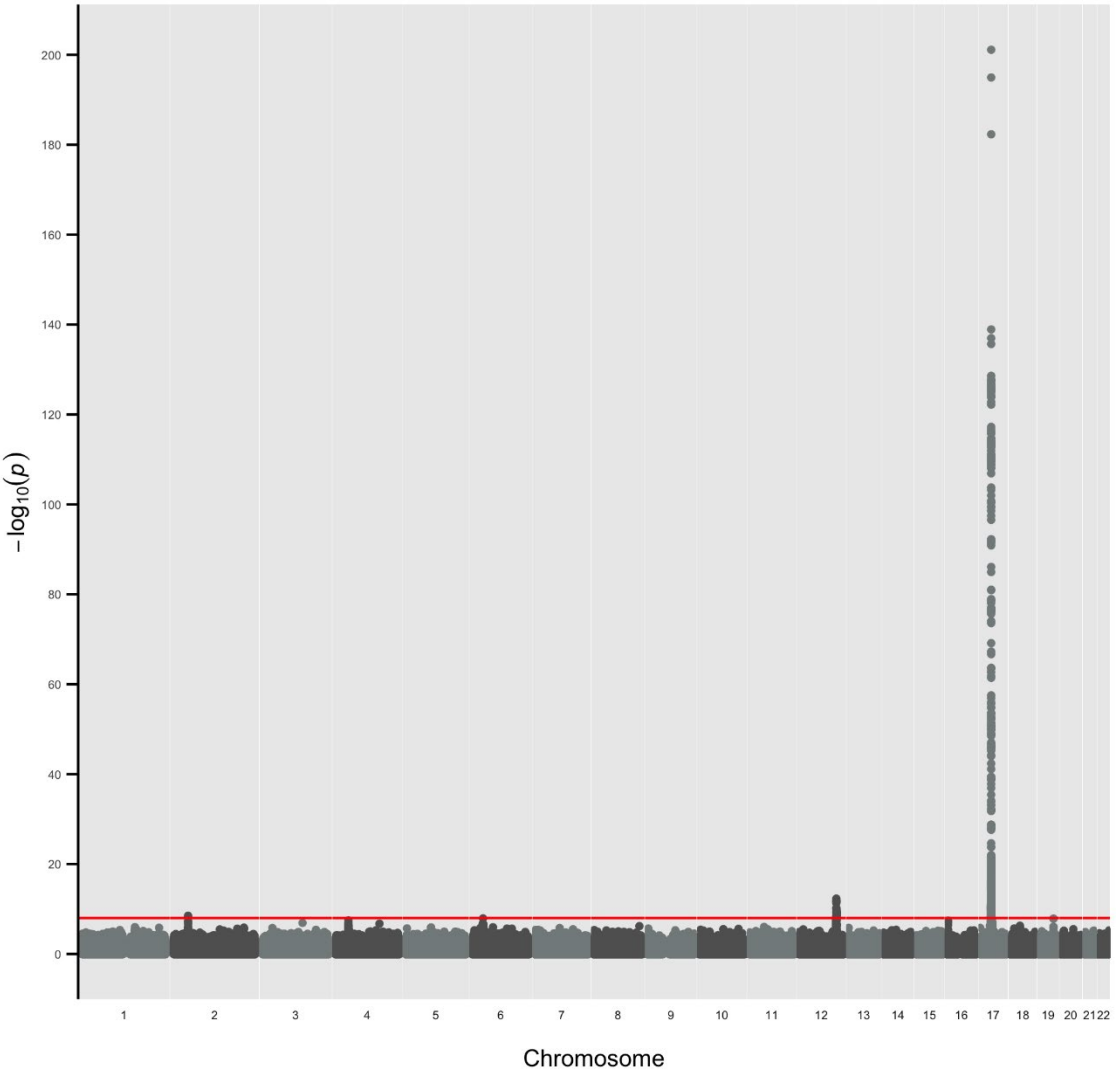

Figure A.1 (cont.)

Manhattan plot for Macrophage inflammatory protein-1 beta (CCL4/MIP-1b)

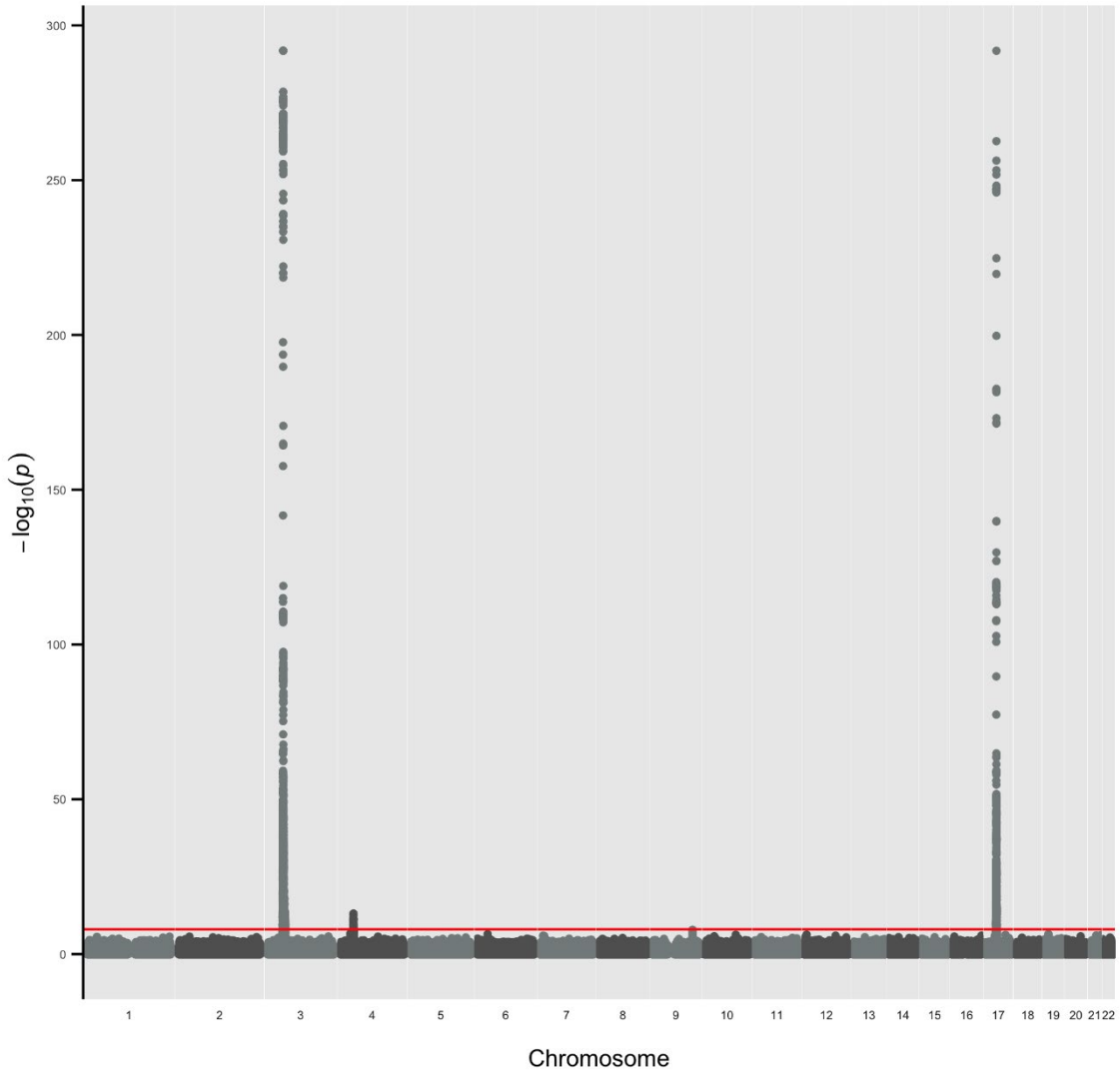

Figure A.1 (cont.)

Manhattan plot for Platelet derived growth factor BB (PDGFbb)

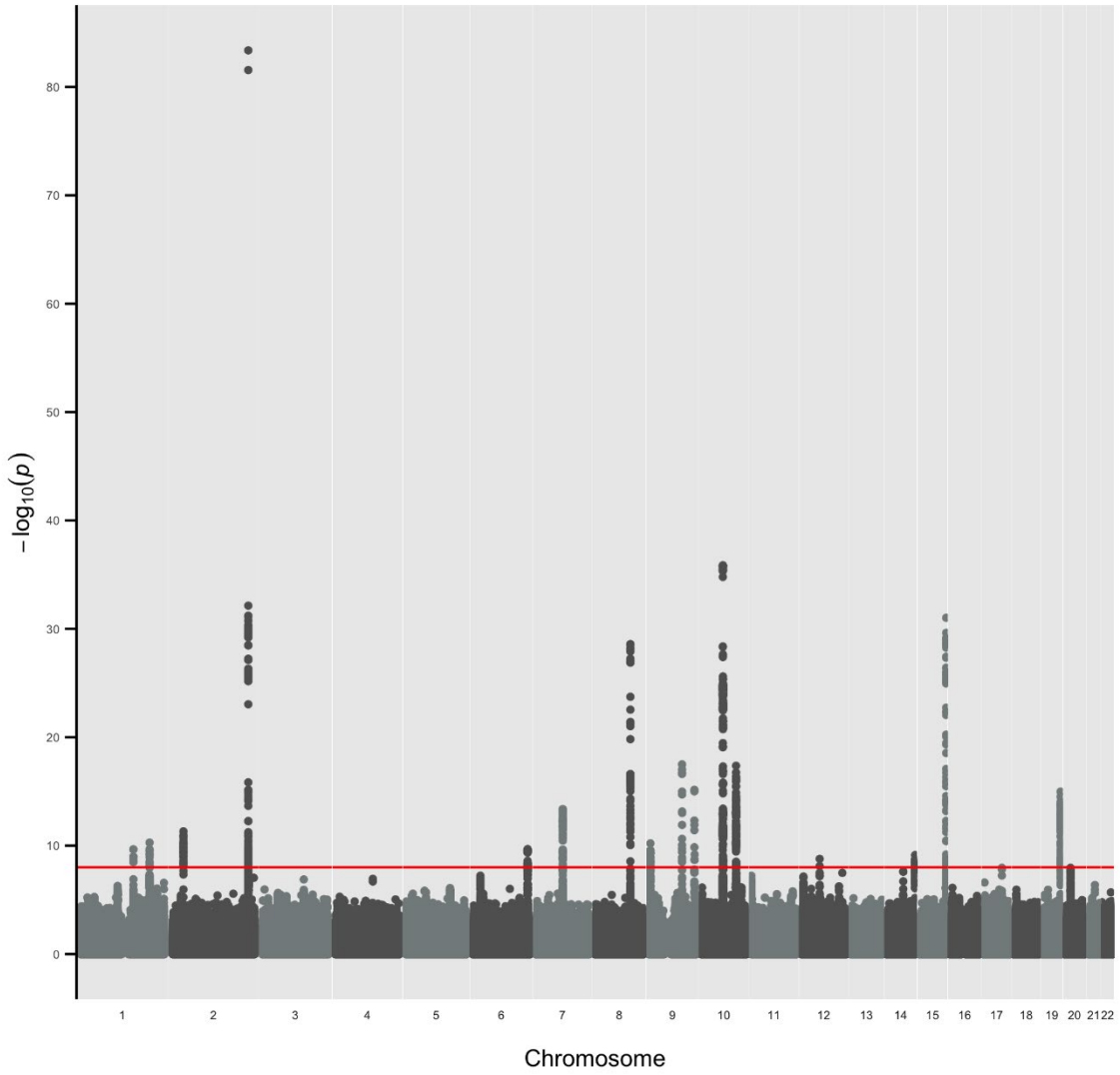

Figure A.1 (cont.)

Manhattan plot for Regulated on Activation, Normal T Cell Expressed and Secreted (RANTES)

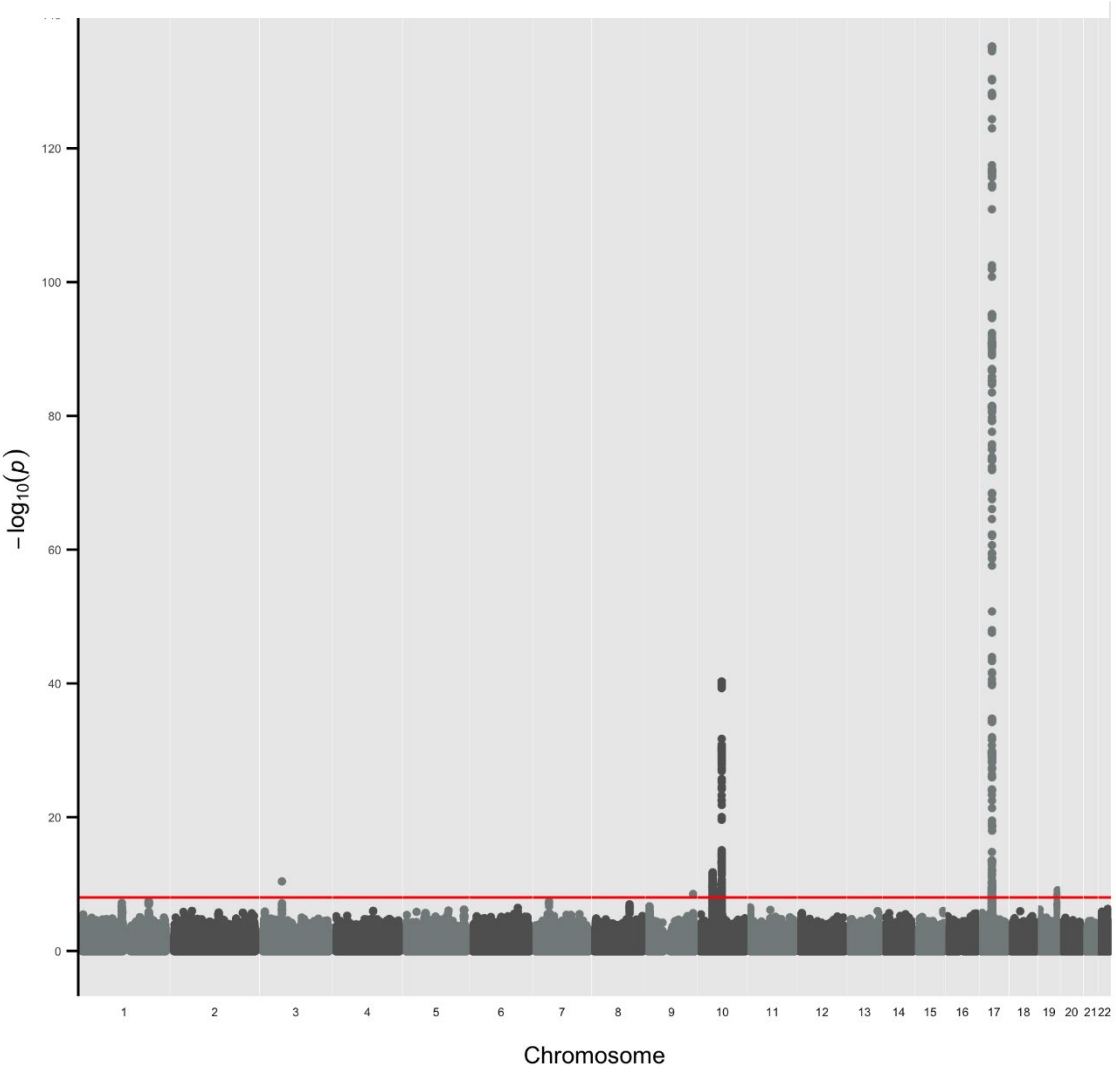

Figure A.1 (cont.)

Manhattan plot for Stem cell factor (SCF)

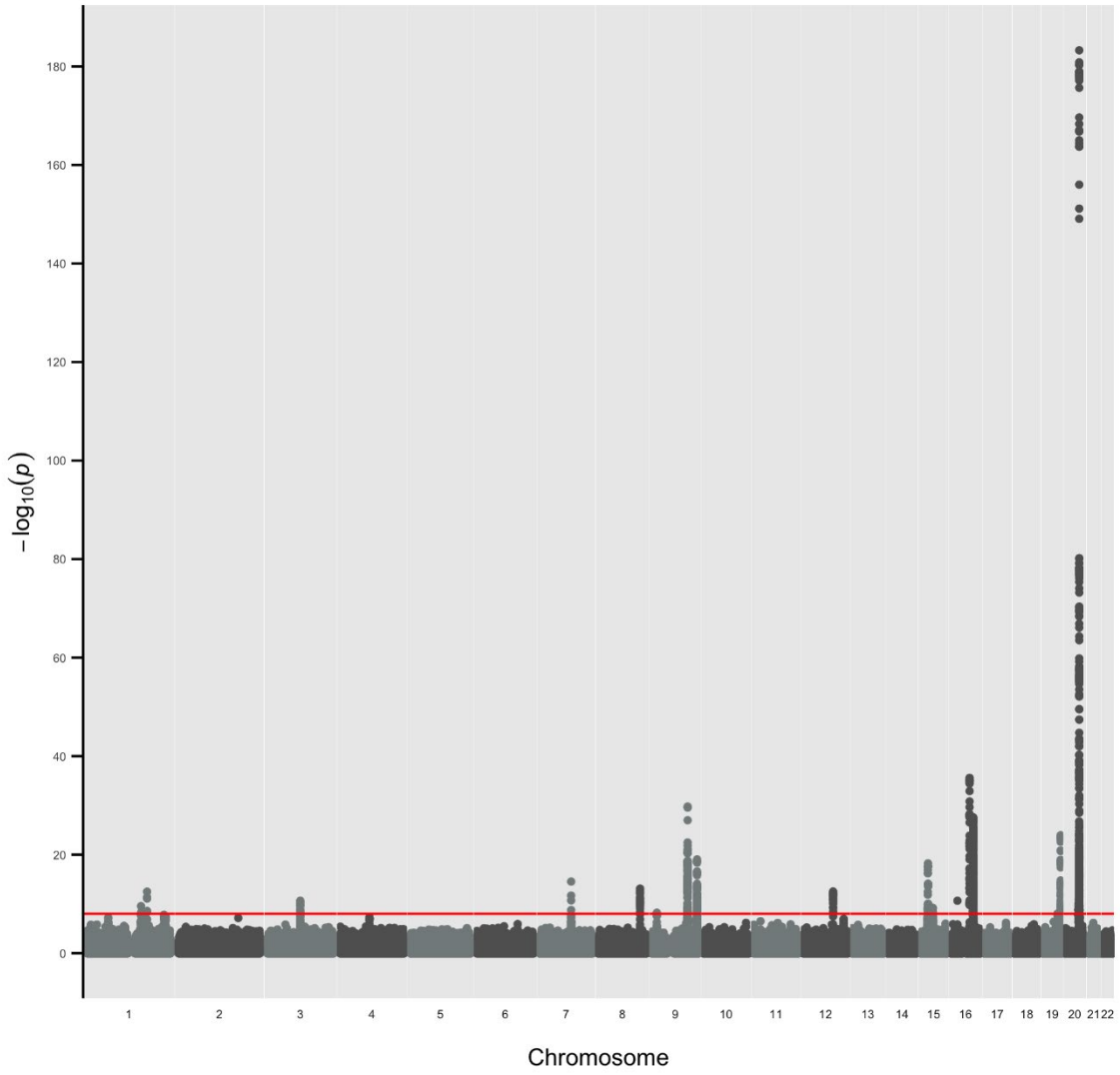

Figure A.1 (cont.)

Manhattan plot for Stromal cell-derived factor-1 alpha (CXCL12/SDF-1a)

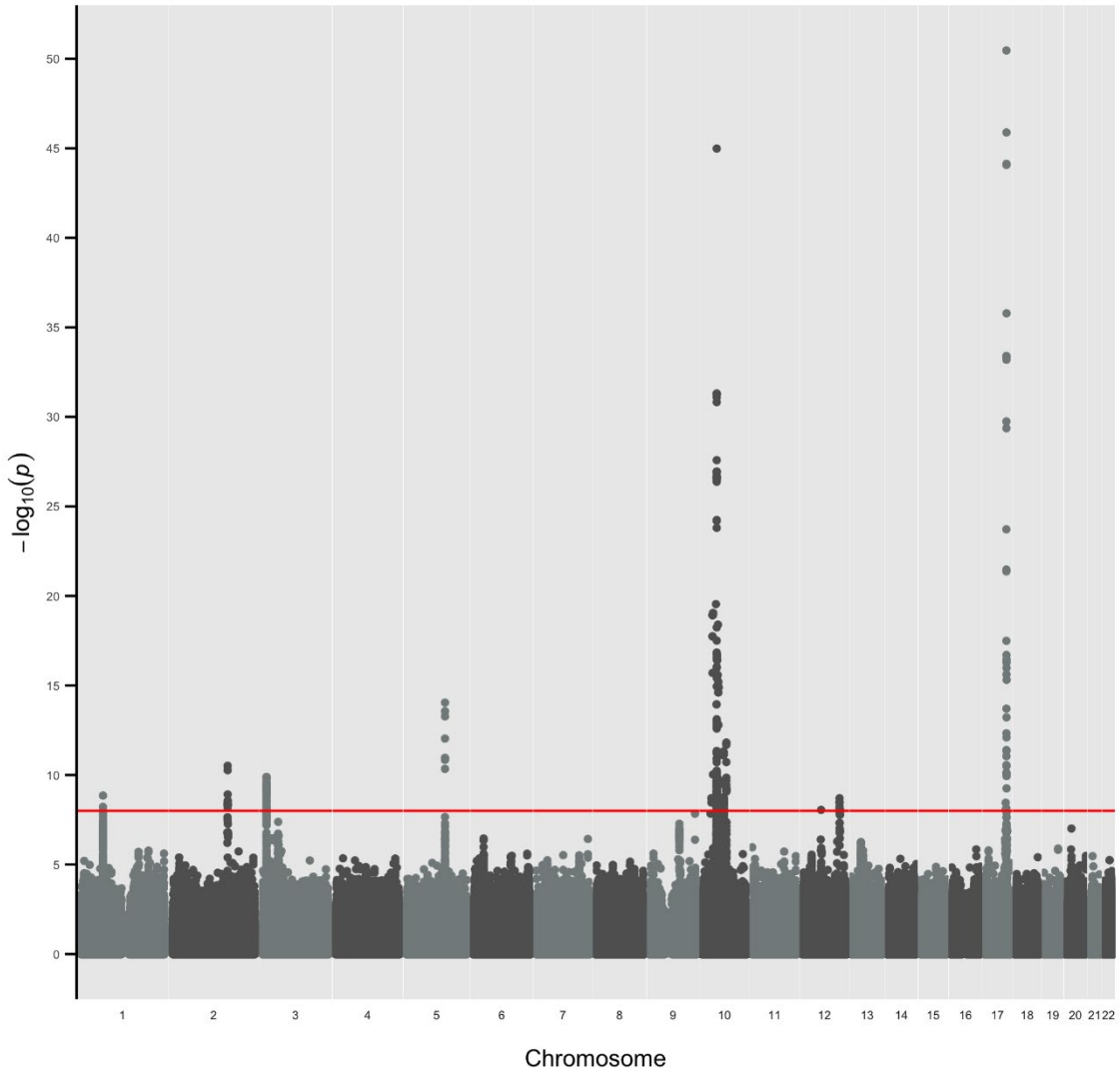

Figure A.1 (cont.)

Manhattan plot for Tumor necrosis factor-alpha (TNF-a)

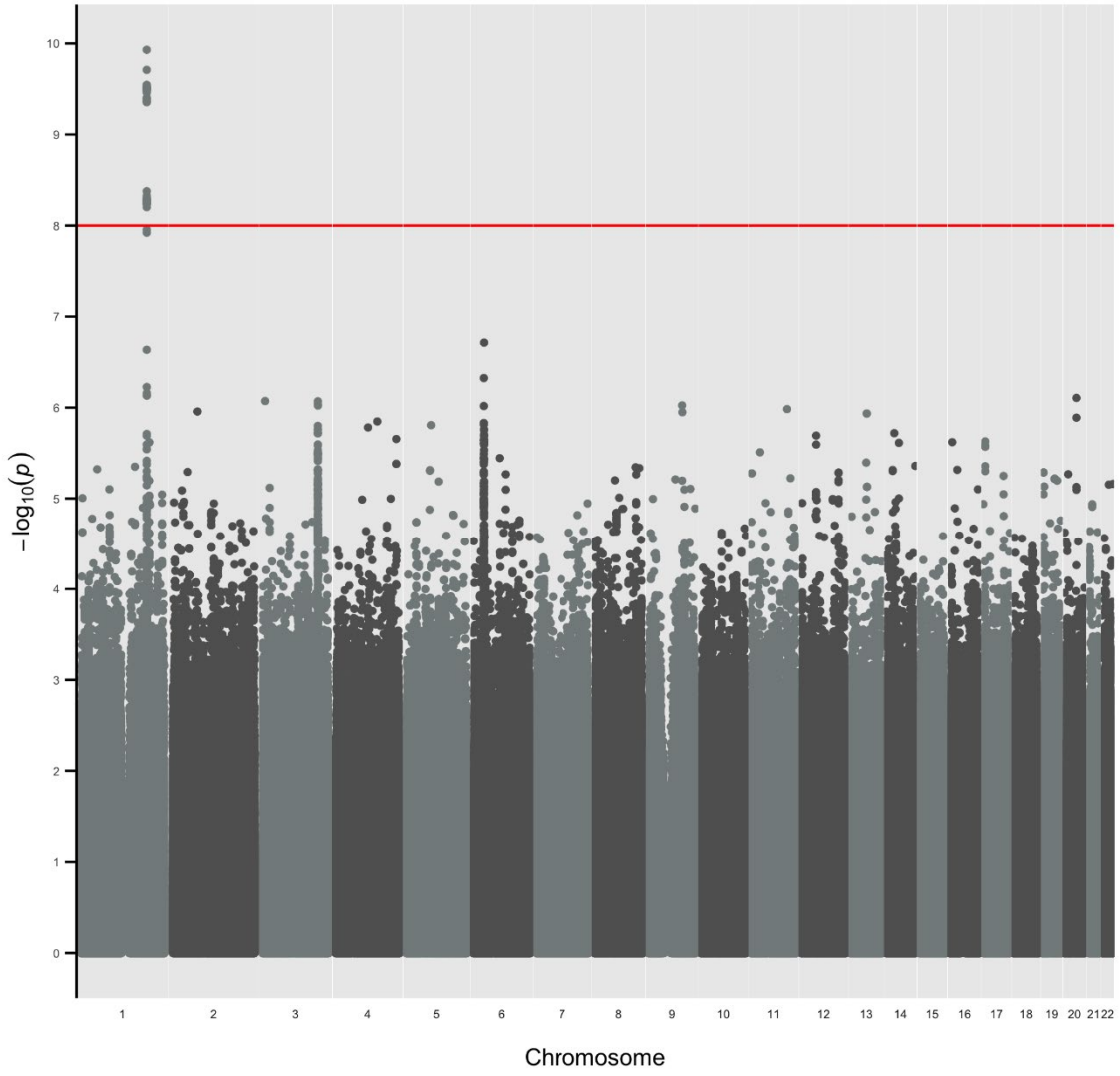

Figure A.1 (cont.)

Manhattan plot for Tumor necrosis factor-beta (TNF-b)

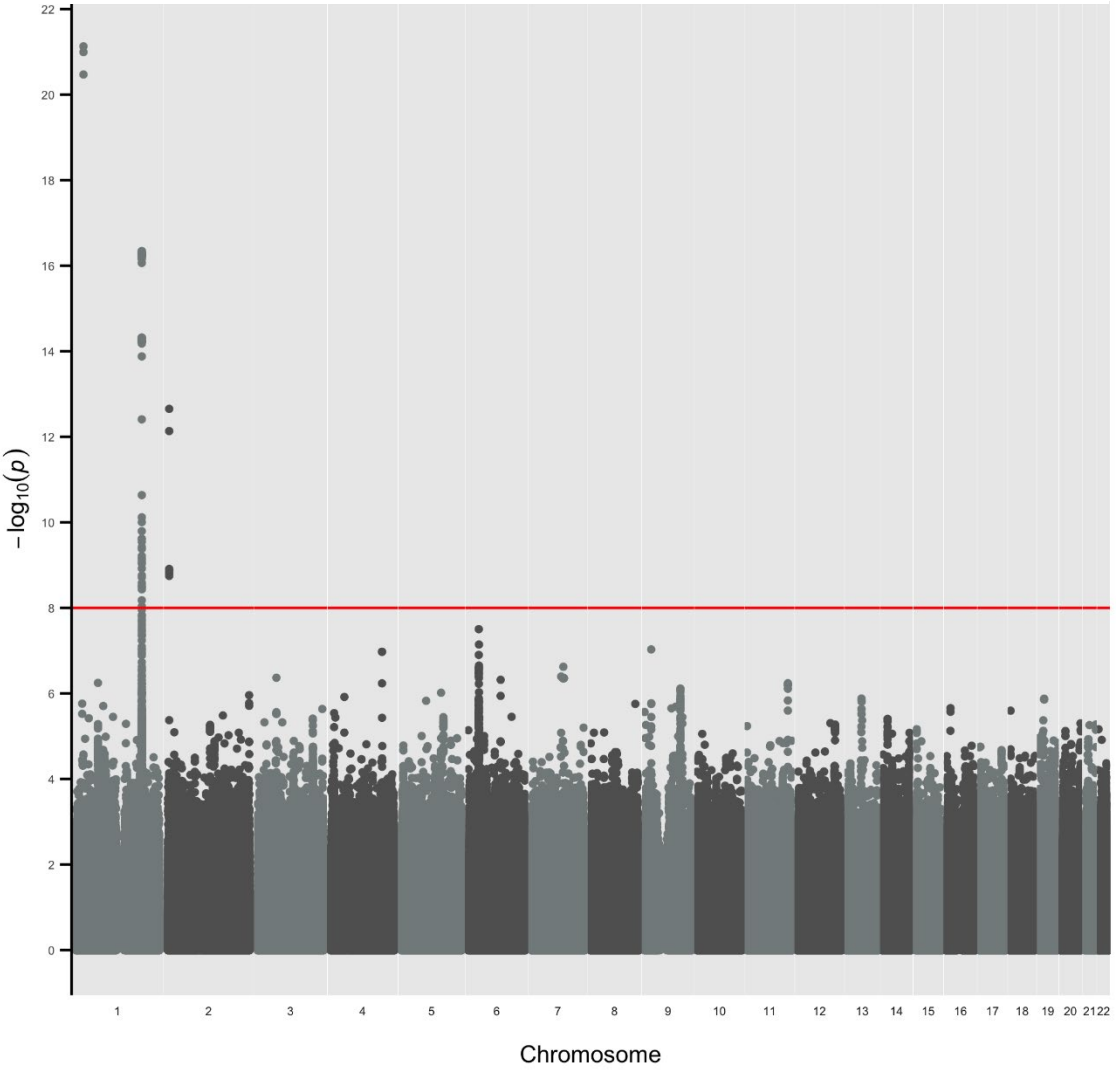

Figure A.1 (cont.)

Manhattan plot for TNF-related apoptosis inducing ligand (TRAIL)

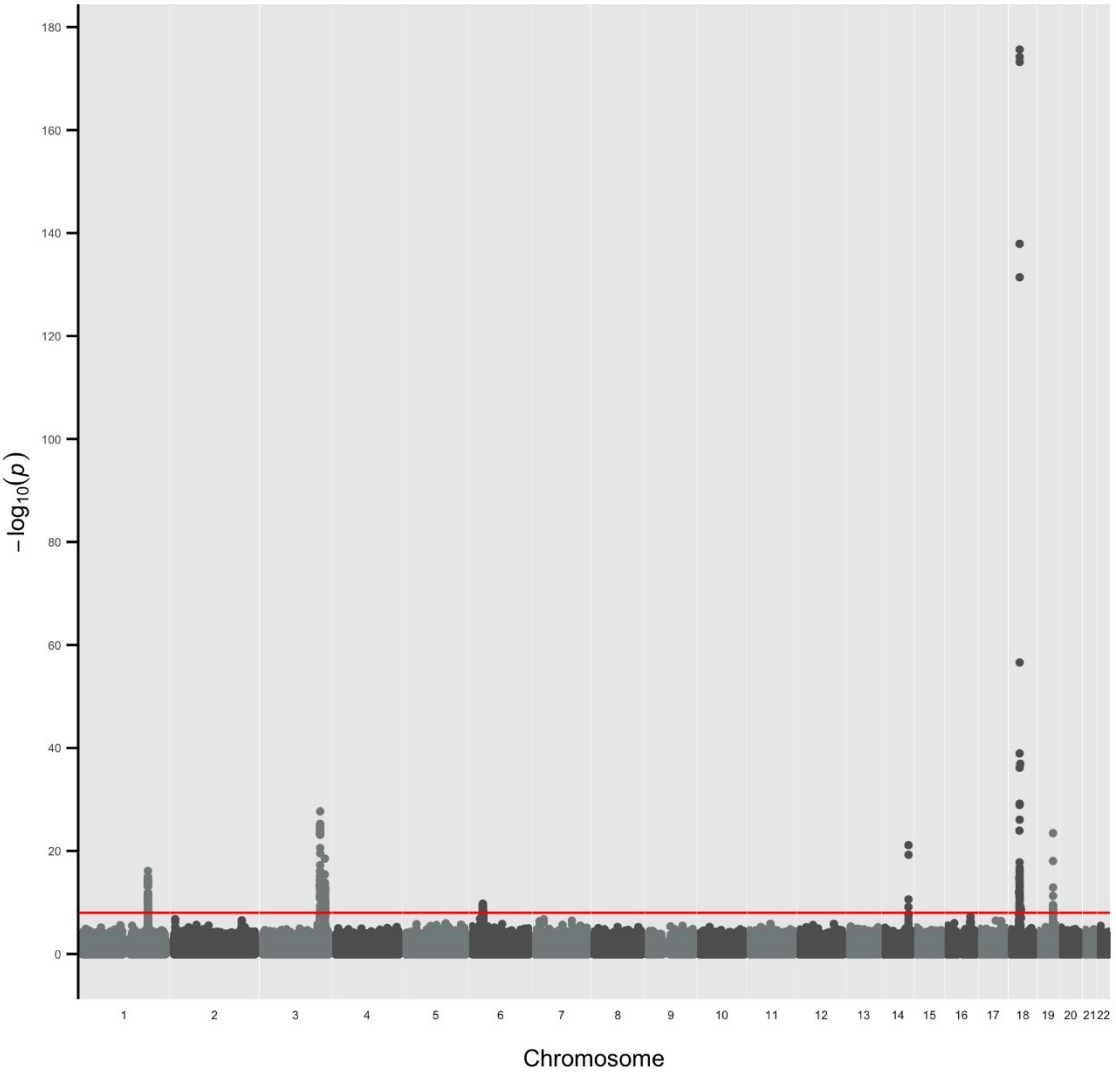

Figure A.1 (cont.)

Manhattan plot for Vascular endothelial growth factor (VEGF)

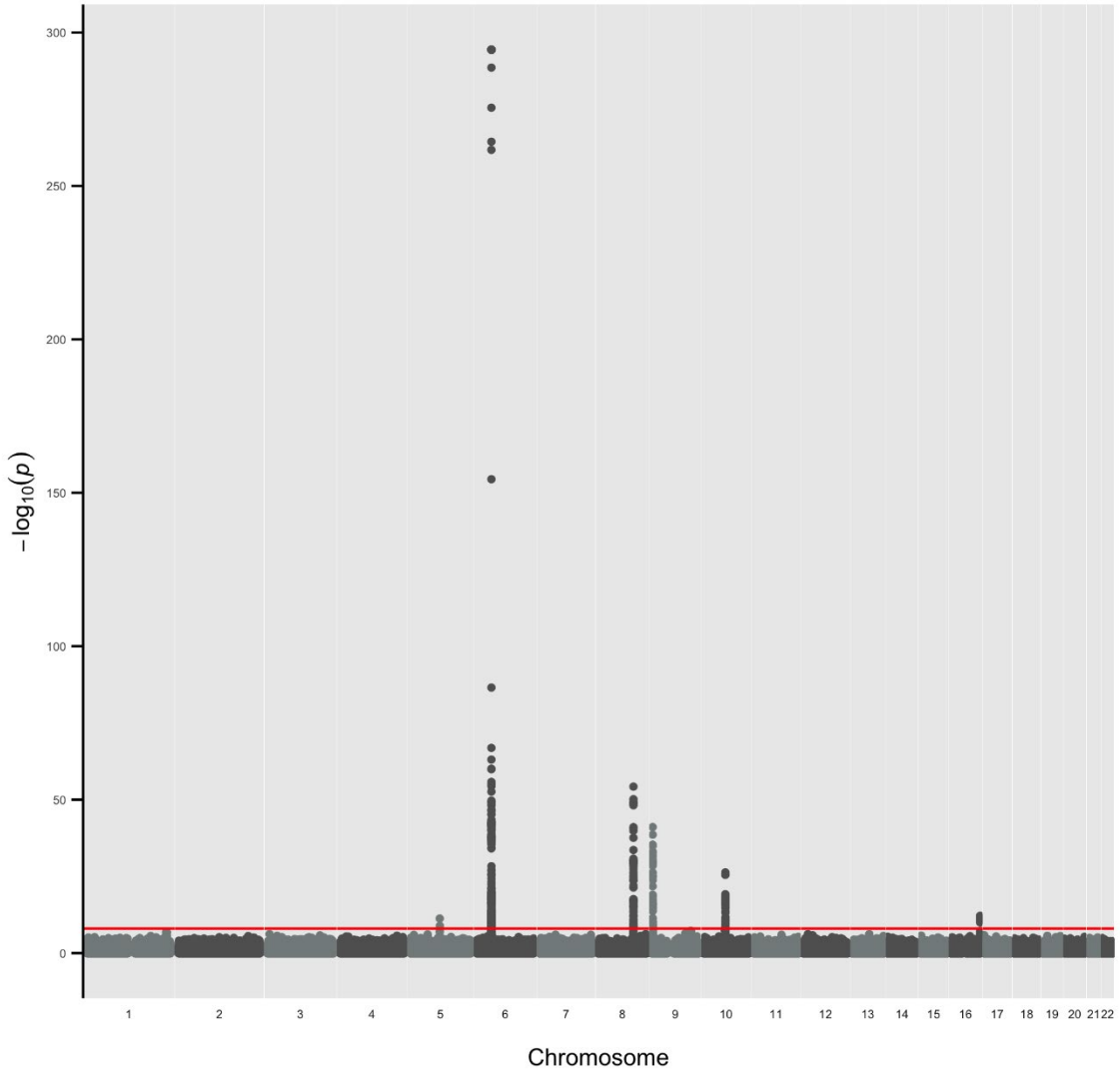

Figure A.2. Locus Zoom plot. Locus zoom plots for the 4 significant cytokine-disease pairings.

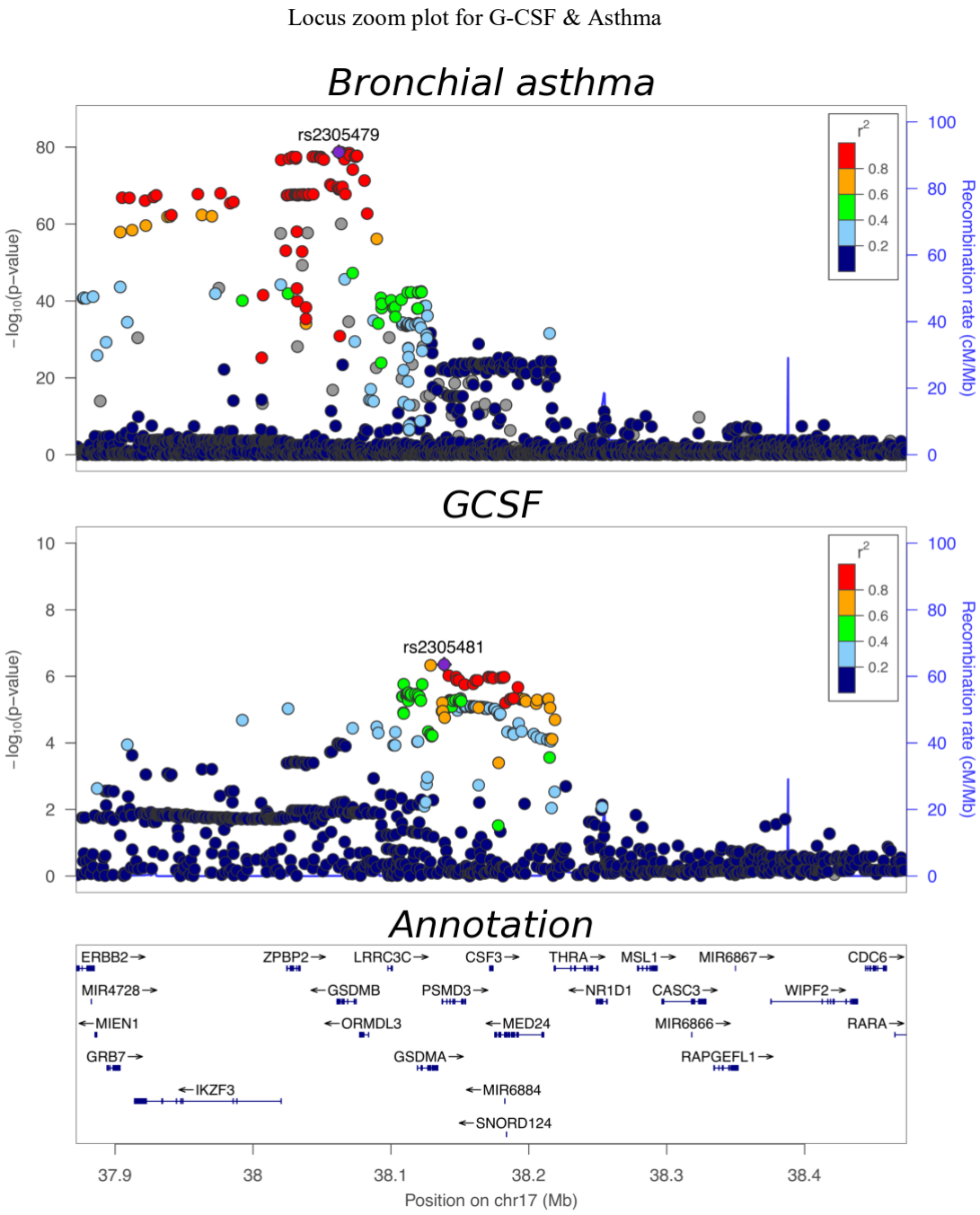

Figure A.2 (cont.)

Locus zoom plot for MIG & Crohn's disease

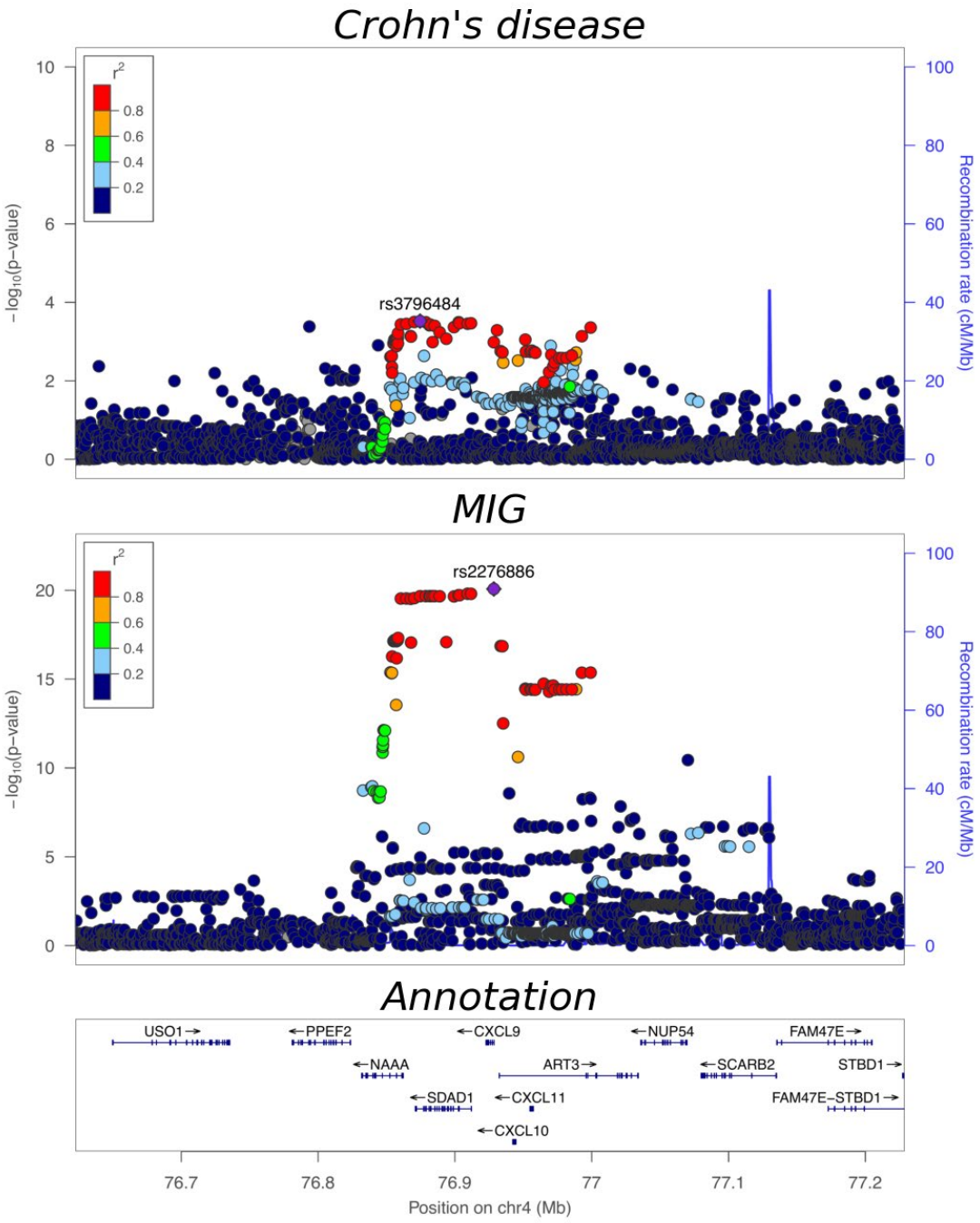

Figure A.2 (cont.)

Locus zoom plot for G-CSF & Crohn's disease

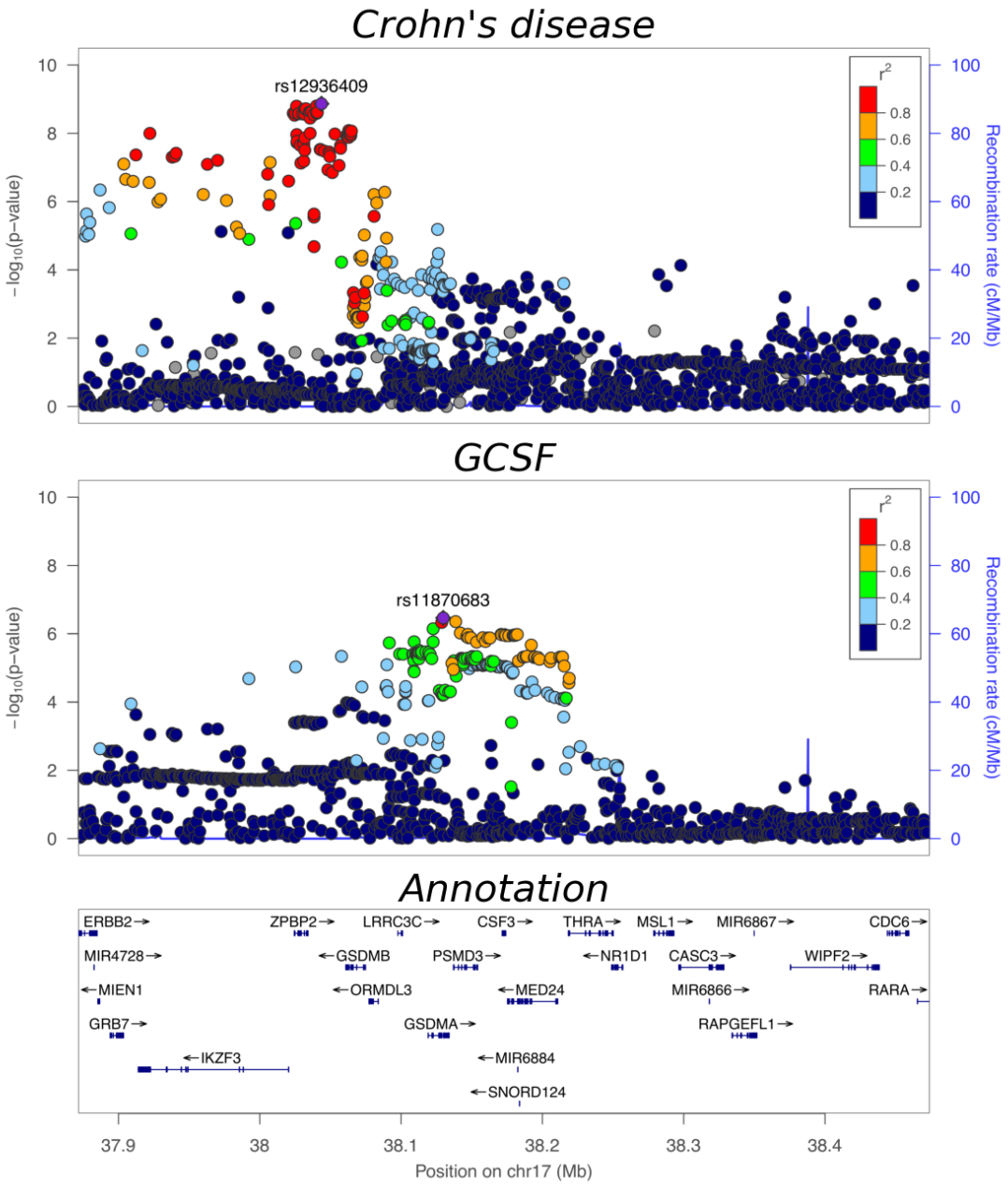

Figure A.2 (cont.)

Locus zoom plot for TNF-b & multiple sclerosis

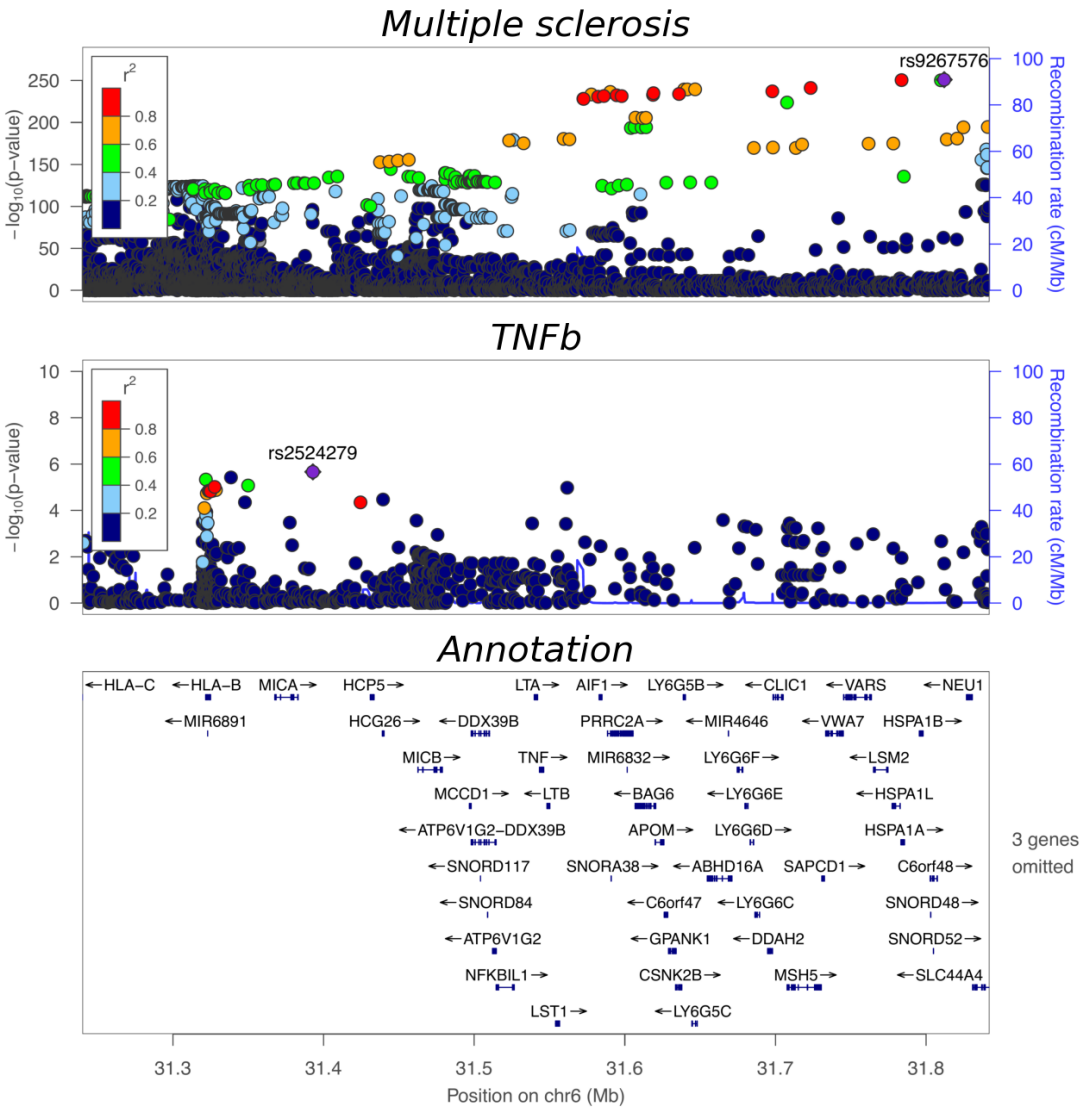

Acknowledgements

First and foremost, I thank my parents, Alina and Richard Konieczny, and my partner, Agnes Heeren, for constant and unconditional love and support through my educational journey. Further, I would like to express my gratitude towards my supervisor, Marios Georgakis, and my colleagues for their scientific and technical input, as well as consistent guidance in the course of my research projects. Lastly, I thank god for my wellbeing and personal strength.

Affidavit

Konieczny, Marek Janusz

Surname, first name

I hereby declare, that the submitted thesis entitled

Inflammatory pathways as drug targets for autoimmune disease - insights from human genomics

is my own work. I have only used the sources indicated and have not made unauthorised use of services of a third party. Where the work of others has been quoted or reproduced, the source is always given.

I further declare that the dissertation presented here has not been submitted in the same or similar form to any other institution for the purpose of obtaining an academic degree.

München, 08.05.2025
Place, Date

Marek Konieczny
Signature doctoral candidate

List of publications

Articles

1) Konieczny MJ, Omarov M, Malik R, Richardson TG, Baumeister SE, Bernhagen J, Dichgans M, Georgakis MK. The genomic architecture of circulating cytokine levels points to drug targets for immune-related diseases. Commun Biol. 2025 Jan 10;8(1):34. doi: 10.1038/s42003-025-07453-w. PMID: 39794498; PMCID: PMC11724035.

2) Konieczny MJ, Dewenter A, Ter Telgte A, Gesierich B, Wiegertjes K, Finsterwalder S, Kopczak A, Hübner M, Malik R, Tuladhar AM, Marques JP, Norris DG, Koch A, Dietrich O, Ewers M, Schmidt R, de Leeuw FE, Duering M. Multi-shell Diffusion MRI Models for White Matter Characterization in Cerebral Small Vessel Disease. Neurology. 2021 Feb 2;96(5):e698-e708. doi: 10.1212/WNL.0000000000011213. Epub 2020 Nov 16. PMID: 33199431.

3) Duering M, Finsterwalder S, Baykara E, Tuladhar AM, Gesierich B, **Konieczny MJ**, Malik R, Franzmeier N, Ewers M, Jouvent E, Biessels GJ, Schmidt R, de Leeuw FE, Pasternak O, Dichgans M. Free water determines diffusion alterations and clinical status in cerebral small vessel disease. Alzheimers Dement. 2018 Jun;14(6):764-774. doi: 10.1016/j.jalz.2017.12.007. Epub 2018 Feb 16. PMID: 29406155; PMCID: PMC5994358.

4) Finsterwalder S, Wuehr M, Gesierich B, Dietze A, **Konieczny MJ**, Schmidt R, Schniepp R, Duering M. Minor gait impairment despite white matter damage in pure small vessel disease. Ann Clin Transl Neurol. 2019 Oct;6(10):2026-2036. doi: 10.1002/acn3.50891. Epub 2019 Sep 16. PMID: 31524338; PMCID: PMC6801180.

5) Gesierich B, Tuladhar AM, Ter Telgte A, Wiegertjes K, **Konieczny MJ**, Finsterwalder S, Hübner M, Pirpamer L, Koini M, Abdulkadir A, Franzmeier N, Norris DG, Marques JP, Zu Eulenburg P, Ewers M, Schmidt R, de Leeuw FE, Duering M. Alterations and test-retest reliability of functional connectivity network measures in cerebral small vessel disease. Hum Brain Mapp. 2020 Jul;41(10):2629-2641. doi: 10.1002/hbm.24967. Epub 2020 Feb 22. PMID: 32087047; PMCID: PMC7294060.

6) Finsterwalder S, Vlegels N, Gesierich B, Araque Caballero MÁ, Weaver NA, Franzmeier N, Georgakis MK, **Konieczny MJ**, Koek HL; Dominantly Inherited Alzheimer Network (DIAN); Karch CM, Graff-Radford NR, Salloway S, Oh H, Allegri RF, Chhatwal JP; DELCODE study group; Jessen F, Düzel E, Dobisch L, Metzger C, Peters O, Incesoy EI, Priller J, Spruth EJ, Schneider A, Fließbach K, Buerger K, Janowitz D, Teipel SJ, Kilimann I, Laske C, Buchmann M, Heneka MT, Brosseron F, Spottke A, Roy N, Ertl-Wagner B, Scheffler K; Alzheimer's Disease Neuroimaging Initiative (ADNI); Utrecht VCI study group; Seo SW, Kim Y, Na DL, Kim HJ, Jang H, Ewers M, Levin J, Schmidt R, Pasternak O, Dichgans M, Biessels GJ, Duering M. Small vessel disease more

than Alzheimer's disease determines diffusion MRI alterations in memory clinic patients. Alzheimers Dement. 2020 Nov;16(11):1504-1514. doi: 10.1002/alz.12150. Epub 2020 Aug 18. PMID: 32808747; PMCID: PMC8102202.

7) Duering M, **Konieczny MJ**, Tiedt S, Baykara E, Tuladhar AM, Leijsen EV, Lyrer P, Engelter ST, Gesierich B, Achmüller M, Barro C, Adam R, Ewers M, Dichgans M, Kuhle J, de Leeuw FE, Peters N. Serum Neurofilament Light Chain Levels Are Related to Small Vessel Disease Burden. J Stroke. 2018 May;20(2):228-238. doi: 10.5853/jos.2017.02565. Epub 2018 May 31. PMID: 29886723; PMCID: PMC6007291.

8) Peters N, van Leijsen E, Tuladhar AM, Barro C, **Konieczny MJ**, Ewers M, Lyrer P, Engelter ST, Kuhle J, Duering M, de Leeuw FE. Serum Neurofilament Light Chain Is Associated with Incident Lacunes in Progressive Cerebral Small Vessel Disease. J Stroke. 2020 Sep;22(3):369-376. doi: 10.5853/jos.2019.02845. Epub 2020 Sep 29. PMID: 33053952; PMCID: PMC7568975.

9) Wollenweber FA, Opherk C, Zedde M, Catak C, Malik R, Duering M, **Konieczny MJ**, Pascarella R, Samões R, Correia M, Martí-Fàbregas J, Linn J, Dichgans M. Prognostic relevance of cortical superficial siderosis in cerebral amyloid angiopathy. Neurology. 2019 Feb 19;92(8):e792-e801. doi: 10.1212/WNL.0000000000006956. Epub 2019 Jan 23. PMID: 30674596.

10) **Konieczny MJ**, Ri SJ, Georgiadis JR. Omental Approach to Functional Recovery After Cerebrovascular Disease. World Neurosurg. 2016 Mar;87:406-16. doi: 10.1016/j.wneu.2015.10.024. Epub 2015 Oct 19. PMID: 26493716.

11) Alberts N*, Groen K*, Klein L*, **Konieczny MJ***, Koopman M*. Dorsal root ganglion neurons carrying a P301S Tau mutation: a valid in vitro model for screening drugs against tauopathies? J Neurosci. 2014 Apr 2;34(14):4757-9. doi: 10.1523/JNEUROSCI.0135-14.2014. PMID: 24695695; PMCID: PMC6802723.

* Authors contributed equally as first authors